INFLUENCE OF STOCKING, CLONE, FERTILIZATION, AND WEED CONTROL ON ABOVE-GROUND BIOMASS AND SOIL CO_2 EFFLUX IN A *PINUS RADIATA* D.DON SILVICULTURAL TRIAL, CANTERBURY, NEW ZEALAND

A thesis
submitted in partial fulfilment
of the requirements for the degree
of
Master of Forestry Science

by

Mohan K C

The New Zealand School of Forestry
University of Canterbury
New Zealand
2018

ABSTRACT

Pinus radiata D. Don is a widely planted exotic tree species in New Zealand as it is a major source of carbon (C) sequestration and industrial timber. Developing precise biomass models is the most essential step in assessing carbon sequestration potential of the forests. Common silvicultural practices comprise site preparation, weed control and fertilization, with clonal forestry playing an increasing role in improving stand productivity and wood quality. These management practices, along with environmental variables, are known to influence above- and below-ground carbon dynamics.

The experimental site was located just south of Rolleston within the Canterbury region of New Zealand. The experiment consisted of 48 permanent plots with a randomized complete block split-split design (Mason, 2008), with an arrangement of factors within four complete blocks. The main plots consisted of three levels of stocking. A first split consisted of four levels of fertilization and follow-up weed control treatment. A second split consisted of five different embryogenic clones randomly allocated to all plots. Three studies were carried out: (a) to find the best models to predict above-ground biomass for *Pinus radiata*; (b) to assess the effects of silvicultural treatments along with environmental variables on soil CO_2 efflux (F_s); and (c) to examine the linkage between above-ground biomass and F_s across silvicultural treatments.

In a first study, two broad procedures were implemented for biomass modelling: (a) independent, and (b) additive. In the independent procedure, linear ordinary least-squares regression with scaled power transformations and y-intercepts produced more precise models than nonlinear biomass estimation methods using power equations and no y-intercepts. In the additive procedure, models fitted in a joint generalized linear least-squares regression, also called seemingly unrelated regression (SUR), provided better goodness-of-fit statistics, standard errors of estimates, residual plots, and histograms of residuals. Compared with independent and additive procedures, additive equations fitted in SUR recorded unbiased estimates of biomass in contrast to linear ordinary least-squares regressions. SUR produced the best goodness-of-fit statistics with unbiased estimates in seven out of ten biomass components. Separate allometric equations were developed to predict biomass for six components, three subtotals of two or more components and total above-ground biomass for *Pinus radiata*.

In a second study, the effects of silvicultural treatments on F_s, soil temperature (T_s), and volumetric water content (θ_v) for the whole period of the experiment, as well as separately for each season, were evaluated using mixed-effect models. The relationships among F_s, T_s, and θ_v were investigated by linear and nonlinear regressions. Season, stocking, and clone had a significant influence on F_s. Estimated mean F_s rate was 22.71 tonnes CO_2 ha^{-1} yr^{-1} (≈ 6.2 tonne C ha^{-1} yr^{-1}). No significant effects of fertilization and follow-up weed control on F_s were observed. Autumn (27.76 tonne CO_2 ha^{-1} yr^{-1}) and winter (15.64 tonne CO_2 ha^{-1} yr^{-1}) exhibited the greatest and smallest rate of F_s, respectively. Greatest F_s rates were observed at 1,250 stems ha^{-1}, without weed control and for clone 3. A soil moisture threshold was determined (i.e. 14.3%) to separate whether F_s was limited by T_s or θ_v. Above this threshold, a clear exponential relationship between F_s and T_s was observed. The values of T_s and θ_v jointly explained relatively high variability (27.90–48.94%) in F_s compared to simply T_s (26.63–47.82%), based on modelling across all silvicultural treatments. Seasonal changes in T_s and θ_v influenced F_s.

In a third study, effects of silvicultural treatments on below-ground soil respiration (BSR), above-ground biomass production (AGB), the ratio (BSR/AGB), tree diameter (DBH), height (H), basal area (G), and leaf area index (LAI) were examined. Mixed-effects analysis of variance was carried out. Stocking, follow-up weed control, and clone significantly influenced above-ground production and below-ground carbon partitioning. Increased above-ground biomass production with stand density was primarily determined by the better use of site resources. Decreased BSR/AGB with stand density was mostly associated to greater resource limitation due to competition. AGB and G increased while DBH and H decreased as stand density increased. Follow-up weed control enhanced above-ground growth by reducing BSR suggesting weed control would decrease competition for below-ground resources. Clones with poorer growth above ground partitioned proportionally more carbon below ground, and vice versa. In conclusion, certain clones were more productive above-ground at the expense of less carbon partitioning below-ground, stocking controlled F_s, T_s and θ_v, and follow-up weed control increased above-ground growth by reducing BSR compared to the treatment without follow-up weed control, which may suggest that weed control reduced competition for below-ground resources.

Key words: *soil CO_2 efflux; Pinus radiata; plantation; soil temperature; soil moisture; below-ground; above-ground; biomass; carbon; partitioning; stocking; clone; fertilization; follow-up herbicide*

ACKNOWLEDGEMENTS

This thesis was started through the initiative of Professor Euan G. Mason (NZ School of Forestry), who suggested that the soil CO_2 efflux could be assessed across silvicultural treatments in a silvicultural experiment with radiata pine located at Rolleston, Canterbury, New Zealand. I would like to especially thank my principal supervisor Professor Euan G. Mason (NZ School of Forestry, University of Canterbury) for his inspiration, empathy, and outstanding supervision. He introduced me to the necessary equipment, measurement and modelling techniques. He provided sound advice in statistical analyses during weekly meetings, and helped enormously with the reviewing and structuring of thesis. Special thanks to my co-supervisor Dr Horacio E. Bown (Faculty of Forestry, University of Chile) for his encouragement, constructive criticism, and support throughout this thesis. I was fortunate to benefit from his expertise to identify key hypotheses, to find the best method of addressing the research question, and to improve the quality of the research. So, thanks to my supervisors! I would not have complete it without your valuable comments and support.

I would like to also thank Dr Daniel Gerhard (Statistics Consulting Unit, University of Canterbury), who guided me to understand the various aspects of mixed-effect modelling. I am grateful to have received a prestigious scholarship "NZAID" from the Ministry of Foreign Affairs and Trade (MFAT), New Zealand, from February 2016 to September 2018. I feel truly indebted to MFAT for this opportunity. I feel thankful also to the Ministry of Forest and Environment, Nepal, for supporting my study leave towards my master's degree. My sincere thank go to Prof Bruce Manley, Prof David Norton, Senior lecturer Justin Morgenroth, Senior lecturer Tara Murray who taught me during my course work. My sincere thanks go to Jeanette Allen, Vicki Wilton, Nigel Pink, and Lachlan Kirk who helped me to arrange the necessary equipment for the field measurement and soil lab activities. I would like to sincerely thank the volunteers involved in my field data collection. I also thank to my friend Hikmah, Thaison, Daniel, Huimin, Poppy, Harry, and Cong Xu for their support and accompanying me during my study.

I would like to thank my parents, brothers, and sisters for their encouragement throughout my study. Finally I would like to extend a heartfelt thanks to my wife, Pratima Bhandari, not only for her love and patience, but also for the support in my seasonal data collection from the field.

Table of Contents

List of figures ix
List of Tables xi
List of symbols xii

Chapter 1. General introduction **1**

Research context 1
Pinus radiata plantations 1
Biomass modelling 1
Soil CO_2 efflux 2
Dynamics of above-ground and below-ground carbon 3
Aim and scope of the research 4
Objectives 4
Hypotheses 5
Synopsis of the experiment and data 5
Thesis structure 10

Chapter 2. Biomass equations for a *Pinus radiata* plantation in the Canterbury plains: A comparison between traditional ordinary least-squares regression and three methods for enforcing additivity **13**

Summary 13
Introduction 14
Materials and methods 16
Study site and experiment 16
Biomass data 17
Modelling procedure 17
Independent procedure for biomass estimation 19
Additive procedure of biomass estimation 20
Model assessment and evaluation 21
Results 22
Measured biomass components 22
Independent procedure of biomass estimation 24
Three additive procedures of biomass estimation 28
Biomass estimates for components, subtotals and AGT 30
Stem 30
Branches 30
Bark 31
New foliage 32
Old foliage 32
Cone 33
Foliage 33
Crown 34
Bole 35
Above-ground total 35
Discussion 42
Measured biomass components 42
Independent procedure for biomass modelling 43

Additive procedure of biomass modelling....44
Conclusion....48

Chapter 3. Seasonal dynamics of soil CO_2 efflux across stocking, clone, fertilization, and understorey-elimination in a *Pinus radiata* plantation in Canterbury, New Zealand 51

Highlights....51
Summary....51
Introduction....53
Materials and methods....55
Study site and experiment....55
Measurement of soil CO_2 efflux....56
Measurement of soil temperature and soil water content....57
Measurement of soil physical properties....57
Statistical analysis....58
Mixed effects modelling....58
Regression analysis....61
Results....64
F_s across stocking, clone, fertilization, and herbicide treatments....64
T_s and θ_v across stocking, clone, fertilization, and follow-up herbicide treatments....67
Soil physical properties across stocking, clone, fertilization, and follow-up herbicide treatments....70
Regression analysis: model performance evaluation....70
Influence of T_s on F_s across silvicultural treatments....72
Influence of T_s and θ_v on F_s across silvicultural treatments....73
Relationships of F_s with soil physical properties....76
Discussion....77
Effects of stocking on F_s....77
Effect of clone on F_s....78
Effects of fertilization on F_s....79
Effects of understorey-elimination on F_s....80
Seasonal variation in F_s....80
Temperature sensitivity of F_s....81
F_s in relation to T_s and θ_v....82
Soil variables influencing F_s....84
Conclusions....85

Chapter 4. Linking above-ground biomass production to below-ground carbon dynamics across stocking, clone, fertilization, and understorey elimination in *Pinus radiata* plantations, New Zealand....87

Highlights....87
Summary....87
Introduction....88
Materials and methods....90
Study site and design of the experiment....90
Above-ground vegetation and biomass....90
Below-ground soil respiration....91
Below-ground to above-ground ratio....91
Stand density index....92

Statistical analysis 92
Results 93
Influence of silvicultural treatments on BSR 93
Influence of silvicultural treatments on AGB 94
Influence of silvicultural treatments on BSR/AGB ratio 95
Influence of silvicultural treatments on DBH 96
Influence of silvicultural treatments on H 97
Influence of silvicultural treatments on G 98
Influence of silvicultural treatments on LAI 99
Discussion 100
Conclusions 103
CHAPTER 5. THESIS SYNTHESIS 105
References 107
Appendixes 120
Appendix 1 120
Appendix 2 130
Appendix 3 137

List of figures

Figure **Short title** **Page**

Figure 1.1: Trial location in Rolleston, Canterbury region of New Zealand. Experimental area boundary in yellow. 7
Figure 1.2: Layout of the experimental trial. 8
Figure 1.3: Schematic representation of the structure of the thesis. 11
Figure 2.1: Model structure with four restrictions (foliage, crown, bole and AGT) for biomass additivity. 21
Figure 2.2: Mean and confidence interval of components, subtotals and AGT biomass 23
Figure 2.3: Partitioning of above-ground total biomass into tree components and subtotal 23
Figure 2.4: Relationship of AGT biomass with variables on original scale of measurement for x and y axes. 24
Figure 2.5: Relationship of AGT biomass with variables on scaled power transformation for x and y axes. 24
Figure 2.6: Residuals vs predicted biomass for the selected best models. The solid black horizontal line across zero represent baseline and the dotted red line is LOESS curve. 42
Figure 2.7: Correlation among the components, subtotals and AGT biomass. The colour indicates the strength of relationship. Darker to lighter indicates high to low correlation, and no colour indicates the relationship is insignificant ($p > 0.05$). 43
Figure 2.8: Effects of follow-up herbicide treatments and clone on biomass production of *P. radiata* in trail site. C and H refers control (no chemical) and herbicide treatment, respectively. 47
Figure 3.1: Histogram showing F_s in a measured scale (upper left) and the same data in a transformed scale (upper right) using Box-Cox transformation, and their corresponding residual distribution (lower left and right). 60
Figure 3.2: (A) ACF for F_s as a response variable, (B) distribution of residuals for the final model fitted in corAR1 autocorrelation structure. 61
Figure 3.3: (A) Relationship between F_s and T_s using all data measured for the whole period of the experiment. (B) Recursive partitioning of the F_s as response variable and T_s at 10 cm soil depth, and θ_v at 10, 20, and 30 cm depth as independent variables in the model. (C) Relationship between F_s and T_s when $\theta_v > 14.3\%$. (D) Relationship between F_s and T_s when $\theta_v < 14.3\%$. The temp indicates T_s and VW_{10} indicates θ_v at 10 cm soil depth. 62
Figure 3.4: Seasonal dynamics of F_s across silvicultural treatments. Values are presented as least square mean (±SE) of F_s, by season. Treatment means within a season followed by the same letter do not differ significantly at $\alpha = 0.05$ level using Tukey's HSD test. 66
Figure 3.5: Predicted vs. residual values of F_s and corresponding histogram of residuals for selected (A) T_s-based equation **3.4** and (B) T_s and θ_v-based equation **3.8.** 72
Figure 3.6: Exponential relationship between F_s and T_s across silvicultural treatments: (A) fertilization (F = fertilization, N = no fertilization), (B) follow-up herbicide (H = herbicide, N = no herbicide), (C) stocking (625, 1,250, and 2,500 stems ha^{-1}) and (D) clones (1–5). Lines were fitted using model parameters of each treatments. T_s was measured at 10 cm soil depth. All fitted models across each treatments were statistically significant ($p < .001$). 73
Figure 3.7: 3D scatter plot showing the relationship between F_s (µmol CO_2 m^{-1} s^{-1}), T_s (°C at 10 cm soil depth), and θ_v (volumetric water content % at 10 cm soil depth) 76
Figure 3.8: The residuals of the best F_s models based on combined T_s and θ_v (Eq. **3.8**) plotted separately with measured (A) T_s and (B) θ_v values. 84

Figure 4.1: Main effects of (A) stocking, and clone (B) on BSR. Treatment means (± SE) indicated by the same letter do not differ significantly at α = 0.05 level using Tukey's HSD test. 94
Figure 4.2: Significant interaction effects of (A) stocking × follow-up herbicide, and (B) clone × follow up herbicide) on AGB. 95
Figure 4.3: Main effects of (A) stocking, (B) clone, and (C) follow-up weed control on BSR/AGB ratio. Treatment means (± SE) indicated by the same letter do not differ significantly at α = 0.05 level using Tukey's HSD test. 96
Figure 4.4: Significant interaction effects of (A) stocking × follow-up herbicide, and (B) clone × follow-up herbicide interaction on DBH. 97
Figure 4.5: Main effects of (A) stocking, (B) clone, and (C) follow-up herbicide treatment on H. Treatment means (± SE) indicated by the same letter do not differ significantly at α = 0.05 level using Tukey's HSD test. 98
Figure 4.6: Significant interaction effects of (A) stocking × follow-up herbicide, and (B) clone × stocking on G. 99

List of Tables

Table	Short title	Page
Table 1.1: Summary of the dataset variables used for each of three studies with their respective units of measurement, data source, and resolution of measurement.		9
Table 2.1: Notations and definitions for biomass modelling of *Pinus radiata*		18
Table 2.2: Measure of goodness of fit statistics		22
Table 2.3: Descriptive statistics of independent variables used in regression models.		23
Table 2.4: Tested linear and nonlinear ordinary least-squares equations with their best fit results.		25
Table 2.5: Goodness-of-fit statistics, regression coefficients and their standard error (±) for the best LINOLS and NLINOLS models.		26
Table 2.6: Regression model with given components as the dependent variable, modelling technique, parameter estimates, their standard error and statistically significant values.		37
Table 2.7: Goodness-of-fit statistics for given biomass components using four methods of modelling.		39
Table 3.1: Lab analysis for the determination of soil physical properties		57
Table 3.2: Different measure of goodness-of-fit statistics to evaluate the model's performance.		64
Table 3.3: Mean soil CO_2 efflux rates.		67
Table 3.4: Mean soil temperature		69
Table 3.5: Mean soil volumetric water content.		69
Table 3.6: Goodness-of-fit statistics for the model evaluation.		71
Table 3.7: Regression models for the relationship between F_s, T_s, and θ_v across the clone (five clones), stocking (625, 1,250, and 2,500 stems ha^{-1}), fertilization (F = fertilization, NF = no fertilization), and follow-up herbicide (H = herbicide, NH = no herbicide) treatments.		75

List of symbols

Symbol	Description	Units
a, b, c, β_0, β_1, β_2	Parameter estimates of model	no units
ACF	Autocorrelation factor	no units
AGB	Above-ground biomass production	tonne C ha^{-1}
AGT	Above-ground total biomass	kg $tree^{-1}$
AIC	Akaike's information criterion	no units
ANOVA	Analysis of variance	no units
BD	Bulk density	g cm^{-3}
BSR	Below-ground soil respiration	tonne C ha^{-1} yr^{-1}
C	Carbon	variable units
CO_2	Carbon dioxide	variable units
CrL	Crown length	m
CV	Coefficient of variation	variable units
DBH, D	Diameter at breast height	cm
DBHq	Quadratic mean diameter	cm
DW	Dry weight	soil (g), wood (kg)
F_s	Soil CO_2 efflux	µmol CO_2 m^2 s^{-1}, tonne CO_2 ha^{-1} yr^{-1}
FW	Fresh weight	soil (g), wood (kg)
G	Basal area	m^2 ha^{-1}
GWC	Gravimetric water content	%
H	Tree height	m
IOA	Index of agreement	no units
LAI	Leaf area index	m^2 m^{-2}
LINADD	Linear model in additive structure	no units
LINOLS	Linear ordinary least square	no unit
LSD	Least significant difference	variable units
MAB	Mean absolute bias	variable units
Max	Maximum	variable units
Min	Minimum	variable units
ML	Maximum likelihood	no unit
MPE	Mean prediction error	variable units
M_s	Mass of fine soil	g
n	Sample size	no unit
NF	New foliage biomass	kg $tree^{-1}$
NLINOLS	Non-linear ordinary least-squares	no unit
NN	No chemical treatment	no unit
OF	Old foliage biomass	kg $tree^{-1}$
PD	Particle density	g cm^{-3}
PORE	Total soil porosity	%

Q_{10}	Increase in F_s rates with 10 °C increase in temperature	no unit
R^2	Coefficient of determination or fit index	variable units
BSR/AGB	Belowground soil respiration/above-ground biomass production	no unit
REML	Restricted maximum likelihood	no unit
RF	Rock fragments in soil	%
RMSE	Root mean square error	variable units
RSE	Residual standard error	variable units
SD	Standard deviation	variable units
SDI	Stand density index	stems ha^{-1}
SLA	Specific leaf area	$cm^2\ g^{-1}$
SUR	Seemingly unrelated regression	no unit
T_s	Soil temperature	°C
V_s	Volume of fine soil	cm^3
WD	Wood density	$kg\ m^{-3}$
WFPS	Water filled pore space	%
$\hat{y}$	Predicted values from the model	variable units
θ_v	Volumetric water content	$m^3\ m^{-3}$, %
λ	Coefficient of transformed variable	no units

Chapter 1. General introduction

Research context

Pinus radiata plantations

Pinus radiata D. Don is an exceptionally important tree species: the world's most widely planted and most valuable tree (Mead, 2013). The total global planted area is now more than 4.2 million hectares (Mead, 2013). In New Zealand, it is the predominant species planted, accounting for about 90% of 1.70 million hectares of forest plantations (Nixon, Gamperle, Pambudi, & Clough, 2017). Common silvicultural practices comprise site preparation, weed control and fertilization, thinning and pruning, among others, with clonal forestry playing an increasing role at improving stand productivity and wood quality. These practices are mainly aimed at enhancing growth and productivity of the trees (Burger, 1994; Lasserre, Mason, & Watt, 2008; Mason, 1992; Mason & Milne, 1999). It has been widely recognized that plantation forests in New Zealand are an important source of industrial timber and fuelwood, while also being a major source of carbon sequestration while growing (Hollinger, Maclaren, Beets, & Turland, 1993).

Biomass modelling

Biomass modelling is a first step to assess carbon sequestration potential of a forest ecosystem. Allometric models are commonly used to assess the biomass contained in the tree species. Allometric relationships can be developed from destructive sampling by using several forms of regression equations. Generally, biomass equations are fitted using nonlinear regressions of the form, $B = aD^b$, where B is the biomass of the tree, or its components, and D is the diameter of the tree (Baskerville, 1972; Beauchamp & Olson, 1973; Sprugel, 1983). Several authors have used this form of equation to estimate the biomass of individual trees (Canadell, Riba, & Andres, 1988; Kitayama & Itow, 1999; Porté, Trichet, Bert, & Loustau, 2002; Santa Regina, Tarazona, & Calvo, 1997). In New Zealand, over the past five decades, many studies were carried out to find the best biomass equations for *P. radiata* using various functional linear and nonlinear forms, with models generally being developed separately for each individual biomass component and for the whole tree (Beets, Pearce, Oliver, & Clinton, 2007; Beets & Pollock, 1987; Madgwick, 1994; Moore, 2010).

Separately calculated biomass equations ignore correlations among the different component equations (Kozak, 1970; Parresol, 1999). The additive system in biomass modelling has long been recognized as a desirable property of systems of equations to predict the biomass of components and the whole tree (Cunia & Briggs, 1984, 1985; Kozak, 1970; Parresol, 1999, 2001). In recent years, the additive procedure of biomass estimation has been extensively used in other parts of the world (Canga, Aranda, Khouri, & Obregón, 2013; Carvalho & Parresol, 2003; Návar, González, Graciano, Dale, & Parresol, 2004; Zhao, Kane, Markewitz, Teskey, & Clutter, 2015). However, there are no studies reporting additive biomass models for any tree species in New Zealand. Therefore, developing additive biomass models for *P. radiata* may assist silviculturists to make better and sounder decisions based on more precise models.

Soil CO_2 efflux

Soil CO_2 efflux (F_s) is an essential component of Earth's carbon budget comprising approximately two thirds of the global carbon budget (Schlesinger & Andrews, 2000). The magnitude of F_s is estimated at approximately 80.4 Pg C yr^{-1} (Raich, Potter, & Bhagawati, 2002). Over recent decades, many studies have been undertaken to evaluate the major drivers affecting F_s in forested land, reporting that F_s is influenced by soil temperature (T_s) (Fang & Moncrieff, 2001; Lloyd & Taylor, 1994), and soil moisture (θ_v) (F. Cook, Orchard, & Corderoy, 1985; Gärdenäs, 2000), nutrients (Zogg, Zak, Burton, & Pregitzer, 1996), and the respiring tissue mass (Vose et al., 1995). Climate change has brought an increasing interest in assessing the spatial and temporal variability of F_s, as well as its main drivers (Yiqi & Zhou, 2010). It has been widely documented that T_s and θ_v are the two most important environmental controls driving F_s (Davidson, Belk, & Boone, 1998; Janssens et al., 2001; Raich et al., 2002; Raich & Schlesinger, 1992; Raich & Tufekciogul, 2000). Although the relationship of F_s with T_s and θ_v have been well documented (Buchmann, 2000; Reiners, 1968; Rustad et al., 2001); the form of the relationship may vary depending on the type of ecosystem (Bowden, Newkirk, & Rullo, 1998; Lomander, Kätterer, & Andrén, 1998; Yiqi & Zhou, 2010). Lloyd & Taylor (1994) showed that F_s scales exponentially with T_s, as other authors have reported (Knorr, Prentice, House, & Holland, 2005). High temperature and high moisture have demonstrated a confounding effect on the temperature sensitivity of F_s as denoted by Q_{10} (Davidson et al., 1998; Yuste, Janssens, Carrara, Meiresonne, & Ceulemans, 2003). Moreover, the temporal dynamics of F_s are also strongly controlled by the photosynthetic activity of plants (Högberg

et al., 2001; Kuzyakov & Cheng, 2001). F_s has also been shown to be affected by the soil physical and chemical properties, such as bulk density, porosity, stoniness, texture, carbon and organic matter content, among others (Aslam, Choudhary, & Saggar, 2000; Yiqi & Zhou, 2010).

Silvicultural practices are known to influence F_s, which is well documented for some tree species (Maier, Albaugh, Lee Allen, & Dougherty, 2004; Yohannes, Shibistova, Asaye, & Guggenberger, 2013). Manipulating silvicultural variables such as stocking (Della-Bianca & Dills, 1960; Litton, Ryan, & Knight, 2004; Noh et al., 2010), nutrients (Bown & Watt, 2016; Gallardo & Schlesinger, 1994; Haynes & Gower, 1995; Olsson, Linder, Giesler, & Högberg, 2005; Phillips & Fahey, 2007), and clones (Bown, Watt, Clinton, Mason, & Whitehead, 2009) have been shown to change F_s. In New Zealand, most research on *P. radiata* plantations has been carried out with the aim of improving growth and wood properties through different silvicultural treatments (Mason, 2008; Mason & Milne, 1999; Mason, South, & Weizhong, 1996). However, studies on the influence of silvicultural treatments and of environmental variables on F_s are scarce; and therefore experimental studies to evaluate the effect of these factors on F_s in *P. radiata* are essential.

Dynamics of above-ground and below-ground carbon

A substantial amount of carbon enters into the soil (75.8 Pg C yr-1) mainly from vegetative inputs (Jenkinson, Adams, & Wild, 1991), being released to the atmosphere (80.4 Pg C yr^{-1}) mainly through F_s (Raich et al., 2002). Dynamics of the carbon in forest ecosystems may vary according to climate, species and site productivity (Jandl et al., 2007). Silvicultural practices such as stocking, clone, fertilization, and herbicide can affect above- and below-ground carbon by altering the microclimatic conditions of the site and soil (Jandl et al., 2007). Above-ground vegetation characteristics such as biomass, tree diameter, height, basal area, and leaf area index may directly affect the soil microclimate, litterfall, and hence root and microbial respiration (Raich & Tufekciogul, 2000). Soil physical as well as chemical properties have a direct and indirect influence on below-ground carbon dynamics (Raich & Tufekciogul, 2000). For instance, pore space filled with small quantities of water may inhibit the soil microbial and root metabolic activity (Gliński & Stępniewski, 1985), and stoniness may affect water availability, soil organic matter and fine-root spread (Rustad, Huntington, & Boone, 2000). Biological factors have also been reported to influence F_s; for instance, positive correlations between net

primary production and F_s (Raich & Nadelhoffer, 1989) and leaf-litter production (Raich & Tufekciogul, 2000) have been observed. Ecological linkages between above-ground vegetation and below-ground processes have been well documented (Coyle, Coleman, & Aubrey, 2008; Murphy, Balser, Buchmann, Hahn, & Potvin, 2008; Wardle et al., 2004). Above-ground vegetation might alter the diversity of soil microorganisms which may further influence below-ground soil respiration (Balvanera et al., 2006; Zak, Holmes, White, Peacock, & Tilman, 2003). Hence, silviculture-induced changes above-ground are expected to have direct effects on soil processes and vice versa (Wardle et al., 2004). For example, certain studies have reported that allocation of carbon from above-ground to below-ground was greater in nutrient-poor sites compared to nutrient-rich sites (Albaugh, Allen, Dougherty, Kress, & King, 1998; Chapin III, 1980; Zerihun & Montagu, 2004). Land-use changes, such as extensive plantations of fast-growing tree species and their management practices, such as fertilization and herbicide application, may have direct effects on carbon sequestration rate by incorporating CO_2 into tree biomass and into the soil (Jandl et al., 2007).

Given the extensive area of *P. radiata* plantations in New Zealand, experimental study is essential to investigate the effects of silvicultural practices on below-ground soil respiration (BSR), above-ground biomass production (AGB), the ratio (BSR/AGB), tree diameter (DBH), height (H), basal area (G), and leaf area index (LAI). Moreover, emphasis should be placed on evaluating the changes in carbon partitioning above- versus that below-ground which might be influenced by silvicultural practices.

Aim and scope of the research

Objectives

The aim of this thesis was to assess the effect of stocking, follow-up weed control, fertilization and genotype on tree biomass, soil respiration and above- versus below-ground carbon processes in a *Pinus radiata* trial in the Canterbury region of New Zealand, and specifically,

1. to develop tree and component biomass models for *Pinus radiata*
2. to assess the soil CO_2 efflux (F_s) across seasons at differing stockings, clones, fertilization, and follow-up weed control treatments, and to examine environmental and soil drivers controlling F_s

3. to examine the linkages between below-ground soil respiration and above-ground biomass production, across stockings, clones, fertilization and follow-up weed control treatments.

Hypotheses

1. Additive biomass models using seemingly unrelated regression (SUR) would provide more precise and unbiased estimates of biomass compared with traditional ordinary least-squares regression (Kozak, 1970; Parresol, 1999, 2001).
2. Fertilization (Castro et al., 1994; Johnson, 1992; Vose et al., 1995), weed control (Carlyle, 1993; Shan, Morris, & Hendrick, 2001), stand density (Della-Bianca & Dills, 1960; Litton, Knight, & Ryan, 2001; Litton et al., 2004), and clone (Bown, Mason, Clinton, & Watt, 2009; Bown, Watt, Clinton, et al., 2009; Bown, Watt, Mason, Clinton, & Whitehead, 2009; Tyree, Seiler, & Maier, 2011, 2014) would bring about changes in below-ground carbon processes, as indicated by F_s. The F_s may vary across the season due to seasonal changes in environmental variables such as T_s and θ_v (Davidson et al., 1998; Yiqi & Zhou, 2010).
3. Silvicultural treatments would affect BSR (Samuelson, Johnsen, Stokes, & Lu, 2004; Shan et al., 2001; Yohannes et al., 2013), AGB (Litton, Ryan, Tinker, & Knight, 2003; Snowdon & Benson, 1992) and vegetation variables such as DBH, H, G, and LAI (Carlyle, 1998; Mason, 1992; Mason & Milne, 1999; McQuillan, 2013; Richardson, 1993; Rubilar et al., 2013), thereby shifting carbon partitioning from below- to above-ground (Haynes & Gower, 1995; Zerihun & Montagu, 2004). Changes in above-ground production will have consequences for below-ground process and vice versa (Wardle et al., 2004).

Synopsis of the experiment and data

Three studies were carried out from 2017 to 2018 from a trial testing the effect of stocking, clones, fertilization, and weed control treatment (Mason, 2008) on growth and wood properties of *P. radiata* in the Canterbury region at Rolleston, New Zealand (Figure 1.1). The experiment was established by the School of Forestry, University of Canterbury, New Zealand, on land owned by Selwyn District Council. The experiment consisted of 48 permanent plots with a

randomized complete block design, having factorial-split plots in 4 complete blocks (Mason, 2008), with an arrangement of factors within the block (Figure 1.2). The first study was designed to find the best model predicting biomass components and total above-ground tree biomass. The second study assessed the effect of stocking, clones, fertilization, and follow-up weed control on soil CO_2 efflux (F_s), and the main environmental and soil variables controlling seasonally collected values of F_s. The third study assessed the linkage between above-ground biomass production and below-ground soil respiration, and how the below/above-ground ratio is changed by silvicultural treatments. The first study was carried out with data collected from destructive sampling of 24 ten-year-old trees of *P. radiata* in 2015. The second and third studies were carried out with data collected in four seasons during 2017 and 2018. In addition, the above-ground biomass models developed for *P. radiata* in the first study, and the soil respiration model developed in the second study, were used for the analysis in the third study, along with other vegetation data collected in 2017. The dataset used in the analysis for each experiment of this thesis is summarized and given in Table 1.1.

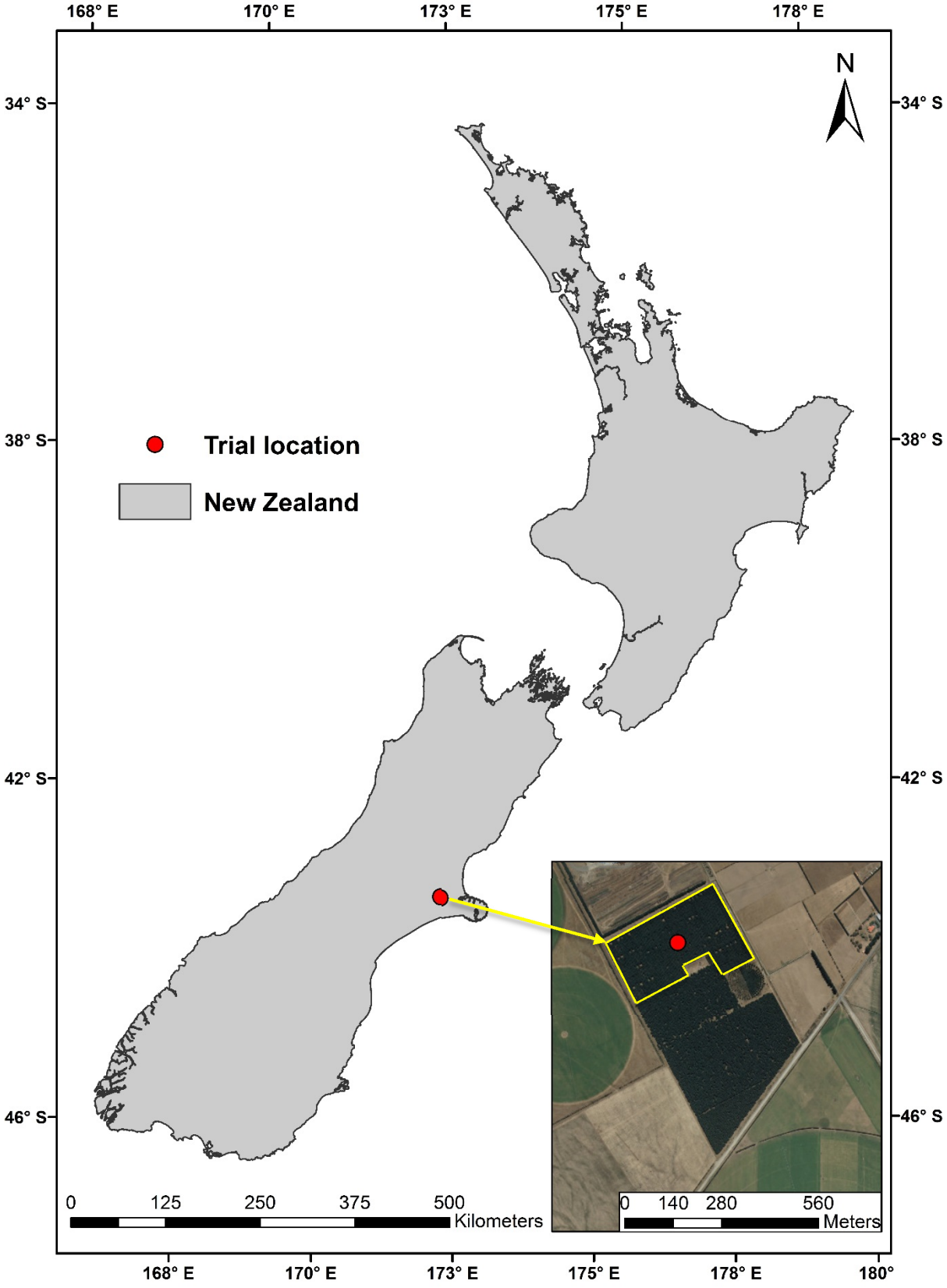

Figure 1.1: Trial location in Rolleston, Canterbury region of New Zealand. Experimental area boundary in yellow.

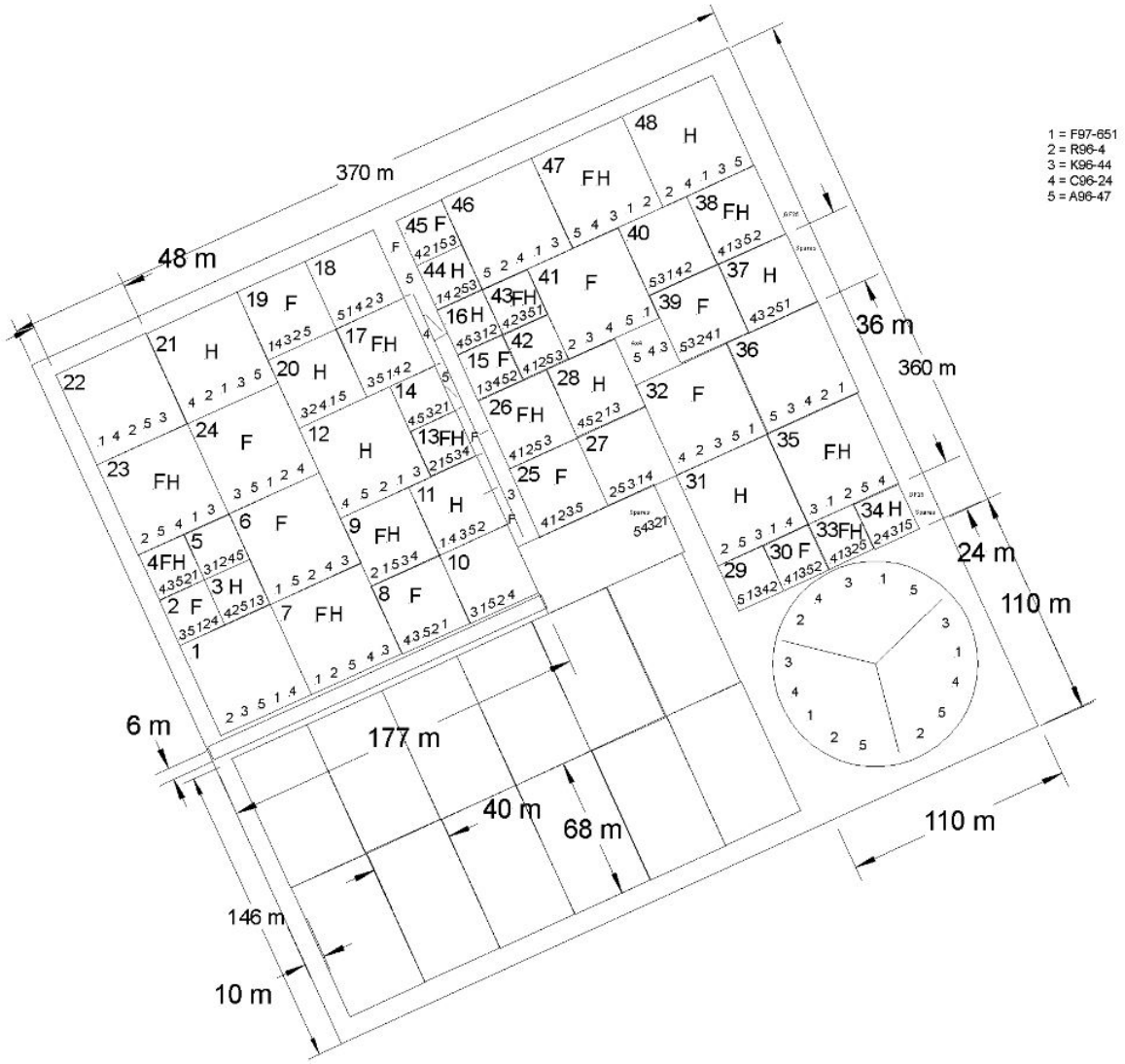

Figure 1.2: Layout of the experimental trial.

Table 1.1: Summary of the dataset variables used for each of three studies with their respective units of measurement, data source, and resolution of measurement.

	Dataset	**Source**	**Resolution***	**Remarks**
First study	DBH (cm)	School of Forestry (2015)	24 sample trees	n = 24
	H (m)	School of Forestry (2015)	24 sample trees	n = 24
	CrL (m)	School of Forestry (2015)	24 sample trees	n = 24
	AGB (kg tree^{-1}) **	School of Forestry (2015)	24 sample trees	n = 24
Second study	F_s (μmol m^2 s^{-1})	Field measured during 4 seasons (2017 & 2018)	clone level	n = 960 (48 plots × 5 records × 4 seasons)
	T_s (°C)	Field measured during 4 seasons (2017 & 2018)	clone level	n = 960 (48 plots × 5 records × 4 seasons)
	θ_v (%)	Field measured and lab analysis during 4 seasons (2017 & 2018)	clone level	n = 960 (48 plots × 5 records × 4 seasons)
	WFPS (%)	Lab analysis (2017 & 2018)	clone level	n = 960 (48 plots × 5 records × 4 seasons)
	BD (g cm^{-3})	Lab analysis (2017 & 2018)	plot level	n = 192 (48 plots × 4 seasons)
	PORE (%)	Lab analysis (2017 & 2018)	plot level	n = 192 (48 plots × 4 seasons)
	RF (%)	Lab analysis (2017 & 2018)	plot level	n = 192 (48 plots × 4 seasons)

Table 1.1 continued overleaf

Table 1.1 continued

	Dataset	Source	Resolution*	Remarks
Third study	DBH (cm)	Field measured once in July 2017	complete enumeration	plot level (n = 48) clone level (n = 240)
	H (m)	Field measured once in July 2017	complete enumeration	plot level (n = 48) clone level (n = 240)
	G (m^2 ha^{-1})	Calculated from data of July 2017	plot level & clone level	plot level (n = 48) clone level (n = 240)
	BSR (tonne C ha^{-1} yr^{-1})	Using model developed in second study	plot level & clone level	plot level (n = 48) clone level (n = 240)
	AGB (tonne ha^{-1})	Using model developed in first study	plot level & clone level	plot level (n = 48) clone level (n = 240)
	LAI (m^2 m^{-2})	Field measured during 4 seasons (2017 & 2018)	plot level	n = 192 (48 plots × 4 seasons)

Note: The abbreviations are as follows: DBH (diameter at breast height), H (total tree height), CrL (crown length), G (basal area), AGB (above-ground biomass), F_s (soil CO_2 efflux), T_s (soil temperature), θ_v (volumetric soil water content), WFPS (water filled pore space), BD (bulk density), PORE (total soil porosity), RF (rock fragments), BSR (below-ground soil reparation), LAI (leaf area index), n = sample size.

** plot level indicates 48 plots, clone level indicates 240 (i.e., 48 plots* × 5 clones)

*** Total tree biomass as well as separate components such cone, new foliage, old foliage, branch, bark, and stem.*

Thesis structure

To achieve the stated objectives and test the listed hypotheses, this thesis comprises five chapters (Figure 1.3). Chapter 1 provides a general introduction and context for the thesis. Chapter 2 compares biomass models using seemingly unrelated regression (SUR) against traditional ordinary least-squares regressions. Chapter 3 addresses the effects of stocking, clones, fertilization, and follow-up weed control on soil CO_2 efflux (F_s), and the main environmental and soil variables controlling seasonally collected values of F_s. Chapter 4 describes the linkage between above-ground biomass production and below-ground soil respiration, and how the below/above-ground ratio was changed by silvicultural treatments. Chapter 5 comprises a synthesis of the previous chapters and summarizes the key findings of this thesis.

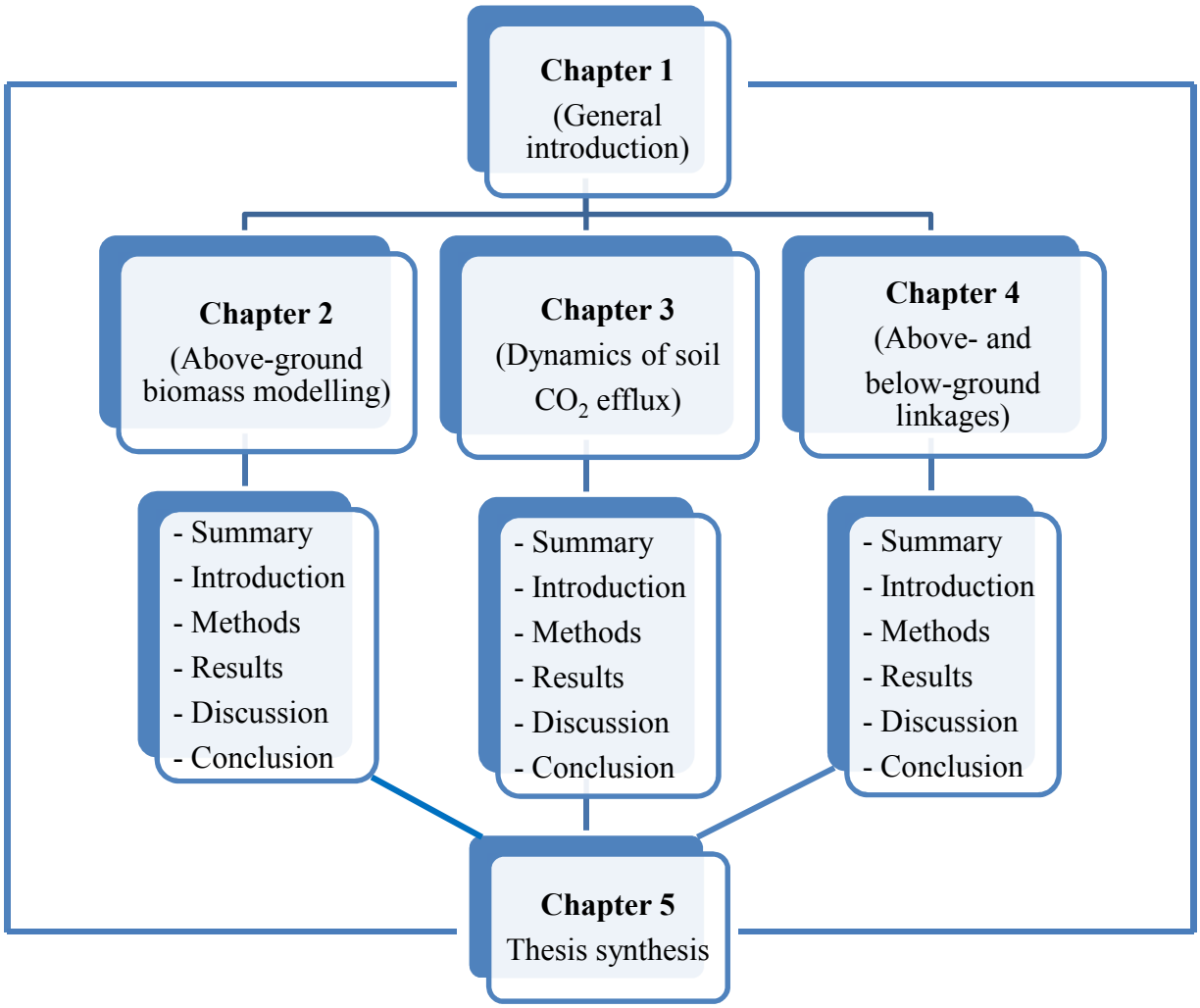

Figure 1.3: Schematic representation of the structure of the thesis.

Chapter 2. Biomass equations for a *Pinus radiata* plantation in the Canterbury plains: A comparison between traditional ordinary least-squares regression and three methods for enforcing additivity

Highlights

- Stem accounted for the largest proportion of above-ground total biomass.
- Linear ordinary least squares-regressions with scaled power transformations and y-intercepts produced more precise models than those from nonlinear biomass estimation methods using power models and no y-intercepts.
- Seemingly unrelated regression (SUR) recorded unbiased estimates of biomass in contrast to linear ordinary least-squares regression.
- SUR is recommended to estimate biomass of *Pinus radiata* plantations in New Zealand.

Summary

The aim of this study was to develop models to estimate components, subtotals and above-ground total biomass for *Pinus radiata* in New Zealand. A total of 24 ten-year-old trees, from a forestry trial designed to test the effect of stocking, clones, fertilizations, and follow-up weed control treatment (Mason, 2008) in the Canterbury region of New Zealand, were felled to assess above-ground biomass. Stems accounted for the highest proportion (58.56%) of above-ground biomass (103.24 ± 30.17 kg tree^{-1}). Two broad procedures were implemented for biomass modelling: (a) independent, and (b) additive. For the independent procedure, traditional linear (LINOLS) models with scaled power transformations and y-intercepts and nonlinear (NLINOLS) power models without y-intercepts were compared. All models were evaluated using goodness-of-fit statistics, standard errors of estimates, residual plots, and histograms of residuals. The result showed that LINOLS models with scaled power transformations and y-intercepts performed better for all components, subtotals and above-ground total biomass in contrast to nonlinear methods. For the additive procedure, the best LINOLS models from the independent procedure were further tested in three different additive structures (LINADD1, LINADD2, and LINADD3). The results indicated that the additive model (LINADD3) in a joint generalized linear least-squares regression, also called seemingly unrelated regression (SUR), provided best goodness-of-fit statistics and residual plots for four out of six components

(stem, branch, new foliage and, old foliage), two out of three subtotals (foliage and crown), and above-ground total biomass compared to other methods. However, bark, cone and bole biomass were better predicted by LINOLS. Separate allometric equations were developed to predict biomass for six components, three subtotal and the total above-ground. SUR is recommended as a sound method to predict biomass of *P. radiata* plantations in New Zealand as it provided best goodness-of-fit statistics with unbiased estimates in 7 out of 10 components. To the best of our knowledge this approach is novel for estimating tree biomass in New Zealand, although it is frequently used in other parts of the world. Further assessment of total tree biomass, including below-ground root biomass, would be the next step recommended.

Key words: *Pinus radiata; above-ground; biomass; linear; nonlinear; additive; SUR*

Introduction

Biomass modelling is a key index and a crucial step to evaluate the potential for carbon sequestration of forest ecosystems. Forests play a vital role in the carbon cycle to mitigate climate change by accumulating and sequestrating atmospheric carbon dioxide (CO_2) (Houghton, 1991). *Pinus radiata* D. Don, native to California, is a widely planted major tree species in the Southern Hemisphere, including New Zealand, Australia, Chile, Spain and South Africa (Lavery & Mead, 2000; Mead, 2013), especially for timber production, as this species is versatile, fast-growing, and has a wide range of end uses (Lavery & Mead, 2000; Lewis, Ferguson, Sutton, Donald, & Lisboa, 1993; Rogers, 2002; Sutton, 1999; Toro & Gessel, 1999). The global plantation area of *P. radiata* is now more than 4.2 million hectares (Mead, 2013). In New Zealand, it is the predominant species planted, and accounts for about 90% of a total 1.70 million hectares of the planted area (Nixon et al., 2017). Plantation forests in New Zealand have not only been recognized as providing financial returns from traditional wood products, but also as providing environmental services by accumulating biomass and storing a substantial amount of carbon through carbon sequestration. To quantify such benefits, a precise biomass model at a required level of accuracy is essential. Biomass estimation of an individual tree or its components is the basis for the forest stand biomass estimation (Zheng et al., 2015).

Clutter et al. (1983) explained various linear and nonlinear additive regression models to estimate the biomass of an individual tree or its components. The additivity system of biomass

equation has long been recognized as a desirable property of a system of component regression, as predictions for tree components biomass added together equals predictions of total tree biomass (Cunia & Briggs, 1984, 1985; Parresol, 1999, 2001). Three procedures of forcing additivity have been proposed (Cunia & Briggs, 1985; Parresol, 1999): (a) adding the best regression functions of the components' biomass to determine the total biomass regression function; (b) using the same independent variables for each component; and (c) using joint generalized least-squares regression, also known as seemingly unrelated regression (SUR), in which statistical dependencies among sample data are accounted for by forcing constraints on the regression coefficients. These three procedures have been applied extensively for estimating tree biomass in some parts of the world (Canga et al., 2013; Návar, González, et al., 2004).

Over 50 years, a substantial number of biomass studies for *P. radiata* have been undertaken in New Zealand. Previous studies have mostly given emphasis to estimating productivity in terms of quantities of dry matter production and nutrients contained in the trees (Beets & Madgwick, 1988; Beets, Pearce, et al., 2007; Beets & Pollock, 1987; Madgwick, 1983, 1985; Madgwick, Jackson, & Knight, 1977; Mead, Draper, & Madgwick, 1984; Webber & Madgwick, 1983; Will, 1964), and some studies evaluated the effects of silvicultural management factors while modelling biomass (Cromer, Barr, Williams, & McNaught, 1985; Mead et al., 1984). Details of modelling about partitioning of tree biomass into different components such as stem, foliage, branch and roots can be found in Beets and Pollock (1987). Madgwick (1994) provided complete coverage of biomass studies for *P. radiata* in New Zealand. Nationally applicable models for *P. radiata* to predict stem biomass and carbon sequestration from the increment in stem wood volume have been developed in New Zealand (Beets, Kimberley, & McKinley, 2007). In recent years, Moore (2010) developed allometric models to predict total above-ground biomass of *P. radiata* using data from the North Island of New Zealand.

Previous equations for *P. radiata* in New Zealand were developed separately for components and total trees. Separately calculated biomass equations ignore correlations among the component equations (Kozak, 1970; Parresol, 1999). Simultaneous fits regarding related equations using additive procedures have greater statistical efficiency, as they take into account statistical dependencies among biomass components recorded from the same tree biomass sample (Parresol, 1999, 2001). Therefore, previously developed equations in New Zealand have not taken into account such statistical dependence among the component equations. As

there are no studies available to estimate biomass of *P. radiata* that meet the additivity requirements, this study is aimed at finding the best allometric equations that predict component biomass, subtotals and total above-ground biomass for *P. radiata* using traditional linear and nonlinear ordinary least-squares regressions, and to contrast these equations with the additive procedures of biomass estimation.

Materials and methods

Study site and experiment

For this study, data were collected from a Rolleston site, in the Canterbury region of New Zealand, planted with *P. radiata* in 2005 (Figure 1.1). This is located at latitude 43° 37.2′ S and longitude 172° 20.4′ E, and about 45 m above sea level on a flat landscape. This site is known to have dry, frosty conditions in winter, and occasional dry and windy conditions in the summer. The site has an air median annual temperature between 11 and 13 °C with a monthly minimum (July) of −2 to +4 °C and a monthly maximum (January) of 20 to 23 °C (Macara, 2016). Annual rainfall is about 618 mm with a monthly range of 38 to 68 mm (Macara, 2016). The major soil type is a Lismore stony silt loam, with aggradation gravel as parent material, which also includes partial glacial gravel (NIWA, 2018; Xue et al., 2013).

The experiment consisted of 48 permanent plots with a randomized complete block split-split design (Figure 1.2), with the arrangement of factors within 4 complete blocks (Mason, 2008). The main plots consisted of three levels of stocking (625, 1250 and 2500 stems ha^{-1}). A first split consisted of four levels of follow-up weed control, and fertilization treatments (fertilization, F; herbicide, H; both, FH; and no chemical, NN). Fertilization was carried out once in year 1 and once in year 3 (NPKS + trace elements @ 80 grams per tree) after planting. Weed control treatment was applied in years 1 and 2 (strip weed control) and follow-up weed control was applied in years 3 (herbicide) and any subsequent year when new weeds appeared after planting. A second split consisted of five different embryogenic clones randomly allocated to all plots, with the clone numbers 1, 2, 3, 4 and 5 (Mason, 2008).

During the summer of 2015 to 2016, a team consisting of Grace Jones, Euan Mason and Horacio Bown harvested and measured the biomass of 24 trees in this experiment from six

plots (Plot 37, 40, 42, 44, 46, and 48), and within each plot four trees were felled. These plots consisted of three levels of stocking (625, 1250 and 2500 stems ha^{-1}), two levels of follow-up weed control treatment (H and NN) and two clones (1 and 2). Clone 1 was recognized as one with a low microfibril angle and high basic density, while clone 2 was reported to have a high microfibril angle and low basic density.

Biomass data

Trees were felled very close to ground level. The over-bark diameter of each tree at breast height was recorded at 1.4 m. Total tree height was measured starting from ground level to the tip of the tree bole. For each tree, the components were separated as stem, branch, bark, foliage, and cones. Foliage as a whole was considered to be foliage along with twigs less than 1 cm in diameter, and this was separated into "new" and "old" foliage. The total fresh weight of all components including subsamples were measured immediately after felling, using a portable balance. All the cones and small branches were weighed separately. The logs were separated into small pieces and weighed in fresh in the field. A subsample of stem disks with bark (cut at the 1.4 m section and every 2 m upwards in the stem) and subsamples of all other components, were taken into the lab where fresh mass was immediately recorded. Subsamples were dried in the oven at 70 °C until constant mass was achieved recording this last value. Dry mass of each component was calculated as the fresh mass recorded in the field for that component multiplied by the ratio of subsample dry to fresh mass (Eq. **2.1**)

$$Y_i = \frac{DW_i}{FW_i} \times TFW_i \qquad \textbf{(2.1)}$$

where Y is the total dry weight (kg), DW and FW refers to the subsampled dry and fresh weight (kg) respectively, TFW is the total fresh weight (kg), and i is the tree component such as stem, bark, branch, new foliage, old foliage and cones.

Modelling procedure

Biomass data generally exhibit non-constant variance in model residuals (Parresol, 1993, 2001). When developing predictive equations, variance can be stabilized either by providing a weight function or by using transformations (Parresol, 1993, 2001). Preliminary visual inspection of the data of this study indicated heteroscedasticity in the model residuals. Scaled-

power transformations were applied, widely known as Box-Cox transformations (Box & Cox, 1964), for dependent as well as independent variables of all linear models to stabilise the variance (Eq. **2.2**). The predicted values of these models were transformed back to the original form using Eq. **2.3**. A similar variance stabilization technique was implemented by Zheng (2015) while using the additive procedure of biomass modelling for *Quercus variabilis* in North China.

$$Y^{(\lambda)} = \begin{cases} \dfrac{Y^{\lambda} - 1}{\lambda}, & \lambda \neq 0 \\ \log(Y), & \lambda = 0 \end{cases} \quad \textbf{(2.2)}$$

$$Y' = \left(\left(\lambda \times Y^{(\lambda)}\right) + 1\right)^{\frac{1}{\lambda}} \quad \textbf{(2.3)}$$

where $Y^{(\lambda)}$ is the transformed variable, and λ is a coefficient of transformed variable that varies normally between −3 and +5 (R. Cook & Weisberg, 2009), Y' is the back-transformed variable. A λ term is chosen to make the frequency distribution of each variable as close to normal as possible, thus promoting linear relationships and stabilising variance.

In this research, broadly two procedures were implemented to estimate components, subtotals and above-ground total biomass: (1) independent, and (2) additive. All models were fitted to estimate biomass in terms of kg tree^{-1}. Throughout this chapter, unless otherwise stated, the following notations and definitions apply (Table 2.1).

Table 2.1: Notations and definitions for biomass modelling of *Pinus radiata*

D	Diameter at breast height (cm)
H	Total tree height (m)
D^2H	Product of H and D^2 (cm^2.m)
WD	Wood density (kg m^{-3})
CrL	Crown length (m)
SLA	Specific leaf area (cm^2 g^{-1})
NF	New foliage
OF	Old foliage
Foliage	Sum of cone, NF and OF biomass (kg)
Crown	Sum of foliage and branch biomass (kg)

Bole	Sum of stem and bark biomass (kg)
Components	Cone, NF, OF, bark, branch, stem
Subtotal	Foliage, crown and bole
AGT	Sum of all components (above-ground total biomass) in kg
λ	Variable-specific transformation coefficient
β	Variable-specific parameter estimate
$\hat{Y}_{co}$, $\hat{Y}_{nf}$, $\hat{Y}_{of}$, $\hat{Y}_{br}$, $\hat{Y}_{ba}$, $\hat{Y}_{st}$, $\hat{Y}_{fol}$, $\hat{Y}_{cr}$, $\hat{Y}_{bol}$, $\hat{Y}_{AGT}$	Predicted biomass in kg for cone, NF, OF, branch, bark, stem, foliage, crown, bole and AGT, respectively.

Independent procedure for biomass estimation

In this procedure, biomass equations were fitted independently using traditional linear ordinary least-squares regressions with scaled power transformations and y-intercepts (denoted as, **LINOLS**; Eq. **2.4**) and nonlinear ordinary least-squares power equations that lacked y-intercepts (denoted as, **NLINOLS**; Eq. **2.5**). The mathematical specifications of these models are as follows.

$$f_l(X_l, \beta_l) = \beta_{lo} + \beta_{l1}X_1 + \beta_{l2}X_2 + \ \ldots\ldots\ldots\ldots \beta_{lp}X_p + \varepsilon_l \quad \textbf{(2.4)}$$

$$f_l(X_l, \beta_l) = \beta_{lo}X_1^{\beta_{l1}}X_2^{\beta_{l2}} + \ \ldots\ldots\ldots\ldots X_p^{\beta_{lp}} + \varepsilon_l \quad \textbf{(2.5)}$$

where X_j is tree dimension variable $j = 1, \ldots, p$ such as D, H and CrL, and $X_l = (X_1, \ldots, X_p)$, and $\beta_l = (\beta_{l0}, \ \beta_{l1,}, \ldots\ldots, \beta_{lp})$.

Each component equation contained its own independent variables. All components, subtotals and AGT biomass equations were fitted separately using the *lm* and *nls* function of R statistical software (R Core Team, 2017), for linear and nonlinear regressions, respectively.

Additive procedure of biomass estimation

The second procedure of biomass estimation is based on three additive procedures, described and compared by Parresol (1999, 2001), as the additivity requirement to estimate biomass of total tree is ensured by the following procedures: (a) adding the separately calculated best regression functions of each component, (b) using the same independent variables for each component, and (c) using joint generalized least-squares methods, also known as SUR, in which statistical dependencies among sample data are accounted for by forcing the constraints in regression coefficients (Cunia & Briggs, 1985; Parresol, 1999). The additive procedure in SUR has been extensively used in the biomass modelling for single species (Cunia & Briggs, 1984, 1985; Green & Reed, 1985; Parresol, 1999; Zheng et al., 2015). In this study, four restrictions were provided for the SUR model: (1) foliage, (2) crown, (3) bole, and (4) AGT, as illustrated in Figure 2.1. For example, foliage biomass is the sum of NF, OF and cone biomass, and so on (Figure 2.1). Mathematically, the additive system of biomass equations in additive error terms with cross-equation correlation is specified in Eq. **2.6** as,

$$
\begin{aligned}
\hat{Y}_{co} &= f_{co}(X_{co}, \beta_{co}) + \varepsilon_{co} \\
\hat{Y}_{nf} &= f_{nf}(X_{nf}, \beta_{nf}) + \varepsilon_{nf} \\
\hat{Y}_{of} &= f_{of}(X_{of}, \beta_{of}) + \varepsilon_{of} \\
\hat{Y}_{br} &= f_{br}(X_{br}, \beta_{br}) + \varepsilon_{br} \\
\hat{Y}_{ba} &= f_{ba}(X_{ba}, \beta_{ba}) + \varepsilon_{ba} \\
\hat{Y}_{st} &= f_{st}(X_{st}, \beta_{st}) + \varepsilon_{st} \\
\hat{Y}_{fol} &= f_{co}(X_{co}, \beta_{co}) + f_{nf}(X_{nf}, \beta_{nf}) + f_{of}(X_{of}, \beta_{of}) + \varepsilon_{fol} \\
\hat{Y}_{cr} &= f_{co}(X_{co}, \beta_{co}) + f_{nf}\left(X_{nf}, \beta_{nf}\right) + f_{of}\left(X_{of}, \beta_{of}\right) + f_{br}(X_{br}, \beta_{br}) + \varepsilon_{cr} \\
\hat{Y}_{bol} &= f_{ba}(X_{ba}, \beta_{ba}) + f_{st}(X_{st}, \beta_{st}) + \varepsilon_{bol} \\
\hat{Y}_{AGT} &= f_{co}(X_{co}, \beta_{co}) + f_{nf}\left(X_{nf}, \beta_{nf}\right) + f_{of}\left(X_{of}, \beta_{of}\right) + f_{br}(X_{br}, \beta_{br}) \\
&\quad + f_{ba}(X_{ba}, \beta_{ba}) + f_{st}(X_{st}, \beta_{st}) + \varepsilon_{AGT}
\end{aligned}
\qquad \textbf{(2.6)}
$$

where $\hat{Y}_i$ represents the predicted biomass of a given component and $f_i(X_i, \beta_i)$ is a regression function for the biomass component, (i = cone, new foliage, old foliage, branch, bark and stem, foliage, crown, bole and AGT biomass). The residuals is ε_j for the i^{th} equation.

All additive biomass equations were analysed in the R statistical software (R Core Team, 2017) using the *systemfit* package (Henningsen & Hamann, 2007) .

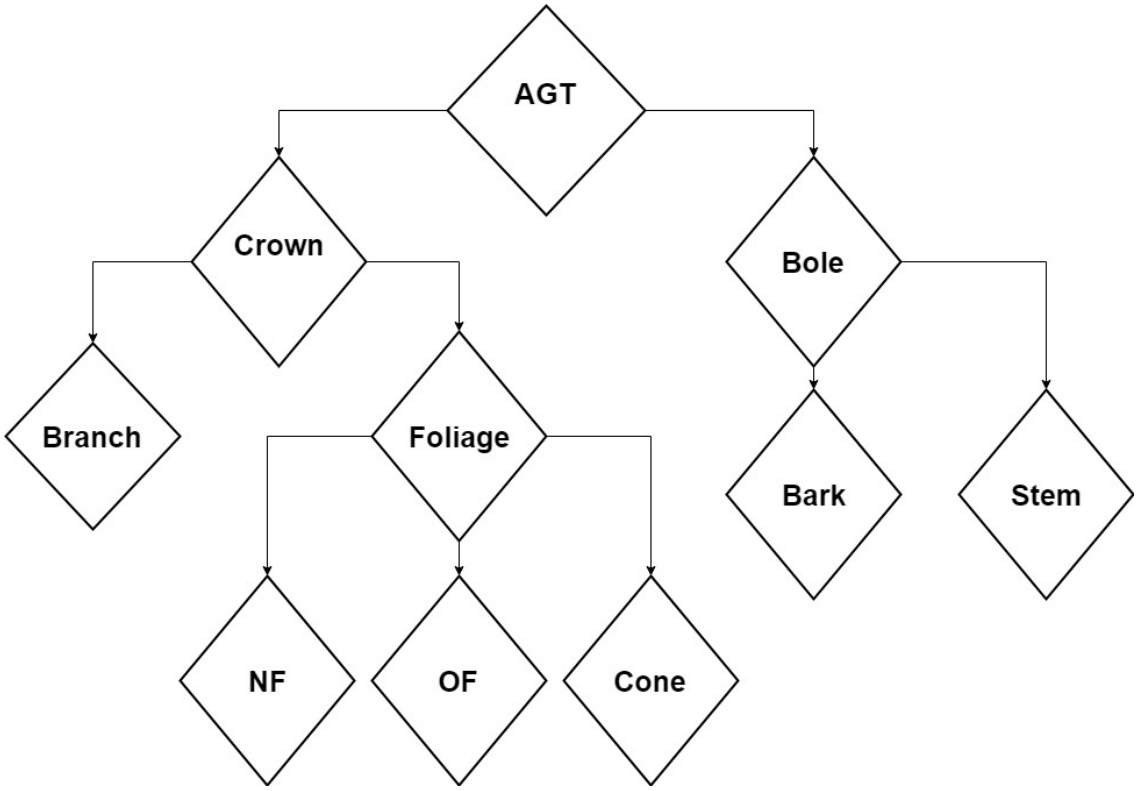

Figure 2.1: Model structure with four restrictions (foliage, crown, bole and AGT) for biomass additivity.

Model assessment and evaluation

The traditional approach of splitting the dataset into "fit data" and "validation data" is essential to examine the model accuracy (Zou, Zeng, Zhang, & Zeng, 2015). However, there was an argument and claim that splitting the data into two portions has not provided any additional evidence of reduced model precision and bias, and more valid parameter estimates (Kozak & Kozak, 2003; Zhang, Peng, Huang, & Zeng, 2016). In this study, a full dataset was used to evaluate the fitting bias, precision, and validity of models using the following goodness-of-fit statistics (Table 2.2): root mean square error (RMSE), mean absolute bias (MAB), mean prediction error (MPE), residual standard error (RSE), coefficient of variation (CV), fit index (R^2), index of agreement (IOA), and Akaike information criterion (AIC). Models were considered better with small AIC, RMSE, MAB, MPE, RSE, and CV of the residuals, and large R^2 and IOA. These fitting statistics were previously interpreted and described (Goicoa, Militino, & Ugarte, 2011; Von Gadow & Hui, 2001). Moreover, models were evaluated by plotting graphs of residual vs predicted values, histograms of residuals and Shapiro-Wilk tests for normality of residuals.

Table 2.2: Measure of goodness of fit statistics

$RMSE_i = \sqrt{\frac{1}{n}\sum_{j=1}^{n}\left(Y_{ij} - \hat{Y}_{ij}\right)^2}$	$MAB_i = \frac{1}{n}\sum_{j=1}^{n}\left\|Y_{ij} - \hat{Y}_{ij}\right\|$
$MPE_i = \frac{1}{n}\sum_{j=1}^{n}\left(Y_{ij} - \hat{Y}_{ij}\right)^2$	$RSE_i = \frac{\sum_{j=1}^{n}\left(Y_{ij} - \hat{Y}_{ij}\right)^2}{n-p}$
$CV_i = \frac{\sqrt{\frac{1}{n}\sum_{j=1}^{n}\left(Y_{ij} - \hat{Y}_{ij}\right)^2}}{\overline{Y}_i} \times 100$	$R_i^2 = 1 - \frac{\sum_{j=1}^{n}\left(Y_{ij} - \hat{Y}_{ij}\right)^2}{\sum_{j=1}^{n}\left(Y_{ij} - \overline{Y}_i\right)^2}$
$IOA = 1 - \frac{\sum_{j=1}^{n}\left(Y_{ij} - \hat{Y}_{ij}\right)^2}{\sum_{j=1}^{n}\left(\left\|\hat{Y}_{ij} - \overline{Y}_{ij}\right\| + \left\|Y_{ij} - \overline{Y}_i\right\|\right)^2}$	$AIC_i = 2p - 2\log L + \frac{2p(p+1)}{n-p-1}$

where Y_{ij} is the j^{th} observed biomass values for the i^{th} components, $\hat{Y}_{ij}$ is the j^{th} predicted biomass values for the i^{th} component, $\overline{Y}_i$ is the mean of n observed values for the components, n is the sample size, and p is the number of model parameters.

Results

Measured biomass components

In this study, the average and confidence intervals (p = 95%) values of biomass (kg tree^{-1}) for all components are as follows: stem (60.46 ± 13.62), branch (17.42 ± 8.83), bark (5.18 ± 1.35), NF (3.37±1.21), OF (13.18 ± 4.91), foliage (20.19 ± 7.37), crown (37.60 ± 15.75), bole (65.62 ±14.92) and AGT (103.24±30.17) (Figure 2.2). Among the six components, stem accounted for the highest proportion (58.56%) of AGT biomass, followed by branch (16.87%), OF (12.76%), bark (5.02%), cone (3.53%) and NF (3.26%); while at the subtotal level, bole accounted for the highest proportion (53.18%), followed by crown (30.47%) and foliage (16.36%) of AGT (Figure 2.3). Descriptive statistics of D, H, WD, and CrL are presented in Table 2.3.

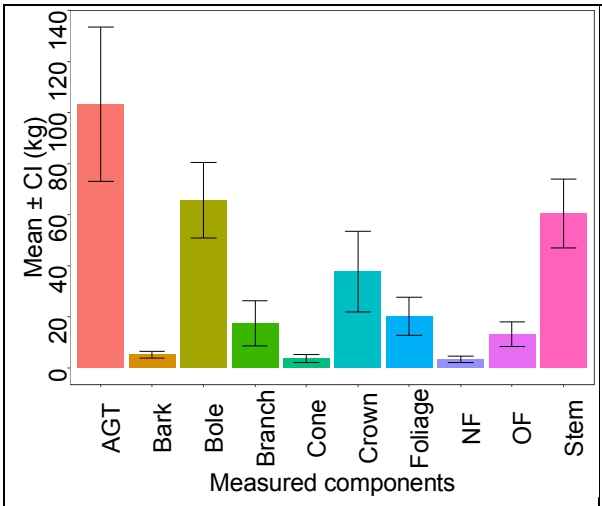

Figure 2.2: Mean and confidence interval of components, subtotals and AGT biomass

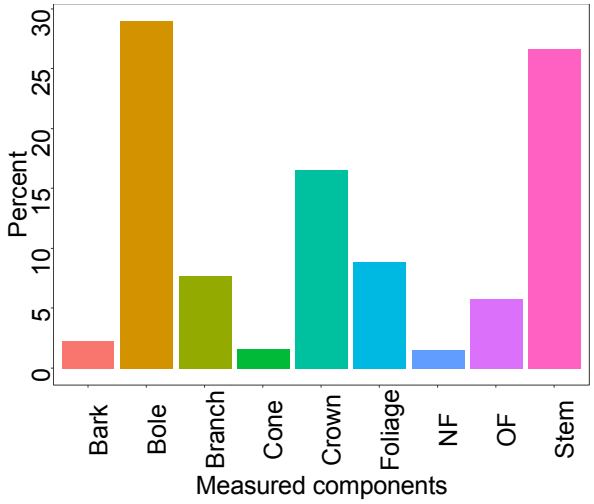

Figure 2.3: Partitioning of above-ground total biomass into tree components and subtotal

Table 2.3: Descriptive statistics of independent variables used in regression models.

Variables	n	Max (cm)	Min (cm)	Mean	SD	CI (p = 95%)
DBH (cm)	24	28	8.2	18.68	5.46	2.30
H (m)	24	13.77	8.85	11.66	1.19	0.50
WD (kg m^{-3})	24	498.67	219.94	336.35	82.89	34.99
CrL (m)	24	6	0.2	3.35	2.07	0.87

Note. n = *sample size, SD = standard deviation, CI = Confidence interval*

A visual examination showed strong relationships between tree components and D, D^2H, H and CrL. For illustrative purposes, an example of a relationship between AGT biomass with D, D^2H, H, and CrL is shown in Figure 2.4. The relationship was linear with D, D^2H, and CrL, whereas it was nonlinear with H, and the variance in AGT biomass increased with increasing values of variables (Figure 2.4). Curvilinearity and heterogeneity in variance were reduced by transforming the variables (Figure 2.5).

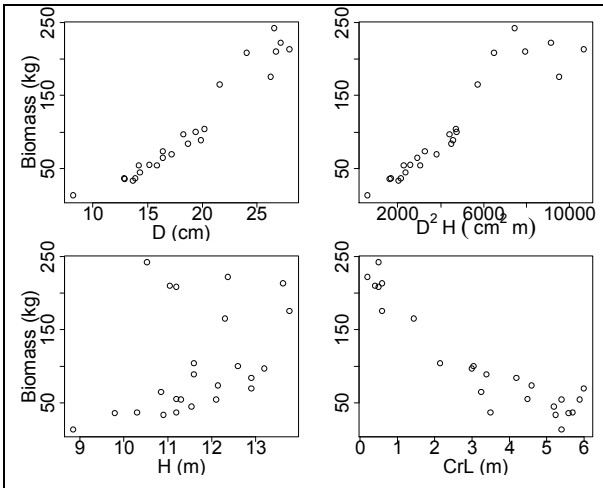

Figure 2.4: Relationship of AGT biomass with variables on original scale of measurement for x and y axes.

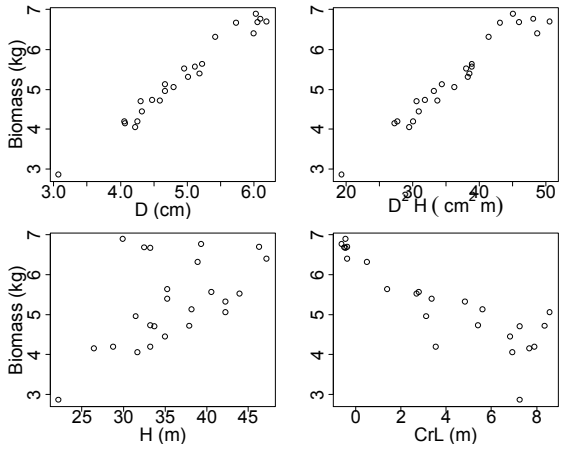

Figure 2.5: Relationship of AGT biomass with variables on scaled power transformation for x and y axes.

Independent procedure of biomass estimation

The goodness-of-fit statistics for all tested LINOLS and NLINOLS equations for components, subtotals and AGT biomass are given in Appendix 1.2. The best-fitted LINOLS and NLINOLS equations for components, subtotals and AGT biomass are given in Table 2.4, and best-fitted statistics with their regression estimates are presented in Table 2.5. The LINOLS model recorded R^2 varying from 0.48 for the cone to 0.98 for stem and bole biomass equations. The CVs of the residuals, which is a measure of precision, varied from 8.05% for stem and bole to 75.23% for the cone biomass models. The IOA varied from 0.78 for the cone to 0.99 for stem and bole biomass. In contrast, the R^2 for NLINOLS models varied from 0.51 for the cone to 0.99 for stem, OF, crown, bole and AGT biomass models, and CVs varied from 8.7% for stem and bole to 72.46% for the cone biomass models. Results demonstrated that all best-fitted LINOLS models with scaled power transformations and y-intercepts and NLINOLS power models that lacked y-intercepts provided consistent fitting statistics (Table 2.5). However, in comparison, LINOLS provided relatively higher R^2 values than NLINOLS for all, except for branch and cone biomass. In addition, compared to LINOLS, NLINOLS regression provided better goodness-of-fit statistics for the cone as well as the branch biomass models (Table 2.5). However, plotting residuals with predicted values and with other variables demonstrated that NLINOLS regression was unsuitable for these two components. Therefore, overall, the best fitted LINOLS model according to goodness-of-fit statistics and residual plots were Eq. (1) for

stem, bark, foliage, bole and AGT biomass, Eq. (2) for cone biomass, Eq. (3) for branch biomass, Eq. (8) for NF and crown biomass, and Eq. (9) for OF biomass (Table 2.4). Finally, these selected equations were further tested in the additive process of biomass estimations.

Table 2.4: Tested linear and nonlinear ordinary least-squares equations with their best fit results.

Equation	LINOLS		NLINOLS	
	Model	**Fitted best with**	**Model**	**Fitted best with**
1	$\hat{Y} = \beta_0 + \beta_1 D$	Stem, Bark, Foliage, Bole AGT	$\hat{Y} = \beta_0 D^{\beta_1}$	Stem, NF, OF, Cone, Foliage, Bole, AGT
2	$\hat{Y} = \beta_0 + \beta_1 D^2$	Cone	$\hat{Y} = \beta_0 H^{\beta_1}$	
3	$\hat{Y} = \beta_0 + \beta_1 D + \beta_2 H$	Branch	$\hat{Y} = \beta_0 (D \times H)^{\beta_1}$	
4	$\hat{Y} = \beta_0 + \beta_1 D^2 H$		$\hat{Y} = \beta_0 (D^2 H)^{\beta_1}$	Bark
5	$\hat{Y} = \beta_0 + \beta_1 D^2 H + \beta_2 H^2$		$\hat{Y} = \beta_0 D^{\beta_1} H^{\beta_2}$	Branch Crown
6	$\hat{Y} = \beta_0 + \beta_1 D^2 H + \beta_2 H^4$		$\hat{Y} = \beta_0 (D \times CrL)^{\beta_1}$	
7	$\hat{Y} = \beta_0 + \beta_1 D^2 H + \beta_2 D^2$		$\hat{Y} = \beta_0 (D \times H^2)^{\beta_1}$	
8	$\hat{Y} = \beta_0 + \beta_1 D + \beta_2 CrL$	NF Crown		
9	$\hat{Y} = \beta_0 + \beta_1 D + \beta_2 CrL^2$	OF		

Table 2.5: Goodness-of-fit statistics, regression coefficients and their standard error (±) for the best LINOLS and NLINOLS models.

		Fit statistics							Parameter estimates		
Comp-onent	**Model**	RMSE	MAB	MPE	RSE	CV%	R^2	IOA	β_0	β_1	β_2
Linear best models											
Stem	1	4.86	3.39	23.66	5.08	8.05	0.98	0.99	−6.691 (0.493) ***	3.264 (0.0986) ***	
Branch	3	8.03	4.93	64.54	8.59	46.12	0.85	0.96	−5.803 (0.666) ***	1.981 (0.149) ***	−0.049 (0.0196) *
Bark	1	0.88	0.6	0.77	0.92	16.99	0.94	0.98	−4.983 (0.373) ***	1.416 (0.074) ***	
NF	8	0.9	0.61	0.8	0.94	26.63	0.92	0.97	−3.803 (0.792) ***	0.992 (0.137) ***	−0.054 (0.033) *
OF	9	2.88	2.11	8.29	3.01	21.85	0.96	0.98	−2.87 (0.441) ***	1.064 (0.079) ***	−0.009 (0.0024) **
Cone	2	2.74	1.78	7.52	2.86	75.23	0.48	0.78	−2.301 (0.769) **	0.132 (0.029) ***	
Foliage	1	4.56	3.18	20.8	4.76	22.59	0.94	0.98	−3.259 (0.393) ***	1.213 (0.079) ***	
Crown	8	15.36	9.02	235.92	16.04	40.85	0.82	0.96	−0.731 (0.51)	0.693 (0.089) ***	−0.046 (0.021) *
Bole	1	5.29	3.77	27.95	5.52	8.05	0.98	0.99	−7.003 (0.51) ***	3.403 (0.102) ***	
AGB	1	17.13	11.42	293.5	17.89	16.59	0.96	0.98	−1.182 (0.244) ***	1.309 (0.049) ***	

Table 2.5 continued on next page

Component	Model	Fit statistics							Parameter estimates		
		RMSE	MAB	MPE	RSE	CV%	R^2	IOA	β_0	β_1	β_2
Nonlinear best models											
Stem	1	5.27	3.88	27.72	5.5	8.71	0.97	0.99	0.292 (0.069) ***	1.803 (0.075) ***	
Branch	5	6.87	4.3	47.18	7.34	39.44	0.89	0.97	0.517 (1.126)	3.791 (0.474) ***	−3.199 (0.645)***
Bark	4	0.9	0.6	0.8	0.94	17.31	0.92	0.98	0.0021 (0.001)	0.931 (0.071) ***	
NF	1	0.88	0.61	0.77	0.92	26.14	0.9	0.97	0.001 (0.0005)	2.868 (0.269) ***	
OF	1	2.42	1.79	5.86	2.53	18.37	0.95	0.99	0.001 (0.0009)	3.044 (0.195) ***	
Cone	1	2.64	1.71	6.98	2.76	72.46	0.51	0.82	0.001 (0.002)	2.861 (0.762) **	
Foliage	1	4.41	3.03	19.42	4.6	21.83	0.93	0.98	0.003 (0.002)	2.985 (0.23) ***	
Crown	5	8.56	5.73	73.19	9.15	22.75	0.95	0.99	0.156 (0.19)	3.456 (0.264) ***	−1.987 (0.379) ***
Bole	1	5.76	4.25	33.15	6.01	8.77	0.97	0.99	0.302 (0.072) ***	1.819 (0.076) ***	
AGB	1	16.34	11.24	266.87	17.06	15.82	0.95	0.99	0.095 (0.045) *	2.347 (0.149) ***	

Note: The estimated parameter values are presented in power transformed scale. Model 1, 2, 3 and so on refers to the best fitted equations given in Table 2.4

Three additive procedures of biomass estimation

In the first procedure, the additivity was ensured by adding individually calculated best regression functions of each component to give a total biomass regression function (Cunia & Briggs, 1985; Parresol, 1999). The best regression functions obtained from the independent procedure of biomass modelling that were fitted separately for each component given in Table 2.4 were used. The additive structure of this model, denoted as **LINADD1,** is specified in Eq. **2.7** as follows:

$$\hat{Y}_{co} = \beta_{10} + \beta_{11}D^2 + \varepsilon_{co}$$

$$\hat{Y}_{nf} = \beta_{20} + \beta_{21}D + \beta_{22}CrL + \varepsilon_{nf}$$

$$\hat{Y}_{of} = \beta_{30} + \beta_{31}D + \beta_{32}CrL^2 + \varepsilon_{of}$$

$$\hat{Y}_{br} = \beta_{40} + \beta_{41}D + \beta_{42}H + \varepsilon_{br}$$

$$\hat{Y}_{ba} = \beta_{50} + \beta_{51}D + \varepsilon_{ba}$$

$$\hat{Y}_{st} = \beta_{60} + \beta_{61}D + \varepsilon_{st}$$

$$\begin{aligned}\hat{Y}_{fol} &= \left(\hat{Y}_{co} + \hat{Y}_{nf} + \hat{Y}_{of}\right) \\ &= (\beta_{10} + \beta_{20} + \beta_{30}) + \beta_{11}D^2 + (\beta_{21} + \beta_{31})D + \beta_{22}CrL + \beta_{32}CrL^2 \\ &\quad + \varepsilon_{fol}\end{aligned}$$

$$\begin{aligned}\hat{Y}_{cr} &= \left(\hat{Y}_{fol} + \hat{Y}_{br}\right) \\ &= (\beta_{10} + \beta_{20} + \beta_{30} + \beta_{40}) + \beta_{11}D^2 + (\beta_{21} + \beta_{31} + \beta_{41})D + \beta_{22}CrL \\ &\quad + \beta_{32}CrL^2 + \beta_{42}H + \varepsilon_{cr}\end{aligned}$$

$$\hat{Y}_{bol} = \left(\hat{Y}_{ba} + \hat{Y}_{st}\right) = (\beta_{50} + \beta_{60}) + (\beta_{51} + \beta_{61})D + \varepsilon_{bol}$$

$$\begin{aligned}\hat{Y}_{AGT} &= \left(\hat{Y}_{cr} + \hat{Y}_{bol}\right) \\ &= (\beta_{10} + \beta_{20} + \beta_{30} + \beta_{40} + \beta_{50} + \beta_{60}) + \beta_{11}D^2 \\ &\quad + (\beta_{21} + \beta_{31} + \beta_{41} + \beta_{51} + \beta_{61})D + \beta_{22}CrL + \beta_{32}CrL^2 + \beta_{42}H \\ &\quad + \varepsilon_{AGT}\end{aligned} \qquad \textbf{(2.7)}$$

In the second procedure, additivity was implemented by using the same explanatory variables for each component. For this, the most frequent independent variable (D) was selected from the best linear regression function as it was best fitted for stem, bark, foliage, bole, and AGT (Table 2.4). Using D as an independent variable for all components, the additive structure of the model, denoted as **LINADD2**, is specified in Eq. **2.8** as follows:

$$\hat{Y}_{co} = \beta_{10} + \beta_{11}D + \varepsilon_{co}$$

$$\hat{Y}_{nf} = \beta_{20} + \beta_{21}D + \varepsilon_{nf}$$

$$\hat{Y}_{of} = \beta_{30} + \beta_{31}D + \varepsilon_{of}$$

$$\hat{Y}_{br} = \beta_{40} + \beta_{41}D + \varepsilon_{br}$$
$$\hat{Y}_{ba} = \beta_{50} + \beta_{51}D + \varepsilon_{ba}$$
$$\hat{Y}_{st} = \beta_{60} + \beta_{61}D + \varepsilon_{st}$$
$$\hat{Y}_{fol} = (\hat{Y}_{co} + \hat{Y}_{nf} + \hat{Y}_{of}) = (\beta_{10} + \beta_{20} + \beta_{30}) + (\beta_{11} + \beta_{21} + \beta_{31})D + \varepsilon_{fol}$$
$$\hat{Y}_{cr} = (\hat{Y}_{fol} + \hat{Y}_{br}) = (\beta_{10} + \beta_{20} + \beta_{30} + \beta_{40}) + (\beta_{11} + \beta_{21} + \beta_{31} + \beta_{41})D + \varepsilon_{cr}$$
$$\hat{Y}_{bol} = \left(\hat{Y}_{ba} + \hat{Y}_{st}\right) = (\beta_{50} + \beta_{60}) + (\beta_{51} + \beta_{61})D + \varepsilon_{bol}$$
$$\hat{Y}_{AGT} = \left(\hat{Y}_{cr} + \hat{Y}_{bol}\right) = (\beta_{10} + \beta_{20} + \beta_{30} + \beta_{40} + \beta_{50} + \beta_{60}) + (\beta_{11} + \beta_{21} + \beta_{31} + \beta_{41} + \beta_{51} + \beta_{61})D + \varepsilon_{AGT} \quad \textbf{(2.8)}$$

In the third procedure, we used different explanatory variables in a joint generalized linear least-squares regression, known as SUR (Cunia and Briggs, 1985; Parresol, 1999). For this, best fitted explanatory variables for each components from the independent procedure of biomass modelling were used, except for bark. We used the second-best regression D^2H as an independent variable for bark (Table 2.4). The additive structure of the model, denoted as **LINADD3,** is specified in Eq. **2.9** as follows:

$$\hat{Y}_{co} = \beta_{10} + \beta_{11}D^2 + \varepsilon_{co}$$
$$\hat{Y}_{nf} = \beta_{20} + \beta_{21}D + \beta_{22}CrL + \varepsilon_{nf}$$
$$\hat{Y}_{of} = \beta_{30} + \beta_{31}D + \beta_{32}CrL^2 + \varepsilon_{of}$$
$$\hat{Y}_{br} = \beta_{40} + \beta_{41}D + \beta_{42}H + \varepsilon_{br}$$
$$\hat{Y}_{ba} = \beta_{50} + \beta_{51}D^2H + \varepsilon_{ba}$$
$$\hat{Y}_{st} = \beta_{60} + \beta_{61}D + \varepsilon_{st}$$
$$\hat{Y}_{fol} = \left(\hat{Y}_{co} + \hat{Y}_{nf} + \hat{Y}_{of}\right) = (\beta_{10} + \beta_{20} + \beta_{30}) + \beta_{11}D^2 + (\beta_{21} + \beta_{31})D + \beta_{22}CrL + \beta_{32}CrL^2 + \varepsilon_{fol}$$
$$\hat{Y}_{cr} = \left(\hat{Y}_{fol} + \hat{Y}_{br}\right) = (\beta_{10} + \beta_{20} + \beta_{30} + \beta_{40}) + \beta_{11}D^2 + (\beta_{21} + \beta_{31} + \beta_{41})D + \beta_{22}CrL + \beta_{32}CrL^2 + \beta_{42}H + \varepsilon_{cr}$$
$$\hat{Y}_{bol} = \left(\hat{Y}_{ba} + \hat{Y}_{st}\right) = (\beta_{50} + \beta_{60}) + \beta_{51}D^2H + \beta_{61}D + \varepsilon_{bol}$$
$$\hat{Y}_{AGT} = \left(\hat{Y}_{cr} + \hat{Y}_{bol}\right) = (\beta_{10} + \beta_{20} + \beta_{30} + \beta_{40} + \beta_{50} + \beta_{60}) + \beta_{11}D^2 + (\beta_{21} + \beta_{31} + \beta_{41} + \beta_{61})D + \beta_{22}CrL + \beta_{32}CrL^2 + \beta_{42}H + \beta_{51}D^2H + \varepsilon_{AGT} \quad \textbf{(2.9)}$$

Biomass estimates for components, subtotals and AGT

The estimated coefficients and goodness of fit statistics for six components, three subtotals, and AGT using four methods (LINOLS, LINADD1, LINADD2 and LINADD3) are shown in Table 2.6 and Table 2.7, respectively.

Stem

All four equations (LINOLS, LINADD1, LINADD2 and LINADD3) showed consistent results. However, on average, LINADD3 provided a slight increase in efficiency to estimate stem biomass by 0.01% compared to the other three equations (Table 2.6). In particular, LINADD3 indicated that RMSE, RSE, and CV simultaneously decreased by 0.1%, MPE decreased by 0.2%, and R^2 increased by 0.005%, in contrast to the other three equations (Table 2.7). In addition, a marginal decrease in the parameter standard error was observed with LINADD3. The distribution of residuals of the LINADD3 model fitted for stem biomass with predicted values is given in Figure 2.6A. The residuals fitted with other variables indicated that this model under-predicted stem biomass for the two trees with the increased values of WD; however, there was no clear evidence of a systematic pattern with D, H and CrL (Appendix 1.1A). A model to predict stem biomass using SUR (Eq. **2.10**) produced lowest values of RMSE, RSE, and CV as compared to an ordinary least-squares method.

$$\hat{Y}_{st} = \left(\lambda_{st} \times \left(\beta_{0_{st}} + \beta_{1_{st}} \left(\frac{D^{\lambda_d} - 1}{\lambda_d} \right) \right) + 1 \right)^{\frac{1}{\lambda_{st}}} \quad \textbf{(2.10)}$$

Branches

LINADD3 increased average efficiency by 9.7% in contrast to the other three equations (Table 2.6). In contrast with the first three equations (LINOLS, LINADD1, and LINADD2), the LINADD3 provided higher efficiencies as the average statistics decreased by RMSE (10.3%), MAB (10.5%), MPE (17.8), RSE (9.7%) and CV (10.3%); and increased by R^2 (7.2%) and IOA (2%) (Table 2.7). In particular, LINADD3 indicated there was a marginal decrease in the goodness-of-fit statistics (e.g. RMSE, RSE, and CV by 1%) in contrast to LINOLS and LINADD1. In contrast to LINADD2, the LINADD3 provided a greater decrease in fit statistics

(e.g. RMSE by 28.74%, RSE by 27.07% and CV by 28.74%) (Table 2.7). The distribution of residuals of the LINADD3 model fitted for branch biomass with predicted values is given in Figure 2.6B. There was some evidence that LINADD3 over-predicted branch biomass for five trees, with the largest values of D and two trees with the largest values of H (Appendix 1.1B), and that it under-predicted with the CrL less than 2 m. However, these trends were found only for a few observations that had the largest values of D and H, and the smallest values of CrL. In addition, the residual plot with WD showed no clear evidence of a trend. A model to predict branch biomass using SUR (Eq. **2.11**) produced lowest values of RMSE, RSE, and CV compared to the ordinary least-squares method.

$$\hat{Y}_{br} = \left(\lambda_{br} \times \left(\beta_{0_{br}} + \beta_{1_{br}}\left(\frac{D^{\lambda_d}-1}{\lambda_d}\right) + \beta_{2_{br}}\left(\frac{H^{\lambda_h}-1}{\lambda_h}\right)\right) + 1\right)^{\frac{1}{\lambda_{br}}} \quad \textbf{(2.11)}$$

Bark

On average, LINOLS provided slightly better efficiency in bark biomass estimates by 0.6%, in contrast to the other three additive equations (Table 2.6). LINOLS simultaneously decreased RMSE, MAB, MPE, RSE and CV by 0.7%, 0.5%, 1.5%, 0.7%, and 0.7%, respectively, and it increased R^2 by 0.1% in contrast to other three equations (Table 2.7). In particular, LINOLS has a marginal decrease in RMSE (2.22%), MAB (1.44%), MPE (4.4%), RSE (2.23%) and CV (2.23%), and an increase in R^2 (0.4%) and IOA (0.07%) in contrast to LINADD1 (Table 2.7). In addition, LINOLS indicated a marginal decrease in the parameter standard error. The distribution of residuals of the LINOLS model fitted for bark biomass with predicted values is given in Figure 2.6C. The residual plot with other variables indicated that LINOLS under-predicted bark biomass for two trees with WD > 450 kg m^{-3}, as well as some trends with H (Appendix 1.1C). However, few observations caused this fluctuation and there was no systematic trend in the residuals with CrL and SLA. Therefore, a LINOLS model (Eq. **2.12**) was considered the best to predict bark biomass.

$$\hat{Y}_{ba} = \left(\lambda_{ba} \times \left(\beta_{0_{ba}} + \beta_{1_{ba}}\left(\frac{D^{\lambda_d}-1}{\lambda_d}\right)\right) + 1\right)^{\frac{1}{\lambda_{ba}}} \quad \textbf{(2.12)}$$

New foliage

On average, the LINADD3 model improved efficiency in NF biomass estimates by 2.7%, and recorded a decrease in fit statistics (e.g., RMSE by 3.7%, RSE by 1.43%), in contrast to LINOLS, LINADD1 and LINADD2 (Table 2.7). The distribution of residuals of the LINADD3 model fitted for NF biomass with predicted values is given in Figure 2.6D. The residual plots indicated that the LINADD3 model over-predicts new foliage biomass for the two trees with H > 13.5 m, two trees with WD < 250 kg m^{-3} and two trees with SLA < 80 cm^2 g^{-1}; and under-predicted trees with WD > 450 kg m^{-3} and SLA > 145 cm^2 g^{-1} (Appendix 1.1D). These terms were included in the model, but results were insignificant ($p > 0.05$) and therefore excluded from the model. Therefore, a model that was fitted in SUR (Eq. **2.13**) was considered best to predict new foliage biomass.

$$\hat{Y}_{nf} = \left(\lambda_{nf} \times \left(\beta_{0_{nf}} + \beta_{1_{nf}} \left(\frac{D^{\lambda_d} - 1}{\lambda_d} \right) + \beta_{2nf} \left(\frac{CrL^{\lambda_{crl}} - 1}{\lambda_{crl}} \right) \right) + 1 \right)^{\frac{1}{\lambda_{nf}}} \quad \textbf{(2.13)}$$

Old foliage

LINADD3 provided a significant increase in efficiency by 9.4% when used to predict OF biomass, in contrast to the other three equations (Table 2.6). In addition, LINADD3 provided a decrease in RMSE (by 10.9%), MAB (by 12.7%), MPE (by 20.3%), RSE (by 9.6%) and CV (by 10.9%), and an increase in R^2 (1.2%) and IOA (0.3%), in contrast to the other three equations (Table 2.7). The distribution of residuals of the LINADD3 model fitted for OF biomass with predicted values is given in Figure 2.6E. The residual plot of the LINADD3 model showed no obvious trend with tree height, but the model under-predicted and over-predicted for trees with WD > 400 kg m^{-3} and WD < 300 kg m^{-3}, respectively (Appendix 1.1E). It means that this model predicted OF biomass better for the trees with a wood density between 300 to 400 kg m^{-3}. In addition, this model over-predicted OF biomass for the trees with SLA < 80 cm^2 g^{-1}. These terms were excluded from the models because they were insignificant ($p > 0.05$). Therefore, a model fitted in SUR (Eq. **2.14**) was considered the best to predict OF biomass.

$$\hat{Y}_{of} = \left(\lambda_{of} \times \left(\beta_{0_{of}} + \beta_{1_{of}} \left(\frac{D^{\lambda_d} - 1}{\lambda_d} \right) + \beta_{2_{of}} \left(\frac{CrL^{\lambda_{crl}} - 1}{\lambda_{crl}} \right)^2 \right) + 1 \right)^{\frac{1}{\lambda_{of}}} \quad \textbf{(2.14)}$$

Cone

On average, LINOLS recorded a slight improvement in cone biomass estimates by 1.6% in contrast to other three additive equations (Table 2.6). The LINOLS equation provided a compatible decrease in RMSE, RSE, and CV by 1.2%; MAB decreased by 0.4%, MPE decreased by 2.4%, R^2 increased by 3% and IOA increased by 1.9%, in contrast to the other three additive equations tested (Table 2.7). The distribution of residuals of the LINOLS model fitted for cone biomass with predicted values is given in Figure 2.6F. The residual plot of the LINOLS model showed that it under-predicts the cone biomass for the trees with H > 12 m, H < 9 m, WD > 450 kg m^{-3} and CrL > 5.5 m, and over-predicts for trees with WD < 250 kg m^{-3} (Appendix 1.1F). These terms were also included in the model but were insignificant ($p > 0.05$) and excluded from the model. In addition, there was no systematic trend of residuals with SLA. Therefore, a model fitted in LINOLS (Eq. **2.15**) was considered the best to predict cone biomass.

$$\hat{Y}_{co} = \left(\lambda_{co} \times \left(\beta_{0_{co}} + \beta_{1_{co}} \left(\frac{D^{\lambda_d} - 1}{\lambda_d}\right)^2\right) + 1\right)^{\frac{1}{\lambda_{co}}} \quad \textbf{(2.15)}$$

Foliage

On average, LINADD3 recorded slightly higher efficiency in foliage biomass estimates by 1.3%. It consistently increased efficiency by 0.7%, 2.6% and 0.6% in contrast to the LINOLS, LINADD1 and LINADD2, respectively (Table 2.6). Using LINADD3, the RMSE, MAB, MPE and CV decreased by 2.1%, 1.6%, 4.1% and 2.1%, respectively, and R^2 by 0.3% and IOA by 0.1% compared with the other three equations (Table 2.7). The distribution of residuals of the LINADD3 model fitted for foliage biomass with predicted values is given in Figure 2.6G. There was some evidence that the LINADD3 model over-predicted the foliage biomass for the trees with H > 13 m, and under-predicted for trees with WD > 425 kg m^{-3}; and there was little evidence of a systematic pattern in residuals with CrL and SLA (Appendix 1.1G). Therefore, the LINADD3 model in SUR (Eq. **2.16**) was considered the best to predict foliage biomass.

$$\hat{Y}_{fol} = \left(\hat{Y}_{co} + \hat{Y}_{nf} + \hat{Y}_{of}\right)$$

$$\hat{Y}_{fol} = \left(\lambda_{\text{co}} \times \left(\beta_{0_{co}} + \beta_{1_{co}}\left(\frac{D^{\lambda_{\text{d}}}-1}{\lambda_{\text{d}}}\right)^2\right)+1\right)^{\frac{1}{\lambda_{\text{co}}}} + \left(\lambda_{nf} \times \left(\beta_{0_{nf}} + \beta_{1_{nf}}\left(\frac{D^{\lambda_d}-1}{\lambda_d}\right) + \beta_{2nf}\left(\frac{CrL^{\lambda_{crl}}-1}{\lambda_{crl}}\right)\right)+1\right)^{\frac{1}{\lambda_{nf}}} + \left(\lambda_{of} \times \left(\beta_{0_{of}} + \beta_{1_{of}}\left(\frac{D^{\lambda_{\text{d}}}-1}{\lambda_{\text{d}}}\right) + \beta_{2_{of}}\left(\frac{CrL^{\lambda_{crl}}-1}{\lambda_{crl}}\right)^2\right)+1\right)^{\frac{1}{\lambda_{of}}} \quad \textbf{(2.16)}$$

Crown

Using LINADD3, average efficiency increased by 17.5% in contrast to the other three equations (Table 2.6). In particular, LINADD3 provided higher efficiencies, as the average fit statistics decreased by 21.5% for RMSE, 16.7% for MAB, 36.3% for MPE, 18.1% for RSE, and 21.5% for CV; and increased R^2 by 7% and IOA by 1.7%, in contrast to other three equations (Table 2.7). The distribution of the residuals of the LINADD3 model fitted for crown biomass with predicted values is given in Figure 2.6H. Plotting residuals with other variables indicated that the model over-predicted for the two trees with H > 13 m and five trees with CrL < 1 m, and under-predicted for the three trees with WD > 425 kg m^{-3}; and there was slight evidence of a trend in residuals with SLA (Appendix 1.1H). Therefore, the additive equation fitted in SUR (Eq. **2.17**) was considered the best to predict crown biomass.

$$\hat{Y}_{cr} = \left(\hat{Y}_{fol} + \hat{Y}_{br}\right)$$

$$\hat{Y}_{cr} = \left(\lambda_{\text{co}} \times \left(\beta_{0_{co}} + \beta_{1_{co}}\left(\frac{D^{\lambda_{\text{d}}}-1}{\lambda_{\text{d}}}\right)^2\right)+1\right)^{\frac{1}{\lambda_{\text{co}}}} + \left(\lambda_{nf} \times \left(\beta_{0_{nf}} + \beta_{1_{nf}}\left(\frac{D^{\lambda_d}-1}{\lambda_d}\right) + \beta_{2nf}\left(\frac{CrL^{\lambda_{crl}}-1}{\lambda_{crl}}\right)\right)+1\right)^{\frac{1}{\lambda_{nf}}} + \left(\lambda_{of} \times \left(\beta_{0_{of}} + \beta_{1_{of}}\left(\frac{D^{\lambda_{\text{d}}}-1}{\lambda_{\text{d}}}\right) + \beta_{2_{of}}\left(\frac{CrL^{\lambda_{crl}}-1}{\lambda_{crl}}\right)^2\right)+1\right)^{\frac{1}{\lambda_{of}}} + \left(\lambda_{br} \times \left(\beta_{0_{br}} + \beta_{1_{br}}\left(\frac{D^{\lambda_{\text{d}}}-1}{\lambda_{\text{d}}}\right) + \beta_{2_{br}}\left(\frac{H^{\lambda_h}-1}{\lambda_h}\right)\right)+1\right)^{\frac{1}{\lambda_{br}}} \quad \textbf{(2.17)}$$

Bole

All four equations (LINOLS, LINADD1, LINADD2 and LINADD3) for bole biomass provided consistent results. However, on average, the LINOLS provided a slight improvement in efficiency to estimate bole biomass by 0.1%, in contrast to other three (Table 2.6). The LINOLS indicated there was a marginal decrease in RMSE (0.1%), MPE (0.2%), RSE (0.1%) and CV (0.1%), compared to the three additive equations (Table 2.7). The distribution of residuals of the LINOLS model fitted for bole biomass with predicted values is given in Figure 2.6I. The residual plots indicated that the LINOLS model over-predicted for the two trees with H > 13 m, four trees with CrL > 5.5 m, three trees with SLA < 80 $cm^2\ g^{-1}$; and under-predicted for the two trees with WD > 450 kg m^{-3} (Appendix 1.1I). Therefore, a LINOLS model (Eq. **2.18**) was considered the best to predict bole biomass.

$$\hat{Y}_{bol} = \left(\lambda_{bol} \times \left(\beta_{0_{bol}} + \beta_{1_{bol}}\left(\frac{D^{\lambda_{\mathrm{d}}} - 1}{\lambda_{\mathrm{d}}}\right)\right) + 1\right)^{\frac{1}{\lambda_{\mathrm{bol}}}} \qquad \textbf{(2.18)}$$

Above-ground total

On average, the LINADD3 provided greater efficiency in AGT biomass estimates by 8% in contrast to the other three equations. LINADD3 increased efficiency by 11.5%, 12.2% and 0.2% compared with the LINOLS, LINADD1, and LINADD2, respectively (Table 2.6). On average, there was a decrease in RMSE by 10.1%, MAB by 9.3%, MPE by 18.7, RSE by 5.8% and CV by 10.1%; and an increase in R^2 by 1.2% and IOA by 0.3% (Table 2.7). The distribution of residuals of the LINADD3 model fitted for AGT biomass with predicted values is given in Figure 2.6J. The residual plots indicated that the LINADD3 model over-predicted the AGT for two trees with the tree H > 13 m, three trees with CrL < 1 m and three trees with SLA < 80 $cm^2\ g^{-1}$; and under-predicted for the two trees with WD > 450 kg m^{-3} (Appendix 1.1J). Although, there were fewer observations that showed these pattern, the resulting model exhibited more satisfactory behaviour to predict the AGT biomass for trees with a H between 10 and 12 m, WD 250 to 425 kg m^{-3}, CrL > 3 m and SLA 100 to 160 $cm^2\ g^{-1}$. Therefore, a LINADD3 model fitted in SUR (Eq. **2.19**) was considered the best to predict AGT biomass.

$$\hat{Y}_{AGT} = \left(\hat{Y}_{cr} + \hat{Y}_{bol}\right)$$

$$\hat{Y}_{AGT} = \left(\lambda_{\mathrm{co}} \times \left(\beta_{0_{co}} + \beta_{1_{co}}\left(\frac{D^{\lambda_{\mathrm{d}}} - 1}{\lambda_{\mathrm{d}}}\right)^2\right) + 1\right)^{\frac{1}{\lambda_{\mathrm{co}}}} + \left(\lambda_{nf} \times \left(\beta_{0_{nf}} + \beta_{1_{nf}}\left(\frac{D^{\lambda_d} - 1}{\lambda_d}\right) + \beta_{2nf}\left(\frac{CrL^{\lambda_{crl}} - 1}{\lambda_{crl}}\right)\right) + 1\right)^{\frac{1}{\lambda_{nf}}} + \left(\lambda_{of} \times \left(\beta_{0_{of}} + \beta_{1_{of}}\left(\frac{D^{\lambda_{\mathrm{d}}} - 1}{\lambda_{\mathrm{d}}}\right) + \beta_{2_{of}}\left(\frac{CrL^{\lambda_{crl}} - 1}{\lambda_{crl}}\right)^2\right) + 1\right)^{\frac{1}{\lambda_{of}}} + \left(\lambda_{br} \times \left(\beta_{0_{br}} + \beta_{1_{br}}\left(\frac{D^{\lambda_{\mathrm{d}}} - 1}{\lambda_{\mathrm{d}}}\right) + \beta_{2_{br}}\left(\frac{H^{\lambda_h} - 1}{\lambda_h}\right)\right) + 1\right)^{\frac{1}{\lambda_{br}}} + \left(\lambda_{\mathrm{ba}} \times \left(\beta_{0_{ba}} + \beta_{1_{ba}}\left(\frac{(D^2H)^{\lambda_{\mathrm{d^2h}}} - 1}{\lambda_{\mathrm{d^2h}}}\right)\right) + 1\right)^{\frac{1}{\lambda_{\mathrm{ba}}}} + \left(\lambda_{st} \times \left(\beta_{0_{st}} + \beta_{1_{st}}\left(\frac{D^{\lambda_{\mathrm{d}}} - 1}{\lambda_{\mathrm{d}}}\right)\right) + 1\right)^{\frac{1}{\lambda_{\mathrm{st}}}} \quad \textbf{(2.19)}$$

Table 2.6: Regression model with given components as the dependent variable, modelling technique, parameter estimates, their standard error and statistically significant values.

Comp-onent	Parameter estimates	Methods				λ value
		LINOLS	LINADD1	LINADD2	LINADD3	
Cone	β_{10}	−2.30074 ** (0.76925)	−2.2253078 ** (0.7674214)	−5.240071 ** (1.483333)	−2.2296709 ** (0.7674720)	$\lambda_d = 0.34$ $\lambda_{co} = 0.27$
	β_{11}	0.13189 *** (0.02936)	0.1288778 *** (0.0292863)	1.262998 *** (0.296479)	0.1290521 *** (0.0292884)	
NF	β_{20}	−4.9588 *** (0.37493)	−4.9589297 *** (0.3747799)	−4.9587980 *** (0.3749312)	−4.2126833 *** (0.6629234)	$\lambda_d = 0.34$ $\lambda_{crl} = 1.45$ $\lambda_{nf} = 0.07$
	β_{21}	1.18411 *** (0.07494)	1.1841332 *** (0.0749077)	1.1841066 (0.0749387)	1.0598911 *** (0.1171656)	
	β_{22}				−0.0347372 (0.0262139)	
OF	β_{30}	−4.08961 *** (0.33052)	−3.20881997 *** (0.33589135)	−4.0896076 *** (0.3305249)	−3.10482979 *** (0.35020813)	$\lambda_d = 0.34$ $\lambda_{crl} = 1.45$ $\lambda_{of} = 0.01$
	β_{31}	1.26626 *** (0.06606)	1.11932096 *** (0.06341561)	1.2662617 *** (0.0660631)	1.10140583 *** (0.06551600)	
	β_{32}		−0.00616425 *** (0.00140122)		−0.00678049 *** (0.00156658)	
Branch	β_{40}	−5.80328 *** (0.66633)	−5.78612845 *** (0.61992780)	−6.485501 *** (0.681185)	−5.75758602 *** (0.61935019)	$\lambda_d = 0.34$ $\lambda_{crl} = 1.67$ $\lambda_{br} = 0.04$
	β_{41}	1.98128 *** (0.14979)	1.98671103 *** (0.12801151)	(1.760100) *** (0.136151)	1.97269196 *** (0.12772204)	
	β_{42}	−0.04958 * (0.01952)	−0.05080977 *** (0.00860345)		−0.04967216 *** (0.00866634)	
Bark	β_{50}	−4.98314 *** (0.37258)	−4.983225 *** (0.372523)	−4.9831405 *** (0.3725848)	−3.34035259 *** (0.27952157)	$\lambda_d{}^2{}_h = 0.3$ $\lambda_{ba} = 0.36$

	β_{51}	1.41585 *** (0.07447)	1.415870 *** (0.074457)	0.3725848 *** (0.0744697)	0.14595384 *** (0.00746132)	
Stem	β_{60}	−6.69072 *** (0.49320)	−6.6907718 *** (0.4931813)	−6.6907242 *** (0.4931963)	−6.6549090 *** (0.4921774)	$\lambda_d = 0.34$ $\lambda_{st} = 0.38$
	β_{61}	3.26444 *** (0.09858)	3.2644484 *** (0.0985736)	3.2644388 *** (0.0985767)	3.2571906 *** (0.0983679)	
Foliage	β_{70}	−3.25917 *** (0.39291)				$\lambda_d = 0.34$ $\lambda_{fol} = 0.03$
	β_{71}	1.21316 *** (0.07853)				
Crown	β_{80}	−0.73115 (0.51011)				$\lambda_d = 0.34$ $\lambda_{crl} = 1.45$ $\lambda_{cr} = -0.13$
	β_{81}	0.69335 *** (0.08859)				
	β_{82}	−0.0461 * (0.02137)				
Bole	β_{90}	−7.00260 *** (0.5102)				$\lambda_d = 0.34$ $\lambda_{bol} = 0.38$
	β_{91}	3.40320 *** (0.1020)				
AGT	β_{100}	−1.18208 *** (0.24429)				$\lambda_d = 0.34$ $\lambda_{AGT} = 0.08$
	β_{101}	1.30925 *** (0.04883)				

Note: The λ value shown in the table indicates that the variables were subjected to a scaled power transformation. The estimated parameter values for each technique are presented in power transformed scale.

Table 2.7: Goodness-of-fit statistics for given biomass components using four methods of modelling.

Biomass	Model	RMSE	MAB	MPE	RSE	CV	R2	IOA	RANK
Stem	LINOLS	4.86415	3.39094	23.66000	5.08044	8.04584	0.976250	0.994010	3
	LINADD1	4.86416	3.39092	23.66003	5.08045	8.04585	0.976253	0.994010	4
	LINADD2	4.86415	3.39094	23.65996	5.08044	8.04584	0.976253	0.994010	2
	LINADD3	4.85914	3.40560	23.61124	5.07521	8.03755	0.976302	0.994008	1
Branch	LINOLS	8.03400	4.93485	64.53760	8.58800	46.12426	0.846160	0.962100	2
	LINADD1	8.04569	4.97038	64.73304	8.60120	46.19406	0.845694	0.962246	3
	LINADD2	11.16751	6.65836	124.71320	11.66408	64.11792	0.702718	0.909118	4
	LINADD3	7.95752	4.84802	63.32210	8.50695	45.68786	0.849057	0.962486	1
Bark	LINOLS	0.88000	0.60400	0.77426	0.91900	16.98693	0.920520	0.979190	1
	LINADD1	0.87992	0.60444	0.77426	0.91905	16.98699	0.920520	0.979191	3
	LINADD2	0.87992	0.60444	0.77426	0.91904	16.98693	0.920520	0.979191	1
	LINADD3	0.89996	0.61281	0.80993	0.93998	17.37388	0.916858	0.978505	4
NF	LINOLS	0.89618	0.60978	0.80315	0.93603	26.62710	0.897760	0.972570	2
	LINADD1	0.89619	0.60979	0.80315	0.93604	26.62714	0.897756	0.972569	4
	LINADD2	0.89618	0.60978	0.80315	0.93603	26.62710	0.897756	0.972568	3
	LINADD3	0.86303	0.59973	0.74482	0.92262	25.64201	0.905182	0.974950	1
OF	LINOLS	2.87917	2.10895	8.28962	3.00720	21.85229	0.936070	0.984630	3
	LINADD1	2.48611	1.75794	6.18075	2.65777	18.86906	0.952332	0.988477	2
	LINADD2	2.87917	2.10895	8.28962	3.00720	21.85229	0.936068	0.984634	3
	LINADD3	2.43621	1.72696	5.93510	2.60441	18.49028	0.954227	0.988881	1
Cone	LINOLS	2.74267	1.77719	7.52225	2.86463	75.22916	0.475160	0.781340	1
	LINADD1	2.76021	1.78295	7.61873	2.88294	75.71009	0.468427	0.774147	3
	LINADD2	2.81134	1.78543	7.90362	2.93635	77.11261	0.448550	0.752992	4

Biomass	Model	RMSE	MAB	MPE	RSE	CV	R2	IOA	RANK
	LINADD3	2.75915	1.78262	7.61292	2.88184	75.68121	0.468832	0.774575	2
Foliage	LINOLS	4.56071	3.17947	20.80010	4.76351	22.59229	0.928750	0.981000	2
	LINADD1	4.50850	3.19432	20.32655	4.93881	22.33363	0.930371	0.982017	2
	LINADD2	4.64822	3.30702	21.60595	4.85491	23.02577	0.925988	0.980798	4
	LINADD3	4.47755	3.17321	20.04843	4.90491	22.18031	0.931324	0.982249	1
Crown	LINOLS	15.35950	9.01933	235.91500	16.04250	40.84526	0.822950	0.955000	4
	LINADD1	10.14552	6.63341	102.93150	11.40258	26.97976	0.922751	0.981048	2
	LINADD2	14.04350	8.40827	197.21980	14.66796	37.34558	0.851989	0.959756	3
	LINADD3	10.02329	6.57037	100.46640	11.2652	26.65473	0.924601	0.981345	1
Bole	LINOLS	5.28687	3.76539	27.95100	5.52195	8.05489	0.976640	0.994110	1
	LINADD1	5.29480	3.76223	28.03491	5.53024	8.06698	0.986765	0.994093	4
	LINADD2	5.29479	3.76221	28.03479	5.53023	8.06696	0.986765	0.994093	2
	LINADD3	5.29279	3.79959	28.01360	5.65823	8.06392	0.986775	0.994085	3
AGT	LINOLS	17.13180	11.41980	293.49700	17.89350	16.59420	0.940010	0.984900	3
	LINADD1	14.70376	9.70185	216.20060	16.52560	14.24236	0.955810	0.989078	2
	LINADD2	17.40499	11.17107	302.93370	18.17892	16.85883	0.938082	0.984020	4
	LINADD3	14.66738	9.70795	215.13220	16.4847	14.20713	0.956028	0.989066	1

Note: RANK indicates the model's performance in comparison. For example, a model in RANK 1 is a best and RANK 4 is a worst in terms of goodness-of-fit statistics, and residual plots.

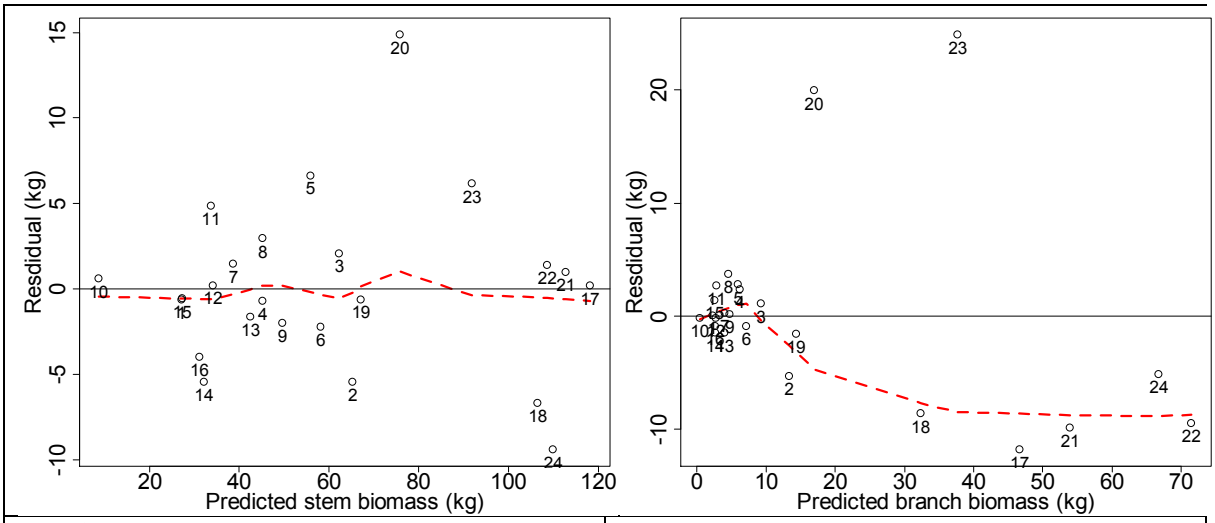

(A) Stem (Eq. **2.10**) | **(B)**) Branch (Eq. **2.11**)

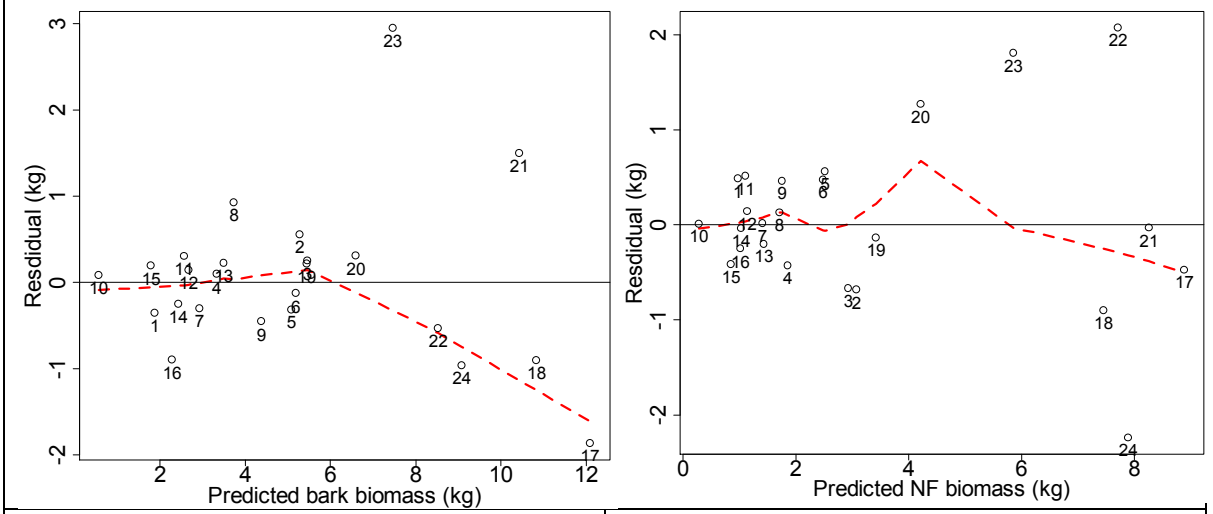

(C) Bark (Eq. **2.12**) | **(D)** NF (Eq. **2.13**)

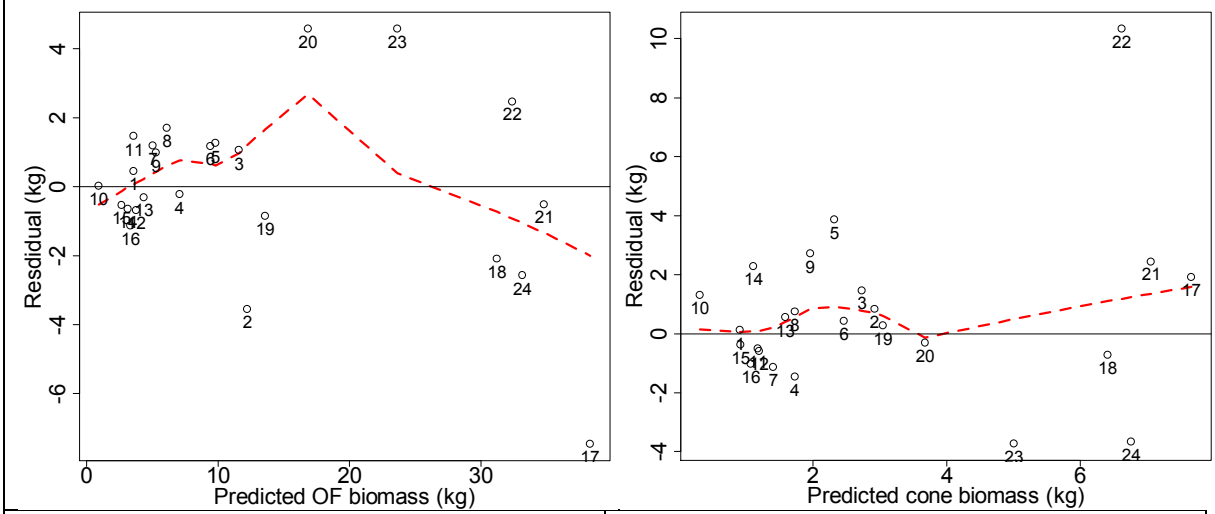

(E) OF (Eq. **2.14**) | **(F)** Cone (Eq. **2.15**)

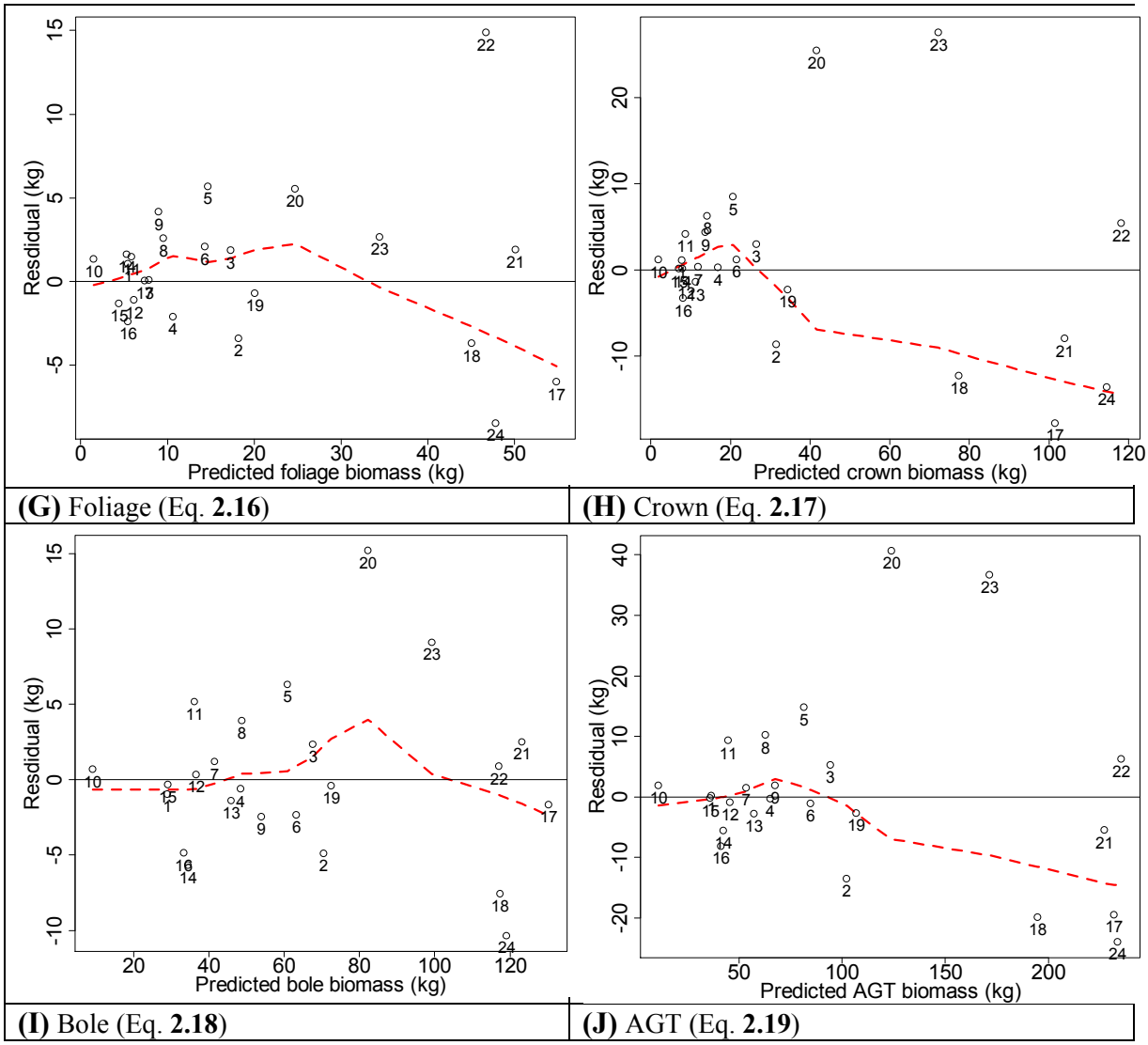

(G) Foliage (Eq. **2.16**) | **(H)** Crown (Eq. **2.17**)

(I) Bole (Eq. **2.18**) | **(J)** AGT (Eq. **2.19**)

Figure 2.6: Residuals vs predicted biomass for the selected best models. The solid black horizontal line across zero represent baseline and the dotted red line is LOESS curve.

Discussion

Measured biomass components

A tree accumulates different amount of biomass into the different components such as stem, branches, and foliage (Beets, Roberston, Ford-Robertson, Gordon, & Maclaren, 1999; Dong, Zhang, & Li, 2015). *P. radiata* in this study accumulated most biomass in the stem (59%), followed by branches (17%), foliage (16%) and cones (3.53%). Our result is similar to Beets et al. (1999), as they developed a function for partitioning tree growth into different components, and reported that partitioning of above-ground production of *P. radiata* in New Zealand varied from 30 to 72% for the stem, 20% for branches and 12 to 40% for the foliage,

with varied across the stand age. In addition, results from this study are comparable to some hard wood species in Northeast China, as the greatest proportion of total above-ground biomass was partitioned to stems (62%), followed by branches (11.1%) (Dong et al., 2015). The highest proportion of biomass in the stem may be attributed to stem diameter, as it showed the highest positive correlation (r = 0.99) between stem biomass and tree diameter (Figure 2.7). Another study also indicated that trees with highest diameters accumulated most biomass compared to tress with smallest diameters (Dong et al., 2015).

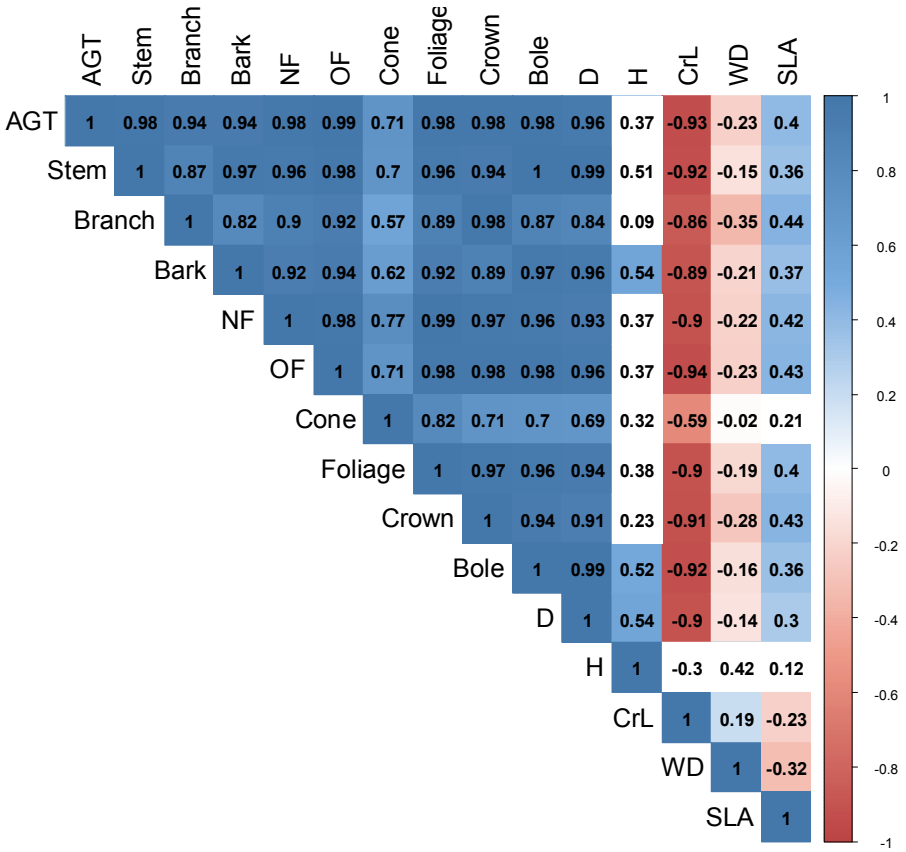

Figure 2.7: Correlation among the components, subtotals and AGT biomass. The colour indicates the strength of relationship. Darker to lighter indicates high to low correlation, and no colour indicates the relationship is insignificant (p > 0.05).

Independent procedure for biomass modelling

We found that the LINOLS model with scaled power transformations and y-intercepts to estimate biomass of components, subtotals and AGT performed better than its NLINOLS counterpart. Moore (2010) also found a better model to predict AGT biomass for *P. radiata* in New Zealand, which was also a linear. In particular, stem, bark, foliage, bole and AGT biomass were better explained by a linear function of D providing unbiased estimates when compared

with other equation forms, while branch biomass was better fitted with D and H as the explanatory variables. NF and OF biomass were better predicted with D and CrL, and D and CrL^2 as explanatory variables, respectively. These explanatory variables are most widely used and commonly fitted functions, which are synthesised and cited by Návar (2010), and consistent with other studies (Bi, Turner, & Lambert, 2004; X. Wang, Fang, Tang, & Zhu, 2006; Zhou, Brandle, Schoeneberger, & Awada, 2007).

The cone biomass model with D^2 as an explanatory variable in this study exhibited poor performance in the goodness-of-fit statistics (e.g., $R^2 = 0.48$). Several attempts were made to improve the cone biomass model by fitting it directly with different variables, including D, H, WD, SLA and CrL in various forms; and indirectly with the best predicted biomass components, such as stem, branch, bark, foliage, bole, and AGT, as explanatory variables. It was observed that cone biomass as a function of predicted foliage biomass exhibited a slightly better fit ($R^2 = 0.60$) than the best model with D^2 as an independent variable. However, unless foliage biomass is predicted, it cannot be used as the independent variable for cone biomass, and it is rarely available from forest inventory data. Therefore, cone biomass prediction from this indirect approach is not recommended. At the subtotal level, the crown biomass as a function of D and CrL as explanatory variables also exhibited a less precise fit ($R^2 = 0.82$). This variability may be associated to differences in crown structure, number and size of the branches, and wood density (Carvalho & Parresol, 2003), as crown biomass in this study was composed of NF, OF, cone, and branches. The best model of each component selected from independent procedures provided the logical base equations for further tests in the additivity of biomass equations. The same approach was used by other researchers (Magalhães & Seifert, 2015; Návar, Méndez, & Dale, 2002) to utilize additive properties in biomass modelling.

Additive procedure of biomass modelling

Biomass additivity reduces the discrepancy between the sum of predicted values for components and those for a total tree (Kozak, 1970), and it has long been documented as a desirable property of systems of equations to predict total tree biomass (Bi et al., 2004; Parresol, 2001). Three procedures were implemented for the additivity in the biomass model (Parresol, 1999, 2001): (1) using a separately calculated best linear function of the biomass of the components (best linear functions were D, D and H, D, D and CrL, D and CrL^2, and D^2 for stem, branch, bark, NF, OF, and cone biomass, respectively); (2) using the most frequently

observed predictor (D) as the same independent variable for all components; and (3) using different independent variables for each component by forcing four linear restrictions on the regression coefficients (Figure 2.1); the SUR technique. The additivity of biomass equations to predict biomass of components, subtotal, and AGT has been explained in some other studies (Carvalho & Parresol, 2003; Magalhães & Seifert, 2015; Návar et al., 2002; Návar, Méndez, et al., 2004; Parresol, 1999, 2001; Zhao et al., 2015).

In this study, one linear ordinary least-squares equation (LINOLS) and three systems of linear additive equations (LINADD1, LINAD2, and LINADD3) were compared. A linear SUR model (LINADD3) provided better results than LINOLS, LINADD1, and LINADD2, in terms of goodness-of-fit statistics, standard error of estimates and residual plots. As there was a strong intrinsic correlation observed among the biomass components (Figure 2.7), it was logically possible to provide a restriction on regression parameters and to estimate the biomass of correlated equations using SUR (Carvalho & Parresol, 2003). Among the three additive equations, LINADD3 fitted in SUR, which considered the correlation between each component equation, provided greater statistical efficiencies, and therefore appeared superior to the other two additive models.

In contrast to our result, a study reported that the additive model (denoted as CON) that uses the same independent variable for all components, similar to our LINADD2 model, was statistically superior to the linear and nonlinear SUR model with the different independent variables in parameter restriction (Magalhães & Seifert, 2015). However, the authors (Magalhães & Seifert, 2015) indicated that the CON method had the limitation that it did not take into account of the contemporaneous correlation. For the precise estimation of biomass using the SUR technique, a system of additive equations must consist of different independent variables for each of the component equations (Srivastava & Giles, 1987). The model of this study LINADD3 is consistent with that of Srivastava & Giles (1987), as different explanatory variables were used in the model for each component, which was more effective than the other two additive models. Model LINADD1 also consisted of the same explanatory variables for two-component equations such as stem and bark, and LINADD2 consisted of the same independent variable for all component equations. Therefore, LINADD1 and LINADD2 was not effective compared to LINADD3, because according to Bhattacharya (2004), a linear SUR model provides biased estimates of a coefficient when that consists of the same independent variables. In addition, the individually calculated best equations for each component (LINOLS)

provided the least efficient biomass estimates for all components except for bark, cone and bole biomass, compared with the linear SUR model (LINADD3). Researchers recommended using SUR to estimate biomass as it provides greater statistical efficiency than separately calculated equations for each component (Bi et al., 2004; Návar, González, et al., 2004; Parresol, 2001).

In particular, LINADD3 recorded noticeable improvement in fit statistics for stem, branch, NF, OF, foliage, crown and AGT biomass, in contrast to the other three equations (LINOLS, LINADD1 and LINADD2) in terms of AIC, RMSE, MAB, MPE, RSE, CV, R^2 and IOA (Table 2.7). Using it for stem biomass caused little change in these statistics, and a decrease in the parameter of standard errors indicated the benefit of using SUR. Application of SUR in additive biomass equations provides lower variance by taking account of the existence of correlations among residuals of the component equations (Carvalho & Parresol, 2003). Therefore, as it provides unbiased parameter estimates, many researchers have tested SUR models and recommended using them in estimating biomass (Bi et al., 2010; Bi et al., 2004; Kozak, 1970; Návar et al., 2002; Návar, Méndez, et al., 2004; Parresol, 2001). Details about the SUR technique are available in Reed (1985), Gallant (1975), Srivastava and Giles (1987).

Allocation of tree dry matter into different components varies with endogenous factors, such as tree species and age, and exogenous factors such as environmental as well as silvicultural factors (Beets & Pollock, 1987). In this study, endogenous factors considered were tree dimension variables, such as D, H, CrL and WD, and exogenous factors were silvicultural practices such as follow-up herbicide, stocking and clone. For example, tree level AGT biomass production was higher with follow-up weed control treatment compared to without follow-up weed control; and clone 1 exhibited a higher biomass production than clone 2 (Figure 2.8). Some previous studies in New Zealand recorded a significant effect of nutrients, and silvicultural practices such as stocking and thinning in the dry-mass production of *P. radiata* (Beets & Madgwick, 1988; Madgwick, 1985; Mead et al., 1984). As explicitly representing these exogenous factors into models could further improve estimation precision, attempts were made to incorporate them into all models as dummy variables. However, it was found that follow-up herbicide, stocking, and clone factors fitted as dummy variables in all models were insignificant ($p > 0.05$) and consequently they were discarded from the modelling. The possible reason for this insignificance may be attributed to allometry as well as biotic factors outweighing the effects of silvicultural treatments. Other attempts were made to include the WD and SLA terms in all fitted best models, but these were also not statistically significant (p

> 0.05). This insignificance is conceivably attributed to the greater negative correlation between biomass components and WD (r = −0.02 to −0.35), and the weak positive correlation with SLA (r = 0.12 to 0.44) (Figure 2.8).

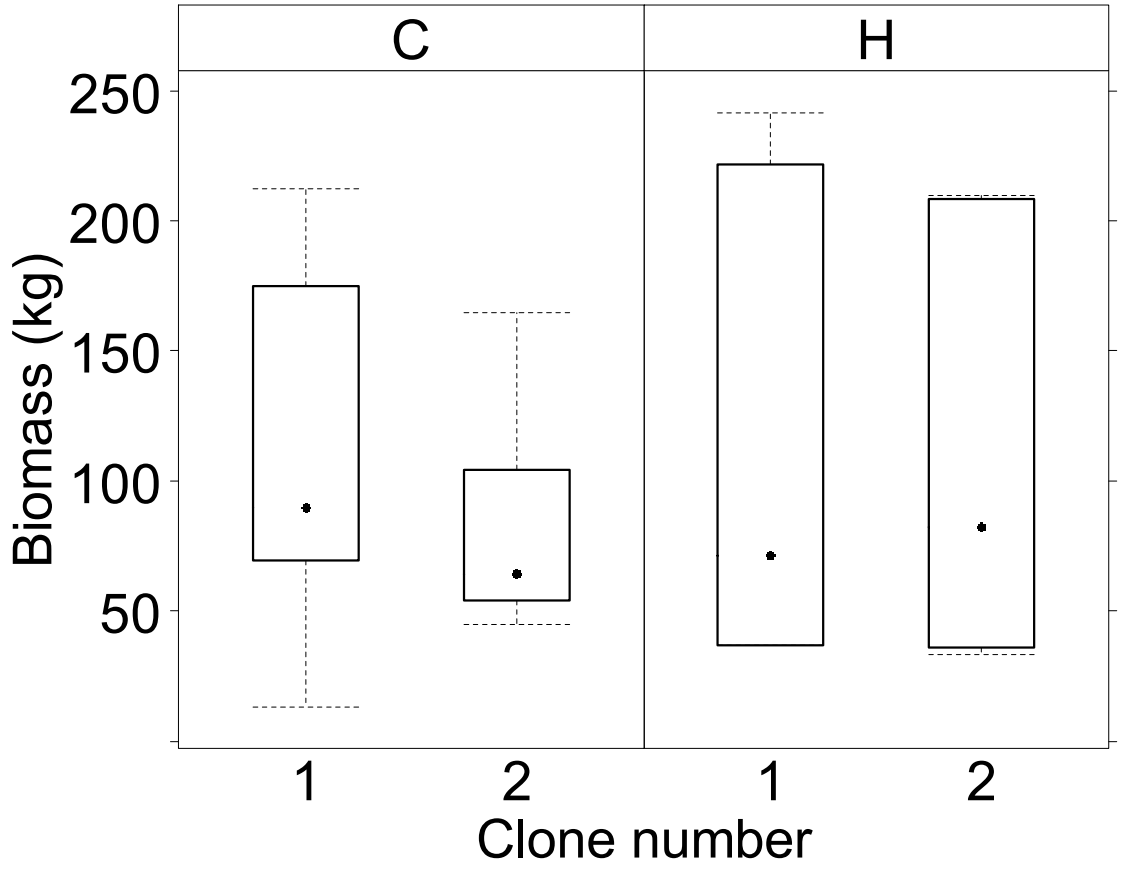

Figure 2.8: Effects of follow-up herbicide treatments and clone on biomass production of P. radiata in trail site. C and H refers control (no chemical) and herbicide treatment, respectively.

In this study, only above-ground biomass components were considered. For total tree biomass including roots, one can estimate and compare models of this study with the C_change model by Beets et al. (1999); however, it is a non-additive model developed with the aim to model the mortality and decay of different components including roots. Estimation of below-ground root biomass is important in order to predict the whole tree biomass of *P. radiata* (Moore, 2010); and also if we wish to compare above- and below-ground processes in terms of biomass partitioning. Root biomass can be estimated by using previously developed equations (Jackson & Chittenden, 1981) or, by using the above- to below-ground biomass ratio (Beets, Pearce, et al., 2007). These indirect methods can provide large prediction errors in estimation. Moreover, as it is expensive and difficult to measure below-ground root biomass, few studies included

root components when modelling total tree biomass of *P. radiata* in New Zealand (Beets, Pearce, et al., 2007; Madgwick, 1994). Only the above-ground biomass components with the available data from destructive sampling were considered in this report. While applying these models, it is advisable to consider the data range, as our models were fitted, with D ranged from 8.2 to 28 cm with an average of 18.68 cm, H ranged from 8.85 to 13.77 m with an average of 11.66 m, and CrL ranged from 0.2 to 6 m with an average of 3.35 m. Outside our data range, using these models to estimate biomass could produce uncertain prediction errors. In addition, site-specific environmental factors (Madgwick, 1994; Mason, 2008), growth condition of trees (Dong et al., 2015), and tree age (Beets & Madgwick, 1988; Beets & Pollock, 1987) may influence the relationship between biomass and linear stem dimensions. Therefore, considering these factors, developed biomass equations of this study are more suitable for the Canterbury region of New Zealand among 10- to 11-year-old radiata pine trees.

Conclusion

Among the six tree components, the stem accounted for the highest proportion of total biomass. Two procedures of biomass modelling were compared, namely, independent and additive. The weakness and robustness of best-selected equations were briefly explained by comparing the goodness-of-fit statistics in terms of AIC, RMSE, MAB, MPE, RSE, CV, R^2, IOA, standard error of estimates and residual plots. For the independent procedure of biomass modelling, LINOLS models with scaled power transformations and y-intercepts and NLINOLS power models that lacked y-intercepts were compared for six components, three subtotals, and AGT biomass. The LINOLS models with scaled power transformations and y-intercepts provided superior results in contrast to NLINOLS power models without y-intercepts. The best fitted component equations from LINOLS models were further tested in an additive procedure. A system of additive equations in SUR with different independent variables for each component (LINADD3) showed better performance than LINOLS, LINADD1, and LINADD2. More specifically, the linear SUR model provided comparatively unbiased estimates for stem (Eq. **2.10**), branch (Eq. **2.11**), NF (Eq. **2.13**), OF (Eq. **2.14**), foliage (Eq. **2.16**), crown (Eq. **2.17**), and AGT (Eq. **2.19**), while LINOLS recorded relatively good fit statistics for bark (Eq. **2.12**), cone (Eq. **2.15**) and bole biomass (Eq. **2.18**) for the dataset of this study. Since 7 out of 10 components were well fitted with SUR, it is recommended that SUR be used to estimate the biomass of *P. radiata* plantations.

To sum up, equations provided in this study will allow users to estimate components, subtotals and AGT biomass, and will help managers to assess the productivity of *P. radiata* in terms of biomass, which would have a major implication in forest carbon modelling.

Chapter 3. Seasonal dynamics of soil CO_2 efflux across stocking, clone, fertilization, and understorey-elimination in a *Pinus radiata* plantation in Canterbury, New Zealand

Highlights

- Estimated mean soil CO_2 efflux (F_s) rate for a *Pinus radiata* plantation in Canterbury, New Zealand was 22.71 tonne CO_2 ha^{-1} yr^{-1} (≈ 6.2 tonne C ha^{-1} yr^{-1}).
- Season, stocking, and clone had a significant influence on F_s.
- No significant effects of fertilization and follow-up weed control on F_s were observed.
- Autumn and winter had the highest and lowest rate of F_s, respectively.
- A soil moisture threshold determining the high and low value of F_s was 14.3%.
- F_s was highly influenced by clone 3, stocking 1,250 stems ha^{-1}, and plots without follow-up weed control.
- Soil temperature (T_s) was the most important variable controlling dynamics of F_s in the studied *P. radiata* plantation.

Summary

Planting trees at different stockings, with different clones, with fertilization, and weed control are commonly used silvicultural practices for *Pinus radiata* plantations in New Zealand. These practices can affect soil CO_2 efflux (F_s). This study was designed to investigate how the F_s differs seasonally with respect to stocking, clone, fertilization, and follow-up herbicide treatments, and to evaluate the relationship between F_s, soil temperature (T_s) and soil volumetric water content (θ_v) for a *P. radiata* plantation trial in the Canterbury region of New Zealand. F_s, T_s, and θ_v, were measured on a seasonal basis in autumn (13–16 April), winter (7–10 July), spring (3–6 October 2017), and summer (13–16 January 2018). Mixed-effects analysis of variance was carried out to examine the effects of silvicultural treatments on F_s, T_s, and θ_v for the whole period of the experiment, as well as separately for each season. The relationships between F_s, T_s, and θ_v were investigated by linear and nonlinear regressions. Correlation analyses were carried out to compare the relationship of F_s with soil physical properties.

F_s rates measured for the whole period of the experiment were significantly affected by the main effects of season, stocking and clone. No significant interaction effects of treatments on F_s were observed. For the whole year, the average rate of F_s estimated from the study site was 22.71 ± 1.02 tonne CO_2 ha^{-1} yr^{-1}. Mean efflux rates, by season, were ranked in the order of autumn (27.76 tonne CO_2 ha^{-1} yr^{-1}) > spring (24.15 tonne CO_2 ha^{-1} yr^{-1}) > summer (23.27 tonne CO_2 ha^{-1} yr^{-1}) > winter (15.64 tonne CO_2 ha^{-1} yr^{-1}). Mean efflux, by clones, were ranked in the order of clone 3 (24.29 tonne CO_2 ha^{-1} yr^{-1}) > clone 5 (23.38 tonne CO_2 ha^{-1} yr^{-1}) > clone 4 (22.02 tonne CO_2 ha^{-1} yr^{-1}) > clone 2 (21.92 tonne CO_2 ha^{-1} yr^{-1}) > clone 1 (21.81 tonne CO_2 ha^{-1} yr^{-1}). By stocking, the mean efflux was consistently higher in stocking 1,250 stems ha^{-1} (26.30 tonne CO_2 ha^{-1} yr^{-1}) across the four seasons. No significant effects on F_s were observed from fertilization and weed control treatments.

The critical value of θ_v separating the high and low value of F_s was 14.3%. For θ_v above 14.3%, a clear exponential relationship between F_s and T_s was observed. The T_s and θ_v jointly explained a relatively high proportion of the variance (27.90–48.94%) in F_s compared with simply T_s (26.63–47.82%) based on modelling across all silvicultural treatments. The combined T_s and θ_v based model suggested that T_s positively affected and moisture negatively affected F_s. Estimated Q_{10} values ranged from 3.03 to 5.19 across all silvicultural treatments. Q_{10} values showed F_s was most sensitive to T_s by silvicultural treatments in the order of clone 3 > 1,250 stems ha^{-1} > non-fertilization > without follow-up weed control treatment. F_s was positively correlated with soil bulk density (r = 0.05–0.29); and correlated negatively with soil porosity (r = −0.05 to −0.3), water-filled pore space (r = −0.13 to −0.51), and rock fragments (r = −0.01 to −0.17).

Planting trees in different stocking and with different clones substantially affected F_s in *P. radiata*; nevertheless, fertilization and follow-up herbicide did not affect it significantly. Seasonal changes in T_s and θ_v influenced F_s.

Key words: *soil CO_2 efflux; Pinus radiata; plantation; soil temperature; soil water content; season; stocking; clone; fertilization; follow-up herbicide*

Introduction

The greenhouse gas emission, carbon dioxide (CO_2) in particular, from the soil is very important as it is the major source of emission from terrestrial ecosystems to the atmosphere (Raich et al., 2002). Globally, forest soils are estimated to contain 383 ± 30 Pg C (44%), while forests 861 ± 66 Pg C (Pan et al., 2011). Soil CO_2 efflux (F_s) estimated to account for 80.4 Pg C yr^{-1} (Raich et al., 2002). Thus, minor alterations in terrestrial F_s by any anthropogenic activities could significantly change soil carbon pools in terrestrial ecosystems, and carbon dynamics influencing global warming (Melillo et al., 2002; Schlesinger & Andrews, 2000). F_s changes due to anthropogenic factors may accelerate global warming by speeding up global carbon cycling (Cox, Betts, Jones, Spall, & Totterdell, 2000; Melillo et al., 2002; Trumbore, Chadwick, & Amundson, 1996). Carbon is accumulating in the atmosphere at the rate of 2.8 Pg yr^{-1}, mainly from anthropogenic activities (Fan et al., 1998). Overall, climate change is predicted to increase air temperature and evapotranspiration, and decrease precipitation, although effects could vary drastically from region to region (Le Quéré et al., 2017). Impacts of human activities on F_s such as soil fertilization, harvesting, irrigation, and land use change are poorly documented and vary at temporal and spatial scales (Raich & Schlesinger, 1992). Therefore, as the vital role of forests in mitigating climate change through carbon sequestration has been well recognized (Schlesinger & Andrews, 2000; Yiqi & Zhou, 2010), the effect of forest management practices on F_s needs to be examined (Lal, 2005; Raich & Tufekciogul, 2000; Shan et al., 2001; Yohannes et al., 2013).

Pinus radiata D. Don, a native of California and Mexico, is the most frequently planted forest species in New Zealand and also in Australia, South Africa and Chile, (Mead, 2013). As it has high productivity and great environmental adaptation, this species has been planted using a wide range of silvicultural regimes, and the planted area across the Southern Hemisphere is now more than 4 million hectares. *P. radiata* yields better tree breeding and silvicultural response and a wider end use for products than many other plantation species (Lavery & Mead, 2000; Lewis et al., 1993; Sutton, 1999; Turner & Lambert, 1986). In New Zealand, *P. radiata* is the predominant planted species, accounting for about 90% of a total of 1.70 million hectares (Nixon et al., 2017). It has been reported that *P. radiata* plantations in New Zealand can play a important role in sequestration of carbon and it's storage (Hollinger et al., 1993), through

enduring products and carbon storage in the soil (Nixon et al., 2017; Scott, Tate, Ford-Robertson, Giltrap, & Smith, 1999).

Fertilization, understorey-elimination, planting at different stockings and with different genotypes are common silvicultural practices for *P. radiata* plantations throughout New Zealand (Mason & Milne, 1999). These practices may have economic implications with sustained productivity (Burger, 1994), as the purpose of fertilization is to enhance growth and productivity, weed control is aimed at reducing competition and improving forest health; and planting at different stocking and with different genotypes is aimed at producing stems with high vigour and quality timber (Mason, 1992). Such silvicultural practices may have a significant effects on F_s by altering the microclimate of the site, including light, soil moisture (θ_v), soil temperature (T_s), and the soil microbial community. Many studies have reported that soil CO_2 varies across temporal and spatial scales (Yiqi & Zhou, 2010) due to T_s (Guidolotti, Rey, D'andrea, Matteucci, & De Angelis, 2013; Lloyd & Taylor, 1994), θ_v (Chang et al., 2014), forest types (Raich & Tufekciogul, 2000), land form (Kang et al., 2003), and soil physical properties (Aslam et al., 2000).

Main research areas for *P. radiata* in New Zealand comprise silviculture, genetics and environment (Lasserre, Mason, & Watt, 2005; Mason, 2008; Mason & Kirongo, 1999), growth and yield modelling, fertilization, weed control and soil cultivation practices (Mason & Milne, 1999; Mason et al., 1996). However, an understanding of how these practices will affect the dynamics of F_s in plantations is still limited. In New Zealand, previous studies on F_s emphasized various factors including influence of temperature (Robinson, 2016), root biomass and soil temperature (Schwendenmann & Macinnis-Ng, 2016), soil tillage practices (Aslam et al., 2000), and comparison of above-ground with below-ground processes (McQuillan, 2013), with suggestions to evaluate the silvicultural impacts on F_s further. However, there are no available published reports evaluating the effects of silvicultural practices on F_s in experimental trials. Therefore, this study aimed: (a) to examine the influence of stocking, clone, fertilization, and weed control on F_s, T_s and θ_v, and (b) to observe the relationship between F_s, T_s and θ_v in a 12-year-old *P. radiata* plantation in the Canterbury region of New Zealand. It was hypothesized that:

(i) fertilization can increase plant growth and productivity, which in turn could increase litterfall input and soil organic matter, thereby increasing F_s (Johnson, 1992);

(ii) understorey-elimination can decrease aboveground litter input in the earlier rotation, and root litter input during the whole rotation (Carlyle, 1993), thereby decrease F_s (Shan et al., 2001);

(iii) stand density would significantly affect F_s due to its influence on in microclimatic, physiological and growth response of trees (Della-Bianca & Dills, 1960; Litton, Raich, & Ryan, 2007). Increase in stand density can increase F_s due to its effects on increased belowground plant biomass (Litton, Ryan, Knight, & Stahl, 2003; Litton, Ryan, Tinker, et al., 2003), and higher litter production as well as decomposition, thereby increasing soil carbon content (Litton et al., 2001).

(iv) different clones would significantly change F_s due to different responses to belowground carbon partitioning and nutrition (Bown, Mason, et al., 2009; Bown, Watt, Clinton, et al., 2009; Bown, Watt, Mason, et al., 2009; Tyree et al., 2011, 2014), corewood properties (Watt et al., 2006), and growth and productivity (Hawkins, Xue, Bown, & Clinton, 2010; Mason, 1992).

(v) F_s may vary across the season due to effects of seasonal changes in environmental variables such as T_s and θ_v (Davidson et al., 1998; Yiqi & Zhou, 2010).

This study is an essential step for understanding the effects of silvicultural practices, and environmental variables on F_s, with potential implications for estimating global carbon budgets from planted forests.

Materials and methods

Study site and experiment

The experiment was located just south of Rolleston (approx. 26 km south west of Christchurch) within the Canterbury region of New Zealand (43° 37.2′ S and 172° 20.4′ E). The experiment was setup by the School of Forestry, University of Canterbury, New Zealand, on land owned by the Selwyn District Council (Figure 1.1) which consists of 7.5 ha of *P. radiata* planted in 2005. At approximately 45 m above sea level on a flat landscape, the site is known to have dry, frosty conditions in winter, and windy and usually arid conditions in the summer. The site has an air median annual temperature between 11 and 13 °C with a monthly minimum (July) of −2

to +4 °C and a monthly maximum (January) of 20 to 23 °C (Macara, 2016). Annual rainfall is about 618 mm with a monthly range of 38 to 68 mm (Macara, 2016). The major soil type is a Lismore stony silt loam, with aggradation gravel as parent material, which also includes partial glacial gravel (NIWA, 2018; Xue et al., 2013).

The design of the experiment consisted of 48 permanent plots with randomized complete block factorial split plots with 4 complete blocks (Mason, 2008), with an arrangement of factors within the block (Figure 1.2). The main plots consisted of 3 levels of stocking (625, 1,250 and 2,500 stems ha^{-1}). A first split consisted of four levels of follow-up weed control and fertilization treatments (fertilization, F; herbicide, H; both, FH; and no chemical, NN). Fertilization was carried out once in year 1 and once in year 3 (NPKS + trace elements @ 80 grams per tree) after planting. Weed control treatment was applied in years 1 and 2 (strip weed control) and follow-up weed control was applied in years 3 (herbicide) and any subsequent year when new weeds appeared after planting. A second split consisted of 5 different clones randomly allocated to all plots, with the clone numbers 1, 2, 3, 4 and 5 indicating the genetic families of F97-651 (low microfibril angle and high basic density), R96-4 (low microfibril angle and low basic density), K96-44 (high microfibril angle and high basic density), C96-24 (high microfibril angle and low basic density), and A96-47 (extremely high microfibril angle and extremely low density), respectively (Mason, 2008).

Measurement of soil CO_2 efflux

Soil CO_2 efflux (F_s) was measured using an infrared gas analyzer (EGM-4, PP Systems, Hitchin, Hertfordshire, England) equipped with a soil respiration chamber (SRC-1) of 10 cm inner diameter. In total, 240 PVC collars (10 cm diameter and 6 cm height) were placed into the soil and left undisturbed to enable F_s measurements to be made. The EGM-4 connected with the SRC-1 gives two CO_2 outputs: the total soil CO_2 concentration at the time of measurement in parts per million (ppm), and the soil CO_2 exchange rate (g CO_2 m^{-2} hr^{-1} (PP Systems, 2016). A record of the soil CO_2 exchange rate in g CO_2 m^{-2} hr^{-1} was converted into tonne CO_2 ha^{-1} yr^{-1} for use in subsequent analyses. F_s values were measured at the centre of all five clones, which have two rows apiece. From the 48 plots, a total of 240 F_s measurements were recorded in each season (48 plots × 5). From four seasons, a total of 960 measurements were made (48 plots × 5 clones × 4 seasons). Field measurements were undertaken between

9:00 AM and 4:00 PM during 13–6 April, 7–10 July, 3–6 October 2017, and 13–6 January 2018.

Measurement of soil temperature and soil water content

Soil temperature (T_s) and soil volumetric water content (θ_v) were measured simultaneously, within 10 cm of the collar, along with F_s measurements. T_s was measured using a built-in temperature probe (STP-1) of the EGM-4 at a soil depth of 10 cm. The θ_v was measured using a portable moisture meter, SM150T (Delta-T Devices, UK), at a depth of 10, 20 and 30 cm. Measurements of the SM150T were calibrated from the lab analysis using a gravimetric method. The gravimetric method of determining θ_v is a standard method that requires oven drying soil samples of a known volume (Walker, Willgoose, & Kalma, 2004).

Measurement of soil physical properties

Soil sampling was carried out using a soil corer of volume 282.7 cm^3 (10 cm height and 6 cm diameter) within 20 cm of the soil collar to depths of 10, 20 and 30 cm. Extracted samples from each plot were placed into plastic bags, tightened to avoid moisture loss, weighed, recorded and labelled. For the lab process, all samples were transferred to paper bags for oven drying and dried at 105 °C for 48 hours. The dried samples were re-weighed, and sieved with a 2 mm sieve to analyse soil physical properties. The following techniques were used to determine the θ_v, bulk density (BD), total porosity (PORE), rock fragments (RF), and water-filled pore space (WFPS) (Table 3.1).

Table 3.1: Lab analysis for the determination of soil physical properties

$\mathrm{GWC} = \frac{\mathrm{FW} - \mathrm{DW}}{\mathrm{DW}} \times 100$	$\mathrm{PORE} = 1 - \frac{\mathrm{BD}}{\mathrm{PD}} \times 100$
$\theta_v = \mathrm{GWC} \times \mathrm{BD}$	$\mathrm{WFPS} = \mathrm{GWC} \times \frac{\mathrm{BD}}{\mathrm{PORE}} \times 100$
$\mathrm{BD} = \frac{\mathrm{Ms}}{\mathrm{Vs}}$	$\mathrm{RF} = \frac{\mathrm{DRF}}{\mathrm{TDW}} \times 100$

Note: GWC = Gravimetric water content (%), FW = Fresh weight of the soil (g), DW = Dry weight of the soil (g), θ_v = Volumetric water content (%), BD = Soil bulk density (g cm^{-3}), Ms = Mass of the fine soil (g), Vs = Volume of the fine soil (cm^3), PORE = Total soil porosity (%), PD = Particle density (g cm^{-3}) with default value (2.65 g cm^{-3}), WFPS = Water filled pore space (%), RF = Rock fragments (%), DRF = Dried weight of the rock fragments > 2 mm (g), and TDW = Total dried weight of the soil sample (g).

Statistical analysis

Mixed effects modelling

Initially, both response and explanatory variables were examined for normality and homogeneity assumptions of the mixed effects modelling. There was some evidence that the response variables were consistently non-normal across the measured data, and also non-homogeneous in variance (e.g., F_s in Figure 3.1). The response variables were therefore transformed before analysis using a scale power transformation technique, also known as "Box-Cox" transformation (Box & Cox, 1964), to satisfy the normality and homogeneity assumptions of the model. However, the results and graphs were presented in back-transformed scale.

All analyses were performed in R version 3.4.1 software (R Core Team, 2017), using mixed effects modelling approaches with the *nlme* package (Pinheiro, Bates, DebRoy, Sarkar, & R Core Team, 2018). Specifically, mixed modelling was undertaken to examine effects of stocking, clone, fertilization, follow-up herbicide, and season on F_s, T_s, and θ_v for the whole period of the experiment as well as separately for each season, with complete blocks as random effects. Analysis started with a sub-optimal model containing as many variables as possible in the fixed components, as suggested by Zuur et al. (2009). For separate seasonal analysis, the hypothesized fixed effects included the stocking, clone, fertilization, and follow-up herbicide treatment and their two-way interaction. For the whole period of the experiment, season was also included as a main effect in the fixed part of the model (Appendix 2.1). In order to account for the dependence of the repeated measurement within the same experimental unit, random effects of experimental units were also specified. The choice of optimal random effect structure was based on the design of the experiment, that is, a nested structure (i.e., complete 48 plots nested within 4 levels of fertilization and follow-up herbicide treatments (fh), which is nested within 3 levels of stockings and again nested within complete 4 blocks. In *nlme* package of R, it was fitted in random part of the model with this structure: ~1|block/stock/fh/plot.

For the separate seasonal analysis, models were fitted directly with the selected optimal fixed and random effect structure for F_s, T_s, and θ_v, according to the design of the experiment, but with blocks as random effects. However, for the whole period of the experiment, inspection of temporal correlation due to repeated measurement on the same experimental unit was required to address the issue of violation of independence, and therefore, for the whole period of the experiment, models were fitted by evaluating the potential autocorrelation. Autocorrelation in a mixed effect model can be examined by a visual inspection of the autocorrelation plot, by incorporating different forms of autocorrelation structures into the model, and comparing models with the AIC values (Zuur et al., 2009). The autocorrelation of the models containing sub-optimal fixed and random effect structures for the whole period of the experiment was therefore examined by plotting model residuals using the *ACF* function in R software. The autocorrelation factor (ACF) for F_s as a response variable at a range of lags up to 30 indicated there is a pattern of a contagious structure running through residuals (Figure 3.2A). The following approaches were undertaken to examine the autocorrelation structure: (a) unstructured correlation; (b) first-order autoregressive covariance using the *corAR1*; (c) a compound symmetry using the *corCompSymm*; and (d) autoregressive moving average, using the *corARMA* function of the *nlme* package in R.

According to Zuur et al.*(Zuur et al., 2009)*, a model fitted with nested random effect structures cannot be compared with the maximum likelihood (ML) method because the estimators for the variance terms are biased, and so restricted maximum likelihood (REML) estimates were used to compare the model with different nested random effects as well as with correlation structures. Fitted models with different correlation structures were compared with unstructured correlation models using Δ Akaike's Information Criterion (Δ AIC) (Appendix 2.1). For F_s and θ_v as the response variable, *corAR1* substantially improved the model fit, as did *corARMA* with ~1|block/stock/fh/plot/clone as an autocorrelation structure for T_s as a response variable (Appendix 2.1).

The final models for the whole period of the experiment for respective response variables were validated through visual inspection of residual plots, which has shown the homogenous distribution of residuals (e.g. F_s in Figure 3.2B). Analysis of variance (ANOVA) was carried out with the results of significant effects of the treatments. The TukeyHSD test was undertaken for the post hoc multiple comparisons of means using the *emmeans* function in R (Lenth,

Singmann, Love, Buerkner, & Herve, 2018), with a confidence level of α = .05 unless otherwise stated.

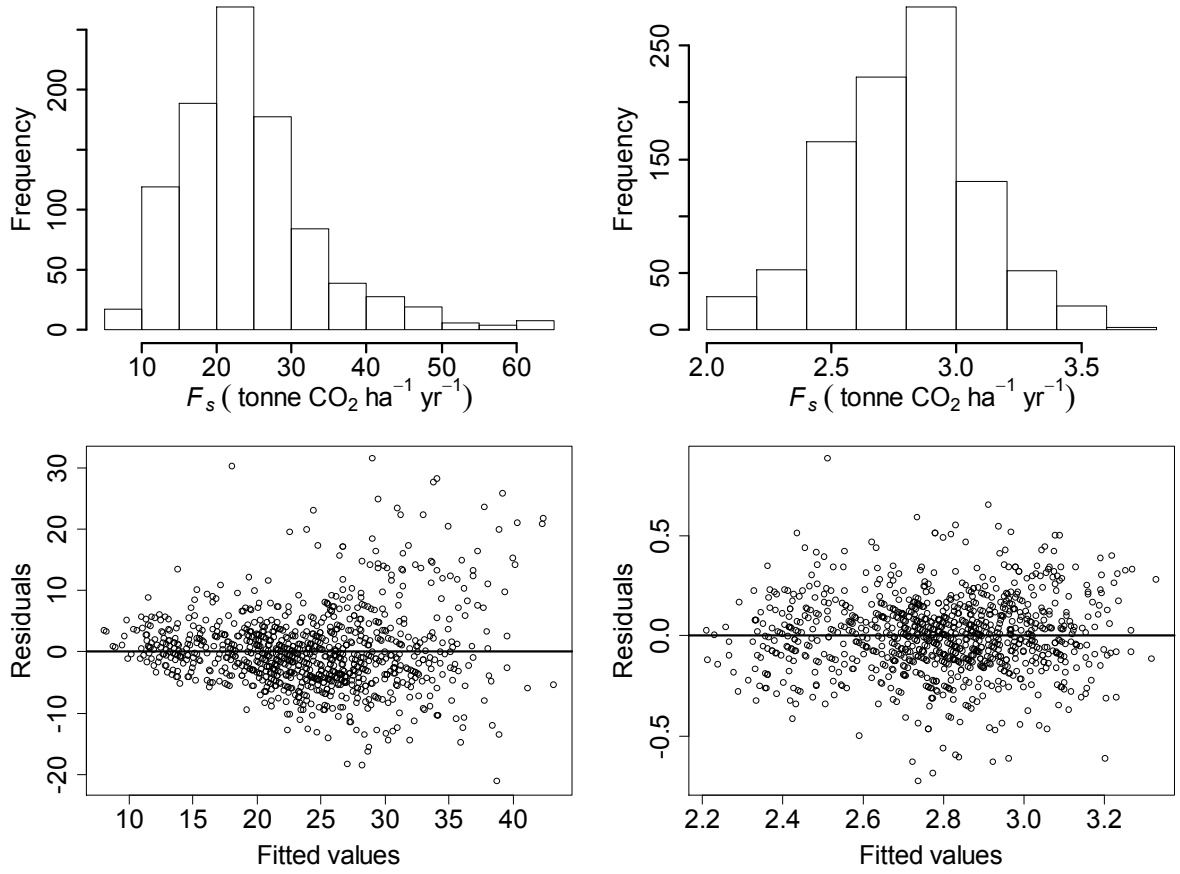

Figure 3.1: Histogram showing F_s in a measured scale (upper left) and the same data in a transformed scale (upper right) using Box-Cox transformation, and their corresponding residual distribution (lower left and right).

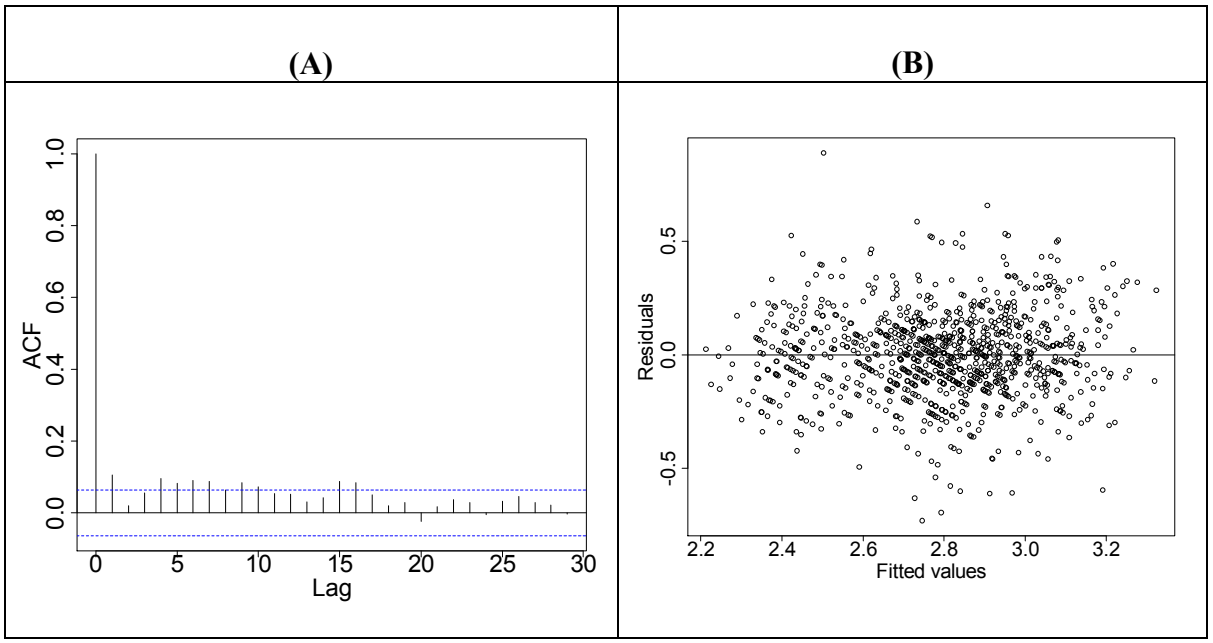

Figure 3.2: (A) ACF for F_s as a response variable, (B) distribution of residuals for the final model fitted in corAR1 autocorrelation structure.

Regression analysis

When all measurements of F_s were plotted against T_s across the whole period of the experiment (n = 960), a clear temperature response of F_s did not appear (Figure 3.3A). As the data were collected on a seasonal basis, it was speculated that soil water is limited by the higher temperature, especially in summer. Therefore, attempts were made to find a critical value of θ_v at which high and low values of F_s could be obtained. Recursive partitioning was applied to search for a θ_v threshold using a *party* package in R software (Hothorn, Hornik, & Zeileis, 2006). The critical value of θ_v separating the high and low value of F_s was 14.3% (Figure 3.3B). With this value, datasets were partitioned into two groups (namely, $\theta_v > 14.3\%$, and $\theta_v < 14.3\%$). When F_s was plotted against T_s, when θ_v was more than 14.3% (n = 616), a clear temperature response of soil respiration appeared (Figure 3.3C). However, the plot of F_s against T_s when θ_v was less than 14.3% (n = 344) exhibited no clear relationship (Figure 3.3D). This type of partitioning technique to determine the moisture threshold in modellling F_s has also been used by others, for example, Chang et al. (2014). Hence, linear and nonlinear regression equations were tested to evaluate the relationship of F_s with T_s, and θ_v using a segmented data set that consisted of a critical value of θ_v greater than 14.3%.

To determine a relationship between F_s and θ_v, linear (Eq. **3.1**) (Davidson et al., 1998), and exponential (Eq. **3.2**) (Davidson, Verchot, Cattanio, Ackerman, & Carvalho, 2000) models were used. While fitting the linear model (Eq. **3.1**), "Box-Cox" transformation (Box & Cox, 1964) was applied for the dependent variable to stabilize the variance.

$$F_s = a + b\theta_v \quad (\mathbf{3.1})$$

$$F_s = ae^{b\theta_v} \quad (\mathbf{3.2})$$

where F_s is the measured soil CO_2 efflux rate (μmol CO_2 $m^{-2}s^{-1}$), θ_v is the measured volumetric water content (%) at 10 cm soil depth and a and b are fitted parameters of the regression.

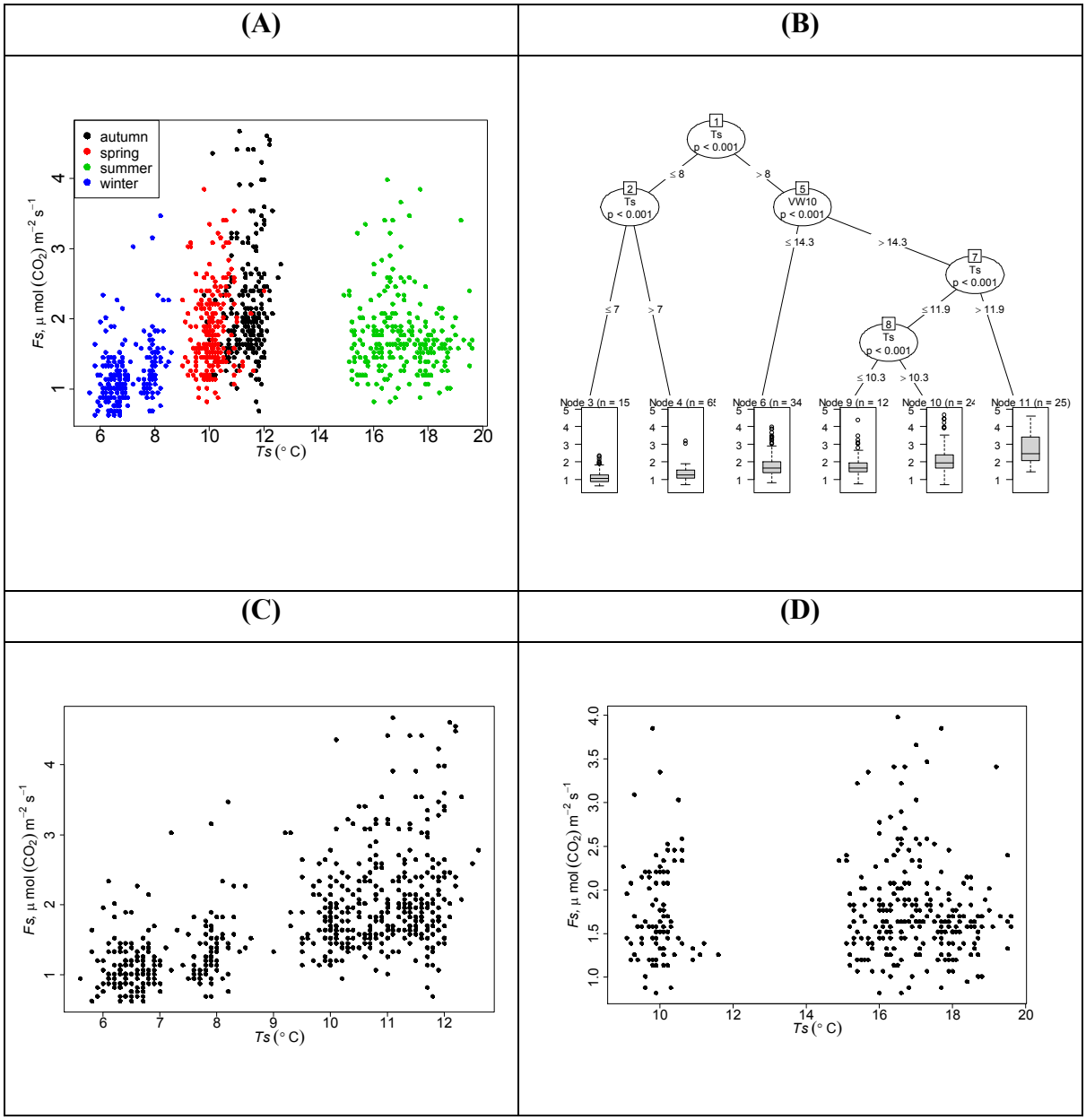

Figure 3.3: (A) Relationship between F_s and T_s using all data measured for the whole period of the experiment. (B) Recursive partitioning of the F_s as response variable and T_s at 10 cm soil depth, and θ_v at 10, 20, and 30 cm depth as independent variables in the model. (C) Relationship between F_s and T_s when θ_v > 14.3%. (D) Relationship between F_s and T_s when θ_v < 14.3%. The temp indicates T_s and VW_{10} indicates θ_v at 10 cm soil depth.

To determine the relationship between F_s and T_s, the two most widely used models were tested: linear (Eq. **3.3**), and exponential (Eq. **3.4**) (Lloyd & Taylor, 1994). Temperature sensitivity (Q_{10}), i.e., the response of F_s to a 10 °C change in T_s values was estimated across all silvicultural treatments using Eq. **3.5** based on the model of Lloyd & Taylor (1994). While fitting the linear model (Eq. **3.3**), a "Box-Cox" transformation (Box & Cox, 1964) was implemented for the response variable to stabilize the variance.

$$F_s = a + bT_s \quad (3.3)$$

$$F_s = ae^{bT_s} \quad (3.4)$$

$$Q_{10} = e^{10b} \quad (3.5)$$

where F_s is the measured soil CO_2 efflux rates (μmol CO_2 $m^{-2}s^{-1}$), T_s is the measured soil temperature at 10 cm soil depth (°C), Q_{10} is the temperature sensitivity response of F_s; a and b are fitted parameters of the regression.

To explore the relationship between F_s, T_s and θ_v, commonly used exponential functions were tested: Eq. **3.6** (Gulledge & Schimel, 2000), Eq. **3.7** (M. Xu & Qi, 2001a), and Eq. **3.8** (Lavigne, Foster, & Goodine, 2004).

$$F_s = ae^{bT_s}\frac{\theta_v}{\theta_v + c} \quad (3.6)$$

$$F_s = ae^{bT_s}{\theta_v}^c \quad (3.7)$$

$$F_s = ae^{bT_s}e^{c\theta_v} \quad (3.8)$$

where F_s is the measured soil CO_2 efflux rate (μmol CO_2 $m^{-2}s^{-1}$), T_s is the measured soil temperature (°C), θ_v is the measured volumetric water content (%) at 10 cm soil depth; and a, b, and c are fitted parameters of the regression.

Models were set up in R statistical software (R Core Team, 2017) using *lm* and *nls* function for linear and nonlinear regressions, respectively. To find the best model to predict F_s, results among fitted functions (Eq. **3.1** to **3.4**, and **3.6** to **3.8**) were evaluated using the following criteria to measure goodness-of-fit statistics (Table 3.2): root mean square error (RMSE), residual standard error (RSE), coefficient of variation (CV), mean absolute bias (MAB), fit index (R^2), index of agreement (IOA), and Akaike's information criterion (AIC). The models that were regarded as best were those with the smallest RMSE, RSE, CV, MAB, AIC of the residuals, and those with the highest R^2 and IOA. Moreover, models were evaluated by plotting graphs of residuals and using the Shapiro-Wilk test of normality. Finally, the best models were chosen to evaluate the relationship between F_s and T_s, and θ_v; and they also examined the relationship across the stocking, clone, fertilization, and herbicide treatments.

Table 3.2: Different measure of goodness-of-fit statistics to evaluate the model's performance.

$\mathrm{RMSE} = \sqrt{\frac{1}{n}\sum_{i=1}^{n}\left(Y_i - \hat{Y}_i\right)^2}$	$\mathrm{RSE} = \frac{\sum_{i=1}^{n}\left(Y_i - \hat{Y}_i\right)^2}{n-p}$
$\mathrm{MAB} = \frac{1}{n}\sum_{i=1}^{n}\left\lvert Y_i - \hat{Y}_i\right\rvert$	$\mathrm{CV} = \frac{\sqrt{\frac{1}{n}\sum_{i=1}^{n}\left(Y_i - \hat{Y}_i\right)^2}}{\overline{Y}_i} \times 100$
$R^2 = 1 - \frac{\sum_{i=1}^{n}\left(Y_i - \hat{Y}_i\right)^2}{\sum_{i=1}^{n}(Y_i - \overline{Y}_i)^2}$	$\mathrm{IOA} = 1 - \frac{\sum_{i=1}^{n}\left(Y_i - \hat{Y}_i\right)^2}{\sum_{i=1}^{n}\left(\left\lvert \hat{Y}_i - \overline{Y}_i\right\rvert + \left\lvert Y_i - \overline{Y}_i\right\rvert\right)^2}$
$\mathrm{AIC} = 2p - 2\log L + \frac{2p(p+1)}{n-p-1}$	
where Y_i and $\hat{Y}_i$ are the observed and predicted F_s, respectively, $\overline{Y}_i$ is the mean of the n observed F_s, n is the sample size, and p is the number of model parameters.	

Results

F_s across stocking, clone, fertilization, and herbicide treatments

For the whole year, the average rate of total F_s estimated from the study site was 22.71 ± 1.02 tonne CO_2 ha^{-1} yr^{-1} (range 15.64 to 27.76). The average values of F_s across four different seasons were as follows: 27.76 ± 1.02 tonne CO_2 ha^{-1} yr^{-1} (range 25.25 to 32.55) for autumn; 24.15 ± 1.02 tonne CO_2 ha^{-1} yr^{-1} (range 20.94 to 29.52) for spring; 23.27 ± 1.02 tonne CO_2 ha^{-1} yr^{-1} (range 20.04 to 26.87) for summer; and 15.64 ± 1.01 tonne CO_2 ha^{-1} yr^{-1} (range 14.38 to 17.42) for winter (Table 3.3).

The ANOVA statistics of the mixed effects analysis for the whole period of the experiment and separate seasonal analysis are given in Appendix 2.2 and Appendix 2.3, respectively. Analysis for the whole period revealed that the values of F_s were strongly controlled by the main effects of season ($F_{3,889} = 319.68$, $p < .001$), stocking ($F_{2,6} = 9.92$, $p < .05$), and clone ($F_{4,889} = 4.32$, $p < .01$). No significant effects of fertilization or follow-up weed control, or two-way interaction between stockings, clone, fertilization, and follow-up weed control treatments on F_s were observed ($p > 0.05$).

When seasonal data were examined separately, clone significantly affected F_s for autumn ($F_{4,172} = 7.74$, $p < .001$), and summer ($F_{4,172} = 2.68$, $p < .05$). The mean F_s rate by clone ranged from a high of 32.55 tonne CO_2 ha^{-1} yr^{-1} for clone 3 in autumn to a low of 15.15 tonne CO_2 ha^{-1} yr^{-1} for clone 1 in winter (Figure 3.4A, Table 3.3). No significant differences between mean efflux rates for any clones were observed during winter and spring. Clone 3 exhibited a significantly higher ($p < .05$) mean efflux rate compared to other clones in autumn, winter, and spring on a consistent basis. However, the mean rate of efflux in summer was significantly higher ($p < 0.05$) in clone 5. For all clones, efflux rates were at their highest in the autumn, and lowest in the winter, while spring and summer showed intermediate rates between these two extremes (Figure 3.4A). All clones showed a similar pattern of change in efflux rates during the whole year.

When seasonal data were examined separately, stocking significantly influenced F_s in spring ($F_{2,6} = 17.69$, $p < .01$), and summer ($F_{2,6} = 7.75$, $p < .05$). Mean F_s by stocking ranged from a high of 31.38 tonne CO_2 ha^{-1} yr^{-1} for the 1,250 stems ha^{-1} stocking in autumn to a low of 14.38 tonne CO_2 ha^{-1} yr^{-1} for the 625 stems ha^{-1} stocking in winter. No significant differences observed between mean efflux rates for all three levels of stocking in autumn and winter (Figure 3.4B). However, efflux rates were significantly higher in medium density stocking throughout all seasons (Figure 3.4B). When examining seasonal data separately, no significant effects of stockings, clone, fertilization, and follow-up herbicide treatments on F_s were observed in the winter season (Figure 3.4), and no significant two-way effects were observed in any season ($p > 0.05$). However, a marginally significant interaction effect was observed between fertilization and clone ($F_{4,172} = 2.35$, $p = .056$), and fertilization and follow-up herbicide ($F_{1,29} = 4.16$, $p = .051$) in the winter when examined separately (Appendix 2.3). The interaction between fertilization and clone in winter indicated that higher mean efflux rates tended to occur in clone 3 in the non-fertilized plot ($p < .05$), and no significant differences were observed between any clones in the fertilized plot ($p > .05$). No significant effects of fertilization and follow-up herbicide treatments on F_s were observed in all seasons investigated (Table 3.3). Although not significantly, overall higher F_s rates occurred in the fertilized plot compared with the non-fertilized plot in all seasons investigated (Table 3.3). In contrast, although not significantly, lower efflux rates tended to occur overall in the understorey-eliminated plot than in the competing vegetation plot in all seasons investigated (Table 3.3). The fertilization × follow-up herbicide interaction showed that higher mean F_s rates were likely to occur in the fertilized plots where no follow-up herbicide treatment applied ($p < .05$), and

no significant difference observed between the fertilized and non-fertilized plots where follow-up herbicide treatment was applied ($p > .05$).

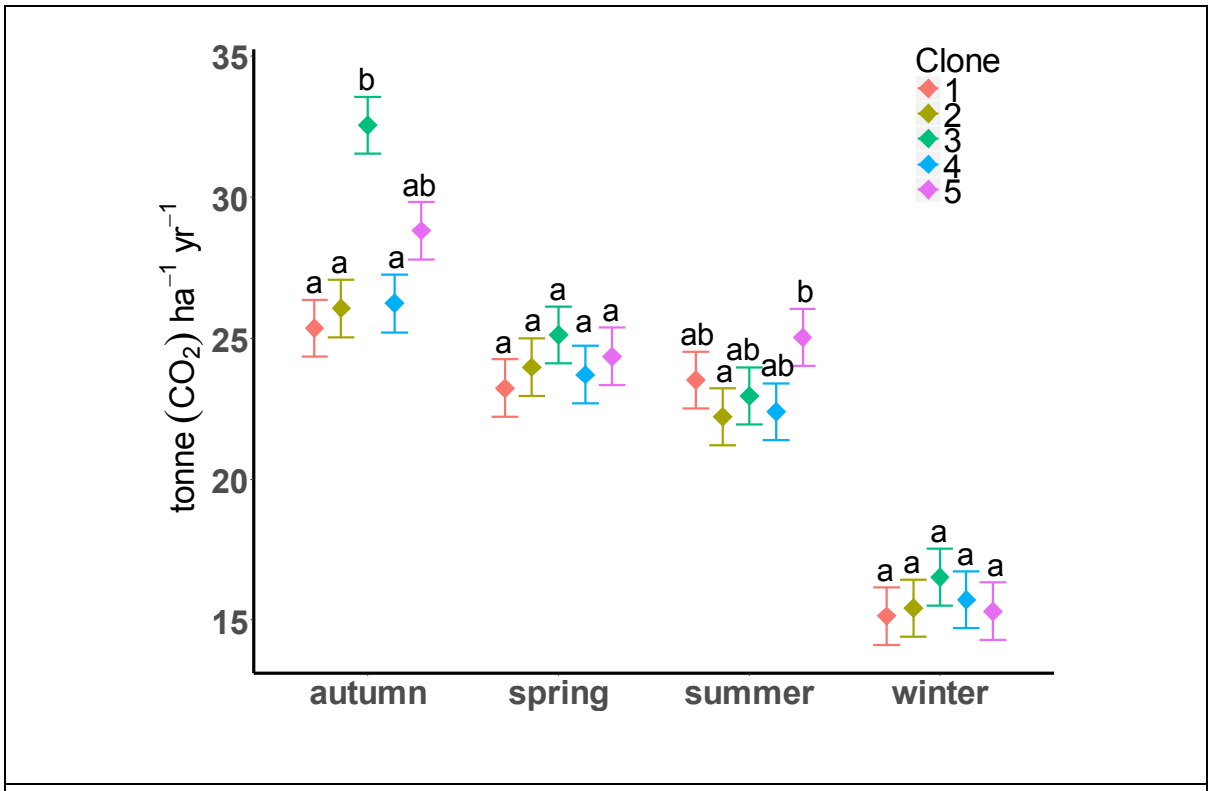

(A) across five clones

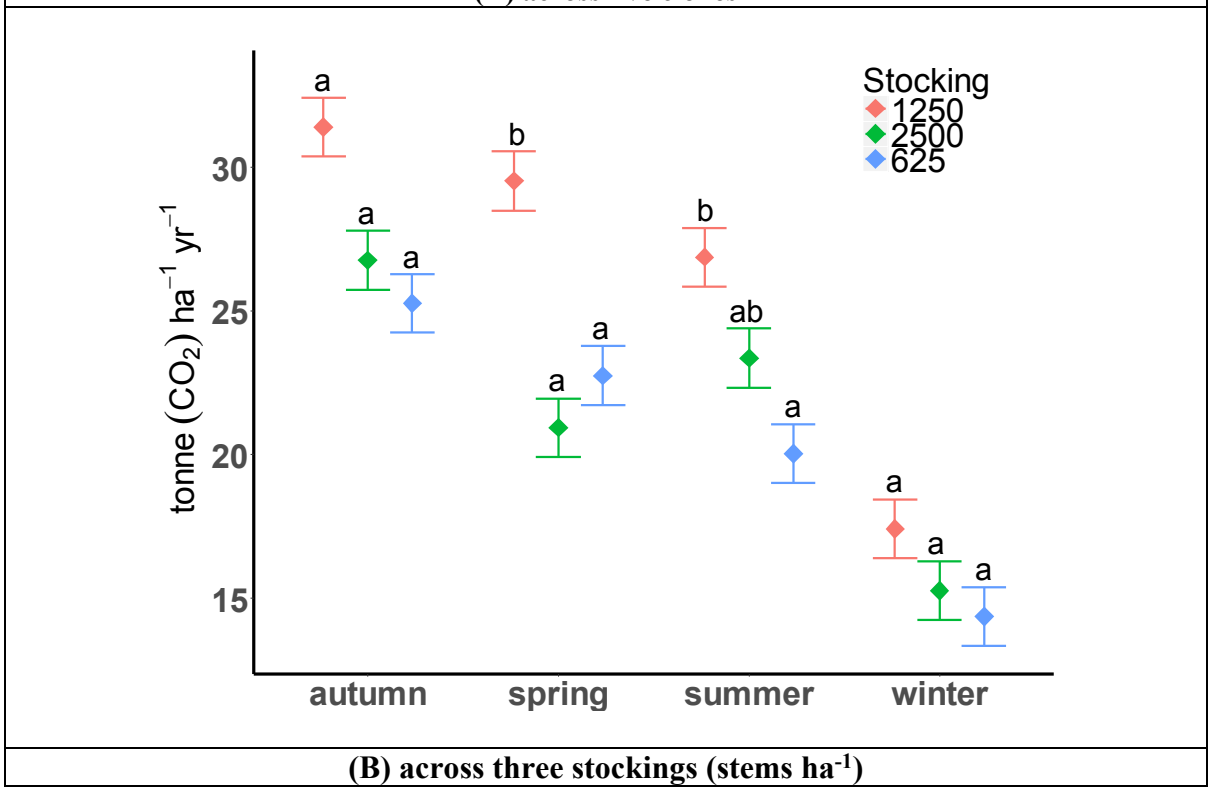

(B) across three stockings (stems ha^{-1})

Figure 3.4: Seasonal dynamics of F_s across silvicultural treatments. Values are presented as least square mean (±SE) of F_s, by season. Treatment means within a season followed by the same letter do not differ significantly at $\alpha = 0.05$ level using Tukey's HSD test.

Table 3.3: Mean soil CO_2 efflux rates.

		Soil CO_2 efflux (tonne CO_2 ha^{-1} yr^{-1})				
Factor	**Level**	**Autumn**	**Winter**	**Spring**	**Summer**	**Overall mean**
STOCK	**625**	25.25±1.02 a	14.38±1.02 a	22.75±1.02 a	20.04±1.02 a	20.61±1.02
	1250	31.38±1.02 a	17.42±1.02 a	29.52±1.02 b	26.87±1.02 b	26.30±1.02
	2500	26.76±1.02 a	15.27±1.02 a	20.94±1.02 a	23.36±1.02 ab	21.58±1.02
CLONE	**1**	25.35±1.02 a	15.15±1.01 a	23.23±1.02 a	23.52±1.02 ab	21.81±1.02
	2	26.06±1.02 a	15.42±1.01 a	23.97±1.02 a	22.21±1.02 a	21.92±1.02
	3	32.55±1.02 b	16.52±1.01 a	25.11±1.02 a	22.96±1.02 ab	24.29±1.02
	4	26.23±1.02 a	15.73±1.01 a	23.71±1.02 a	22.39±1.02 ab	22.02±1.02
	5	28.81±1.02 ab	15.32±1.01 a	24.35±1.02 a	25.03±1.02 b	23.38±1.02
FERT	**F**	28.47±1.02 a	16.13±1.01 a	24.56±1.02 a	23.28±1.01 a	23.11±1.02
	NF	26.85±1.02 a	15.12±1.01 a	23.58±1.02 a	23.10±1.01 a	22.16±1.02
HERB	**H**	26.51±1.02 a	15.10±1.01 a	23.83±1.02 a	22.38±1.01 a	21.96±1.02
	NH	28.85±1.02 a	16.16±1.01 a	24.30±1.02 a	24.05±1.01 a	23.34±1.02
Overall mean		27.76±1.02	15.64±1.01	24.15±1.02	23.27±1.02	22.71±1.02

Note: Mean values observed by stockings (stems ha^{-1}), clones (1 – 5), fertilization (F = fertilized, NF = non-fertilized), and follow-up herbicide (H = herbicide, NH = no herbicide) treatments in P. radiata plantations during four seasons. Treatment means within a season followed by the same letter do not differ significantly at $\alpha = 0.05$ level using Tukey's HSD test.

T_s and θ_v across stocking, clone, fertilization, and follow-up herbicide treatments

Values of T_s changed seasonally, being greater in summer (16.96 ± 1 °C) compared to winter (6.83 ± 1 °C), autumn (11.4 ± 6.8 °C), and spring (10.05 ± 1 °C) (Table 3.4). The ANOVA statistics of the mixed effects analysis for the whole period of the experiment and separate seasonal analyses are given in Appendix 2.2 and Appendix 2.3 respectively. T_s was strongly controlled by the main effects of season ($F_{3,889} = 9677$, $p < .001$), and clone ($F_{4,889} = 9.37$, $p < .001$) for the analysis during the whole period of the experiment. No significant effects of stocking, fertilization, and follow-up herbicide treatments on T_s were observed ($p > 0.05$). In

addition, no significant ($p > .05$) two-way interaction effects were observed between stocking, clone, fertilization, and follow-up herbicide treatments on T_s for the analysis during the whole period of the experiment.

When examined by separate seasons, T_s was significantly influenced by the main effect of clone in autumn, spring, summer, and winter ($F_{4,172} = 7.43$, $p < .001$), ($F_{4,172} = 7$, $p < .001$), ($F_{4,172} = 3.27$, $p < .05$), and ($F_{4,172} = 4$, $p < .01$) respectively. Clone 3 tended to have the highest mean T_s in all seasons except summer and exhibited the highest overall mean temperature (11.4 °C) compared with all other clones (Table 3.4). Although not significant, stocking 1,250 stems ha^{-1} tended to have the highest mean T_s in all seasons except in summer, with the highest overall mean T_s (11.42 °C) compared to stocking 625 and 2,500 stems ha^{-1} (Table 3.4). Overall, mean values of T_s ranged from a high of 17.17 °C in stocking 625 stems ha^{-1} in autumn to a low of 6.69 °C for the same stocking in winter (Table 3.4).

The values of θ_v followed an opposite trend to T_s, being lower in summer (7.32 ± 1 %) and increasing in spring (14.63 ± 1.6%), winter (17.15 ± 1%), and autumn (17.68 ± 1%) (Table 3.5). The ANOVA statistics of the mixed effects model for the whole period of the experiment and for each season are given in Appendix 2.2 and Appendix 2.3 respectively. The analysis for the whole period of the experiment revealed that θ_v was strongly affected by the interacting effects of stocking × follow-up herbicide ($F_{2,29} = 8.06$, $p < .01$). When examined on a seasonal basis, the interacting effects of stocking × follow-up herbicide on θ_v were also observed in autumn ($F_{2,29} = 11$, $p < .001$), and winter ($F_{2,29} = 5$, $p < .05$). Significant interacting effects of stocking × fertilization ($F_{2,29} = 5$, $p < .05$) and follow-up herbicide × clone ($F_{4,172} = 2.54$, $p < .05$) were observed in autumn and spring respectively. Clone had a significant effect on θ_v in winter ($F_{4,172} = 6$, $p < .001$). No significant ($p > .05$) effects of silvicultural treatments on θ_v were observed in summer. For the autumn season, significant stocking × follow-up herbicide interaction on θ_v indicated that θ_v differed between the plots with and without follow-up herbicide treatments across the 625 and 1,250 stems ha^{-1} ($p < .05$), and 2,500 stems ha^{-1} ($p < .05$). The θ_v in the plots with follow-up herbicide treatment applied, and with 625 stems ha^{-1} had an average increase of θ_v by 0.14 % and 0.16% more than those in the plots with 1,250 and 2,500 stems ha^{-1} respectively %) (Table 3.5). There was no evidence that at any level of stocking θ_v differed significantly from plots without follow-up herbicide treatment applied.

Table 3.4: Mean soil temperature.

Soil temperature (°C)						
Factors	**Level**	**Autumn**	**Winter**	**Spring**	**Summer**	**Overall mean**
STOCK	**625**	11.4±7.01 a	6.69±1 a	10.00±1 a	17.17±1 a	11.32±2.5
	1250	11.42±7.01 a	7.05±1 a	10.15±1 a	17.06±1 a	11.42±2.5
	2500	11.37±7.01 a	6.77±1 a	10.00±1 a	16.66±1 a	11.20±2.5
CLONE	**1**	11.35±6.67 a	6.83±1 ab	10.05±1 b	17.00±1 ab	11.31±2.42
	2	11.33±6.67 a	6.76±1 a	10.03±1 ab	16.97±1 ab	11.27±2.42
	3	11.55±6.67 b	6.95±1 b	10.15±1 b	16.95±1 ab	11.40±2.42
	4	11.37±6.67 a	6.81±1 ab	9.93±1 a	16.77±1 a	11.22±2.42
	5	11.39±6.67 a	6.81±1 ab	10.09±1 b	17.12±1 b	11.35±2.42
FERT	**F**	11.38±6.72 a	6.84±1 a	10.08±1 a	16.88±1 a	11.30±2.43
	NF	11.42±6.72 a	6.82±1 a	10.02±1 a	17.05±1 a	11.33±2.43
HERB	**H**	11.45±6.72 a	6.84±1 a	10.07±1 a	17.10±1 a	11.37±2.43
	NH	11.35±6.72 a	6.82±1 a	10.03±1 a	16.83±1 a	11.26±2.43
Overall mean		11.4±6.77	6.83±1	10.05±1	16.96±1	11.31±2.44

Note: Mean values observed across stockings (stems ha−1), clones (1 – 5), fertilization (F = fertilized, NF = non-fertilized), and follow-up herbicide (H = herbicide, NF = no herbicide) treatments in P. radiata plantations during four seasons. Treatment means within a season followed by the same letter do not differ significantly at α = 0.05 level using Tukey's HSD test.

Table 3.5: Mean soil volumetric water content.

Soil moisture (%)						
Factors	**Level**	**Autumn**	**Winter**	**Spring**	**Summer**	**Overall mean**
STOCK	**625**	17.86±1 a	17.19±1 ab	15.11±1.69 b	7.31±1 a	14.37±1.17
	1250	17.75±1 a	17.03±1 a	14.72±1.69 ab	7.40±1 a	14.23±1.17
	2500	17.44±1 a	17.23±1 b	14.07±1.69 a	7.26±1 a	14.00±1.17
CLONE	**1**	17.75±1 a	17.11±1 ab	14.50±1.62 a	7.40±1 a	14.19±1.16
	2	17.66±1 a	17.12±1 ab	14.76±1.62 a	7.33±1 a	14.22±1.16
	3	17.41±1 a	17.28±1 c	14.57±1.62 a	7.26±1 a	14.13±1.16
	4	17.80±1 a	17.19±1 bc	14.59±1.62 a	7.31±1 a	14.22±1.16
	5	17.78±1 a	17.05±1 a	14.74±1.62 a	7.31±1 a	14.22±1.16
FERT	**F**	17.61±1 a	17.16±1 a	14.61±1.6 a	7.32±1 a	14.18±1.15
	NF	17.75±1 a	17.13±1 a	14.65±1.6 a	7.33±1 a	14.22±1.15
HERB	**H**	17.89±1 b	17.08±1 a	14.89±1.6 b	7.37±1 a	14.31±1.15
	NH	17.48±1 a	17.22±1 b	14.38±1.6 a	7.27±1 a	14.09±1.15
Overall mean		17.68±1	17.15±1	14.63±1.63	7.32±1	14.20±1.16

Note: Mean values observed across stockings (stems ha−1), clones (1 – 5), fertilization (F = fertilized, NF = non-fertilized), and follow-up herbicide (H = herbicide, NH = no herbicide) treatments in P. radiata plantations during four seasons. Treatment means within a season followed by the same letter do not differ significantly at α = 0.05 level using Tukey's HSD test.

Soil physical properties across stocking, clone, fertilization, and follow-up herbicide treatments

Overall, the average values of soil physical properties (10 cm depth) recorded from the experimental site across all silvicultural treatments were 0.81 g cm^{-3} (range 0.61–1.1) for BD, 14.92% (range 1.83–45.14) for RF, 23.67% (range 5.62–53.11) for WFPS, and 69.27% (range 58.51–76.95) for PORE (Appendix 2.4).

The BD did not differ significantly across the clones (same values 0.81 g cm^{-3}), stocking (range 0.79–0.84 g cm^{-3}), or season (same values 0.81 g cm^{-3}). The BD was higher in the fertilized and understorey-eliminated plots (0.83 g cm^{-3}) compared with non-fertilized and competing vegetation plots (0.80 g cm^{-3}). RF was not significantly different across the clones (same values 14.89%), stocking (range 13.13–16.54%), and season (same values 14.89%). The value of WFPS showed no significant difference across clones (same 23.57%), stocking (range 21.86–25.16%), and fertilizer treatment (23.55 vs. 23.6%). WFPS differed significantly across the season, which was highest in winter (32.73%) than in summer (11.6%), while spring (26.5%) and autumn (25.3%) showed no difference and were intermediate between these two extremes. PORE was not significantly different across the clone (same values 69.27%), stockings (range 68.36–70.04%), and seasons (same value 69.27%), but it differed across the fertilization and follow-up herbicide treatments (range 68.83– 69.71%) (Appendix 2.4).

Regression analysis: model performance evaluation

Moisture-based models (Eq. **3.1** and Eq. **3.2**) provided insignificant results of the estimates and poor goodness-of-fit statistics compared to T_s-based and combined T_s and θ_v-based models (Table 3.6). When comparing two T_s-based models, the exponential model (Eq. **3.4**) provided a better result than its linear counterpart (Eq. **3.3**). The values of RMSE (0.5860), MB (−0.0007), CV (33.9114), and RSE (0.5869) were relatively low and R^2 (0.36437) and IOA (0.718) were somewhat higher for the exponential model than for the linear model (Table 3.6). Among three T_s and θ_v-based models, the exponential–exponential model (Eq. **3.8**) provided better results, indicating that the values of RMSE (0.5823), MB (0.00004), CV (33.6957), and RSE (0.5837) were relatively low and R^2 (0.37243) and IOA (0.713) were higher than other models (Table 3.6). Comparing all three models, the poorest performance was from models that only included θ_v.

Overall, when comparing between univariate T_s-based models and bi-variate models based on T_s and θ_v, little improvement was observed in the combined model (Table 3.6). Therefore, the exponential model (Eq. **3.4**) and the exponential-exponential model (Eq. **3.8**) were selected separately as best for the T_s-based and combined model based on T_s and θ_v, respectively. The graph of residual vs. predicted values of F_s, the associated histogram of the residuals, and Shapiro-Wilk test of normality for the selected two models are given in Figure 3.5. Moreover, to ascertain whether the models could capture some of the detailed features across silvicultural treatments, these two models were further tested separately across the different level of stocking, clone, fertilization, and follow-up herbicide treatments.

Table 3.6: Goodness-of-fit statistics for the model evaluation.

Models	θ_v based		T_s-based		combined (based on θ_v and T_s)		
Equation	**3.1**	**3.2**	**3.3**	**3.4**	**3.6**	**3.7**	**3.8**
AIC	NA	1373.95	NA	1095.79	1090	1089.96	1089.93
RMSE	0.7489	0.7345	0.5925	0.586	0.5824	0.5823	0.5823
MB	0.1464	3.59E-05	0.084	-0.0007	0.00009	0.00007	0.00004
CV	43.3459	42.50102	34.2873	33.9114	33.6976	33.6964	33.6957
RSE	0.7501	0.7357	0.5935	0.5869	0.5838	0.5838	0.5837
R^2	-0.0381	0.0016	0.3502	0.36437	0.37236	0.3724	0.37243
IOA	0.227	0.045	0.703	0.718	0.722	0.721	0.713
a	0.77**	2.27***	-0.75***	0.49***	0.32***	1.99*	0.79***
b	-0.02 ns	-0.02 ns	0.13***	0.13***	0.14***	0.14***	0.14***
c					-5.63***	-0.51**	-0.03**
Q_{10}	0.82	0.85	3.6	3.7	3.84	3.85	3.86

Note: Abbreviations are as follows: root mean square error (RMSE), residual standard error (RSE), and coefficient of variation (CV), mean absolute bias (MAB), fit index (R^2), index of agreement (IOA), and Akaike information criterion (AIC). AICs for the linear model denoted as NA were subject to scaled power transformation and therefore transformed values were not comparable with other values in their original form.

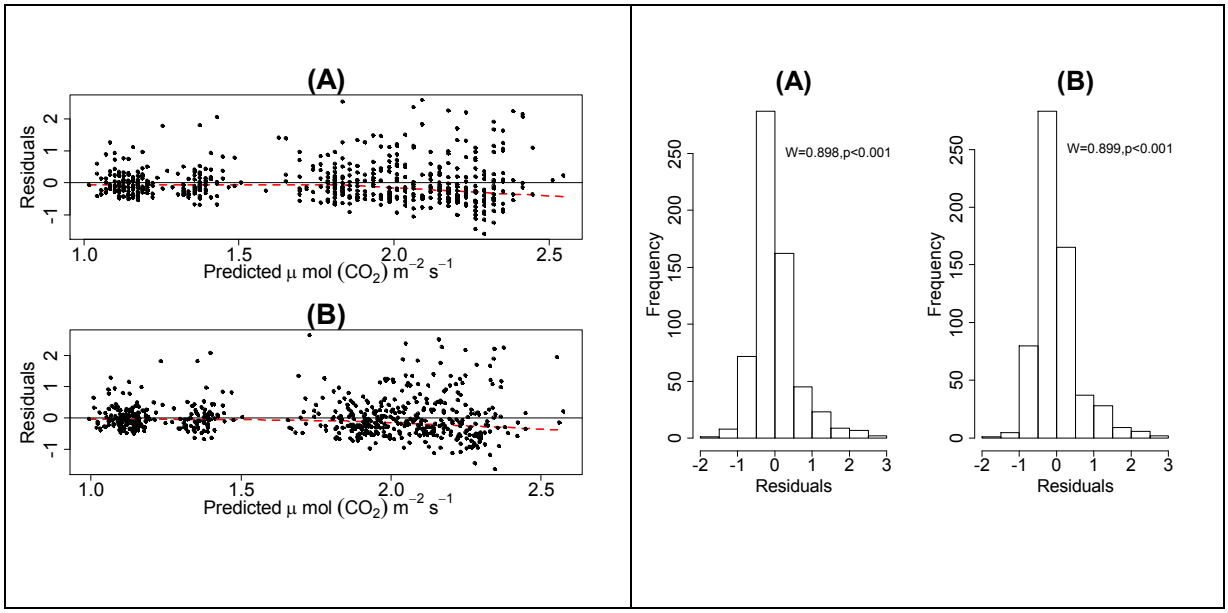

Figure 3.5: Predicted vs. residual values of F_s and corresponding histogram of residuals for selected (A) T_s-based equation **3.4** and (B) T_s and θ_v-based equation **3.8.**

Influence of T_s on F_s across silvicultural treatments

The T_s-based model (Eq. **3.4**) was applied separately for five clones, three level of stockings, two level of fertilizations, and two level of follow-up herbicide treatments to further examine the relationship between F_s and T_s; and the results are given in Table 3.7A. The T_s explained 26.63–47.82% of the variability in F_s, with the highest variation from a model with stocking of 1,250 stems ha^{-1}, and the lowest from a model with clone 1 (Table 3.7A). The applied Q_{10} values ranged from 2.98 to 5.03 across all silvicultural treatments, with the highest Q_{10} in clone 3 and the lowest in clone 2. The slope between T_s and F_s increased exponentially and was higher in the fertilized plot (Figure 3.6A), and in the plots without follow-up weed control treatment (Figure 3.6B) than in the non-fertilized and understorey-eliminated plot, respectively. The slope of the relationship between T_s and F_s tended to be higher for stocking 1,250 stems ha^{-1} than for 625 and 2,500 stems ha^{-1} (Figure 3.6C). For the model with clones, the slope of T_s with F_s was significantly higher in clone 3 than in the other four clones (Figure 3.6D). Comparing across separate silvicultural treatments in the T_s-based model, the Q_{10} values were higher in clone 3, stocking 1,250 stems ha^{-1}, plots with non-fertilizaton and without follow-up herbicide treatment (Table 3.7A), indicating that F_s was most sensitive to T_s in those levels of treatments.

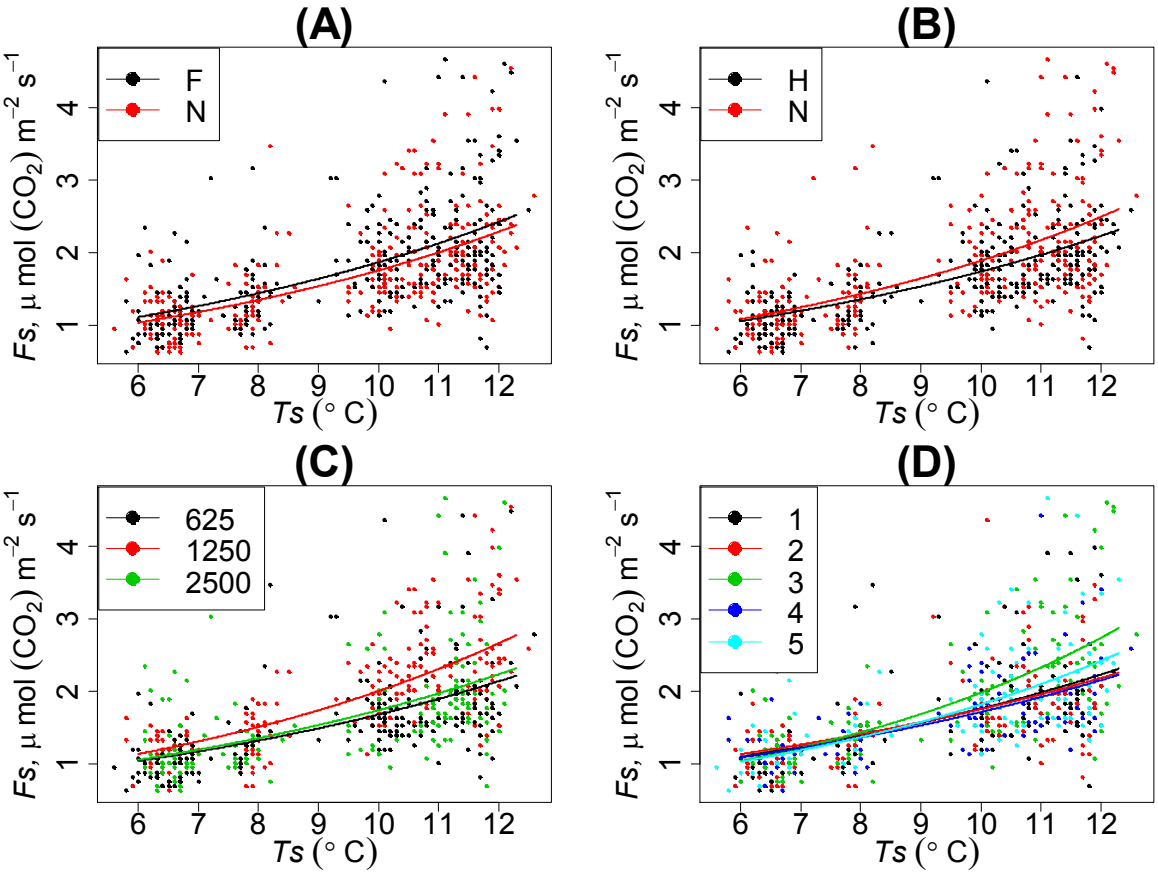

Figure 3.6: Exponential relationship between F_s and T_s across silvicultural treatments: (A) fertilization (F = fertilization, N = no fertilization), (B) follow-up herbicide (H = herbicide, N = no herbicide), (C) stocking (625, 1,250, and 2,500 stems ha^{-1}) and (D) clones (1–5). Lines were fitted using model parameters of each treatments. T_s was measured at 10 cm soil depth. All fitted models across each treatments were statistically significant ($p < .001$).

Influence of T_s and θ_v on F_s across silvicultural treatments

The combined T_s and θ_v-based model (Eq. **3.8**) was fitted separately five clones, three level of stockings, two level of fertilizations, and two level of follow-up herbicide treatments, to examine further the combined effects of T_s and θ_v on F_s; and the results are given in Table 3.7B.

The combined model yielded relatively higher R^2 values and lower RMSE values than simply T_s based model (Table 3.7B). The combined model explained a 27.90– 48.94% variation in F_s across all levels of treatment. However, the effect of θ_v is insignificant for some levels of treatment (Table 3.7B). Unlike the Q_{10} values in the T_s based model, the fitted Q_{10} values of the combined model were marginally higher, ranging from 2.91 to 5.23 across all the treatments, with the highest in clone 3 and lowest in clone 2. Compared with separate silvicultural treatments, the Q_{10} values in the combined model were higher in clone 3 than the other four

clones, higher in the stocking 1,250 stems ha^{-1} than in the other two stockings, higher in the non-fertilized plots than in the fertilized, and higher in plots without follow-up herbicide treatment than in the understorey-eliminated plots (Table 3.7B). In the combined model, the slope of the T_s was positive but the slope of the θ_v was negative across all levels of treatments, indicating that T_s has positive effects and θ_v has negative effects on F_s (Table 3.7B). A three-dimensional (3D) scatter plot also indicates that F_s increase with the increase in T_s, while it decreases when θ_v is higher (Figure 3.7).

Table 3.7: Regression models for the relationship between F_s, T_s, and θ_v across the clone (five clones), stocking (625, 1,250, and 2,500 stems ha^{-1}), fertilization (F = fertilization, NF = no fertilization), and follow-up herbicide (H = herbicide, NH = no herbicide) treatments.

(A) T_s-based: $F_s = ae^{bT_s}$						
Factors	**Levels**	**a**	**b**	**R^2**	**Q_{10}**	**RMSE**
Clone	1	0.5401***	0.1182***	0.2663	3.2592	0.6563
	2	0.5882***	0.1093***	0.2975	2.9816	0.5658
	3	0.3938***	0.1615***	0.4692	5.0288	0.6319
	4	0.5473***	0.1141***	0.4126	3.1294	0.4407
	5	0.4357***	0.1429***	0.4313	4.1723	0.5447
Stock	625	0.5023***	0.1206***	0.3314	3.3402	0.5446
	1,250	0.4839***	0.1419***	0.4782	4.1366	0.5373
	2,500	0.4976***	0.1251***	0.3106	3.4927	0.6194
Fert.	F	0.5074***	0.1302***	0.3556	3.6780	0.6096
	NF	0.4664***	0.1324***	0.3797	3.7592	0.5561
Herb.	H	0.5005***	0.1245***	0.3913	3.4719	0.5167
	NH	0.4707***	0.1389***	0.3592	4.0121	0.6377
(B) T_s and θ_v-based: $F_s = ae^{bT_s}e^{c\theta_v}$						
Factors	**Level**	**a**	**b**	**c**	**R^2**	**Q_{10}**	**RMSE**
Clone	1	0.9801*	0.1227***	−0.0376 ns	0.2790	3.4110	0.6506
	2	0.4119*	0.1068***	0.0222 ns	0.3011	2.9104	0.5643
	3	0.7873*	0.1654***	−0.0433 ns	0.4822	5.2284	0.6241
	4	0.8550*	0.1177***	−0.0281 ns	0.4223	3.2449	0.4371
	5	0.6908**	0.1485***	−0.0306 ns	0.4407	4.4159	0.5401
Stock	625	1.0052**	0.1264***	−0.0440*	0.3502	3.5403	0.5369
	1,250	0.7822***	0.1475***	-0.0316 *	0.4894	4.3714	0.5315
	2,500	0.4951*	0.1250***	0.0003 ns	0.3106	3.4919	0.6194
Fert.	F	0.7373***	0.1323***	−0.0232 ns	0.3604	3.7552	0.6073
	NF	0.8296***	0.1386***	−0.0374 *	0.3917	3.9998	0.5507
Herb.	H	0.9232***	0.1303***	−0.0393 **	0.4081	3.6801	0.5014
	NH	0.6058**	0.14056***	−0.0158 ns	0.3610	4.0776	0.6474

Note: Given a, b, and c are parameter estimates of the regression, RMSE is the root mean square error, R^2 is the fit index, Q_{10} *is the temperature sensitivity index for* F_s *(at 10 °C increase in* T_s*).*

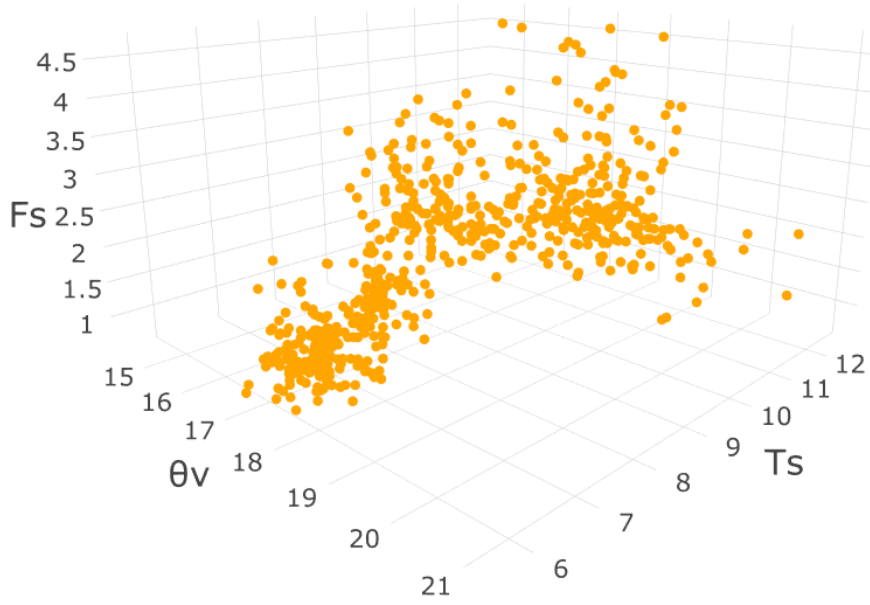

Figure 3.7: 3D scatter plot showing the relationship between F_s (µmol CO_2 m^{-1} s^{-1}), T_s (°C at 10 cm soil depth), and θ_v (volumetric water content % at 10 cm soil depth).

Relationships of F_s with soil physical properties

Separate correlation analyses for F_s and T_s with soil physical properties across the silvicultural treatments are given in Appendix 2.5 and Appendix 2.6, respectively. F_s correlated significantly with T_s, which explains much about the changes of F_s across all levels of treatments (r = 0.53–0.69; $p < 0.001$). In particular, the correlation between F_s and T_s was notably the highest ($p < 0.001$) in clone 3 (r = 0.69), stocking 1,250 stems ha^{-1} (r = 0.65), non-fertilized plots (r = 0.63), and follow-up weed control plots (r = 0.63). Although the relationship was weak, a positive correlation observed between F_s and BD at 10, 20 and 30 cm soil depth (r = 0.05–0.29), and WFPS at 20 cm soil depth (r = 0.02–0.3; $p < 0.05$) across the all levels of treatment. A significant negative correlation was observed between F_s and θ_v at 20 and 30 cm depth (r = −0.06 to −0.41), PORE at 10, 20 and 30 cm depth (r = −0.05 to −0.3), WFPS at 10 and 30 cm depth (r = −0.02 to −0.32), and RF at 10, 20 and 30 cm depth (r = −0.01 to −0.17) across the all treatments. In particular, the correlation between F_s and θ_v at 20 cm soil depth was significantly negative in stocking 1,250 stems ha^{-1} ($p < 0.001$). Significant correlations were not observed between F_s and θ_v at 10 cm depth across all level of treatments

($p > 0.05$), except for stocking 1,250 and 2,500 stems ha^{-1} ($p < 0.05$) and plots without follow-up weed control ($p < 0.001$).

T_s was positively related to WFPS at 20 cm soil depth ($p < 0.05$). A significantly negative correlation between T_s with θ_v was observed at 20 and 30 cm depth (r = −0.14 to −0.41; $p < 0.05$), whereas it was not significantly related to θ_v at 10 cm depth ($p > 0.05$) across all levels of treatment. Similarly, T_s correlated negatively with WFPS (r = −0.13 to −0.51) at 10 cm ($p < 0.001$) and 30 cm soil depth ($p < 0.05$) across all levels of treatment.

Discussion

Effects of stocking on F_s

As expected the value of F_s did not increase with stand density. However, plots with 1,250 stems ha^{-1} exhibited consistently higher efflux rates, increasing by 22% and 18%, compared with 625 and 2,500 stems ha^{-1}, respectively across all seasons. F_s across stocking in this study (20.61–26.30 tonne CO_2 ha^{-1} yr^{-1}) was within a range investigated by Noh et al. (2010) for a *P. densifolia* forest in Korea (22.77–27.32 tonne CO_2 ha^{-1} yr^{-1}) with the highest value in medium density stocking. The rate of F_s was highest in medium density stocking (600 stems ha^{-1}) with 7.45 tonne C ha^{-1} yr^{-1} (≈ 27.32 tonne CO_2 ha^{-1} yr^{-1}) compared to low stocking (375 stems ha^{-1}) with 6.96 tonne C ha^{-1} yr^{-1} (≈ 25.52 tonne CO_2 ha^{-1} yr^{-1}), and high stocking (938 stems ha^{-1}) with 6.21 tonne C ha^{-1} yr^{-1} (≈ 22.77 tonne CO_2 ha^{-1} yr^{-1}) (Noh et al., 2010).

In contrast, Litton, Ryan, & Knight (2004) reported that the below-ground allocation of carbon increased with the stand density in 13-year-old *P. contorta* of the same age, with 68, 237, and 306 g C m^{-2} yr^{-1} for low (< 1,000 stems ha^{-1}), medium (7,000–40,000 stems ha^{-1}), and high (> 50,000 stems ha^{-1}) stocking. Another study also found that F_s measured during the growing season of 13-year-old *P. contorta* increased with the tree density by 1.0, 1.8, and 2.1 µmol CO_2 m^{-2} s^{-1} for low, medium, and high-density stands (Litton, Ryan, Knight, et al., 2003). Although F_s differed significantly with stand density and higher efflux rates observed in medium density stocking of the same age, the hypothesis of this study did not support an increase in F_s with stand density. However, differences were mostly attributed to seasonal changes in T_s as the highest T_s values were observed at the 1,250 stems ha^{-1} stocking (Table 3.4). Some studies reported that stocking can directly influence soil physical properties such as T_s, θ_v, and soil nutrient availability (Litton et al., 2004; Litton, Ryan,

Knight, et al., 2003; Tang, Qi, Xu, Misson, & Goldstein, 2005). These effects of stocking on soil physical properties can also directly affect F_s, such as through competition for limited resources (Gower, Vogt, & Grier, 1992), and a shift of carbon partitioning from above- to below-ground (Giardina & Ryan, 2002; Litton et al., 2007). Further studies, therefore, are recommended to evaluate the effects of stocking on the microclimatic conditions of the site and the physiological conditions of the trees, such as root biomass, total photosynthesis, and thereby their effects on F_s.

Effect of clone on F_s

The hypothesis regarding the effects of the clone on F_s was supported by the results of this study as the main effect of clone on F_s was statistically significant for the whole period of the experiment, separately for the autumn and summer season. This result suggests that clone 3 had a high influence on F_s and produced overall higher mean values of F_s (about 3 to 10 %) compared with other clones (Table 3.3). This higher efflux rate from clone 3 is attributed to T_s, as higher overall mean T_s were observed in clone 3 (about 0.4 to 1.6%) compared with the other clones (Table 3.4). Clone 3 in this study is initially chosen for its high microfibril angle and high basic wood density. A study in 11-year-old *P. radiata* plantations in New Zealand reported a significant influence of clones on the microfibril angle of the wood (Lasserre, Mason, Watt, & Moore, 2009). The faster-growing genotypes exhibit greater carbon partitioning to aboveground net primary production (ANNP) at the expense of total below-ground carbon flux (TBCF) (Bown, Watt, Clinton, et al., 2009). This indicates that clone 3 could allocate more carbon with higher amount of light capture and photosynthesis, which may have influenced the overall carbon assimilation (Bown, Watt, Clinton, et al., 2009).

Although there were no field studies available on the differences in F_s across different clones, this study can be compared to findings from a greenhouse experiment, which examined four distinct *P. radiata* clones that represented different growth performance within the central North Island of New Zealand. The greenhouse study found a significant effect of nutrient treatment on a ratio of F_s to TBCF, with a greater effect of low nitrogen and low phosphorus addition (61%) compared with combined nitrogen and phosphorous supply (49%) (Bown, Watt, Clinton, et al., 2009). This greenhouse study also explained significant genotypic variation in aboveground growth rates suggesting higher gains in carbon use efficiency. Therefore, further comparison in different sites with different levels of nutrient could provide insight into how fertility regulates the F_s across the different clones. Moreover, the results of this study are from a site that experiences seasonal water limitations,

and so further comparison on sites that do not experience water limitations over the growing season could benefit the findings of clonal effect on F_s.

Effects of fertilization on F_s

The initial hypothesis expecting an increase in F_s with fertilization was not supported by the results of this study at any season during the year. This result was consistent with a study on planted slash pine (Castro et al., 1994; Shan et al., 2001), planted ponderosa pine (Vose et al., 1995), and natural red pine stands (Jeong, Bolan, & Kim, 2016), as no significant effects of fertilization on F_s were observed. Authors suggested that changes in F_s could be related to the differences in soil carbon among treatments (Baker, Oliver, & Hodgkiss, 1986; Johnson, 1992; Nohrstedt, Arnebrant, Bååth, & Söderström, 1989; Shan et al., 2001). Soil carbon was increased by fertilization in most of the cases when the available literature on soil carbon storage was reviewed and reported by Johnson (1992). The increase in soil carbon by fertilization can be due to increases in productivity, thereby increasing the soil organic matter input, and stabilisation of soil organic matter in the soil throughout the rotation (Johnson, 1992). There are several contrasting results, however, on the effects of fertilization on F_s (Brumme & Beese, 1992; Dulohery, Morris, & Lowrance, 1996; Kim, Jeong, Bolan, & Naidu, 2012; Shrestha, Strahm, Sucre, Holub, & Meehan, 2014; Van Lear, Kapeluck, & Parker, 1995). There are two possible reasons for the insignificant effects of fertilization on F_s in this study: (a) as the last fertilization was applied in Year 3 after planting, the effects after 9 years after fertilization might have already ceased and smoot over time to produce measurable differences in soil carbon; therefore, differences in F_s were insignificant, and (b) two opposite effects reported by Vose et al. (1995) show that, firstly, there was an increase in autotrophic respiration by the addition of nitrogen (Ryan, Hubbard, Pongracic, Raison, & McMurtrie, 1996), and secondly, there was a decrease in heterotrophic respiration due to a decrease in microbial activity (Söderström, Bååth, & Lundgren, 1983), so both an increase and a decrease in the effects may provide insignificant effects on F_s. However, the results of this study can be expected to change with increases in stand age, as some studies pointed out that F_s may vary across stand age (Bown & Watt, 2016; Shrestha et al., 2014; Wiseman & Seiler, 2004). Fertilization can have long-term implications that would produce a measurable change in soil carbon, and thereby F_s (Kim et al., 2012). It is recommended that further research evaluates and compares the F_s response to fertilization in older age *P. radiata* plantations.

Effects of understorey-elimination on F_s

The hypothesis that follow-up herbicide would decrease F_s was not supported by the results of this study. In contrast to this result, some studies indicated that understorey elimination significantly affected F_s (Carlyle, 1993; Shan et al., 2001; Wan et al., 2014). These studies found that the effects of understorey elimination on F_s was mainly associated with significant change in organic materials from above- to below-ground in the earlier rotation, and change in input by root litter throughout the rotation. Hence, the possible reasons for the insignificant effects of understorey elimination on F_s in this study could be an insignificant change in fine-root turnover and inadequate input of root litter into the soil as suggested by Shan et al. (2001).

Seasonal variation in F_s

Strong seasonal differences in F_s, T_s, and θ_v were observed. The average annual rate of F_s estimated from this study (22.71 ± 1.02 tonne CO_2 ha^{-1} yr^{-1}, range 15.64 to 27.76) was consistent with the figure estimated by Raich & Schlesinger (1992) from temperate coniferous forests (681 ± 95 g C m^{-2} yr^{-1} ≈ 24.97 ± 3.49 tonne CO_2 ha^{-1} yr^{-1}). The mean value of F_s was highest in autumn (27.76 tonne CO_2 ha^{-1} yr^{-1}) and lowest in winter (15.64 tonne CO_2 ha^{-1} yr^{-1}), which generally followed the seasonal cycle of T_s and θ_v. This result is consistent to previous studies, which reported that these variations were primarily attributed to environmental factors such as T_s and θ_v (Davidson et al., 1998; Martin & Bolstad, 2005; Walker et al., 2004); vegetation characteristics, such as stand density and tree physiology (Olajuyigbe, Tobin, Saunders, & Nieuwenhuis, 2012; Raich & Tufekciogul, 2000); soil microbial populations (Asaye, 2015), and the quantity and lability of dead organic matter (Olajuyigbe et al., 2012). The seasonal pattern of F_s may vary across geographic locations and seasons (Yiqi & Zhou, 2010).

The highest efflux rates were observed in autumn, when T_s was moderate (11 °C) and θ_v was higher (17.68%), and the lowest efflux was observed in winter, when T_s was lowest (6.83 °C) and θ_v was moderate (17.15%) (Table 3.3, Table 3.4, Table 3.5). This showed that T_s was the limiting factor in winter, and θ_v was the limiting factor during summer. The study site has a typical cool temperate climate with the lowest rainfall in winter, and highest temperatures in summer (NIWA, 2018). A study pointed out that belowground microbial activities and root respiration are sensitive to T_s and θ_v, which in turn may affect the seasonal variation in F_s (Asaye, 2015). Therefore, the high value of F_s in this study in autumn may be attributed to the higher growth rate of the plant due to moderate T_s

and θ_v conditions that stimulate plant root respiration and accelerate the rate of microbial decomposition because of the optimal environment for microbes (Tang et al., 2005). In contrast, the low value of the F_s in winter could be due to slow microbial decomposition at low temperature and decreased root respiration (Dörr & Münnich, 1987). This study explored the seasonal variation in F_s in relation to T_s and θ_v. The changes in environmental conditions such as T_s and θ_v could affect forest productivity and growth, which in turn may affect soil microbial activity and root respiration. Therefore, further study is suggested to examine separate auto-and heterotrophic components of F_s in relation to seasonal growth and productivity of forests.

Temperature sensitivity of F_s

In modelling F_s, the temperature sensitivity of F_s (Q_{10}) has been discussed frequently (Gulledge & Schimel, 2000; Lloyd & Taylor, 1994; M. Xu & Qi, 2001a, 2001b), and Q_{10} indicate the response of F_s when temperature increases by 10 °C (Lloyd & Taylor, 1994; Van't Hoff & Lehfeldt, 1899). Recorded values of Q_{10} in this study (2.91 to 5.23) across all treatments were in the range of other reports (Davidson et al., 1998; Gulledge & Schimel, 2000; Kirschbaum, 1995, 2000; Raich & Schlesinger, 1992; M. Xu & Qi, 2001b), as widely discussed that Q_{10} may vary (1 to 10) depending on the type of ecosystem. However, Q_{10} values in this study were varied compared to the range of 3.45–3.77 reported for old (70-year) natural *P. densiflora* in Korea (Noh et al., 2010); they were lower than the range 3.28–6.22 for oak natural forests in central Korea (Yi et al., 2005); higher than the range 1.78–2.45 for old *P. densiflora* in Japan (Nakane, Tsubota, & Yamamoto, 1984; Nakane, Yamamoto, & Tsubota, 1983); and within the range 2.61–3.75 for temperate forests in China (C. Wang, Yang, & Zhang, 2006). These variations in Q_{10} value are attributed to the type of ecosystem and climatic conditions that were reported (Davidson et al., 1998; Raich & Schlesinger, 1992).

The Q_{10} value in this study was highest in clone 3, stocking 1,250 stems ha^{-1}, fertilized plots and plots without follow-up weed control compared with the other (four) clones, stocking 625 and 2,500 stems ha^{-1}, non-fertilized plots, and plots with follow-up weed control. This highest Q_{10} value from those levels of treatments suggested that they have the highest influence on temperature sensitivity of F_s. In clone 3 the high value of Q_{10} is probably due to the highest T_s compared with other clones. The Q_{10} value is a temperature dependent that is a response of F_s with 10 °C increase in temperature, which has been widely recognized by many authors (Kirschbaum, 1995; Lloyd & Taylor, 1994; Thierron & Laudelout, 1996), and availability of the respiratory substrate can play a vital role for Q_{10} to F_s (Liu et al., 2006). The increased supply of the respiratory substrate can accelerate Q_{10} (Dhillion,

Roy, & Abrams, 1995). Therefore, in this study, the higher respiratory substrates from plant root as well as from soil organic matter could have resulted in high Q_{10} in those levels of treatments. In addition, F_s from forest soil mostly depends on translocation of the amount of photosynthetic materials from the above-to below-ground of the tree (Högberg et al., 2001). A study also reported that F_s rates likely to be most sensitive to photosynthetic activity of the plant across different seasons (Janssens, Carrara, & Ceulemans, 2004), and so the sensitivity of T_s to F_s across different treatments in this study could be associated with the seasonal changes in photosynthetic phenomena.

F_s in relation to T_s and θ_v

In regression analysis, F_s was modelled using T_s and θ_v at 10 cm soil depth as 10 cm depth has been widely used to explain relationships between F_s, T_s, and θ_v (Yiqi & Zhou, 2010). In this study, the θ_v threshold (> 14.3%) was determined, at which the clear exponential relationship between F_s and T_s was observed. This threshold indicated that response of F_s to T_s was increased when θ_v was > 14.3%, and vice versa. Like the findings in this study, the F_s response to T_s was higher (Q_{10} = 1.8) when θ_v was > 14%, and was lower (Q_{10} = 1.4) when θ_v was < 14% (M. Xu & Qi, 2001a). However, the θ_v threshold may vary across different ecosystems depending on the factors constraining water uptake by plants and microbes (Chang et al., 2014). There were no comparable field studies available that investigated the F_s response to T_s and θ_v in different ecosystem types in New Zealand. However, studies in other areas reported that F_s depend only on T_s when θ_v was more than 17% (Chang et al., 2014), 10% (Almagro, López, Querejeta, & Martínez-Mena, 2009), 9% (Chang et al., 2016), and 20% (Rey et al., 2002), and suggested that below this threshold the relationship was weakened. Other researchers also modelled F_s with T_s by determining the θ_v threshold (Fang & Moncrieff, 2001; Lellei-Kovács et al., 2011; Palmroth et al., 2005; B. Wang et al., 2014).

In regression analysis of a segmented data set in which θ_v > 14.3%, T_s explained the highest variability (26.63–47.82 %) in F_s across all silvicultural treatments (Table 3.7). T_s at 10 cm soil depth correlates significantly positively to F_s (r = 0.53–0.69), while θ_v at 10, 20 and 30 cm soil depth correlates negatively and weakly (r = −0.01 to +0.41) across all silvicultural treatments (Appendix 2.5). These results are supported by other studies which indicated that T_s is an important driver for predicting F_s (Jonsson & Sigurdsson, 2009; Jonsson & Sigurdsson, 2010; Kim et al., 2012; Maier & Kress, 2000; Noh et al., 2010; Raich & Potter, 1995; Raich & Schlesinger, 1992; Saiz et al., 2006), as T_s directly influences the respiratory enzymes of both plant roots and soil microbes (Chang et al., 2014; J. Xu et

al., 2011; Yiqi & Zhou, 2010). These results are also comparable to studies on loblolly pine (Maier et al., 2016; Pangle & Seiler, 2002; Samuelson et al., 2004).

The negative relationship between F_s and θ_v observed in this study was similar with other studies (Lai et al., 2012; Rey et al., 2002; Saiz et al., 2006; M. Xu & Qi, 2001a), indicating the modelling of F_s as a function of θ_v has no significant usefulness because of the statistically insignificant result . The negative response of θ_v to F_s could have two possible reasons: (a) a decrease in substrate supply (Davidson, Janssens, & Luo, 2006), due to drying out of surface soil, and (b) a decrease in photosynthesis, which affect the translocation of photosynthetic material from above- to below-ground (Bhupinderpal et al., 2003; Chang et al., 2014; Högberg et al., 2001), which in turn simultaneously influences F_s. It was also reported that a low θ_v condition can limit F_s by reducing the supply of substrate, and the respiratory enzymes and soil microbes, due to an increase in diffusion resistance (Davidson et al., 2006; Orchard & Cook, 1983; Yu et al., 2011). However, Raich & Potter (1995) noted that when θ_v was sufficient up to the physiological requirement of plants and soil microbes, it might have been an important variable affecting F_s. The value of θ_v is likely to become a limiting factor for F_s under two conditions: (a) when soils are dry, and (b) when soils are saturated up to a level of anaerobic conditions (Raich & Potter, 1995). In this study, the former could be a reason for limiting F_s, as soils in the study site were relatively dry, particularly in summer (Figure 3.3A).

Many studies suggest that θ_v can contribute to the highest variability in F_s when considered with other variables, such as T_s (Davidson et al., 1998; Raich & Tufekciogul, 2000; Reichstein et al., 2003). The results of this study are consistent with those previous studies, as T_s and θ_v jointly provided relatively high variability (27.90–48.94 %) in F_s compared to T_s across all silvicultural treatments (Table 3.7A, Table 3.7B). This result is supported by other previous studies, which reported that the combination of T_s and θ_v can explain most of the variations in F_s, and are important factors in controlling F_s (Borken, Xu, Davidson, & Beese, 2002; Jia, Zhou, Wang, Wang, & Wang, 2006). Although the combined T_s and θ_v based model better predicted F_s across all silvicultural treatments, in terms of the applicability of this model, the residual analysis showed that F_s rates were estimated accurately at low temperatures when T_s is below 10 °C (Figure 3.8A); with soil moisture, it was slightly over-estimated across the whole θ_v range (Figure 3.8B). Moreover, in the combined model, estimated values of a, and b were always positive, and values of c were always negative (Table 3.7B), indicating that temperature contributes positively to F_s, while θ_v contributes negatively to F_s. The positive effect of soil temperature on F_s is consistent with other studies (Jonsson & Sigurdsson, 2010; Kim et al.,

2012; Maier & Kress, 2000; Noh et al., 2010), and therefore T_s is the more important predictor compared to θ_v in modelling F_s in *P. radiata* plantations.

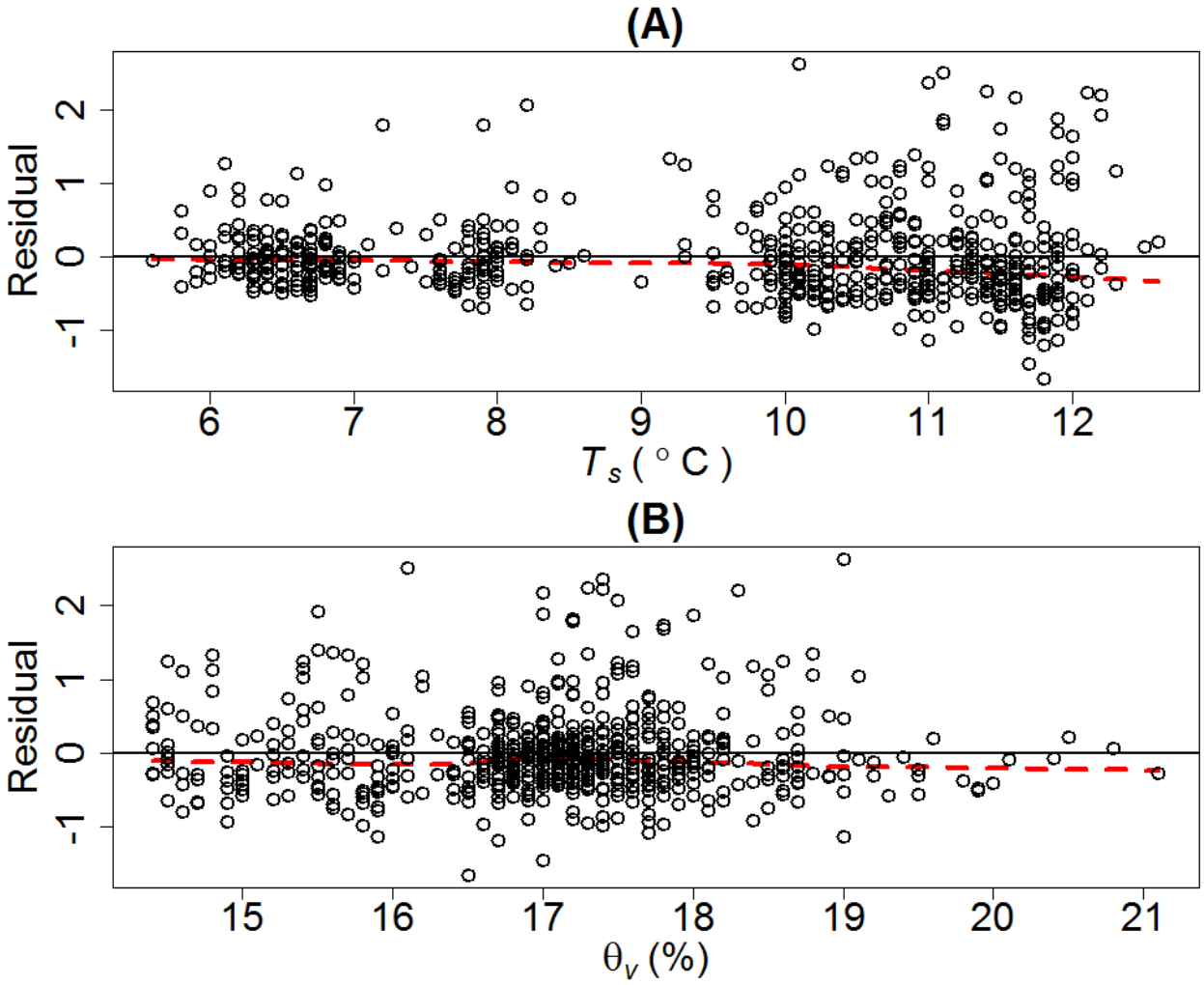

*Figure 3.8: The residuals of the best F_s models based on combined T_s and θ_v (Eq. **3.8**) plotted separately with measured (A) T_s and (B) θ_v values.*

Soil variables influencing F_s

The significant positive relationship between F_s and BD (r = 0.05–0.29) observed in this study (Appendix 2.5) is similar to that of a previous study (Godwin, Kobziar, & Robertson, 2017). F_s correlates negatively with PORE (r = −0.05 to −0.3) and WFPS (r = −0.02 to −0.32) (Appendix 2.5). This negative relationship may suggest that pore space filled with high water content may reduce the accumulation of CO_2, and pore space filled with less water may inhibit the soil microbial and root metabolic activity, as suggested by Gliński & Stępniewski (1985). A negative correlation was also observed between T_s and WFPS (r = −0.13 to −0.51) at 10 cm soil depth across all silvicultural treatments (Appendix 2.6), suggesting that T_s may influence F_s through its influence on the WFPS.

The negative relationship between F_s and RF ($r = -0.01$ to -0.17) was observed (Appendix 2.5). This result is supported by a previous study that showed F_s had a significantly negative relationship with rock fragments, with 21.7% variability in explaining F_s (Wiseman & Seiler, 2004). Another study also reported decrease in F_s with an increase in RF (Pangle, 2000). The reason for this decrease of F_s due to an increase of RF may be associated with a decrease in water availability, soil organic matter and fine-root spread (Rustad et al., 2000).

Conclusions

Season, stocking, and clone had a significant, positive influence on F_s in a *P. radiata* plantations in the Canterbury region of New Zealand. The rate of F_s was by far the highest in autumn (27.76 tonne CO_2 ha^{-1} yr^{-1}) and lowest in winter (15.64 tonne CO_2 ha^{-1} yr^{-1}). T_s was highest in summer (16.96 °C) and lowest in winter (6.83 °C), while θ_v was lowest in summer (7.32 %) and highest in autumn (17.68 %). Clone 3, initially chosen for its high microfibril angle and high basic wood density, significantly increased F_s (about 3–10%) compared with the other four clones. F_s increased significantly in plots with 1,250 stems ha^{-1}, compared with 625 (by 22%) and 2,500 (by 18%) stems ha^{-1}. A moisture threshold (> 14.3%) was identified after which a clear exponential relationship between F_s and T_s was observed. A model with combination of T_s and θ_v explained the relatively high percentage of observed variation (27.90–48.94%) in F_s compared with T_s only (26.63–47.82%). However, the combined model indicated that T_s had positive effects and θ_v had negative effects on F_s, as the gradient of T_s across all silvicultural treatments was positive, and the gradient of θ_v across those treatments was negative. Therefore, T_s was the most important predictor for modelling F_s.

As silvicultural treatments have been shown to influence F_s in this experiment, these practices could have significant impacts on carbon budget, given the extensive *P. radiata* plantation in New Zealand. Although F_s is only a part of the carbon budget, the F_s has to be analysed together with gross primary productivity in order to determine the regional emissions of CO_2 from plantations.

Chapter 4. Linking above-ground biomass production to below-ground carbon dynamics across stocking, clone, fertilization, and understorey elimination in *Pinus radiata* plantations, New Zealand

Highlights

- Stocking, follow-up weed control, and clone significantly influenced above-ground biomass production and soil respiration.
- Above-ground biomass production increased while the BSR/AGB ratio decreased as stand density increased.
- Follow-up weed control enhanced above-ground biomass.
- Slow growing clones exhibited a greater BSR/AGB ratio compared to faster growing clones, suggesting carbon partitioning as a mechanism explaining clones' growth performance.
- Above-ground biomass production and basal area increased with stand density. Tree diameter and height decreased with stand density.

Summary

The linkage between above-ground biomass production and below-ground carbon (C) fluxes as influenced by silviculture has been little studied, and changes in allocation above- versus below-ground may assist understanding the physiological mechanisms underlying silviculture. This study aimed to investigate the effects of stocking, clone, fertilization, and follow-up herbicide treatments on below-ground soil respiration (BSR), above-ground biomass production (AGB), the ratio (BSR/AGB), tree diameter (DBH), height (H), basal area (G), and leaf area index (LAI). The experiment was planted with *Pinus radiata* in 2005 in a dry site in the Canterbury region of New Zealand, and was measured for this study in the period 2017–2018, when trees were 12-13 years old. Mixed-effects analysis of variance was carried out using data at the plot and clone levels.

The BSR rate was significantly affected by the main effects of stocking and clone. Significant interactions of both stocking × follow-up herbicide and clone × follow-up herbicide were observed for AGB and DBH. Significant interaction of both stocking × follow-up herbicide

and stocking × clone were observed for G. The BSR/AGB ratio and H were significantly affected by main effects of clone, follow-up herbicide, and stocking. No significant effects of silvicultural treatments on LAI were observed. No significant effects of fertilization on above-ground and below-ground variables were observed.

Estimated mean values of variables at age 12 were as follows: 6.58 tonne C ha^{-1} yr^{-1} (range 5.93–7.52) for BSR, 55.25 tonne C ha^{-1} (range 49.39–59.61) for AGB, 19.45 cm (range 14.79–24.28) for DBH, 13.10 m (range 12.8–13.56) for H, 36.62 m^2 ha^{-1} (range 29.32–43.50) for G, and 3.27 m^2 m^{-2} (range 3.15–3.35) for LAI. BSR increased by 26.8% from 625 to 1,250 stems ha^{-1}, and then decreased by 16.4% from 1,250 to 2,500 stems ha^{-1}. Clones 1 and 3 exhibited greater AGB and smaller BSR/AGB ratio, compared to slower growing clones (i.e., Clones 4 and 5). BSR/AGB ratio was greatest at 625 stems ha^{-1} by 19.1% and 31.6% compared with 1,250 and 2,500 stems ha^{-1}, respectively. Values of AGB, and G increased with stand density, while DBH and H decreased with stand density. The AGB was higher by 20.7% and 5% at 2,500 stems ha^{-1}, compared with 625 and 1,250 stems ha^{-1} respectively. AGB, DBH, H, and G were significantly greater with follow-up weed control treatment than in those without follow-up weed control.

Stocking, follow-up herbicide, and clone, in that order, had the greatest influence on DBH followed by G, AGB, and H. Results suggest that stocking, weed control and clone shifted carbon partitioning above-and below-ground.

Key words: *Pinus radiata; below-ground; above-ground; carbon; partitioning; stocking; clone; fertilization; follow-up herbicide*

Introduction

Pinus radiata is a widely planted tree species in New Zealand, Australia, South Africa, and Chile, (Mead, 2013). Due to higher productivity and greater adaptability to varied environmental conditions, the planted area across the Southern Hemisphere is now more than 4 million hectares, with a wider range of end-use products than other plantation forest species (Lavery & Mead, 2000; Lewis et al., 1993; Sutton, 1999; Turner & Lambert, 1986). In New

Zealand, *P. radiata* is the predominantly planted species, accounting for about 90% of a total of 1.70 million hectares (Nixon et al., 2017). The *P. radiata* plantations in New Zealand can play a significant role in sequestration of carbon and it's storage (Hollinger et al., 1993), both by using wood products for a longer period of time as well as by storing carbon in the soil and biomass (Nixon et al., 2017; Scott et al., 1999). Assessment of the significance of plantation forestry in mitigating climate change requires better knowledge of fundamental ecosystem processes and fluxes, particularly between soil, plants, and the atmosphere (Cao & Woodward, 1998). Planting trees at different stockings and with different clones, fertilization, and herbicides are the most common silvicultural practices for *P. radiata* in New Zealand. Most silvicultural studies of *P. radiata* in New Zealand have been focused on the assessment of above-ground productivity (Arneth, Kelliher, McSeveny, & Byers, 1998; Hollinger et al., 1993; Kauppi & Tomppo, 1993; Madgwick, 1983; McMurtrie, Rook, & Kelliher, 1990; McQuillan, 2013; Snowdon & Benson, 1992). However, these studies did not consider below-ground processes resulting from silvicultural treatments above ground. In addition, understanding of the above- and below-ground linkages would assist better and sounder planning of silvicultural regimes and adaptation strategies to contribute to mitigate climate change.

Because little is known about the above- and below-ground carbon allocation responses of *P. radiata* plantations to silvicultural treatments, this study is carried out to examine the effects of stocking, clone, fertilization, and follow-up herbicide treatments on below-ground soil respiration (BSR), above-ground biomass production (AGB), the ratio (BSR/AGB), tree diameter (DBH), height (H), basal area (G), and leaf area index (LAI) in a 12 to 13-year-old *P. radiata* trial in the Canterbury region of New Zealand. It was hypothesized that silvicultural treatments outlined above would change absolute magnitudes of BSR (Samuelson et al., 2004; Shan et al., 2001; Yohannes et al., 2013), AGB (Litton, Ryan, Tinker, et al., 2003; Snowdon & Benson, 1992) and some other relevant stand and tree variables such as G, DBH, H and LAI (Carlyle, 1998; Mason, 1992; Mason & Milne, 1999; McQuillan, 2013; Richardson, 1993). It was also hypothetized that silvicultural treatments would bring about relative changes in the BSR/AGB ratio, as already reported by other researchers (Haynes & Gower, 1995; Rubilar et al., 2013; Wardle et al., 2004; Zerihun & Montagu, 2004).

Materials and methods

Study site and design of the experiment

The experimental site was located just south of Rolleston (approx. 26 km south-west of Christchurch) within the Canterbury region of New Zealand (43° 37.2′ S and 172° 20.4′ E). The experiment was established by the School of Forestry, University of Canterbury, New Zealand, on land owned by the Selwyn District Council (Figure 1.1). At approximately 45 m above sea level on a flat landscape, the site is known to have wet and frosty conditions in winter, and windy and usually arid condition in summer. The site has an air median annual temperature between 11 and 13 °C with a monthly minimum (July) of −2 to +4 °C and a monthly maximum (January) of 20 to 23 °C (Macara, 2016). Annual rainfall is about 618 mm with a monthly range of 38 to 68 mm (Macara, 2016). The major soil type is a Lismore stony silt loam, with aggradation gravel as parent material, which also includes partial glacial gravel (NIWA, 2018; Xue et al., 2013).

The experiment consisted of 48 permanent plots of variable size with a randomized complete block factorial split design with 4 complete blocks (Mason, 2008), and an arrangement of factors within each block (Figure 1.2). The main treatment consisted of 3 levels of stocking (625, 1,250 and 2,500 stems ha^{-1}). A first split consisted of four levels of weed control and fertilization treatments (fertilization, F; herbicide, H; both, FH; and no chemical, NN). Fertilization was carried out once in year 1 and once in year 3 (NPKS + trace elements at a rate of 80 g per tree) after planting. Weed control treatment was applied in years 1 and 2 (strip weed control) and follow-up weed control in years 3 (herbicide) and any subsequent year when new weeds appeared after planting. A second split consisted of 5 different clones randomly allocated to all plots, with the clone numbers 1, 2, 3, 4 and 5 indicating preselected wood anatomical properties (Mason, 2008).

Above-ground vegetation and biomass

A forest inventory carried out in July 2017 was used to estimate above-ground biomass (AGB) and other stand level variables for each plot. Diameters at breast height (DBH), total tree height (H), and crown length (CrL) for all trees across 48 plots were measured. A Haglöf Vertex IV Ultrasonic Hypsometer was used to measure the H and CrL, and a graduated diameter tape to measure DBH.

LAI at a fertilization × follow-up weed control plot level was measured during four seasons (n = 4 seasons × 48 plots = 192) with a plant canopy analyser (LAI 2000, LI-COR Inc., Lincoln, Nebraska). Basal area (G) was computed using the DBH data and plot size in terms of m^2 ha^{-1}. Total AGB was computed from DBH, H, and CrL data; and an additive biomass model developed for this experiment (Chapter 2). Tree level above-ground biomass values (kg $tree^{-1}$) calculated from the additive biomass model were scaled to estimate plot level biomass production (tonne C ha^{-1}). It was assumed that carbon concentration was 50% of dry mass. All measured data were summarized and organized by using a *summaryBy* function of the *doBy* package in R software (Højsgaard, Halekoh, Robison-Cox, Wright, & Leidi, 2016), at the plot level (n = 48) and clone level (n = 240).

Below-ground soil respiration

Below-ground soil respiration (BSR) was measured using an EGM-4 (PP Systems, Hitchin, Hertfordshire, England) equipped with a soil respiration chamber (SRC-1) of 10 cm inner diameter. The EGM-4 is a closed static chamber system that provides an estimate of the soil CO_2 efflux (BSR) rate (g CO_2 m^{-2} hr^{-1}). From the 48 plots, a total of 240 BSR measurements were recorded in each season (48 plots × 5 clones). In four seasons, a total of 960 measurements were made (48 plots × 5 clones × 4 seasons). The total of 960 records collected over a year were summarized and organized by using the *summaryBy* function of the *doBy* package in R (Højsgaard et al., 2016), at the plot level (n = 48) and clone level (n = 240) for use in the analysis. Values of BSR were scaled into tonnes C ha^{-1} yr^{-1} using the equations of soil CO_2 efflux (F_s) vs soil temperature (T_s) and volumetric water content (θ_v) developed in Chapter 3 and continuous measurements of T_s and θ_v by in-site micrometeorological stations.

Below-ground to above-ground ratio

This ratio of BSR (tonne C ha^{-1} yr^{-1}) to AGB (tonne C ha^{-1}) (BSR/AGB) was used as a surrogate of carbon patitioning above versus below-ground. In order to determine the exact ecosystem root/shoot ratio, an estimation of both above-ground as well as below-ground net primary productivity (NPP) would be required. The data of this study did not include above-ground leaf litterfall production, nor below-ground components for the estimation of ecosystem

NPP. Readers should be aware that this index cannot be considered as an exact ecosystem root/shoot ratio, and therefore the ratio estimated in this study should be taken as a reference only.

Stand density index

To estimate stand density index (SDI), inventory data collected from the experiment from 2008 to 2017 were analyzed. These time series were subsequently summarized and organized, by using a *summaryBy* function of the *doBy* package in R (Højsgaard et al., 2016). The stand density of three levels (625, 1,250, and 2,500 stems ha^{-1}) of this experiment were treated as continuous variables for the SDI analysis. SDI was estimated by using the most commonly used equation (Eq. **4.1**) (Reineke, 1933).

$$SDI = tpha\left(\frac{DBH_q}{25}\right)^{1.6} \quad \textbf{(4.1)}$$

where SDI = Reineke's stand-density index, tpha = observed trees ha^{-1}, DBHq = quadratic mean diameter (cm)

Statistical analysis

All statistical analyses were carried out using the R system for statistical computing (R Core Team, 2017). Linear mixed effects models were implemented using the *nlme* package in R (Pinheiro et al., 2018). Variables were transformed using "Box-Cox" transformations (Box & Cox, 1964) (Eq. **4.2**), as necessary, to meet the fundamental assumptions (e.g., normality and homogeneity of variance) of the models used. However, results were reported in their original forms using a back transformation (Eq. **4.3**). The effects of stocking, clone, fertilization and follow-up herbicide treatments on BSR, AGB, BSR/AGB ratio, DBH, H, G, and LAI were examined using mixed-effects analysis of variance.

Data analysis was carried out separately at the plot level (n = 48) and clone level (n = 240). For the plot level data, stocking, fertilization and follow-up herbicide were considered as fixed effects and their interactions tested. For the clone level data, the fixed part of the model of each response variable included the stocking, clone, fertilization, and follow-up herbicide treatments, and their two-way interactions. For the plot and clone level analysis, the non-independence of repeated measurements structure was modelled as a random effect according

to the design of the experiment. The selected random effect structure was block/stock/fertilization-herbicide [i.e., fertilization and follow-up herbicide treatments (4 levels) nested within stocking (3 levels), which is again nested within block (4 levels)]. Tukey's LSD test was used for the post hoc multiple comparisons of treatment means using the *emmeans* function in R (Lenth et al., 2018) at a significance level of α = .05 unless noted otherwise.

$$Y^{(\lambda)} = \begin{cases} \dfrac{Y^{\lambda} - 1}{\lambda}, & \lambda \neq 0 \\ \log(Y), & \lambda = 0 \end{cases} \quad \textbf{(4.2)}$$

$$Y' = \left(\left(\lambda \times Y^{(\lambda)}\right) + 1\right)^{\frac{1}{\lambda}} \quad \textbf{(4.3)}$$

where $Y^{(\lambda)}$ is the transformed variable, λ is the power transformation coefficient, and Y' is the back transformed variable. A λ term is chosen to make the frequency distribution of each variable as close to normal as possible, thus promoting linear relationships and stabilising variance.

Results

Influence of silvicultural treatments on BSR

The estimated mean ± standard error value of BSR rate using a mixed-effects analysis was 6.58 ± 0.26 tonne C ha^{-1} yr^{-1} (range 5.93–7.52) (Appendix 3.3). At the plot level, BSR was influenced by the main effects of stocking only ($F_{2,6} = 7.96$, $p < .05$) (Appendix 3.1). The mean BSR was significantly higher at 1,250 stems ha^{-1} (7.52 tonne C ha^{-1} yr^{-1}) compared with 625 stems ha^{-1} (by 26.8%) and 2,500 stems ha^{-1} (by 19.6%) (Figure 4.1A). Fertilization and weed control treatments did not significantly influence BSR. No significant interactions were observed between stocking, fertilization, and follow-up herbicide treatments on BSR (Appendix 3.1).

In the clone level analysis, BSR was significantly influenced by the main effects of clone ($F_{4,172} = 3.7$, $p < .01$), and stocking ($F_{2,6} = 7.96$, $p < .05$) (Appendix 3.2). Clone 3 exhibited significantly higher BSR (7.07 tonne C ha^{-1} yr^{-1}) compared to other clones, and there were no significant differences in BSR between clones 2 and 4, and between clones 1 and 5 (Figure 4.1B; Appendix 3.4).

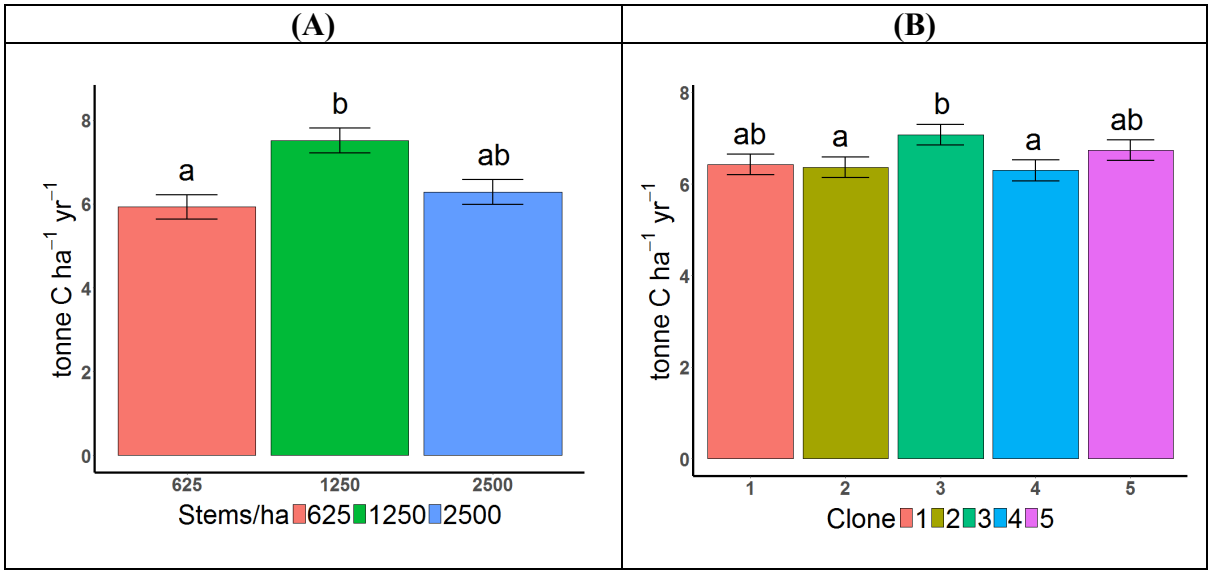

Figure 4.1: Main effects of (A) stocking, and clone (B) on BSR. Treatment means (± SE) indicated by the same letter do not differ significantly at α = 0.05 level using Tukey's HSD test.

Influence of silvicultural treatments on AGB

The estimated mean ± standard error value of AGB from the mixed-effects analysis across stocking, fertilization, and follow-up herbicide treatments was 55.25 ± 0.8 tonne C ha^{-1} (range 49.39–59.61) (Appendix 3.3). At the plot level, results showed that AGB was significantly influenced by the stocking × follow-up herbicide interaction ($F_{2,27}$ = 4.17, p < .05) (Appendix 3.1), although values of AGB were consistently higher in the follow-up weed control treatment compared with the without follow-up weed control treatment across all levels of stocking (Figure 4.2A). Compared with treatment without follow-up weed control, the AGB was higher in follow-up weed control treatment by 15.3, 8.3 and 2.7% for stand densities of 625, 1,250, and 2,500 stems ha^{-1} respectively (Figure 4.2A). On average, AGB was higher for 2,500 stems ha^{-1} (59.6 tonne C ha^{-1}) compared with 625 (by 20.7 %) and 1,250 stems ha^{-1} (5%) (Figure 4.2A; Appendix 3.3).

At the clone level, AGB was influenced significantly by the interactions of stocking × follow-up herbicide ($F_{2,29}$ = 4.03, p < .05), and clone × follow-up herbicide ($F_{4,172}$ = 2.43, p < .05) (Appendix 3.2). The clone × follow-up herbicide interaction showed that mean values of AGB were consistently higher in the follow-up weed control treatment compared with the without follow-up weed control treatment across clones (Figure 4.2B). Compared with the without follow-up weed control treatment, AGB was higher in follow-up weed control treatment by 4, 17.9, 4.7, 7.3, and 8.6 % in clone 1, clone 2, clone 3, clone 4, and clone 5 respectively (Figure

4.2B). On average, AGB was higher for clone 1 (62.81 tonne C ha^{-1}) and lower for clone 4 (48.63 tonne C ha^{-1}) in the follow-up weed control and without follow-up weed control treatment (Figure 4.2B; Appendix 3.4).

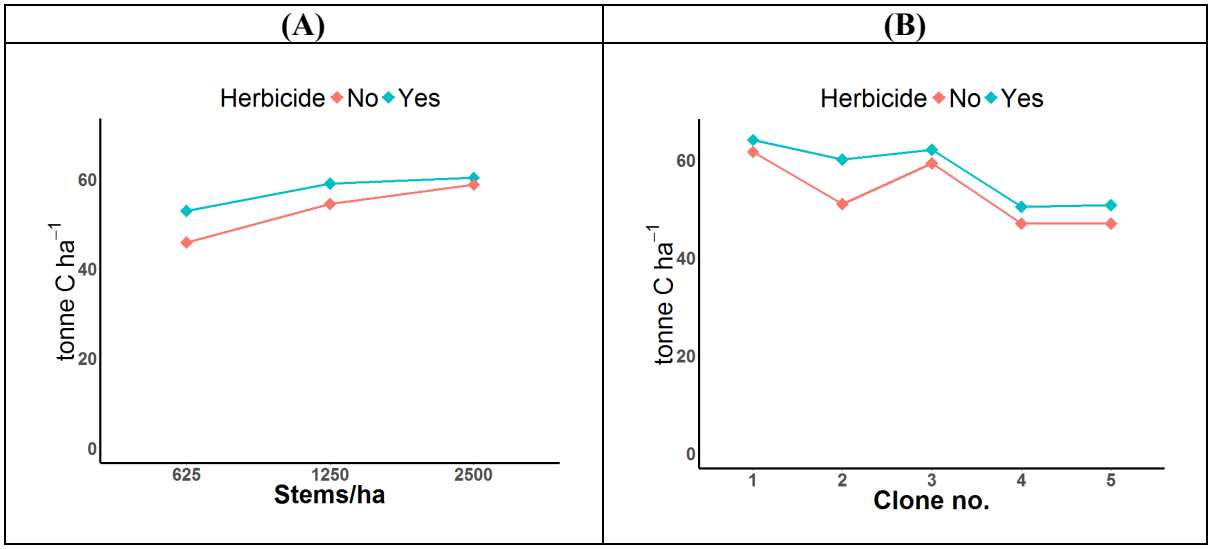

Figure 4.2: Significant interaction effects of (A) stocking × follow-up herbicide, and (B) clone × follow up herbicide) on AGB.

Influence of silvicultural treatments on BSR/AGB ratio

The estimated mean ± standard error value of BSR/AGB ratio was 0.16 ± 0.01 (range 0.11–0.25) (Appendix 3.3). At the plot level, BSR/AGB ratio was influenced significantly by the main effects of follow-up herbicide ($F_{1,27}$ = 10.9, p < .01) and stocking ($F_{2,6}$ = 5.37, p < .05) (Appendix 3.1). No significant effects of fertilization or the interactions between treatments on BSR/AGB ratio were observed. BSR/AGB ratio was significantly higher (i.e., 0.25) at 625 stems ha^{-1} compared with 1,250 (by 19.1%) and 2,500 stems ha^{-1} (by 31.6%) (Figure 4.3A; Appendix 3.3). There was no difference in BSR/AGB ratio between the 1,250 and 2,500 stems ha^{-1} (Figure 4.3A, Appendix 3.3). BSR/AGB ratio was significantly higher in without follow-up weed control treatment (by 18.2%) than in the follow-up weed control (Figure 4.3C; Appendix 3.3).

At the clone level, BSR/AGB ratio was significantly affected by the main effects of clone ($F_{4,172}$ = 14.87, p < .001), follow-up herbicide ($F_{1,29}$ = 10.67, p < .01), and stocking ($F_{2,6}$ = 6.43, p < .05) (Appendix 3.2). Clone 5 exhibited a significantly higher BSR/AGB ratio (i.e., 0.14) compared with other clones and, although differences are very small, all clones differed significantly from each other (Figure 4.3B; Appendix 3.4). It is worth noting that clone 5 was the one with the smallest AGB (Figure 4.2B) and greatest BSR/AGB ratio (Figure 4.3B)

suggesting that carbon allocation is one of the reasons why this was a slow-growing clone. Also clone 4 had the second greatest BSR/AGB ratio (Figure 4.3B) and also exhibited slow growth similar to clone 5 (Figure 4.2B). The fastest growing clones, 1 and 3 (Figure 4.2B), exhibited the smallest and the third-smallest BSR/AGB ratio (Figure 4.3B) among clones which also suggest this was a cause of rapid above-ground growth.

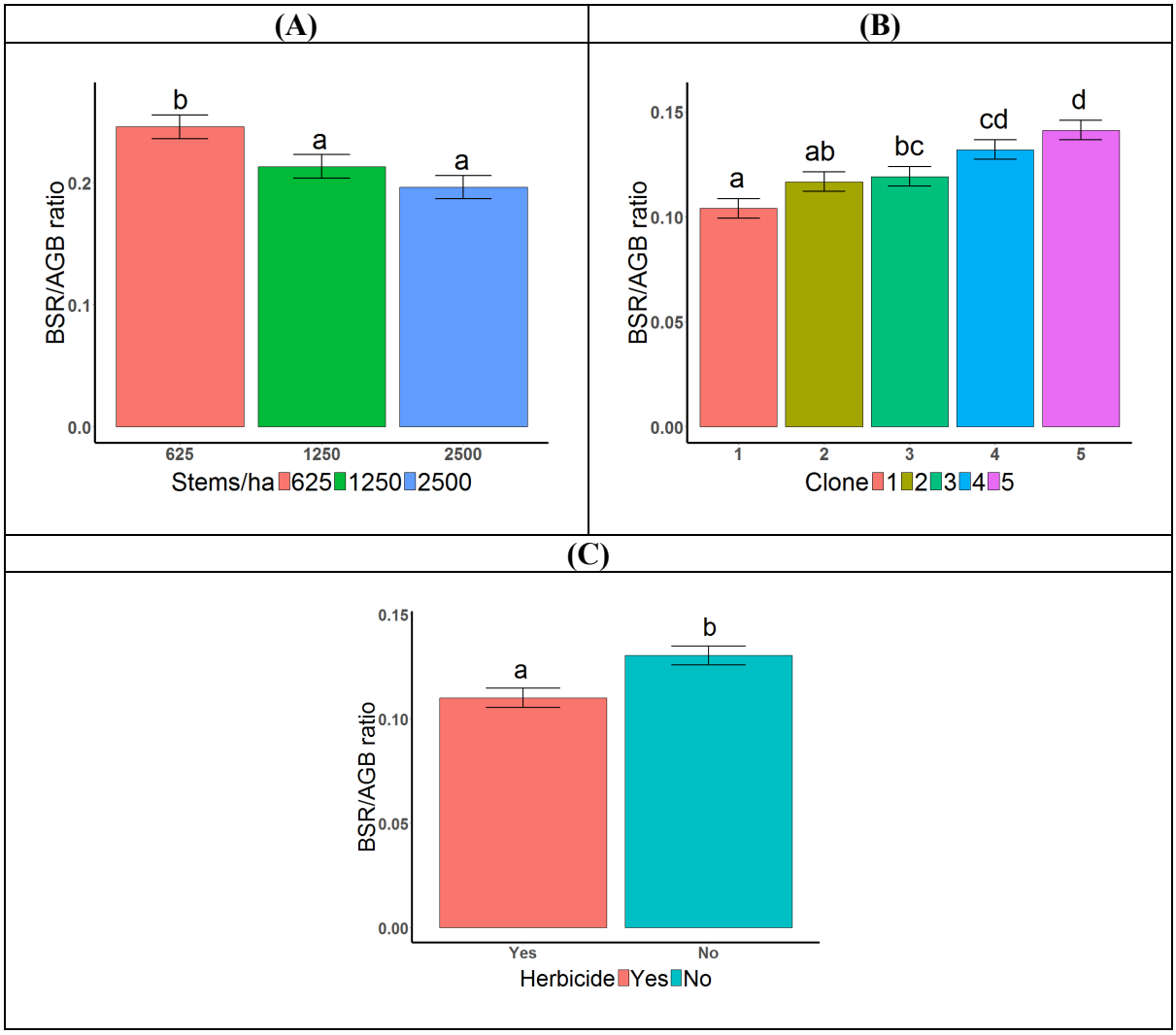

Figure 4.3: Main effects of (A) stocking, (B) clone, and (C) follow-up weed control on BSR/AGB ratio. Treatment means (± SE) indicated by the same letter do not differ significantly at α = 0.05 level using Tukey's HSD test.

Influence of silvicultural treatments on DBH

The estimated mean ± standard error value of DBH across stocking, fertilization, and follow-up weed control treatments was 19.45 ± 0.12 cm (range 14.79–24.28) (Appendix 3.3). At the plot level, DBH was significantly influenced by the interaction of stocking × follow-up herbicide ($F_{2,27} = 11.57, p < .001$) (Appendix 3.1). The interaction showed that the mean values

of DBH were consistently higher in the follow-up weed control treatment compared with without follow-up weed control across all levels of stocking (Figure 4.4A). Consequently, the DBH was greater in the weed control treatment by 7.9, 4.9 and 2.9% for the 625, 1,250, and 2,500 stems ha^{-1} stockings, respectively (Figure 4.4A). As expected, the DBH was higher at 625 stems ha^{-1} (24.28 cm) than at 1,250 (by 26%) and 2,500 stems ha^{-1} (64.2%) (Figure 4.4A; Appendix 3.3).

At the clone level, DBH was influenced significantly by the stocking × follow-up herbicide ($F_{2,29}$ = 12.02, p < .001) and clone × follow-up herbicide ($F_{4,172}$ = 2.8, p < .05) interactions (Appendix 3.2). The clone × follow-up herbicide interaction showed that DBH was consistently greater with the follow-up weed control treatment than in the treatment without follow-up weed control, independent of clones (Figure 4.4B). Compared with the treatment without follow up weed control, the DBH was greater in the follow-up weed control treatment by 4.5, 9.7, 3.7, 5.3, and 5.1% in clone 1, clone 2, clone 3, clone 4, and clone 5 respectively (Figure 4.4B). On average, the value of DBH was greater in clone 1 (20.56 cm) and smaller in clone 4 (18.26 cm) independent of follow-up weed control treatment (Figure 4.4B; Appendix 3.4).

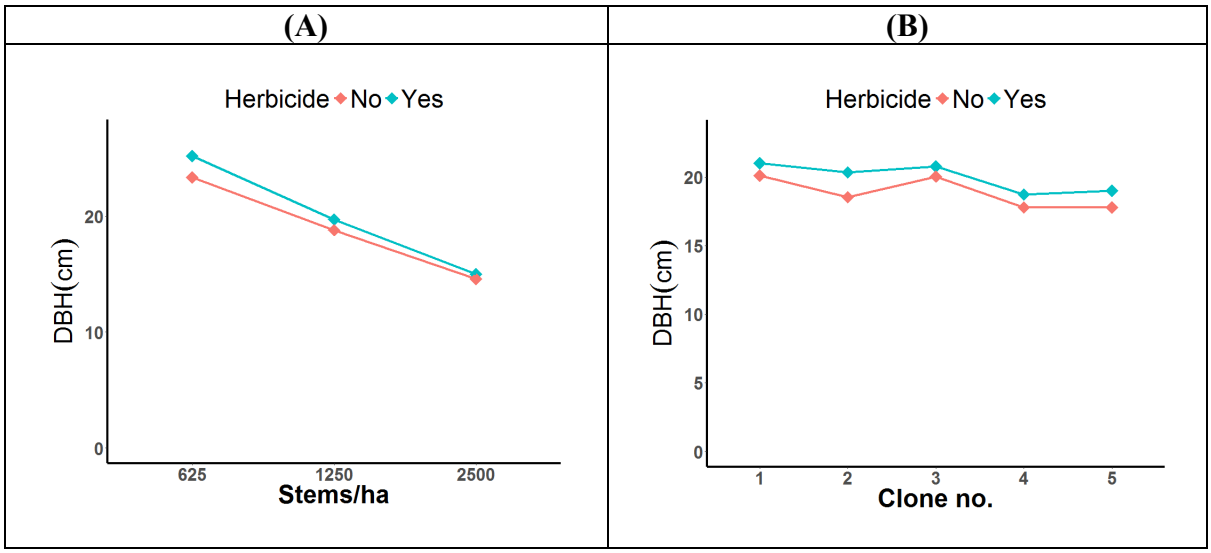

Figure 4.4: Significant interaction effects of (A) stocking × follow-up herbicide, and (B) clone × follow-up herbicide interaction on DBH.

Influence of silvicultural treatments on H

The estimated mean ± standard error value of H across stocking, fertilization, and follow-up herbicide treatments was 13.10 ± 0.16 m (range 12.8–13.56) (Appendix 3.3). At the plot level, H was influenced significantly by the main effects of follow-up herbicide ($F_{1,27}$ = 22.74, p <

.001), and stocking ($F_{2,6}$ = 17.58, p < .01) while all other interactions were insignificant (Appendix 3.1). Mean H was greater at 625 stems ha^{-1} (13.56 m) and 1,250 stems ha^{-1} (13.21 m), than at 2,500 stems ha^{-1} (12.53 m) (Figure 4.5A; Appendix 3.3). Mean H was significantly greater in the follow-up weed control treatment (by 4.7%) compared to the treatment without follow-up weed control (Figure 4.5C; Appendix 3.3).

At the clone level, mean H was influenced significantly by the main effects of clone ($F_{4,172}$ = 61.46, p < .001), follow-up herbicide ($F_{1,29}$ = 23.53, p < .001), and stocking ($F_{2,6}$ = 17.49, p < .01) (Appendix 3.2). Although differences were small, clones 3 and 4 showed the greatest and smallest H values (13.87 m and 12.38 m respectively), while other clones were intermediate between these two extremes (Figure 4.5B; Appendix 3.4).

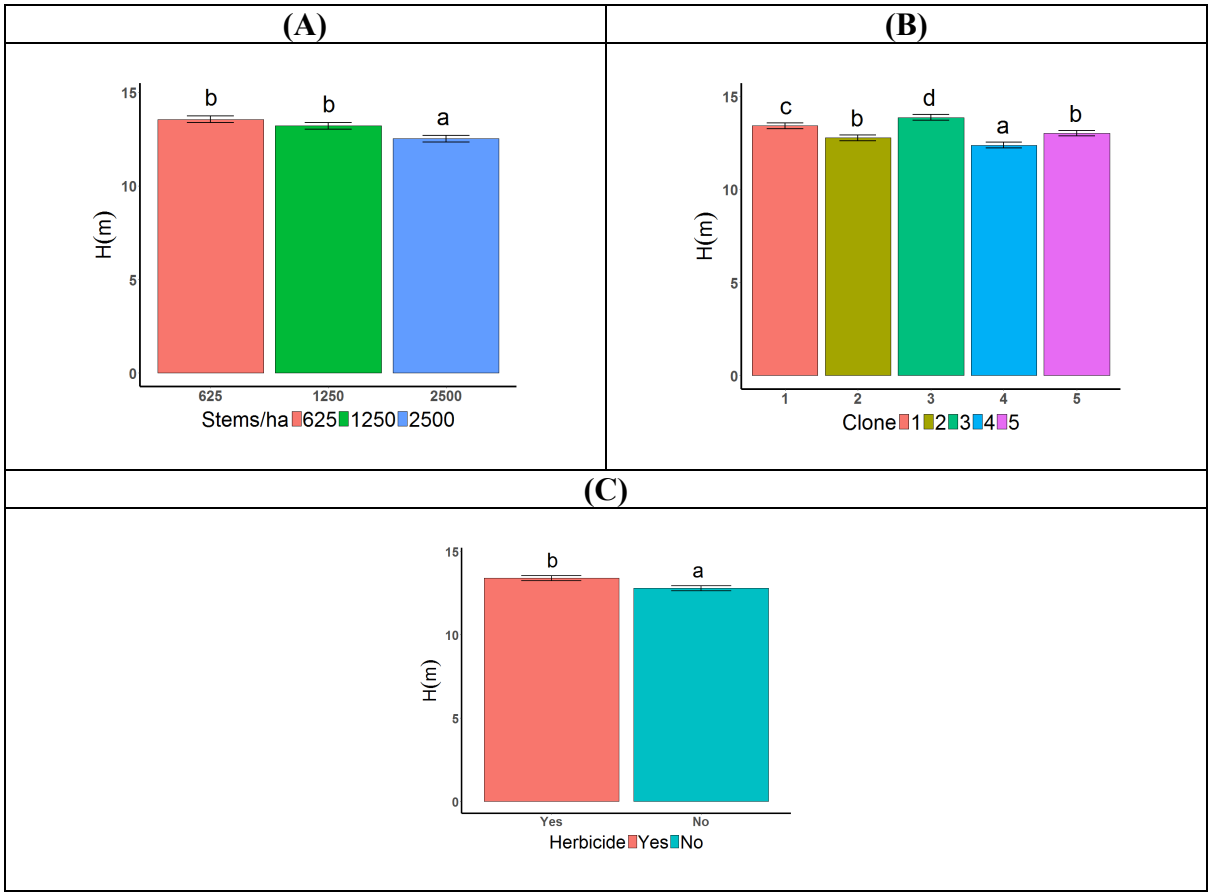

Figure 4.5: Main effects of (A) stocking, (B) clone, and (C) follow-up herbicide treatment on H. Treatment means (± SE) indicated by the same letter do not differ significantly at α = 0.05 level using Tukey's HSD test.

Influence of silvicultural treatments on G

The estimated mean ± standard error value of G across stocking, fertilization, and follow-up herbicide treatments was 36.62 ± 0.36 m^2 ha^{-1} (range 29.32–43.50) (Appendix 3.3). At the plot

level, results showed that G was influenced significantly by the interaction of stocking × follow-up herbicide ($F_{2,27}$ = 4.16, p < .05) (Appendix 3.1). The interaction, which was weak compared with the main effects, showed that mean values of G were consistently greater in the follow-up weed control treatment compared to the treatment without follow-up weed control, across all levels of stocking (Figure 4.6A). Compared with treatment without follow-up weed control, the G was greater in the follow-up weed control treatment by 15.6, 9.2 and 2.9% for the 625, 1,250, and 2,500 stems ha^{-1} stockings, respectively (Figure 4.6A). Across weed control treatments, the G was greater at 2,500 stems ha^{-1} (43.5 m^2 ha^{-1}) compared with 625 (by 48.4%) and 1,250 stems ha^{-1} (17.5%) (Figure 4.6A, Appendix 3.3).

At the clone level, G was significantly influenced by the stocking × follow-up herbicide ($F_{2,29}$ = 3.37, p < .05), and stocking × clone ($F_{8,172}$ = 2.39, p < .05) interactions (Appendix 3.2). The stocking × clone interaction, although weak compared with the main effects, showed that G decreased in the order 2,500, 1,250 and 625 stems ha^{-1}, across all clones (Figure 4.6B). Clones 1 and 3 exhibited collectively greater G across stockings compared to the other clones, particularly clones 4 and 5 (Figure 4.6B).

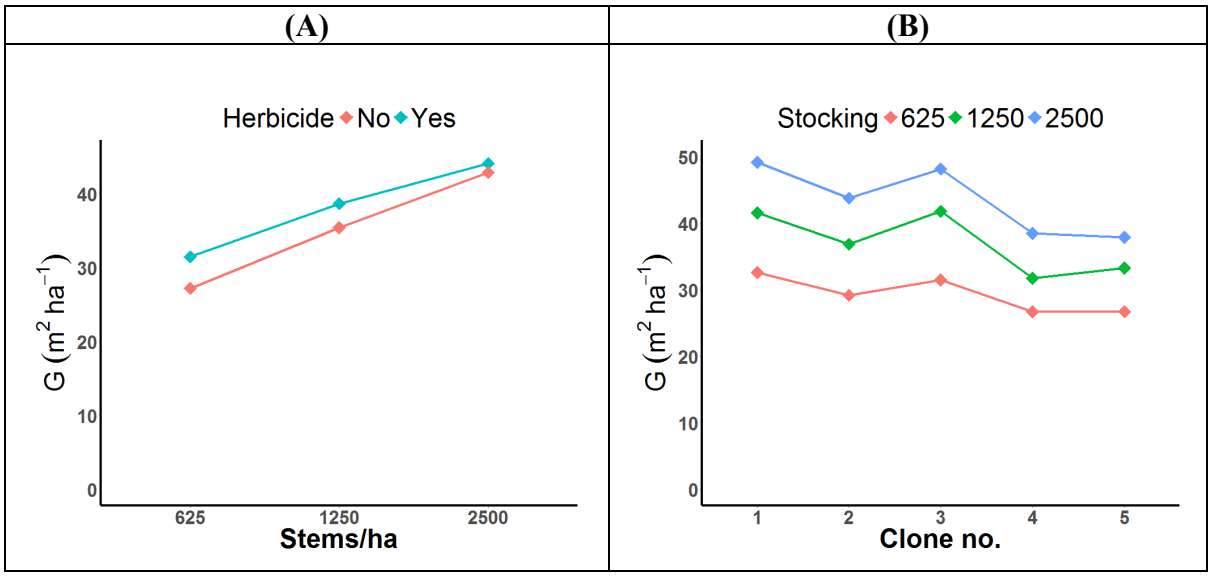

Figure 4.6: Significant interaction effects of (A) stocking × follow-up herbicide, and (B) clone × stocking on G.

Influence of silvicultural treatments on LAI

The estimated mean ± standard error value of LAI across stocking, fertilization, and follow-up herbicide treatments was 3.27 ± 0.12 m^2 m^{-2} (range 3.15–3.35) (Appendix 3.3). At the plot

level, the main and interactive effects of stocking, fertilization, and follow-up weed control on LAI were insignificant ($p > .05$) (Appendix 3.1). The clone level LAI results are not reported as there are uncertainties concerning the spatial extent of the LAI 2000 measurements which may comprise several clones.

Discussion

The hypothesis that stocking would influence BSR is partially supported by this study, although a surprising result was that BSR was maximized at 1,250 stems ha^{-1} with similar lower values at 625 and 1,250 stems ha^{-1}. The increase in BSR from 625 to 1,250 stems ha^{-1} may be attributed to greater above- and below-ground growth and microbial activity at 1,250 stems ha^{-1} with full site occupancy, and competition for site resources at a level that plants can still tolerate without being strongly stressed. We may speculate that reductions in BSR from 1,250 to 2,500 stems ha^{-1} may be associated with highly stressful conditions for resource capture and trees becoming space limited at 2,500 stems ha^{-1}. The stand density index (SDI) analysis supported this phenomena (Appendix 3.5). SDI indicated that natural mortality was higher in plots planted with an initial stocking of 2,500 stems ha^{-1} than in the plots planted with 1,250 stems ha^{-1} and 625 stems ha^{-1} (Appendix 3.5A). The growth trajectory of the *P. radiata* plantation revealed that natural mortality increased with the increase in stand age, and that the rate of reduction was higher at the highest stocking (Appendix 3.5B). Stand density can influence soil climate and canopy density, and ultimately in soil carbon fluxes (Gower et al., 1992; Litton et al., 2007; Litton et al., 2004). Some studies have found that above-ground productivity and below-ground carbon fluxes of *P. radiata* can be highly constrained by water availability (Álvarez et al., 2013; Benecke, 1980; Benson, Myers, & Raison, 1992; Cromer, Tompkins, & Barr, 1983; Jackson, Gifford, & Chittenden, 1976; Raison et al., 1992; Schlatter & Gerding, 1984). The highest stocking in this study exhibited the greatest mortality, which may be due to a high water stress in the site during summer. Chapter 3 showed that soil volumetric water content was lower at 2,500 stems ha^{-1} by 2.6% and 1.6% than at 625 and 1,250 stems ha^{-1}, respectively. In addition, the significant effects of follow-up weed control and no effects from fertilization suggests that moisture availability could be the driving factor constraining above-ground biomass production (Rubilar et al., 2013). Increased competition for below-ground resources and potential water stress due to high stockings could be a reasonable explanation for the greater mortality observed, which may explain the observed decrease of below-ground carbon flux from 1,250 to 2,500 stems ha^{-1}.

The hypothesis that stocking would influence the BSR/AGB ratio is supported by this study. The BSR/AGB ratio decreased as stand density increased. The carbon allocation was significantly higher in plots planted with 625 stems ha^{-1} by 19.1% and 31.6% compared with 1,250 and 2,500 stems ha^{-1} respectively. Giardina & Ryan (2002) reported the opposite, with total below-ground carbon allocation (TBCA) being 18% higher at a high stocking (10^4 stems ha^{-1}) than at low stocking (1,111 stems ha^{-1}). However, the decrease of BSR/AGB ratio with the increase in stand density in this study might be attributed to solar radiation being more limiting than water or nutrients at 2,500 stems ha^{-1}, reason why trees would potentially allocate more carbon aboveground. A greater competition for light at 2,500 stems ha^{-1} would also explain the greater mortality observed compared to lower densities.

Follow-up weed control was the second most important factor after stocking controlling most stand and tree variables. The weed control treatment consistently exhibited greater values of AGB (Figure 4.2A), DBH (Figure 4.4A), and G (Figure 4.6A) across the stockings. Weed control eliminated competing vegetation in strips in all plots up to age 2, and follow-up complete weed control (herbicide) applied at ages 3 and above. The departure of competing vegetation from plots without follow-up weed control is very recent, particularly at 625 stems ha^{-1} in the study site. Greater growth performance above ground with follow-up weed control could be attributed to reduced competition for resource availability below ground, particularly for water, following herbicide application. This result is consistent with a study that reported a significant increase of above-ground growth of *P. radiata* plantation after weed control (Mason & Milne, 1999; Mead, Lucas, & Mason, 1993; Rubilar et al., 2013). It is also worth noting that the BSR/AGB ratio decreased significantly with the follow-up weed control treatment (Figure 4.3C), while above-ground growth increased significantly (Figure 4.2A). This result suggests that follow-up weed control shifted carbon allocation above ground at the expense of below ground processes. Allocation theory would predict this effect if weed control had increased water but also nutrient availability for this dry site. This inference is supported by the fact that mean soil volumetric water content was greater in the plots with follow-up weed control by 1.6% compared to the plots without follow-up weed control treatment (Chapter 3).

The hypothesis that clones would differ on both above-ground biomass production and below-ground carbon partitioning was supported by the results of this study. This result is qualified with an assumption that biomass equations applied to all clones in an unbiased manner. This is

because biomass models developed for this study included two clones only (clones 1 and 2) and clone type did not significantly influence any form of the biomass equations (Chapter 2). Considering this assumptions, it was observed that clone 1 and clone 3 were the most productive above ground (Figure 4.2B) allocating the least carbon below ground (Figure 4.3B), while clone 4 and clone 5 were the least productive above ground (Figure 4.2B) allocating the most carbon below ground (Figure 4.3B). The results suggest that carbon partitioning above versus below ground is one of the underlying mechanisms for certain clones to be more productive above ground. Results of this study are similar to those by Chmura et al. (2013), who reported a significant effect of genotypes on root to shoot ratio for *P. sylvestris*, and clones with a poorer performance above ground showed proportionally higher carbon partitioning below ground. Similar results to this study for *P. radiata* were also found by Li, Allen, & McKeand (1991) and Snowdon (1985). Although the five different clones compared in this study represent preselected wood anatomical properties, they also showed significant differences in above-ground production, below-ground soil carbon respiration and its ratio. The significant differences in below-ground carbon respiration across clones is consistent also with Bown et al. (2009), who reported that carbon partitioning differed significantly between slow- and fast-growing clones, coinciding with greater carbon partitioning below ground in the former and smaller in the latter. Hence, the faster-growing clones of *P. radiata* exhibited greater carbon partitioning to above-ground net primary production at the expense of total below-ground carbon flux and vice versa (Bown, Watt, Clinton, et al., 2009).

Some authors advocate for a strong genotype × environment interaction related to forest productivity (Lee Allen, Fox, & Campbell, 2005; Li et al., 1991; Teskey, Bongarten, Cregg, Dougherty, & Hennessey, 1987). A non-existing interaction would mean that fast-growing clones will always grow rapidly irrespective of the environment where they grow and vice versa. A significant interaction would mean, for instance, that a clone could outperform in a poor site and underperform in a good site compared with other clones. We found the interactions between genotype and silvicultural treatment (i.e. stocking, herbicide, fertilization), which may change resource availability, were weak to non-existent. For instance, the significant clone × follow-up herbicide interaction for AGB and DBH showed that the mean values of AGB and DBH were consistently greater in the follow-up weed control treatment, compared to the treatment without follow-up weed control across clones, although reductions were not strictly proportional and hence the interaction became significant although weak

(Figure 4.2B, Figure 4.4B). This weakly significant clone × follow-up herbicide interaction also indicates that clones may not assist greatly to reduce the space limited by higher competition belowground. A similar study for *P. radiata* in the Canterbury region of New Zealand (Mead et al., 1993), reported a lack of interaction between weed control and clones. Another case for a weak genotype × environment interaction, is provided by Carson et al. (2004) who suggested that irrespective of nutrient availability some clones would have higher assimilation and partitioning of carbon above-ground. However, it should be noted that in our experiment global growth inputs such as radiation, rainfall and temperature very likely varied very little between treatments, and so the test for a genotype × environment interaction in this experiment was relatively weak. A study in New Zealand also reported that survival and growth of *P. radiata* varied significantly across clones, with insignificant clone × weed interaction (Mason & Kirongo, 1999). Neither the main effect nor the interactive effect of fertilization and other treatments were significant for most variables studied at the plot and clone level. Similarly, Snowdon and Benson (1992) found that fertilization did not influence either above- or below-ground productivity for young *P. radiata*. Giardina and Ryan (2002) found that, although not significant, total below-ground carbon flux in *Eucalyptus* plantations in Hawaii, was smaller in fertilized plots than in non-fertilized plots. We also found a marginal, insignificant decrease in BSR/AGB ratio with fertilization.

In summary, this study shows that silviculture changes above- versus below-ground carbon partitioning, providing some new insight into the underlying mechanisms by which stocking, follow-up weed control, and clone operate. The results of this study suggests that: (a) below-ground carbon allocation decreased as the stocking increased, (b) herbicide influenced the above-ground growth by shifting carbon partitioning above ground at the expense of below-ground processes, and (c) certain clones were more productive above-ground at the expense of smaller carbon partitioning below-ground than others.

Conclusions

Stocking, follow-up herbicide and clone strongly affected above-ground productivity and carbon partitioning above and below ground for *P. radiata* in a dry site in Canterbury. Biomass yield and basal area by age 12 increased with stocking, but BSR/AGB ratio was significantly greater at 625 stems ha^{-1} compared to both 1,250 and 2,500 stems ha^{-1}. It is worth noting, however, that the BSR/AGB ratio was insignificantly greater at 1,250 compared to 2,500 stems

ha^{-1}. A smaller BSR/AGB ratio at 2,500 stems ha^{-1} compared to lower densities, would suggest that trees were highly stressed being space limited which probably induced strong limitation to soil resources, particularly water and nutrients. Greater resource limitations and competition at 2,500 stems ha^{-1} compared to lower densities is also supported by the greater mortality at this density. Weed control, although applied at a young age, brought about significant increases in AGB and a smaller BSR/AGB ratio, suggesting that follow-up weed control alleviated understorey-induced water and nutrient stresses. Assuming that biomass equations applied to all clones in an unbiased manner, clones 1 and 3 were the fastest growing clones above ground, and allocated the least carbon below ground. In contrast, clones 4 and 5 were the least productive above ground, but allocated the greatest carbon below ground. This suggested that shifts in carbon allocation from above to below ground is one of the mechanisms by which certain clones are more productive above ground.

Chapter 5. THESIS SYNTHESIS

The overall aim of the thesis was to assess above-ground biomass and soil CO_2 effluxes of *P. radiata* plantations across silvicultural treatments in the Canterbury region of New Zealand.

In a first study, two broad procedures of biomass modelling, namely independent and additive, were compared. Precision and bias of both approaches were compared using goodness-of-fit statistics, standard error of estimates and residual plots. Separate allometric equations were developed for *P. radiata* to predict biomass for components, subtotal and total above ground. Seemingly Unrelated Regression (SUR) provided unbiased estimates in 7 out of 10 components, having clear advantages over other methods tested.

In a second study, seasonal dynamics of soil CO_2 efflux across silvicultural and environmental variables were examined. Season, stocking, and clone had a significant, positive influence on F_s. The rate of F_s was greatest in autumn and smallest in winter. Clone 3 exhibited the greatest F_s compared to other clones. F_s was greater at 1,250 stems ha^{-1} compared to 625 and 2,500 stems ha^{-1}. A clear exponential relationship between F_s and T_s was observed when θ_v was greater than 13.4%.

In a third study, linkages between above-ground biomass production and below-ground carbon fluxes in *P. radiata* were evaluated. The BSR rate was significantly affected by the main effects of stocking and clone. The significant interaction effects of both stocking × follow-up herbicide and clone × follow-up herbicide were observed for AGB, DBH, and G. The significant effects of clone, follow-up herbicide, and stocking were observed for BSR/AGB ratio and H. No significant effects of fertilization on any above- or below-ground variables were observed. Increased above-ground biomass yield with stand density was likely to be associated to greater site occupancy and resource use. Decreased BSR/AGB ratio with stand density would suggest that light was a primary limitation at higher densities, triggering greater carbon allocation aboveground at the expense of the belowground. Follow-up weed control increased above-ground growth and decreased the below-ground carbon partitioning, which suggests that follow-up weed control reduced competition for below-ground resources. Slower growing clones exhibited greater AGB and smaller BSR/AGB ratio compared to faster growing clones,

suggesting that the former allocated proportionally more carbon below-ground, and less aboveground compared to the latter.

To sum up, (a) best biomass equations were found when fitting additive models using SUR compared to traditional approaches; (b) soil respiration changed with season, stocking and weed control, and scaled with soil temperature and soil volumetric water content; and (c) AGB increased with stocking, weed control, and differed among clones, the BSR/AGB ratio decreased with stocking and weed control, and faster growing clones exhibited smaller BSR/AGB ratio than slow growing clones, suggesting a tradeoff between above-ground productivity and belowground carbon allocation.

References

Albaugh, T. J., Allen, H. L., Dougherty, P. M., Kress, L. W., & King, J. S. (1998). Leaf area and above- and belowground growth responses of loblolly pine to nutrient and water additions. *Forest Science, 44*(2), 317-328.

Almagro, M., López, J., Querejeta, J., & Martínez-Mena, M. (2009). Temperature dependence of soil CO_2 efflux is strongly modulated by seasonal patterns of moisture availability in a Mediterranean ecosystem. *Soil Biology and Biochemistry, 41*(3), 594-605.

Álvarez, J., Allen, H. L., Albaugh, T. J., Stape, J. L., Bullock, B. P., & Song, C. (2013). Factors influencing the growth of radiata pine plantations in Chile. *Forestry: An International Journal of Forest Research, 86*(1), 13-26. https://doi.org/10.1093/forestry/cps072

Arneth, A., Kelliher, F., McSeveny, T., & Byers, J. (1998). Net ecosystem productivity, net primary productivity and ecosystem carbon sequestration in a *Pinus radiata* plantation subject to soil water deficit. *Tree physiology, 18*(12), 785-793.

Asaye, Z. (2015). Temporal dynamics of soil CO_2 efflux in thinned and un-thinned stands of *Cupressus lusitanica* in Munessa Forest, Southern Ethiopia. *International Journal of Agriculture and Forestry, 5*(3), 190-198.

Aslam, T., Choudhary, M., & Saggar, S. (2000). Influence of land-use management on CO_2 emissions from a silt loam soil in New Zealand. *Agriculture, ecosystems & environment, 77*(3), 257-262.

Baker, T., Oliver, G., & Hodgkiss, P. (1986). Distribution and cycling of nutrients in *Pinus radiata* as affected by past lupin growth and fertiliser. *Forest Ecology and Management, 17*(2-3), 169-187.

Balvanera, P., Pfisterer, A., Buchmann, N., He, J., Nakashizuka, T., Raffaelli, D., & Schmid, B. (2006). Biodiversity and ecosystem functioning: A meta-analysis of experimental results. *Ecology Letters, 9*, 1146-1156.

Baskerville, G. (1972). Use of logarithmic regression in the estimation of plant biomass. *Canadian Journal of Forest Research, 2*(1), 49-53.

Beauchamp, J. J., & Olson, J. S. (1973). Corrections for bias in regression estimates after logarithmic transformation. *Ecology, 54*(6), 1403-1407.

Beets, P., Kimberley, M., & McKinley, R. (2007). Predicting wood density of *Pinus radiata* annual growth increments. *New Zealand Journal of Forestry Science, 37*(2), 241.

Beets, P., & Madgwick, H. (1988). Above-ground dry matter and nutrient content of *Pinus radiata* as affected by lupin, fertiliser, thinning, and stand age. *New Zealand Journal of Forestry Science, 18*(1), 43-64.

Beets, P., Pearce, S., Oliver, G., & Clinton, P. (2007). Root/shoot ratios for deriving below-ground biomass of *Pinus radiata* stands. *New Zealand Journal of Forestry Science, 37*(2), 267.

Beets, P., & Pollock, D. (1987). Accumulation and partitioning of dry matter in *Pinus radiata* as related to stand age and thinning. *New Zealand Journal of Forestry Science, 17*(2), 246-271.

Beets, P., Roberston, K., Ford-Robertson, J., Gordon, J., & Maclaren, J. (1999). Description and validation of C_Change: A model for simulating carbon content in managed *Pinus radiata* stands. *New Zealand Journal of Forestry Science, 29*(3), 409-427.

Benecke, U. (1980). Photosynthesis and transpiration of *Pinus radiata* D. Don under natural conditions in a forest stand. *Oecologia, 44*(2), 192-198.

Benson, M., Myers, B., & Raison, R. (1992). Dynamics of stem growth of *Pinus radiata* as affected by water and nitrogen supply. *Forest Ecology and Management, 52*(1-4), 117-137.

Bhattacharya, D. (2004). Seemingly unrelated regressions with identical regressors: A note. *Economics Letters, 85*(2), 247-255.

Bhupinderpal, S., Nordgren, A., Ottosson Löfvenius, M., Högberg, M., Mellander, P. E., & Högberg, P. (2003). Tree root and soil heterotrophic respiration as revealed by girdling of boreal Scots pine forest: Extending observations beyond the first year. *Plant, Cell & Environment, 26*(8), 1287-1296.

Bi, H., Long, Y., Turner, J., Lei, Y., Snowdon, P., Li, Y., . . . Ximenes, F. (2010). Additive prediction of aboveground biomass for *Pinus radiata* D. Don plantations. *Forest Ecology and Management, 259*(12), 2301-2314.

Bi, H., Turner, J., & Lambert, M. J. (2004). Additive biomass equations for native eucalypt forest trees of temperate Australia. *Trees, 18*(4), 467-479.

Borken, W., Xu, Y. J., Davidson, E. A., & Beese, F. (2002). Site and temporal variation of soil respiration in European beech, Norway spruce, and Scots pine forests. *Global Change Biology, 8*(12), 1205-1216.

Bowden, R. D., Newkirk, K. M., & Rullo, G. M. (1998). Carbon dioxide and methane fluxes by a forest soil under laboratory-controlled moisture and temperature conditions. *Soil Biology and Biochemistry, 30*(12), 1591-1597.

Bown, H., Mason, E., Clinton, P., & Watt, M. (2009). Chlorophyll fluorescence response of *Pinus radiata* clones to nitrogen and phosphorus supply. *Ciencia e investigación agraria, 36*(3), 451-464.

Bown, H., & Watt, M. (2016). Stem and soil CO_2 efflux responses of *Pinus radiata* plantations to temperature, season, age, time (day/night) and fertilization. *Ciencia e investigación agraria, 43*(1), 95-109.

Bown, H., Watt, M., Clinton, P., Mason, E., & Whitehead, D. (2009). The influence of N and P supply and genotype on carbon flux and partitioning in potted *Pinus radiata* plants. *Tree physiology, 29*(7), 857-868. https://doi.org/https://doi.org/10.1093/treephys/tpp030

Bown, H., Watt, M., Mason, E., Clinton, P., & Whitehead, D. (2009). The influence of nitrogen and phosphorus supply and genotype on mesophyll conductance limitations to photosynthesis in *Pinus radiata*. *Tree physiology, 29*(9), 1143-1151. https://doi.org/https://doi.org/10.1093/treephys/tpp051

Box, G. E., & Cox, D. R. (1964). An analysis of transformations. *Journal of the Royal Statistical Society. Series B (Methodological)*, 211-252.

Brumme, R., & Beese, F. (1992). Effects of liming and nitrogen fertilization on emissions of CO_2 and N_2O from a temperate forest. *Journal of Geophysical Research: Atmospheres, 97*(D12), 12851-12858.

Buchmann, N. (2000). Biotic and abiotic factors controlling soil respiration rates in *Picea abies* stands. *Soil Biology and Biochemistry, 32*(11), 1625-1635.

Burger, J. (1994). Cumulative effects of silvicultural technology on sustained forest productivity. *IEA proceedings, Fredericksto*n, *New Brunswick, Canada*, 59-70.

Canadell, J., Riba, M., & Andres, P. (1988). Biomass equations for *Quercus ilex L.* in the Montseny Massif, Northeastern Spain. *Forestry: An International Journal of Forest Research, 61*(2), 137-147.

Canga, L., Aranda, U., Khouri, A., & Obregón, C. (2013). Above-ground biomass equations for *Pinus radiata* D. Don in Asturias. *Forest Systems*.

Cao, M., & Woodward, F. I. (1998). Net primary and ecosystem production and carbon stocks of terrestrial ecosystems and their responses to climate change. *Global Change Biology, 4*(2), 185-198.

Carlyle, J. (1993). Organic carbon in forested sandy soils: Properties, processes, and the impact of forest management. *New Zealand Journal of Forestry Science, 23*, 390-402.

Carlyle, J. (1998). Relationships between nitrogen uptake, leaf area, water status and growth in an 11-year-old *Pinus radiata* plantation in response to thinning, thinning residue, and nitrogen fertiliser. *Forest Ecology and Management, 108*(1-2), 41-55.

Carson, S., Skinner, M., Lowe, A., & Kimberley, M. (2004). Performance differences in *Pinus radiata* progeny with differing site nutrient availability. *Canadian Journal of Forest Research, 34*(12), 2410-2423.

Carvalho, J. P., & Parresol, B. R. (2003). Additivity in tree biomass components of Pyrenean oak (*Quercus pyrenaica Willd.*). *Forest Ecology and Management, 179*(1-3), 269-276.

Castro, M. S., Peterjohn, W. T., Melillo, J. M., Steudler, P. A., Gholz, H. L., & Lewis, D. (1994). Effects of nitrogen fertilization on the fluxes of N_2O, CH_4, and CO_2 from soils in a Florida slash pine plantation. *Canadian Journal of Forest Research, 24*(1), 9-13.

Chang, C., Sabaté, S., Sperlich, D., Poblador, S., Sabater, F., & Gracia, C. (2014). Does soil moisture overrule temperature dependence of soil respiration in Mediterranean riparian forests? *Biogeosciences, 11*(21), 6173-6185.

Chang, C., Sperlich, D., Sabaté, S., Sánchez-Costa, E., Cotillas, M., Espelta, J. M., & Gracia, C. (2016). Mitigating the stress of drought on soil respiration by selective thinning: Contrasting effects of drought on soil respiration of two oak species in a Mediterranean forest. *Forests, 7*(11), 263.

Chapin III, F. S. (1980). The mineral nutrition of wild plants. *Annual Review of Ecology and Systematics, 11*(1), 233-260.

Chmura, D. J., Guzicka, M., Rożkowski, R., & Chałupka, W. (2013, 2013/12/01). Variation in aboveground and belowground biomass in progeny of selected stands of *Pinus sylvestris*. *Scandinavian Journal of Forest Research, 28*(8), 724-734. https://doi.org/10.1080/02827581.2013.844269

Clutter, J. L., Fortson, J. C., Pienaar, L. V., Brister, G. H., & Bailey, R. L. (1983). *Timber management: a quantitative approach*. New York: John Wiley & Sons, Inc.

Cook, F., Orchard, V. A., & Corderoy, D. M. (1985). Effects of lime and water content on soil respiration. *New Zealand Journal of Agricultural Research, 28*(4), 517-523.

Cook, R., & Weisberg, S. (2009). *Applied regression including computing and graphics*. New York: John Wiley & Sons.

Cox, P. M., Betts, R. A., Jones, C. D., Spall, S. A., & Totterdell, I. J. (2000). Acceleration of global warming due to carbon-cycle feedbacks in a coupled climate model. *Nature, 408*(6809), 184.

Coyle, D. R., Coleman, M. D., & Aubrey, D. P. (2008). Above-and below-ground biomass accumulation, production, and distribution of sweetgum and loblolly pine grown with irrigation and fertilization. *Canadian Journal of Forest Research, 38*(6), 1335-1348.

Cromer, R., Barr, N., Williams, E., & McNaught, A. (1985). Response to fertiliser in a *Pinus radiata* plantation. 1. Above-ground biomass and wood density. *New Zealand Journal of Forestry Science, 15*(1), 59-70.

Cromer, R., Tompkins, D., & Barr, N. (1983). Irrigation of *Pinus radiata* with waste water: Tree growth in response to treatment. *Australian Forest Research, 13*, 57-65.

Cunia, T., & Briggs, R. (1984). Forcing additivity of biomass tables: Some empirical results. *Canadian Journal of Forest Research, 14*(3), 376-384.

Cunia, T., & Briggs, R. (1985). Forcing additivity of biomass tables: Use of the generalized least squares method. *Canadian Journal of Forest Research, 15*(1), 23-28.

Davidson, E. A., Belk, E., & Boone, R. D. (1998). Soil water content and temperature as independent or confounded factors controlling soil respiration in a temperate mixed hardwood forest. *Global Change Biology, 4*(2), 217-227.

Davidson, E. A., Janssens, I. A., & Luo, Y. (2006). On the variability of respiration in terrestrial ecosystems: Moving beyond Q_{10}. *Global Change Biology, 12*(2), 154-164.

Davidson, E. A., Verchot, L. V., Cattanio, J. H., Ackerman, I. L., & Carvalho, J. (2000). Effects of soil water content on soil respiration in forests and cattle pastures of eastern Amazonia. *Biogeochemistry, 48*(1), 53-69.

Della-Bianca, L., & Dills, R. (1960). Some effects of stand density in a Red Pine plantation on soil moisture, soil temperature, and radial growth. *Journal of Forestry, 58*(5), 373-377.

Dhillion, S. S., Roy, J., & Abrams, M. (1995). Assessing the impact of elevated CO_2 on soil microbial activity in a Mediterranean model ecosystem. *Plant and Soil, 187*(2), 333-342.

Dong, L., Zhang, L., & Li, F. (2015). Developing additive systems of biomass equations for nine hardwood species in Northeast China. *Trees, 29*(4), 1149-1163.

Dörr, H., & Münnich, K. (1987). Annual variation in soil respiration in selected areas of the temperate zone. *Tellus B, 39*(1-2), 114-121.
Dulohery, C. J., Morris, L. A., & Lowrance, R. (1996). Assessing forest soil disturbance through biogenic gas fluxes. *Soil Science Society of America Journal, 60*(1), 291-298.
Fan, S., Gloor, M., Mahlman, J., Pacala, S., Sarmiento, J., Takahashi, T., & Tans, P. (1998). A large terrestrial carbon sink in North America implied by atmospheric and oceanic carbon dioxide data and models. *Science, 282*(5388), 442-446.
Fang, C., & Moncrieff, J. (2001). The dependence of soil CO_2 efflux on temperature. *Soil Biology and Biochemistry, 33*(2), 155-165.
Gallant, A. R. (1975). Seemingly unrelated nonlinear regressions. *Journal of Econometrics, 3*(1), 35-50.
Gallardo, A., & Schlesinger, W. H. (1994). Factors limiting microbial biomass in the mineral soil and forest floor of a warm-temperate forest. *Soil Biology and Biochemistry, 26*(10), 1409-1415.
Gärdenäs, A. I. (2000). Soil respiration fluxes measured along a hydrological gradient in a Norway spruce stand in south Sweden (Skogaby). *Plant and Soil, 221*(2), 273-280.
Giardina, C. P., & Ryan, M. G. (2002). Total belowground carbon allocation in a fast-growing *Eucalyptus* plantation estimated using a carbon balance approach. *Ecosystems, 5*(5), 487-499.
Gliński, J., & Stępniewski, W. (1985). *Soil aeration and its role for plants*. Place of publication: CRC Press, Inc.
Godwin, D. R., Kobziar, L. N., & Robertson, K. M. (2017). Effects of fire frequency and soil temperature on soil CO_2 efflux rates in Old-Field Pine-Grassland forests. *Forests, 8*(8), 274.
Goicoa, T., Militino, A., & Ugarte, M. (2011). Modelling aboveground tree biomass while achieving the additivity property. *Environmental and Ecological Statistics, 18*(2), 367-384.
Gower, S. T., Vogt, K. A., & Grier, C. C. (1992). Carbon dynamics of Rocky Mountain Douglas-fir: Influence of water and nutrient availability. *Ecological Monographs, 62*(1), 43-65.
Green, E. J., & Reed, D. D. (1985). Compatible tree volume and taper functions for pitch pine. *Northern Journal of Applied Forestry, 2*(1), 14-16.
Guidolotti, G., Rey, A., D'andrea, E., Matteucci, G., & De Angelis, P. (2013). Effect of environmental variables and stand structure on ecosystem respiration components in a Mediterranean beech forest. *Tree physiology, 33*(9), 960-972.
Gulledge, J., & Schimel, J. P. (2000). Controls on soil carbon dioxide and methane fluxes in a variety of taiga forest stands in interior Alaska. *Ecosystems, 3*(3), 269-282.
Hawkins, B. J., Xue, J., Bown, H., & Clinton, P. (2010). Relating nutritional and physiological characteristics to growth of *Pinus radiata* clones planted on a range of sites in New Zealand. *Tree physiology, 30*(9), 1174-1191.
Haynes, B. E., & Gower, S. T. (1995). Belowground carbon allocation in unfertilized and fertilized red pine plantations in northern Wisconsin. *Tree physiology, 15*(5), 317-325.
Henningsen, A., & Hamann, J. (2007). systemfit: A package for estimating systems of simultaneous equations in R. *Journal of statistical software, 23*(4), 1-40.
Högberg, P., Nordgren, A., Buchmann, N., Taylor, A. F. S., Ekblad, A., Högberg, M. N., . . . Read, D. J. (2001, 06/14/online). Large-scale forest girdling shows that current photosynthesis drives soil respiration. *Nature, 411*, 789. https://doi.org/10.1038/35081058
Højsgaard, S., Halekoh, U., Robison-Cox, J., Wright, K., & Leidi, A. (2016). doBy: Groupwise statistics, LSmeans, linear contrasts, utilities. *R package version 4.5-15, 4*, 5-13.
Hollinger, D., Maclaren, J., Beets, P., & Turland, J. (1993). Carbon sequestration by New Zealand's plantation forests. *New Zealand Journal of Forestry Science, 23*(2), 194-208.
Hothorn, T., Hornik, K., & Zeileis, A. (2006). Unbiased recursive partitioning: A conditional inference framework. *Journal of Computational and Graphical statistics, 15*(3), 651-674.
Houghton, R. A. (1991, September 01). Tropical deforestation and atmospheric carbon dioxide. *Climatic Change, 19*(1-2), 99-118. https://doi.org/10.1007/bf00142217

Jackson, D., & Chittenden, J. (1981). Estimation of dry matter in *Pinus radiata* root systems I. Individual trees. *New Zealand Journal of Forestry Science, 11*(2), 164-182.
Jackson, D., Gifford, H., & Chittenden, J. (1976). Environmental variables influencing the increment of *Pinus radiata*:(2) effects of seasonal drought on height and diameter increment. *New Zealand Journal of Forestry Science, 5*(3), 265-286.
Jandl, R., Lindner, M., Vesterdal, L., Bauwens, B., Baritz, R., Hagedorn, F., . . . Byrne, K. A. (2007). How strongly can forest management influence soil carbon sequestration? *Geoderma, 137*(3), 253-268.
Janssens, I., Carrara, A., & Ceulemans, R. (2004). Annual Q_{10} of soil respiration reflects plant phenological patterns as well as temperature sensitivity. *Global Change Biology, 10*(2), 161-169.
Janssens, I., Lankreijer, H., Matteucci, G., Kowalski, A., Buchmann, N., Epron, D., . . . Grünwald, T. (2001). Productivity overshadows temperature in determining soil and ecosystem respiration across European forests. *Global Change Biology, 7*(3), 269-278.
Jenkinson, D. S., Adams, D., & Wild, A. (1991). Model estimates of CO_2 emissions from soil in response to global warming. *Nature, 351*(6324), 304.
Jeong, J., Bolan, N., & Kim, C. (2016). Heterotrophic soil respiration affected by compound fertilizer types in red pine (*Pinus densiflora S. et Z.*) stands of Korea. *Forests, 7*(12), 309.
Jia, B., Zhou, G., Wang, Y., Wang, F., & Wang, X. (2006). Effects of temperature and soil water-content on soil respiration of grazed and ungrazed *Leymus chinensis* steppes, Inner Mongolia. *Journal of Arid Environments, 67*(1), 60-76.
Johnson, D. W. (1992, August 01). Effects of forest management on soil carbon storage. *Water, Air, and Soil Pollution, 64*(1), 83-120. https://doi.org/10.1007/bf00477097
Jonsson, J., & Sigurdsson, B. (2009). Effects of thinning and fertilization on soil respiration in a cottonwood plantation in Iceland. *Biogeosciences Discussions, 6*(5), 9257-9278.
Jonsson, J., & Sigurdsson, B. D. (2010). Effects of early thinning and fertilization on soil temperature and soil respiration in a poplar plantation. *Icelandic Agricultural Sciences, 23*, 97-109.
Kang, S., Doh, S., Lee, D., Lee, D., Jin, V. L., & Kimball, J. S. (2003). Topographic and climatic controls on soil respiration in six temperate mixed-hardwood forest slopes, Korea. *Global Change Biology, 9*(10), 1427-1437.
Kauppi, P. E., & Tomppo, E. (1993, October 01). Impact of forests on net national emissions of carbon dioxide in West Europe. *Water, Air, and Soil Pollution, 70*(1), 187-196. https://doi.org/10.1007/bf01104996
Kim, C., Jeong, J., Bolan, N. S., & Naidu, R. (2012). Short-term effects of fertilizer application on soil respiration in red pine stands. *Journal of Ecology and Environment, 35*(4), 307-311.
Kirschbaum, M. U. (1995). The temperature dependence of soil organic matter decomposition, and the effect of global warming on soil organic C storage. *Soil Biology and Biochemistry, 27*(6), 753-760.
Kirschbaum, M. U. (2000). Will changes in soil organic carbon act as a positive or negative feedback on global warming? *Biogeochemistry, 48*(1), 21-51.
Kitayama, K., & Itow, S. (1999). Aboveground biomass and soil nutrient pools of a *Scalesia pedunculata* montane forest on Santa Cruz, Galápagos. *Ecological research, 14*(4), 405-408.
Knorr, W., Prentice, I. C., House, J., & Holland, E. (2005). Long-term sensitivity of soil carbon turnover to warming. *Nature, 433*(7023), 298.
Kozak, A. (1970). Methods for ensuring additivity of biomass components by regression analysis. *The Forestry Chronicle, 46*(5), 402-405.
Kozak, A., & Kozak, R. (2003). Does cross validation provide additional information in the evaluation of regression models? *Canadian Journal of Forest Research, 33*(6), 976-987.
Kuzyakov, Y., & Cheng, W. (2001). Photosynthesis controls of rhizosphere respiration and organic matter decomposition. *Soil Biology and Biochemistry, 33*(14), 1915-1925.

Lai, L., Zhao, X., Jiang, L., Wang, Y., Luo, L., Zheng, Y., . . . Rimmington, G. M. (2012). Soil respiration in different agricultural and natural ecosystems in an arid region. *PloS one, 7*(10), e48011.

Lal, R. (2005). Forest soils and carbon sequestration. *Forest Ecology and Management, 220*(1-3), 242-258.

Lasserre, J.-P., Mason, E., & Watt, M. (2005). The effects of genotype and spacing on *Pinus radiata* D. Don corewood stiffness in an 11-year old experiment. *Forest Ecology and Management, 205*(1-3), 375-383.

Lasserre, J.-P., Mason, E., & Watt, M. (2008). Influence of the main and interactive effects of site, stand stocking and clone on *Pinus radiata* D. Don corewood modulus of elasticity. *Forest Ecology and Management, 255*(8-9), 3455-3459.

Lasserre, J.-P., Mason, E., Watt, M., & Moore, J. R. (2009). Influence of initial planting spacing and genotype on microfibril angle, wood density, fibre properties and modulus of elasticity in *Pinus radiata* D. Don corewood. *Forest Ecology and Management, 258*(9), 1924-1931.

Lavery, P. B., & Mead, D. J. (2000). *Pinus radiata*: A narrow endemic from North America takes on the world. In D. M. Richardson (Ed.), *Ecology and Biogeography of Pinus* (pp. 432-449). Cambridge UK: Cambridge University Press

Lavigne, M., Foster, R., & Goodine, G. (2004). Seasonal and annual changes in soil respiration in relation to soil temperature, water potential and trenching. *Tree physiology, 24*(4), 415-424.

Le Quéré, C., Andrew, R. M., Friedlingstein, P., Sitch, S., Pongratz, J., Manning, A. C., . . . Jackson, R. B. (2017). Global carbon budget 2017. *Earth System Science Data*, 1-79.

Lee Allen, H., Fox, T. R., & Campbell, R. G. (2005). What is ahead for intensive pine plantation silviculture in the South? *Southern Journal of Applied Forestry, 29*(2), 62-69.

Lellei-Kovács, E., Kovács-Láng, E., Botta-Dukát, Z., Kalapos, T., Emmett, B., & Beier, C. (2011). Thresholds and interactive effects of soil moisture on the temperature response of soil respiration. *European Journal of Soil Biology, 47*(4), 247-255.

Lenth, R., Singmann, H., Love, J., Buerkner, P., & Herve, M. (2018). Emmeans: Estimated marginal means, aka least-squares means. *R Package Version 1.2.3.* Retrieved from https://CRAN.R-project.org/package=emmeans

Lewis, N. B., Ferguson, I. S., Sutton, W., Donald, D., & Lisboa, H. (1993). *Management of radiata pine*. Melbourne: Inkata Press Pty Ltd/Butterworth-Heinemann.

Li, B., Allen, H., & McKeand, S. (1991). Nitrogen and family effects on biomass allocation of loblolly pine seedlings. *Forest Science, 37*(1), 271-283.

Litton, C. M., Knight, D. H., & Ryan, M. G. (2001). Above-and belowground carbon allocation in post-fire lodgepole pine forests: Effects of tree density and stand age. *University of Wyoming National Park Service Research Center Annual Report, 25*(1), 123-129.

Litton, C. M., Raich, J. W., & Ryan, M. G. (2007). Carbon allocation in forest ecosystems. *Global Change Biology, 13*(10), 2089-2109.

Litton, C. M., Ryan, M. G., & Knight, D. H. (2004). Effects of tree density and stand age on carbon allocation patterns in postfire lodgepole pine. *Ecological Applications, 14*(2), 460-475.

Litton, C. M., Ryan, M. G., Knight, D. H., & Stahl, P. D. (2003). Soil-surface carbon dioxide efflux and microbial biomass in relation to tree density 13 years after a stand replacing fire in a lodgepole pine ecosystem. *Global Change Biology, 9*(5), 680-696.

Litton, C. M., Ryan, M. G., Tinker, D. B., & Knight, D. H. (2003). Belowground and aboveground biomass in young postfire lodgepole pine forests of contrasting tree density. *Canadian Journal of Forest Research, 33*(2), 351-363.

Liu, H. S., Li, L. H., Han, X. G., Huang, J. H., Sun, J. X., & Wang, H. Y. (2006). Respiratory substrate availability plays a crucial role in the response of soil respiration to environmental factors. *Applied Soil Ecology, 32*(3), 284-292.

Lloyd, J., & Taylor, J. (1994). On the temperature dependence of soil respiration. *Functional ecology*, 315-323.

Lomander, A., Kätterer, T., & Andrén, O. (1998). Modelling the effects of temperature and moisture on CO_2 evolution from top-and subsoil using a multi-compartment approach. *Soil Biology and Biochemistry, 30*(14), 2023-2030.

Macara, G. R. (2016). *The climate and weather of Canterbury*. NIWA Sceience and Technology Series, Taihoro Nukurangi. Retrieved from https://www.niwa.co.nz/static/web/canterbury_climatology_second_ed_niwa.pdf.

Madgwick, H. (1983). Estimation of the oven-dry weight of stems, needles, and branches of individual *Pinus radiata* trees. *New Zealand Journal of Forestry Science, 13*(1), 108-109.

Madgwick, H. (1985). Dry matter and nutrient relationships in stands of *Pinus radiata*. *New Zealand Journal of Forestry, 15*(3), 324-336.

Madgwick, H. (1994). *Pinus radiata: biomass, form and growth*. Rotorua NZ: HAI Madgwick.

Madgwick, H., Jackson, D. S., & Knight, P. (1977). Above-ground dry matter, energy, and nutrient contents of trees in an age series of *Pinus radiata* plantations. *New Zealand Journal of Forestry Science, 7*(3), 445-468.

Magalhães, T. M., & Seifert, T. (2015). Biomass modelling of *Androstachys johnsonii Prain*: A comparison of three methods to enforce additivity. *International Journal of Forestry Research, 2015*.

Maier, C. A., Albaugh, T. J., Lee Allen, H., & Dougherty, P. M. (2004). Respiratory carbon use and carbon storage in mid-rotation loblolly pine (*Pinus taeda L.*) plantations: The effect of site resources on the stand carbon balance. *Global Change Biology, 10*(8), 1335-1350.

Maier, C. A., Anderson, P., Butnor, J. R., Dougherty, P. M., Johnsen, K., & McInnis, D. (2016). *Temporal and spatial patterns of soil CO_2 efflux, soil carbon, and root biomass associated with bedding in young loblolly pine plantations.* Paper presented at the Proceedings of the 18th Biennial Southern Silvicultural Research Conference. e-Gen. Tech. Rep. SRS-212. Asheville, NC: US Department of Agriculture, Forest Service, Southern Research Station. 614 p.

Maier, C. A., & Kress, L. (2000). Soil CO_2 evolution and root respiration in 11 year-old loblolly pine (*Pinus taeda*) plantations as affected by moisture and nutrient availability. *Canadian Journal of Forest Research, 30*(3), 347-359.

Martin, J. G., & Bolstad, P. V. (2005). Annual soil respiration in broadleaf forests of northern Wisconsin: Influence of moisture and site biological, chemical, and physical characteristics. *Biogeochemistry, 73*(1), 149-182.

Mason, E. (1992). *Decision-support systems for establishing radiata pine plantations in the Central North Island of New Zealand*. (Doctoral Thesis). University of Canterbury, Christchurch, New Zealand.

Mason, E. (2008). Influences of silviculture, genetics and environment on radiata pine corewood properties: Results from recent studies and a future direction. *New Zealand Journal of Forestry Science, 53*(2), 26-31.

Mason, E., & Kirongo, B. (1999). Responses of radiata pine clones to varying levels of pasture competition in a semiarid environment. *Canadian Journal of Forest Research, 29*(7), 934-939.

Mason, E., & Milne, P. (1999). Effects of weed control, fertilization, and soil cultivation on the growth of *Pinus radiata* at midrotation in Canterbury, New Zealand. *Canadian Journal of Forest Research, 29*(7), 985-992.

Mason, E., South, D. B., & Weizhong, Z. (1996). Performance of *Pinus radiata* in relation to seedling grade, weed control, and soil cultivation in the central North Island of New Zealand. *New Zealand Journal of Forestry Science, 26*(1/2), 173-183.

McMurtrie, R., Rook, D., & Kelliher, F. (1990). Modelling the yield of *Pinus radiata* on a site limited by water and nitrogen. *Forest Ecology and Management, 30*(1-4), 381-413.

McQuillan, S. (2013). *Above and below ground assessment of Pinus radiata.* (Unpublished BForSci Thesis). University of Canterbury, Christchurch, New Zealand.

Mead, D. (2013). *Sustainable management of Pinus radiata plantations*: FAO Forestry Paper No. 170. Rome: FAO.
Mead, D., Draper, D., & Madgwick, H. (1984). Dry matter production of a young stand of *Pinus radiata*: Some effects of nitrogen fertiliser and thinning. *New Zealand Journal of Forestry Science, 14*(1), 97-108.
Mead, D., Lucas, R., & Mason, E. (1993). Studying interactions between pastures and *Pinus radiata* in Canterbury's subhumid temperate environment—the first two years. *New Zealand Journal of Forestry Science, 38*(1), 26-31.
Melillo, J. M., Steudler, P. A., Aber, J. D., Newkirk, K., Lux, H., Bowles, F. P., . . . Morrisseau, S. (2002). Soil warming and carbon-cycle feedbacks to the climate system. *Science, 298*(5601), 2173-2176. https://doi.org/10.1126/science.1074153
Moore, J. (2010). Allometric equations to predict the total above-ground biomass of *radiata pine* trees. *Annals of Forest Science, 67*(8), 806.
Murphy, M., Balser, T., Buchmann, N., Hahn, V., & Potvin, C. (2008). Linking tree biodiversity to belowground process in a young tropical plantation: Impacts on soil CO_2 flux. *Forest Ecology and Management, 255*(7), 2577-2588.
Nakane, K., Tsubota, H., & Yamamoto, M. (1984, March 01). Cycling of soil carbon in a Japanese red pine forest I. Before a clear-felling. *The Botanical Magazine, 97*(1), 39-60. https://doi.org/10.1007/bf02488146
Nakane, K., Yamamoto, M., & Tsubota, H. (1983). Estimation of root respiration rate in a mature forest ecosystem. *JAPANESE JOURNAL OF ECOLOGY, 33*(4), 397-408. https://doi.org/10.18960/seitai.33.4_397
Návar, J. (2010). Measurement and assessment methods of forest aboveground biomass: A literature review and the challenges ahead. In Maggie Momba, M., & Faizal, B. (Eds). *Biomass. Rijeka, Croatia: Sciyo*, 27-64.
Návar, J., González, N., Graciano, L., Dale, V., & Parresol, B. (2004). Additive biomass equations for pine species of forest plantations of Durango, Mexico. *Madera y Bosques, 10*(2).
Návar, J., Méndez, E., & Dale, V. (2002). Estimating stand biomass in the Tamaulipan thornscrub of northeastern Mexico. *Annals of Forest Science, 59*(8), 813-821.
Návar, J., Méndez, E., Nájera, A., Graciano, J., Dale, V., & Parresol, B. (2004). Biomass equations for shrub species of Tamaulipan thornscrub of North-eastern Mexico. *Journal of Arid Environments, 59*(4), 657-674.
NIWA. (2018). *Eastern South Island*. Retrieved from https://www.niwa.co.nz/education-and-training/schools/resources/climate/overview/map_e_south
Nixon, C., Gamperle, D., Pambudi, D., & Clough, P. (2017). *Plantation forestry statistics: Contribution of forestry to New Zealand*. Wellington, NZ.
Noh, N. J., Son, Y., Lee, S. K., Yoon, T. K., Seo, K. W., Kim, C., . . . Hwang, J. (2010). Influence of stand density on soil CO_2 efflux for a *Pinus densiflora* forest in Korea. *Journal of Plant Research, 123*(4), 411-419.
Nohrstedt, H.-Ö., Arnebrant, K., Bååth, E., & Söderström, B. (1989). Changes in carbon content, respiration rate, ATP content, and microbial biomass in nitrogen-fertilized pine forest soils in Sweden. *Canadian Journal of Forest Research, 19*(3), 323-328.
Olajuyigbe, S., Tobin, B., Saunders, M., & Nieuwenhuis, M. (2012). Forest thinning and soil respiration in a Sitka spruce forest in Ireland. *Agricultural and Forest Meteorology, 157*, 86-95.
Olsson, P., Linder, S., Giesler, R., & Högberg, P. (2005). Fertilization of boreal forest reduces both autotrophic and heterotrophic soil respiration. *Global Change Biology, 11*(10), 1745-1753.
Orchard, V. A., & Cook, F. (1983). Relationship between soil respiration and soil moisture. *Soil Biology and Biochemistry, 15*(4), 447-453.
Palmroth, S., Maier, C. A., McCarthy, H. R., Oishi, A. C., Kim, H.-S., Johnsen, K. H., . . . Oren, R. (2005). Contrasting responses to drought of forest floor CO_2 efflux in a loblolly pine plantation and a

nearby Oak-Hickory forest. *Global Change Biology, 11*(3), 421-434. https://doi.org/doi:10.1111/j.1365-2486.2005.00915.x

Pan, Y., Birdsey, R. A., Fang, J., Houghton, R., Kauppi, P. E., Kurz, W. A., . . . Hayes, D. (2011). A large and persistent carbon sink in the world's forests. *Science, 333*(6045), 988-993. https://doi.org/10.1126/science.1201609

Pangle, R. (2000). *Soil CO_2 efflux in response to fertilization and mulching treatments in a two-year-old loblolly pine (Pinus taeda L.) plantation in the Virginia Piedmont*. (Master's Thesis). Virginia Tech, Blacksburg, Virginia.

Pangle, R., & Seiler, J. (2002). Influence of seedling roots, environmental factors and soil characteristics on soil CO_2 efflux rates in a 2-year-old loblolly pine (*Pinus taeda L.*) plantation in the Virginia Piedmont. *Environmental Pollution, 116*, S85-S96.

Parresol, B. (1993). Modeling multiplicative error variance: An example predicting tree diameter from stump dimensions in baldcypress. *Forest Science, 39*(4), 670-679.

Parresol, B. (1999). Assessing tree and stand biomass: A review with examples and critical comparisons. *Forest Science, 45*(4), 573-593.

Parresol, B. (2001). Additivity of nonlinear biomass equations. *Canadian Journal of Forest Research, 31*(5), 865-878.

Phillips, R. P., & Fahey, T. J. (2007). Fertilization effects on fineroot biomass, rhizosphere microbes and respiratory fluxes in hardwood forest soils. *New Phytologist, 176*(3), 655-664.

Pinheiro, J., Bates, D., DebRoy, S., Sarkar, D., & R Core Team. (2018). nlme: Linear and nonlinear mixed effects models. (Version 3.1-137). Retrieved from https://CRAN.R-project.org/package=nlme

Porté, A., Trichet, P., Bert, D., & Loustau, D. (2002). Allometric relationships for branch and tree woody biomass of Maritime pine (*Pinus pinaster Aıt.*). *Forest Ecology and Management, 158*(1-3), 71-83.

PP Systems. (2016). EGM-4: Environmental Gas Monitor Operator's Manual. Version 4.18. Retrieved from http://www.vtpup.cz/common/manual/PrF_biofyz_PPSystems_EGM4_manual_EN.pdf

R Core Team. (2017). *R: A language and environment for statistical computing*. R Foundation for Statistical Computing, Vienna, Austria. Retrieved from https://www.R-project.org/.

Raich, J., & Nadelhoffer, K. (1989). Belowground carbon allocation in forest ecosystems: Global trends. *Ecology, 70*(5), 1346-1354.

Raich, J., & Potter, C. S. (1995). Global patterns of carbon dioxide emissions from soils. *Global Biogeochemical Cycles, 9*(1), 23-36.

Raich, J., Potter, C. S., & Bhagawati, D. (2002). Interannual variability in global soil respiration, 1980–94. *Global Change Biology, 8*(8), 800-812.

Raich, J., & Schlesinger, W. H. (1992). The global carbon dioxide flux in soil respiration and its relationship to vegetation and climate. *Tellus B, 44*(2), 81-99.

Raich, J., & Tufekciogul, A. (2000). Vegetation and soil respiration: Correlations and controls. *Biogeochemistry, 48*(1), 71-90.

Raison, R., Khanna, P., Benson, M., Myers, B., McMurtrie, R., & Lang, A. (1992). Dynamics of *Pinus radiata* foliage in relation to water and nitrogen stress: Needle loss and temporal changes in total foliage mass. *Forest Ecology and Management, 52*(1-4), 159-178.

Reed, D. D., & Green, E. J. (1985). A method of forcing additivity of biomass tables when using nonlinear models. *Canadian Journal of Forest Research, 15*(6), 1184-1187.

Reichstein, M., Rey, A., Freibauer, A., Tenhunen, J., Valentini, R., Banza, J., . . . Irvine, J. (2003). Modeling temporal and large-scale spatial variability of soil respiration from soil water availability, temperature and vegetation productivity indices. *Global Biogeochemical Cycles, 17*(4).

Reineke, L. H. (1933). Perfecting a stand-density index for even-aged forests. *Journal of agricultural research, 46*, 627 - 638.

Reiners, W. (1968). Carbon dioxide evolution from the floor of three Minnesota forests. *Ecology, 49*(3), 471-483.

Rey, A., Pegoraro, E., Tedeschi, V., De Parri, I., Jarvis, P. G., & Valentini, R. (2002). Annual variation in soil respiration and its components in a coppice oak forest in central Italy. *Global Change Biology, 8*(9), 851-866.

Richardson, B. (1993). Vegetation management practices in plantation forests of Australia and New Zealand. *Canadian Journal of Forest Research, 23*(10), 1989-2005.

Robinson, J. M. (2016). *Temperature sensitivity of soil respiration*. (Master's Thesis). University of Waikato, Hamilton NZ.

Rogers, D. L. (2002). In situ genetic conservation of Monterey pine (*Pinus radiata* D. Don): Information and recommendations. *New Zealand Journal of Forestry Science, 32*(23), 395-398.

Rubilar, R. A., Albaugh, T. J., Allen, H. L., Alvarez, J., Fox, T. R., & Stape, J. L. (2013). Influences of silvicultural manipulations on above- and belowground biomass accumulations and leaf area in young *Pinus radiata* plantations, at three contrasting sites in Chile. *Forestry: An International Journal of Forest Research, 86*(1), 27-38. https://doi.org/10.1093/forestry/cps055

Rustad, L., Campbell, J., Marion, G., Norby, R., Mitchell, M., Hartley, A., . . . Gurevitch, J. (2001). A meta-analysis of the response of soil respiration, net nitrogen mineralization, and aboveground plant growth to experimental ecosystem warming. *Oecologia, 126*(4), 543-562.

Rustad, L., Huntington, T. G., & Boone, R. D. (2000). Controls on Soil Respiration: Implications for Climate Change. *Biogeochemistry, 48*(1), 1-6.

Ryan, M. G., Hubbard, R. M., Pongracic, S., Raison, R. J., & McMurtrie, R. E. (1996, Mar). Foliage, fine-root, woody-tissue and stand respiration in *Pinus radiata* in relation to nitrogen status. *Tree physiology, 16*(3), 333-343.

Saiz, G., Green, C., Butterbach-Bahl, K., Kiese, R., Avitabile, V., & Farrell, E. P. (2006, September 01). Seasonal and spatial variability of soil respiration in four Sitka spruce stands. *Plant and Soil, 287*(1), 161-176. https://doi.org/10.1007/s11104-006-9052-0

Samuelson, L. J., Johnsen, K., Stokes, T., & Lu, W. (2004). Intensive management modifies soil CO_2 efflux in 6-year-old *Pinus taeda L.* stands. *Forest Ecology and Management, 200*(1-3), 335-345.

Santa Regina, I., Tarazona, T., & Calvo, R. (1997). Aboveground biomass in a beech forest and a Scots pine plantation in the Sierra de la Demanda area of Northern Spain. *Annals of Forest Science, 54*(3), 261-269.

Schlatter, J., & Gerding, V. (1984). Important site factors for *Pinus radiata* growth in Chile. In: Grey, D.C., Schonau, A.P.G., Schutz, C.J. (Eds.), Proceedings, IUFRO Sypmosium on Site and Productivity of Fast Growing Plantations. Pretoria and Pietermaritzburg, South Africa, 30 April–11 May. 1984. ISBN 0 621 08513 8., 541–550.

Schlesinger, W. H., & Andrews, J. A. (2000). Soil respiration and the global carbon cycle. *Biogeochemistry, 48*(1), 7-20.

Schwendenmann, L., & Macinnis-Ng, C. (2016). Soil CO_2 efflux in an old-growth southern conifer forests (*Agathis australis*) – magnitude, components, and controls. *Soil, 2*(3), 1-38. https://doi.org/10.5194/soil-2016-21

Scott, N. A., Tate, K. R., Ford-Robertson, J., Giltrap, D. J., & Smith, C. T. (1999). Soil carbon storage in plantation forests and pastures: Land-use change implications. *Tellus B: Chemical and Physical Meteorology, 51*(2), 326-335. https://doi.org/doi:10.1034/j.1600-0889.1999.00015.x

Shan, J., Morris, L. A., & Hendrick, R. L. (2001). The effects of management on soil and plant carbon sequestration in slash pine plantations. *Journal of Applied Ecology, 38*(5), 932-941.

Shrestha, R. K., Strahm, B. D., Sucre, E. B., Holub, S. M., & Meehan, N. (2014). Fertilizer management, parent material, and stand age influence forest soil greenhouse gas fluxes. *Soil Science Society of America Journal, 78*, 2041-2053. https://doi.org/10.2136/sssaj2014.03.0118

Snowdon, P. (1985). Effects of fertilizer and family on the homogeneity of biomass regressions for young *Pinus radiata*. *Australian Forest Research, 15*, 135-140.

Snowdon, P., & Benson, M. (1992). Effects of combinations of irrigation and fertilisation on the growth and above-ground biomass production of *Pinus radiata*. *Forest Ecology and Management, 52*(1-4), 87-116.

Söderström, B., Bååth, E., & Lundgren, B. (1983, 1983/11/01). Decrease in soil microbial activity and biomasses owing to nitrogen amendments. *Canadian Journal of Microbiology, 29*(11), 1500-1506. https://doi.org/10.1139/m83-231

Sprugel, D. (1983). Correcting for bias in log-transformed allometric equations. *Ecology, 64*(1), 209-210.

Srivastava, V. K., & Giles, D. E. (1987). *Seemingly unrelated regression equations models: Estimation and inference* (Vol. 80): CRC Press.

Sutton, W. R. J. (1999). The need for planted forests and the example of radiata pine. *New Forests, 17*(1), 95-110. https://doi.org/10.1023/a:1006567221005

Tang, J., Qi, Y., Xu, M., Misson, L., & Goldstein, A. H. (2005). Forest thinning and soil respiration in a ponderosa pine plantation in the Sierra Nevada. *Tree physiology, 25*(1), 57-66.

Teskey, R., Bongarten, B., Cregg, B., Dougherty, P., & Hennessey, T. (1987). Physiology and genetics of tree growth response to moisture and temperature stress: An examination of the characteristics of loblolly pine (*Pinus taeda L.*). *Tree physiology, 3*(1), 41-61.

Thierron, V., & Laudelout, H. (1996, 1996/07/01). Contribution of root respiration to total CO_2 efflux from the soil of a deciduous forest. *Canadian Journal of Forest Research, 26*(7), 1142-1148. https://doi.org/10.1139/x26-127

Toro, J., & Gessel, S. (1999, July 01). Radiata pine plantations in Chile. *New Forests, 18*(1), 33-44. https://doi.org/10.1023/a:1006597823190

Trumbore, S. E., Chadwick, O. A., & Amundson, R. (1996). Rapid exchange between soil carbon and atmospheric carbon dioxide driven by temperature change. *Science, 272*(5260), 393-396. https://doi.org/10.1126/science.272.5260.393

Turner, J., & Lambert, M. J. (1986). Nutrition and nutritional relationships of *Pinus radiata*. *Annual Review of Ecology and Systematics, 17*(1), 325-350.

Tyree, M. C., Seiler, J. R., & Maier, C. A. (2011). Short-term impacts of soil amendments on belowground C cycling and soil nutrition in two contrasting *Pinus taeda L.* genotypes. *Forest Ecology and Management, 262*(8), 1473-1482.

Tyree, M. C., Seiler, J. R., & Maier, C. A. (2014). Contrasting genotypes, soil amendments, and their interactive effects on short-term total soil CO_2 efflux in a 3-year-old *Pinus taeda L.* plantation. *Soil Biology and Biochemistry, 69*, 93-100.

Van't Hoff, J. H., & Lehfeldt, R. A. (1899). *Lectures on theoretical and physical chemistry*. London: Edwin Arnold.

Van Lear, D. H., Kapeluck, P. R., & Parker, M. M. (1995). Distribution of carbon in a Piedmont soil as affected by loblolly pine management. In *Carbon Forms and Functions in Forest Soils* (pp. 489-501). Madison, WI: Soil Science Society of America

Von Gadow, K., & Hui, G. (2001). *Modelling forest development* (Vol. 57): Springer Science & Business Media.

Vose, J. M., Elliott, K. J., Johnson, D. W., Walker, R. F., Johnson, M. G., & Tingey, D. T. (1995). Effects of elevated CO_2 and N fertilization on soil respiration from ponderosa pine (*Pinus ponderosa*) in open-top chambers. *Canadian Journal of Forest Research, 25*(8), 1243-1251.

Walker, J. P., Willgoose, G. R., & Kalma, J. D. (2004). In situ measurement of soil moisture: A comparison of techniques. *Journal of Hydrology, 293*(1), 85-99.

Wan, S., Zhang, C., Chen, Y., Zhao, J., Zhu, X., Wu, J., . . . Fu, S. (2014). Interactive effects of understory removal and fertilization on soil respiration in subtropical *Eucalyptus* plantations. *Journal of Plant Ecology, 8*(3), 284-290.

Wang, B., Zha, T. S., Jia, X., Wu, B., Zhang, Y. Q., & Qin, S. G. (2014). Soil moisture modifies the response of soil respiration to temperature in a desert shrub ecosystem. *11*(2), 259-268. https://doi.org/10.5194/bg-11-259-2014

Wang, C., Yang, J., & Zhang, Q. (2006). Soil respiration in six temperate forests in China. *Global Change Biology, 12*(11), 2103-2114. https://doi.org/doi:10.1111/j.1365-2486.2006.01234.x

Wang, X., Fang, J., Tang, Z., & Zhu, B. (2006). Climatic control of primary forest structure and DBH–height allometry in Northeast China. *Forest Ecology and Management, 234*(1-3), 264-274.

Wardle, D. A., Bardgett, R. D., Klironomos, J. N., Setälä, H., Van Der Putten, W. H., & Wall, D. H. (2004). Ecological linkages between aboveground and belowground biota. *Science, 304*(5677), 1629-1633.

Watt, M., Moore, J., Façon, J., Downes, G., Clinton, P., Coker, G., . . . Bown, H. (2006). Modelling the influence of stand structural, edaphic and climatic influences on juvenile *Pinus radiata* dynamic modulus of elasticity. *Forest Ecology and Management, 229*(1), 136-144. https://doi.org/https://doi.org/10.1016/j.foreco.2006.03.016

Webber, B., & Madgwick, H. (1983). Biomass and nutrient content of 29-year-old *Pinus radiata* stand. *New Zealand Journal of Forestry Science, 13*(2), 222-228.

Will, G. (1964). Dry matter production and nutrient uptake by *Pinus radiata* in New Zealand. *The Commonwealth Forestry Review*, 57-70.

Wiseman, P. E., & Seiler, J. R. (2004, 2004/05/06/). Soil CO_2 efflux across four age classes of plantation loblolly pine (*Pinus taeda L.*) on the Virginia Piedmont. *Forest Ecology and Management, 192*(2), 297-311. https://doi.org/https://doi.org/10.1016/j.foreco.2004.01.017

Xu, J., Chen, J., Brosofske, K., Li, Q., Weintraub, M., Henderson, R., . . . Shao, C. (2011, 2011/12/01). Influence of timber harvesting alternatives on forest soil respiration and its biophysical regulatory factors over a 5-year period in the Missouri Ozarks. *Ecosystems, 14*(8), 1310-1327. https://doi.org/10.1007/s10021-011-9482-2

Xu, M., & Qi, Y. (2001a). Soil-surface CO_2 efflux and its spatial and temporal variations in a young ponderosa pine plantation in Northern California. *Global Change Biology, 7*(6), 667-677.

Xu, M., & Qi, Y. (2001b). Spatial and seasonal variations of Q_{10} determined by soil respiration measurements at a Sierra Nevadan forest. *Global Biogeochemical Cycles, 15*(3), 687-696. https://doi.org/doi:10.1029/2000GB001365

Xue, J., Dungey, H., Clinton, P., Henley, D., Niollet, S., & Leckie, A. (2013). *The potential for using foliar carbon isotopic signature to screen drought tolerant radiata pine genotypes for dryland plantation forests in New Zealand*. Wellington NZ: Ministry for Primary Industries.

Yi, M.-J., Son, Y., Jin, H.-O., Park, I.-H., Kim, D.-Y., Kim, Y.-S., & Shin, D.-M. (2005). Belowground carbon allocation of natural *Quercus mongolica* forests estimated from litterfall and soil respiration measurements. *Korean Journal of Agricultural and Forest Meteorology, 7*(3), 227-234.

Yiqi, L., & Zhou, X. (2010). *Soil respiration and the environment*. London: Elsevier.

Yohannes, Y., Shibistova, O., Asaye, Z., & Guggenberger, G. (2013). Forest management influence on the carbon flux of *Cupressus lusitanica* plantation in the Munessa forest, Ethiopia. *Forest Research, 2*, 111. https://doi.org/10.4172/2168-9776.1000111

Yu, X., Zha, T., Pang, Z., Wu, B., Wang, X., Chen, G., . . . Wu, H. (2011). Response of soil respiration to soil temperature and moisture in a 50-year-old oriental arborvitae plantation in China. *PloS one, 6*(12), e28397. https://doi.org/10.1371/journal.pone.0028397

Yuste, J. C., Janssens, I., Carrara, A., Meiresonne, L., & Ceulemans, R. (2003). Interactive effects of temperature and precipitation on soil respiration in a temperate maritime pine forest. *Tree physiology, 23*(18), 1263-1270.

Zak, D. R., Holmes, W. E., White, D. C., Peacock, A. D., & Tilman, D. (2003). Plant diversity, soil microbial communities, and ecosystem function: Are there any links? *Ecology, 84*(8), 2042-2050.

Zerihun, A., & Montagu, K. D. (2004). Belowground to aboveground biomass ratio and vertical root distribution responses of mature *Pinus radiata* stands to phosphorus fertilization at planting. *Canadian Journal of Forest Research, 34*(9), 1883-1894.

Zhang, C., Peng, D.-L., Huang, G.-S., & Zeng, W.-S. (2016). Developing aboveground biomass equations both compatible with tree volume equations and additive systems for single-trees in poplar plantations in Jiangsu province, China. *Forests, 7*(2), 32.

Zhao, D., Kane, M., Markewitz, D., Teskey, R., & Clutter, M. (2015). Additive tree biomass equations for midrotation loblolly pine plantations. *Forest Science, 61*(4), 613-623.

Zheng, C., Mason, E., Jia, L., Wei, S., Sun, C., & Duan, J. (2015). A single-tree additive biomass model of *Quercus variabilis Blume* forests in North China. *Trees, 29*(3), 705-716.

Zhou, X., Brandle, J. R., Schoeneberger, M. M., & Awada, T. (2007). Developing above-ground woody biomass equations for open-grown, multiple-stemmed tree species: Shelterbelt-grown Russian-olive. *Ecological Modelling, 202*(3-4), 311-323.

Zogg, G. P., Zak, D. R., Burton, A. J., & Pregitzer, K. S. (1996). Fine root respiration in northern hardwood forests in relation to temperature and nitrogen availability. *Tree physiology, 16*(8), 719-725.

Zou, W.-T., Zeng, W.-S., Zhang, L.-J., & Zeng, M. (2015). Modeling crown biomass for four pine species in China. *Forests, 6*(2), 433-449.

Zuur, A., Ieno, E., Walker, N., Saveliev, A., & Smith, G. (2009). *Mixed Effects Models and Extensions in Ecology with R*. New Work, USA: Springer.

Appendixes

Appendix 1

Appendix 1.1: Residual distribution of selected best models with predicting and other variables: (A) Stem (Eq. **2.10**), (B) Branch (Eq. **2.11**), (C) Bark (Eq. **2.12**), (D) NF (Eq. **2.13**), (E) OF (Eq. **2.14**), (F) Cone (Eq. **2.15**), (G) Foliage (Eq. **2.16**), (H) Crown (Eq. **2.17**), (I) Bole (Eq. **2.18**), and (J) AGT (Eq. **2.19**). The solid black horizontal line across zero represent baseline and the dotted red line is LOESS curve).

(A) Stem biomass

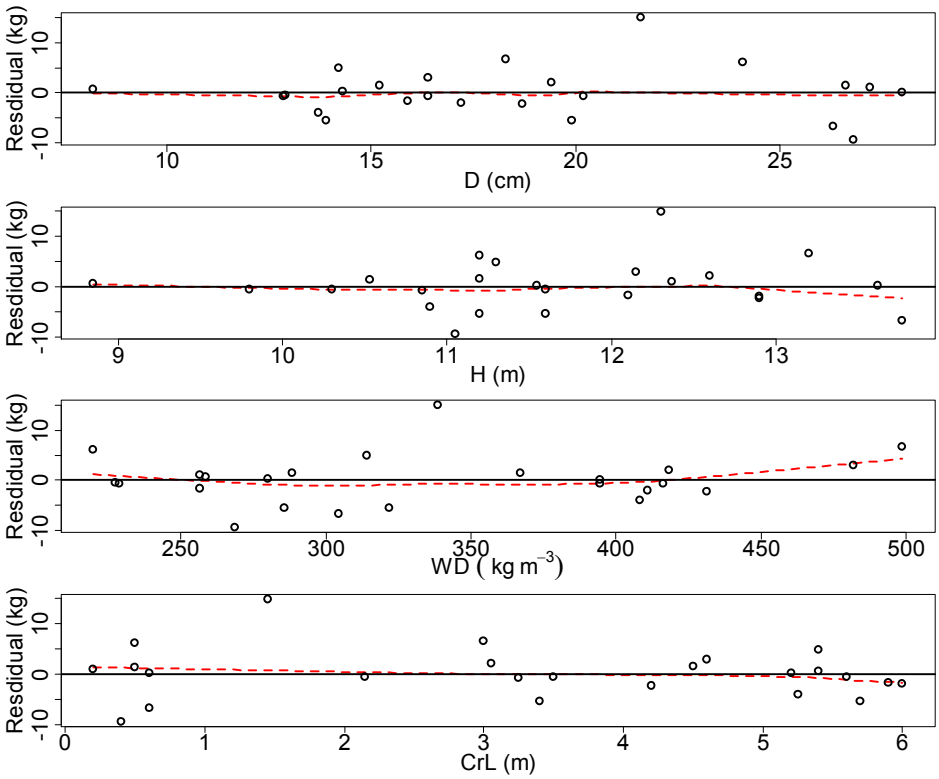

(B) Branch biomass

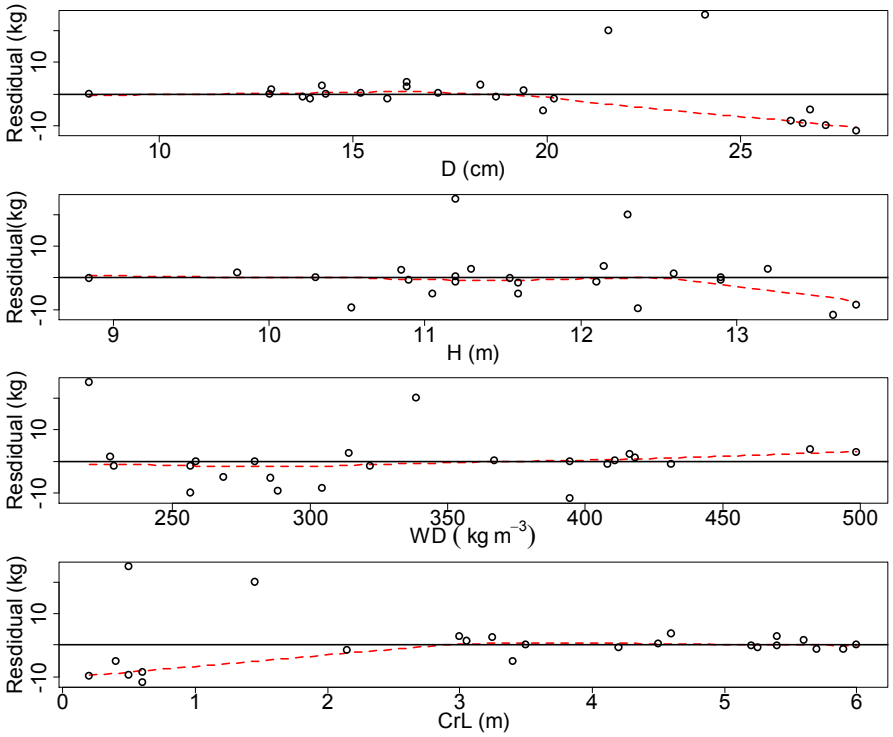

(C) Bark biomass

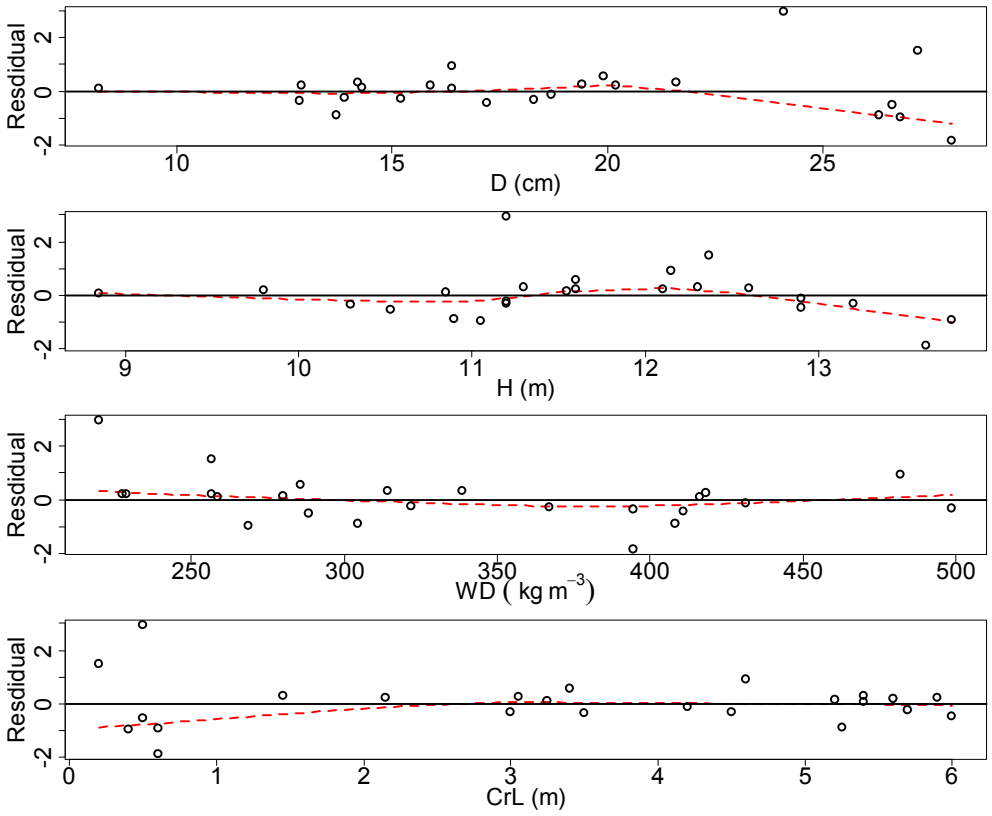

(D) New foliage biomass

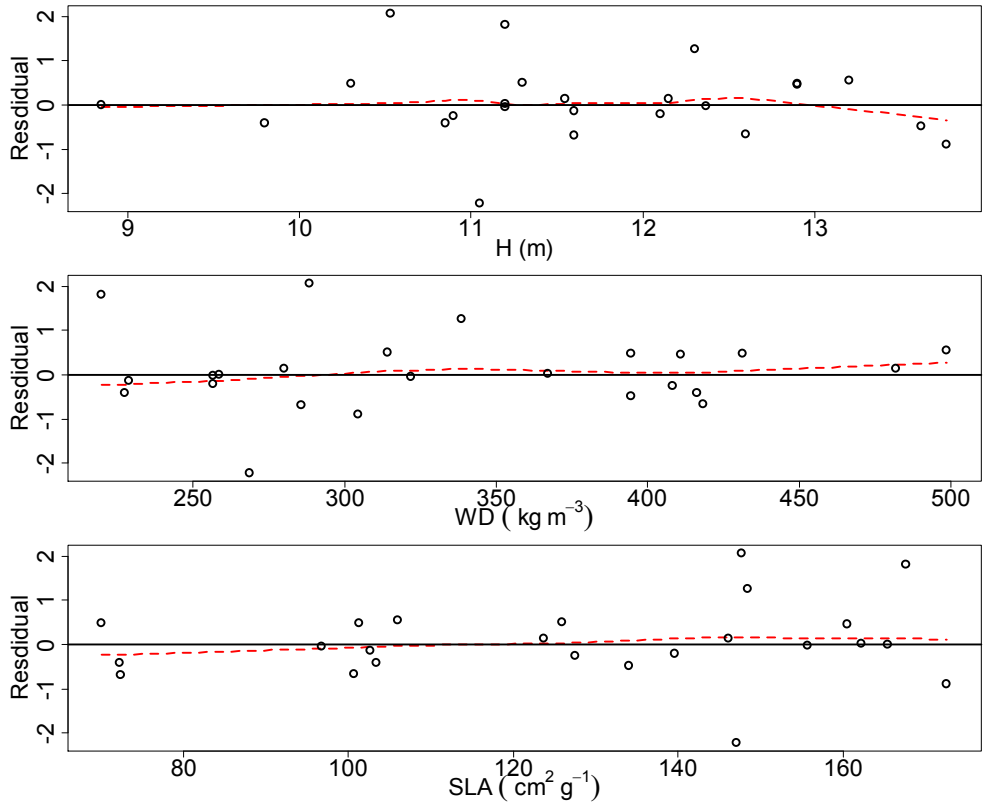

(E) Old foliage biomass

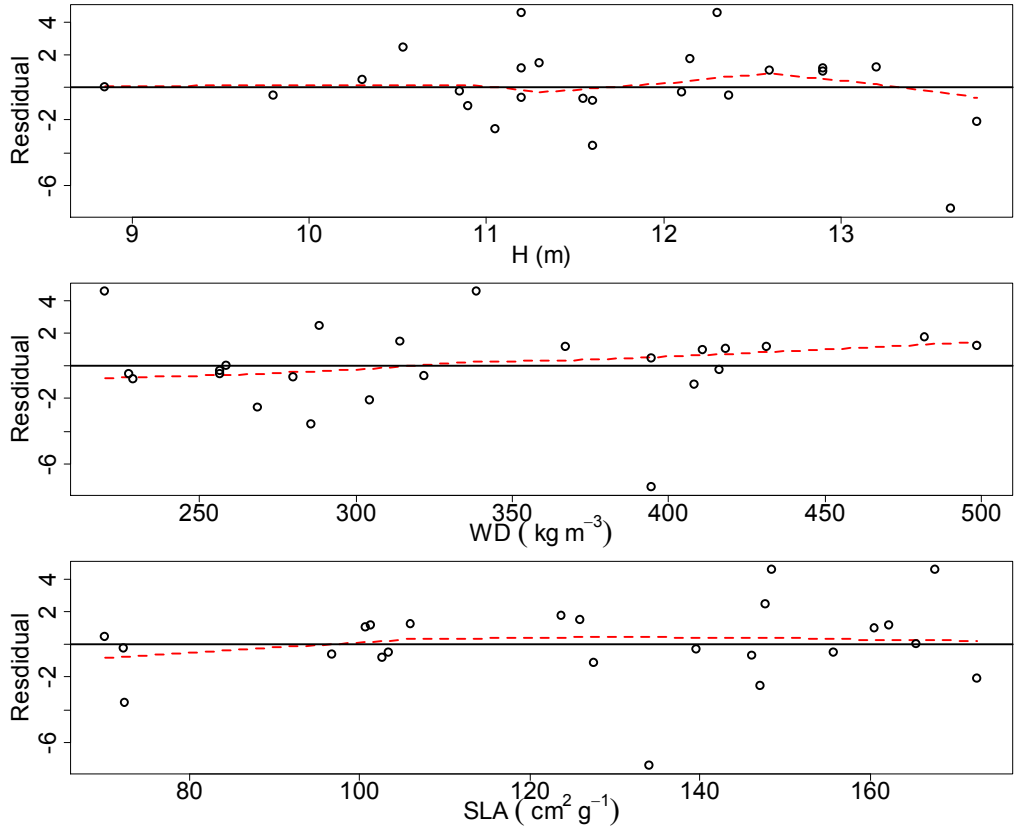

(F) Cone biomass

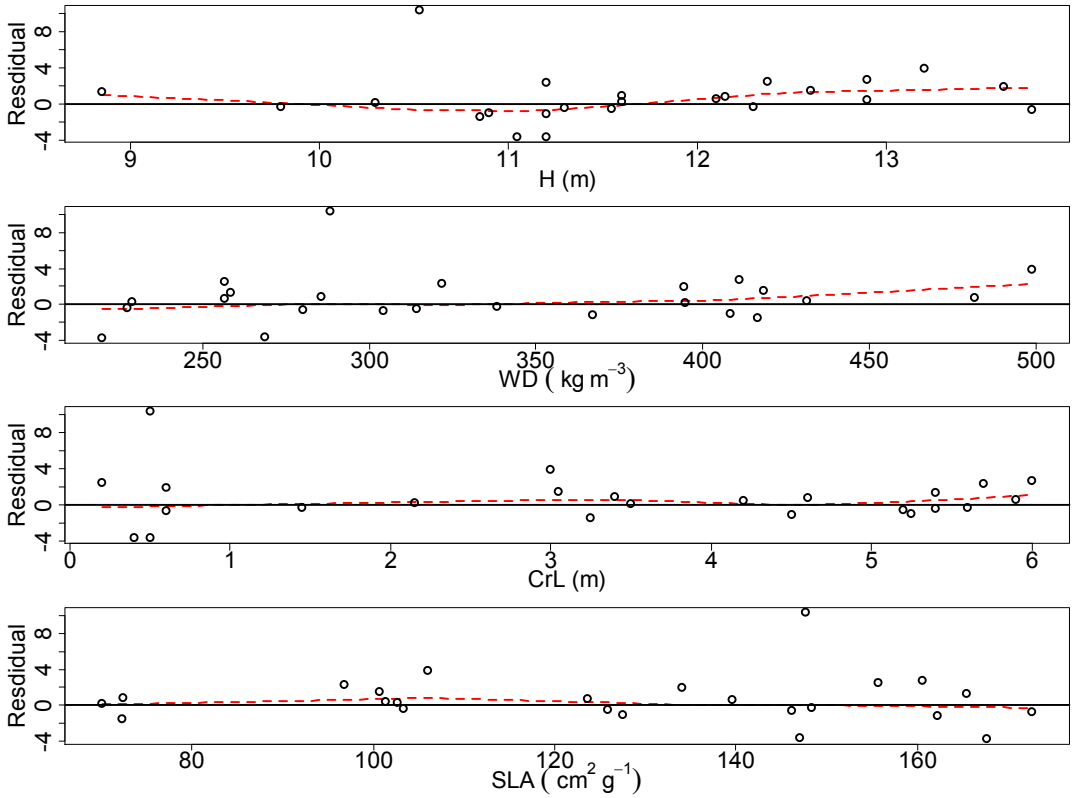

(G) Foliage biomass

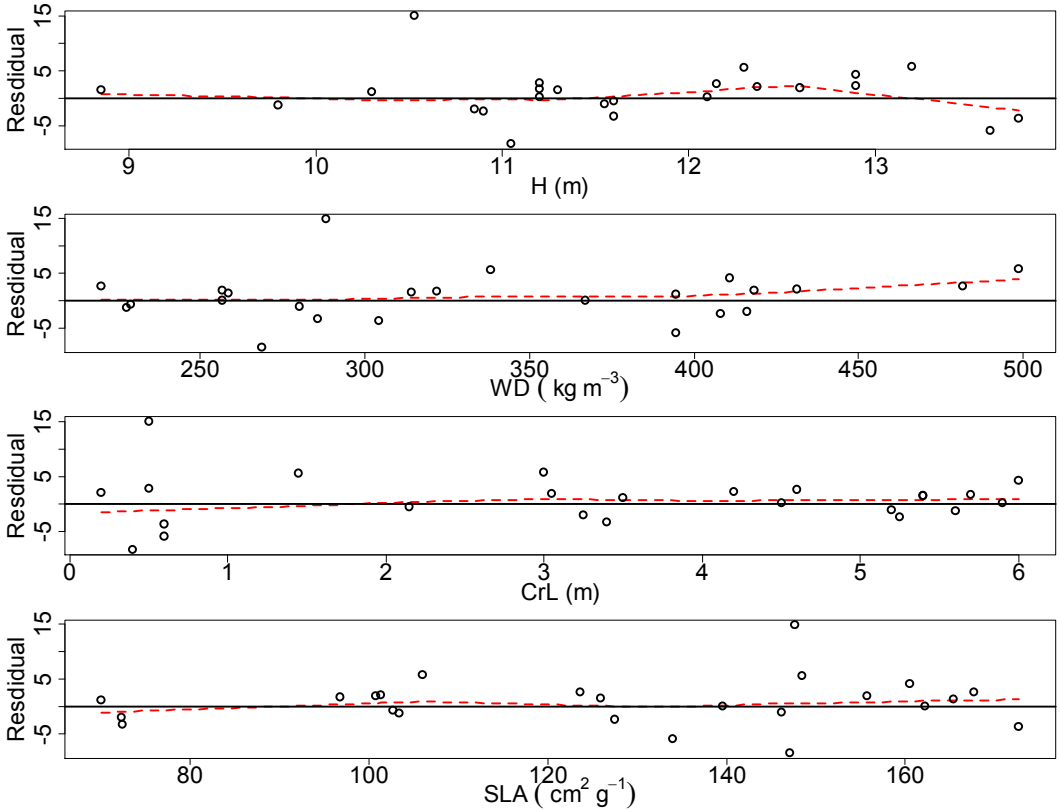

(H) Crown total biomass

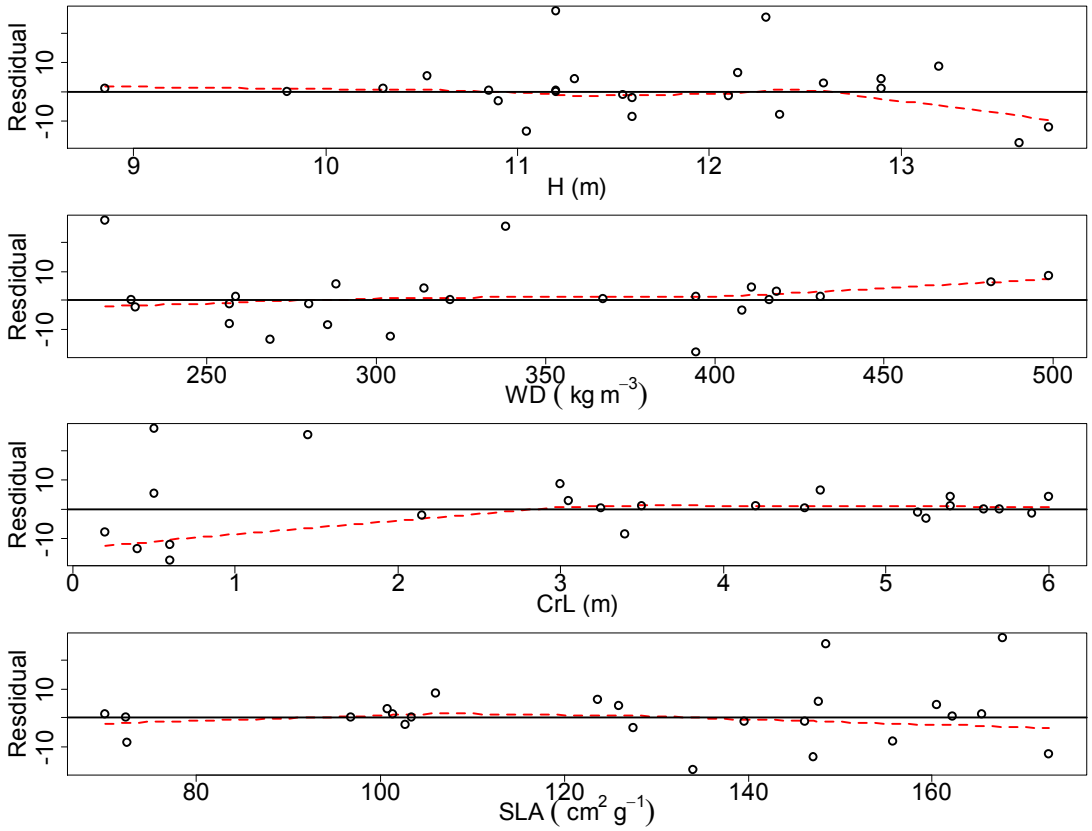

(I) Bole total biomass

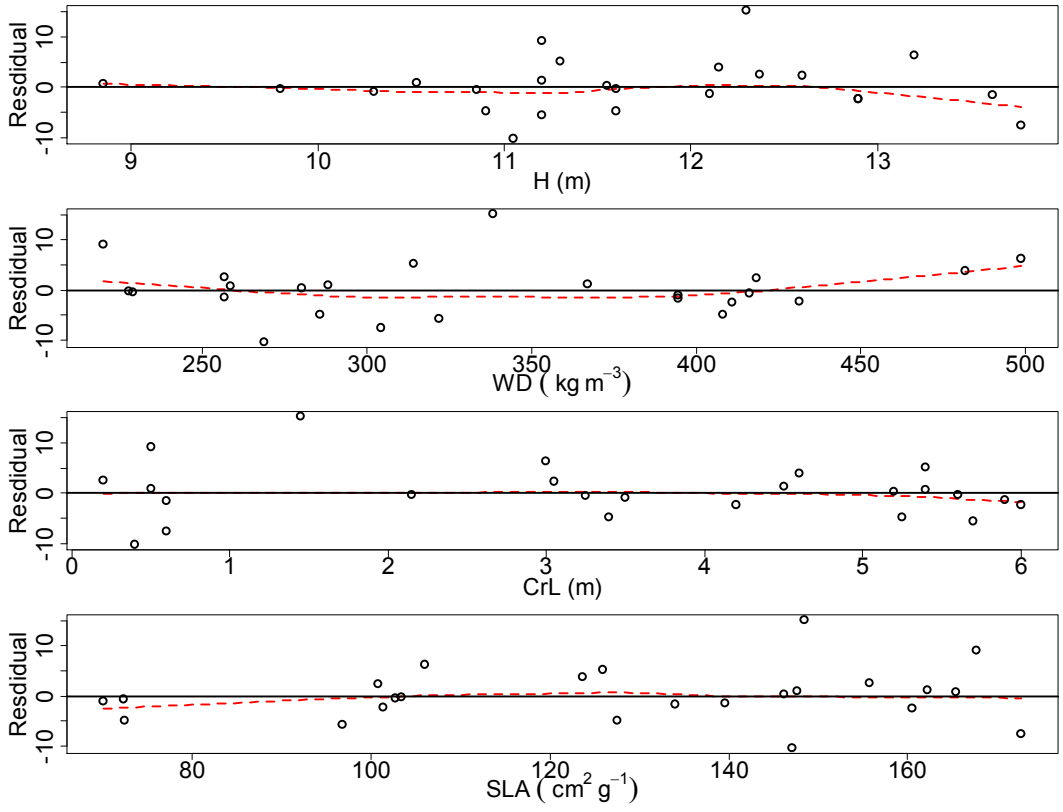

(J) Above ground total biomass

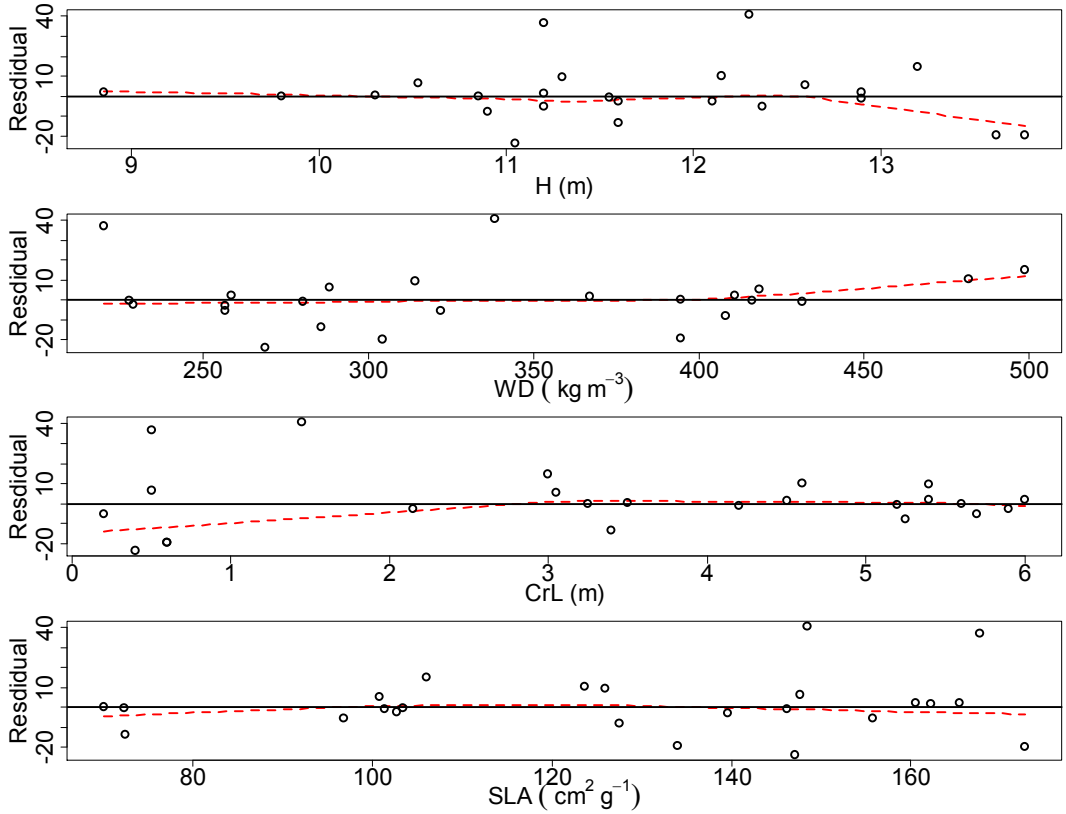

Appendix 1.2: Comparison of ordinary least square models with their goodness of fit statistics: (A) LINOLS, and (B) NLINOLS. The estimated parameter values are presented in power transformed scale. Model 1, 2, 3 and so on refers to the model equations tested in Table 2.4. RANK indicates the model's performance in comparison. For example, a model in RANK 1 is a best and RANK 4 is a worst in terms of goodness-of-fit statistics, and residual plots.

(A) Linear OLS

	MOD	AIC	RMSE	MAB	MPE	RSE	CV	R2	IOA	RANK
Stem	1	25.443	4.864	3.391	23.660	5.080	8.046	0.976	0.994	1
	2	36.147	6.014	4.385	36.173	6.282	9.948	0.964	0.991	4
	4	37.711	7.121	4.851	50.703	7.437	11.778	0.949	0.987	5
	5	30.787	5.425	4.026	29.436	5.800	8.974	0.970	0.993	3
	6	28.735	5.088	3.777	25.884	5.439	8.415	0.974	0.994	2
Branch	1	40.943	11.168	6.658	124.713	11.664	64.118	0.703	0.909	3
	2	43.512	12.098	7.017	146.363	12.636	69.461	0.651	0.903	4
	3	36.513	8.034	4.935	64.538	8.588	46.124	0.846	0.962	1
	4	50.742	15.701	9.164	246.536	16.400	90.150	0.412	0.808	5
	5	39.308	8.634	5.221	74.550	9.230	49.573	0.822	0.956	2
Bark	1	11.981	0.880	0.604	0.774	0.919	16.987	0.921	0.979	1
	2	16.150	0.975	0.691	0.951	1.019	18.827	0.902	0.976	3

	4	10.712	0.901	0.614	0.812	0.941	17.393	0.917	0.979	2
NF	1	12.283	0.896	0.610	0.803	0.936	26.627	0.898	0.973	2
	2	14.074	0.989	0.709	0.978	1.033	29.378	0.876	0.969	3
	4	15.354	1.255	0.758	1.575	1.311	37.285	0.800	0.947	4
	8	11.387	0.850	0.599	0.723	0.909	25.260	0.908	0.976	1
OF	1	6.232	2.879	2.109	8.290	3.007	21.852	0.936	0.985	3
	2	10.613	3.925	2.668	15.409	4.100	29.793	0.881	0.974	4
	4	12.951	5.307	3.241	28.168	5.543	40.282	0.783	0.949	5
	8	-0.283	2.522	1.843	6.358	2.696	19.138	0.951	0.989	2
	9	-2.634	2.379	1.690	5.659	2.543	18.055	0.956	0.989	1
Cone	1	78.297	2.811	1.785	7.904	2.936	77.113	0.449	0.753	3
	2	77.114	2.743	1.777	7.522	2.865	75.229	0.475	0.781	1
	4	76.856	2.850	1.718	8.122	2.977	78.169	0.433	0.750	2
Foliage	1	14.531	4.561	3.179	20.800	4.764	22.592	0.929	0.981	1
	2	12.748	5.204	3.709	27.083	5.436	25.780	0.907	0.978	2
	4	15.680	7.335	4.030	53.797	7.661	36.333	0.816	0.952	3
Crown	1	-6.906	15.360	9.019	235.915	16.043	40.845	0.823	0.955	2
	2	-3.795	18.980	11.134	360.252	19.824	50.474	0.730	0.939	4
	4	1.497	26.138	14.444	683.211	27.301	69.509	0.487	0.871	5
	5	-3.452	16.412	10.166	269.338	17.545	43.643	0.798	0.953	3
	8	-9.707	14.178	8.493	201.024	15.157	37.704	0.849	0.963	1
Bole	1	27.070	5.287	3.765	27.951	5.522	8.055	0.977	0.994	1
	2	37.807	6.594	4.886	43.486	6.888	10.047	0.964	0.991	5
	4	38.458	7.617	5.235	58.013	7.955	11.604	0.952	0.988	6
	5	31.856	5.854	4.293	34.264	6.258	8.918	0.971	0.993	3
	6	29.714	5.456	4.010	29.770	5.833	8.313	0.975	0.994	2
	7	35.013	6.412	4.729	41.117	6.855	9.769	0.966	0.992	4
AGT	1	-8.281	17.132	11.420	293.497	17.894	16.594	0.940	0.985	1
	2	0.903	20.701	13.738	428.549	21.622	20.052	0.912	0.979	3
	4	7.756	28.826	17.558	830.938	30.108	27.921	0.830	0.957	4
	5	-1.638	18.746	12.888	351.398	20.040	18.157	0.928	0.983	2

(B) Nonlinear OLS

	Model	**AIC**	**RMSE**	**MB**	**MAB**	**MPE**	**RSE**	**CV**	**R2**	**IOA**	**RANK**
Stem	1	153.84	5.27	-0.26	3.88	27.72	5.50	8.71	0.97	0.99	1
	2	232.67	27.20	-0.07	22.72	739.97	28.41	45.00	0.26	0.64	7
	3	185.52	10.19	-0.41	7.51	103.78	10.64	16.85	0.90	0.97	4
	4	167.89	7.06	-0.30	4.99	49.77	7.37	11.67	0.95	0.99	3

	5	155.68	5.25	-0.25	3.94	27.53	5.61	8.68	0.97	0.99	2
	6	213.17	18.12	-0.38	14.57	328.33	18.93	29.97	0.67	0.89	6
	7	203.85	14.92	-0.48	11.26	222.71	15.59	24.69	0.78	0.93	5
Branch	1	187.59	10.63	-0.74	7.24	113.10	11.11	61.06	0.73	0.91	2
	3	204.72	15.20	-1.08	11.35	230.96	15.87	87.26	0.45	0.75	5
	4	198.73	13.41	-1.10	9.64	179.93	14.01	77.01	0.57	0.83	4
	5	168.61	6.87	-0.72	4.30	47.18	7.34	39.44	0.89	0.97	1
	6	193.41	12.01	-1.55	9.21	144.14	12.54	68.93	0.66	0.87	3
	7	210.55	17.16	-0.79	13.04	294.45	17.92	98.52	0.30	0.62	6
Bark	1	69.77	0.91	-0.04	0.65	0.83	0.95	17.64	0.91	0.98	2
	2	120.66	2.64	-0.01	2.18	6.95	2.75	50.91	0.29	0.66	6
	3	77.87	1.08	-0.06	0.73	1.17	1.13	20.88	0.88	0.97	3
	4	68.88	0.90	-0.04	0.60	0.80	0.94	17.31	0.92	0.98	1
	6	100.11	1.72	-0.03	1.50	2.95	1.80	33.19	0.70	0.90	5
	7	92.52	1.47	-0.07	1.08	2.15	1.53	28.33	0.78	0.93	4
NF	1	67.97	0.88	-0.03	0.61	0.77	0.92	26.14	0.90	0.97	1
	3	90.18	1.40	-0.08	0.94	1.95	1.46	41.53	0.75	0.92	3
	4	80.15	1.13	-0.06	0.77	1.29	1.18	33.69	0.84	0.95	2
	6	94.64	1.53	-0.11	1.23	2.35	1.60	45.57	0.70	0.90	4
	7	101.07	1.75	-0.08	1.24	3.08	1.83	52.11	0.61	0.86	5
OF	1	116.53	2.42	-0.18	1.79	5.86	2.53	18.37	0.95	0.99	1
	3	153.52	5.23	-0.43	3.93	27.35	5.46	39.69	0.79	0.93	3
	4	139.57	3.91	-0.35	2.83	15.29	4.08	29.68	0.88	0.97	2
	6	156.40	5.55	-0.52	4.49	30.84	5.80	42.15	0.76	0.92	4

	7	166.64	6.87	-0.39	5.20	47.25	7.18	52.17	0.64	0.87	5
Cone	1	120.73	2.64	0.05	1.71	6.98	2.76	72.46	0.51	0.82	1
	3	124.65	2.87	-0.06	1.75	8.21	2.99	78.61	0.43	0.75	3
	4	122.69	2.75	-0.02	1.71	7.57	2.87	75.47	0.47	0.79	2
	6	128.80	3.12	-0.04	2.19	9.76	3.26	85.71	0.32	0.67	5
	7	127.43	3.04	-0.07	1.80	9.22	3.17	83.30	0.36	0.68	4
Foliage	1	145.29	4.41	-0.14	3.03	19.42	4.60	21.83	0.93	0.98	1
	3	174.76	8.14	-0.56	5.46	66.26	8.50	40.32	0.77	0.93	2
	6	180.28	9.13	-0.66	7.30	83.41	9.54	45.24	0.71	0.90	3
	7	186.69	10.44	-0.53	7.32	108.93	10.90	51.70	0.63	0.86	4
Crown	1	197.78	13.15	-0.78	8.73	172.92	13.73	34.97	0.87	0.96	2
	3	223.52	22.48	-1.66	16.71	505.52	23.48	59.79	0.62	0.86	4
	5	179.14	8.56	-0.61	5.73	73.19	9.15	22.75	0.95	0.99	1
	6	215.66	19.08	-2.10	14.09	364.23	19.93	50.75	0.73	0.91	3
	7	232.14	26.91	-1.36	20.33	723.91	28.10	71.55	0.46	0.76	5
Bole	1	158.13	5.76	-0.30	4.25	33.15	6.01	8.77	0.97	0.99	1
	2	236.93	29.73	-0.08	24.90	883.93	31.05	45.30	0.26	0.64	6
	3	189.10	10.98	-0.46	8.14	120.48	11.46	16.72	0.90	0.97	3
	4	171.17	7.55	-0.34	5.34	57.07	7.89	11.51	0.95	0.99	2
	6	217.14	19.68	-0.41	16.02	387.42	20.56	29.99	0.68	0.89	5
	7	207.76	16.19	-0.55	12.27	262.09	16.91	24.67	0.78	0.93	4
AGB	1	208.19	16.34	-0.62	11.24	266.87	17.06	15.82	0.95	0.99	1
	3	241.69	32.83	-1.65	23.72	1077.80	34.29	31.80	0.78	0.93	3
	4	228.93	25.16	-1.24	17.28	633.19	26.28	24.37	0.87	0.96	2

	6	246.02	35.93	-1.85	29.21	1290.89	37.53	34.80	0.74	0.91	4
	7	254.31	42.70	-1.65	31.83	1823.02	44.60	41.36	0.63	0.87	5

Appendix 2

Appendix 2.1: Comparison of different forms of correlation structures with an unstructured model (without correlation structure) for soil CO_2 efflux (F_s), soil temperature (T_s), and soil volumetric water content (θ_v) for the whole period of the experiment. Data fitted in *nlme* package of R. The change in AIC (Δ AIC) denotes the increase in AIC with an autocorrelation structure. The corAR1, corCompSymm, and corARMA indicate first-order autoregressive, compound symmetry, and autoregressive moving average autocorrelation structures, respectively. Models are fitted with restricted maximum likelihood (REML) estimates. The fixed effects in the model were stocking, clone, fertilization, follow-up herbicide, and their two-way interaction and season.

Structures	Random effects	Autocorrelation	AIC	Δ AIC	*p*-value
		F_s			
unstructured	~1|block/stock/fh/plot		-85.74		
corAR1	~1|block/stock/fh/plot	~1|block/stock/fh/plot/clone	-125.34	39.61	<.0001
corCompSymm	~1|block/stock/fh/plot	~1|block/stock/fh/plot/clone	-116.41	30.67	<.0001
corARMA	~1|block/stock/fh/plot	~1|block/stock/fh/plot/clone	-123.01	37.26	<.0001
		T_s			
unstructured	~1|block/stock/fh/plot		-2,780.46		
corAR1	~1|block/stock/fh/plot	~1|block/stock/fh/plot/clone	-2,879.69	99.24	<.0001
corCompSymm	~1|block/stock/fh/plot	~1|block/stock/fh/plot/clone	-2,891.49	111.04	<.0001
corARMA	~1|block/stock/fh/plot	~1|block/stock/fh/plot/clone	-2,917.72	137.27	<.0001
		θ_v			
unstructured	~1|block/stock/fh/plot		22,986.78		
corAR1	~1|block/stock/fh/plot	~1|block/stock/fh/plot/clone	22,963.20	23.58	<.0001
corCompSymm	~1|block/stock/fh/plot	~1|block/stock/fh/plot/clone	22,969.77	17.01	<.0001
corARMA	~1|block/stock/fh/plot	~1|block/stock/fh/plot/clone	22,965.46	21.32	<.0001

Appendix 2.2: ANOVA statistics for the fixed components of the linear mixed effect model for soil CO_2 efflux (F_s), soil temperature (T_s), and soil volumetric water content (θ_v) fitted for the whole period of the experiment. Fixed effects included stocking, clone, fertilization, and follow-up herbicide, and their two-way interactions and season.

F_s				
Factors	**numDF**	**denDF**	**F-value**	**p-value**
(Intercept)	1	889	22873.63	<.0001
Stock (S)	2	6	9.92	0.0125
Fert (F)	1	29	0.94	0.3414
Herb (H)	1	29	2.52	0.1231
Clone (C)	4	889	4.32	0.0018
Season (Se)	3	889	319.68	<.0001
S × F	2	29	0.05	0.9536
S × H	2	29	0.60	0.5548
F × C	4	889	1.64	0.1632
H × C	4	889	1.86	0.1172
F × H	1	29	2.05	0.1632
S × C	8	889	0.55	0.8194

T_s				
Factors	**numDF**	**denDF**	**F-value**	**p-value**
(Intercept)	1	889	21515.07	<.0001
Stock (S)	2	6	1.41	0.3155
Fert (F)	1	29	0	0.9871
Herb (H)	1	29	0.78	0.3836
Clone (C)	4	889	9.37	<.0001
Season (Se)	3	889	9,676.54	<.0001
S × F	2	29	1.39	0.2631
S × H	2	29	1.24	0.3053
F × C	4	889	1.13	0.3426
H × C	4	889	1.38	0.2405
F × H	1	29	1.37	0.2509
S × C	8	889	1.50	0.1519
θ_v				
Factors	**numDF**	**denDF**	**F-value**	**p-value**
(Intercept)	1	889	2708.53	<.0001
Stock (S)	2	6	10.29	0.0115
Fert (F)	1	29	0.01	0.9253
Herb (H)	1	29	11.07	0.0024
Clone (C)	4	889	0.57	0.6865
Season (Se)	3	889	2001.12	<.0001
S × F	2	29	3.16	0.0572
S × H	2	29	8.06	0.0016
F × C	4	889	0.46	0.7662
H × C	4	889	0.39	0.8108
F × H	1	29	2.29	0.1407
S × C	8	889	0.29	0.9701

Appendix 2.3: ANOVA statistics for the fixed components of linear mixed effect model for soil CO_2 efflux (F_s), soil temperature (T_s), and soil volumetric water content (θ_v) fitted with the data separately for each season. Fixed effects included stocking (S), clone (C), fertilization (F), and follow-up herbicide (H) treatment, and their two-way interaction. Only significant results (p <.05) were reported in the table.

Season	Factor	F_s				T_s				θ_v			
		num DF	den DF	F-value	p-value	num DF	den DF	F-value	p-value	num DF	den DF	F-value	p-value
Autumn	H									1	29	10	0.0031
	C	4	172	7.74	<.0001	4	172	7.43	<.0001				
	S × F									2	29	5	0.011
	S × H									2	29	11	0.0004
Winter	H									1	29	7	0.0137
	C					4	172	4	0.0043	4	172	6	0.0001
	S × H									2	29	5	0.0172
Spring	S	2	6	17.69	0.003					2	6	5.99	0.0371
	H									1	29	4.95	0.034
	C					4	172	7	<.0001				
	H × C									4	172	2.54	0.0419
Summer	S	2	6	7.75	0.0218								
	C	4	172	2.68	0.0336	4	172	3.27	0.0129				

Appendix 2.4: Soil physical properties across silvicultural treatments and season. Soil physical properties are denoted as BD, RF, WFPS, and PORE indicating the bulk density, rock fraction, water filled pore space, total soil porosity at 10 cm soil depth, respectively. Different letters along the column within the same silvicultural treatments denote significant differences at $p \leq 0.05$ using mixed effects ANOVA ($p < .05$), TukeyHSD test.

Factors	Level	BD	RF	WFPS	PORE
Clone	1	0.81 (0.01) a	14.89 ± 1.21 a	23.57 ± 1.77 a	69.27 ± 28.32 a
	2	0.81 ± 0.01 a	14.89 ± 1.21 a	23.57 ± 1.77 a	69.27 ± 28.32 a
	3	0.81 ± 0.01 a	14.89 ± 1.21 a	23.57 ± 1.77 a	69.27 ± 28.32 a
	4	0.81 ± 0.01 a	14.89 ± 1.21 a	23.57 ± 1.77 a	69.27 ± 28.32 a
	5	0.81 ± 0.01 a	14.89 ± 1.21 a	23.57 ± 1.77 a	69.27 ± 28.32 a
	Mean	0.81 ± 0.01	14.89 ± 1.21	23.57 ± 1.77	69.27 ± 28.32
Stock	625	0.81 ± 0.01 a	13.13 ± 1.34 a	25.16 ± 1.85 a	69.39 ± 29.18 a
	1250	0.79 ± 0.01 a	15.16 ± 1.34 a	23.73 ± 1.85 a	70.04 ± 29.18 a
	2500	0.84 ± 0.01 a	16.54 ± 1.34 a	21.86 ± 1.85 a	68.36 ± 29.18 a
	Mean	0.81 ± 0.01	14.94 ± 1.34	23.59 ± 1.85	69.27 ± 29.18
Fert	F	0.83 ± 0.01 b	14.86 ± 1.2 a	23.6 ± 1.76 a	68.83 ± 28.14 a
	NF	0.8 ± 0.01 a	14.92 ± 1.2 a	23.54 ± 1.76 a	69.71 ± 28.14 b
	Mean	0.81 ± 0.01	14.89 ± 1.2	23.57 ± 1.76	69.27 ± 28.14
Herb	H	0.83 ± 0.01 b	13.33 ± 1.2 a	24.94 ± 1.76 b	68.84 ± 28.14 a
	NH	0.8 ± 0.01 a	16.58 ± 1.2 b	22.23 ± 1.76 a	69.71 ± 28.14 b
	Mean	0.81 ± 0.01	14.96 ± 1.2	23.59 ± 1.76	69.27 ± 28.14
Season	autumn	0.81 ± 0.01 a	14.89 ± 1.21 a	25.3 ± 1.76 b	69.27 ± 28.26 a
	winter	0.81 ± 0.01 a	14.89 ± 1.21 a	32.73 ± 1.76 c	69.27 ± 28.26 a
	spring	0.81 ± 0.01 a	14.89 ± 1.21 a	26.5 ± 1.76 b	69.27 ± 28.26 a
	summer	0.81 ± 0.01 a	14.89 ± 1.21 a	11.66 ± 1.76 a	69.27 ± 28.26 a
	Mean	0.81 ± 0.01	14.89 ± 1.21	24.05 ± 1.76	69.27 ± 28.26
Overall mean		0.81 ± 0.01	14.92 ± 1.23	23.67 ± 1.78	69.27 ± 28.41

Appendix 2.5: Correlation analyses between soil CO_2 efflux (F_s) and soil temperature (T_s), soil volumetric water content (θ_v), bulk density (BD), total soil porosity (PORE), water filled pore space (WFPS), and rock fragments (RF) across the clone (1 – 5), stocking (stems ha^{-1}), fertilization (F = fertilized, NF = non-fertilized), and follow-up herbicide (H = herbicide, NH = no herbicide). The subscript values 10, 20 and 30 associated with given variables are soil depth. Correlation values are Pearson's coefficient. Notation of asterisk indicates significant correlations at *$p < 0.05$, **$p < 0.01$, and **$p < 0.001$.

Variables	CLONE					STOCK			FERT		HERB	
	1	**2**	**3**	**4**	**5**	**625**	**1250**	**2500**	**F**	**NF**	**H**	**NH**
T_s	0.53***	0.55***	0.69***	0.65***	0.65***	0.59***	0.65***	0.58***	0.58***	0.63***	0.63***	0.59***
θ_{v10}	-0.07	0.06	-0.11	-0.06	0.04	-0.06	0.14*	-0.18*	-0.02	-0.06	-0.06	-0.01***
θ_{v20}	-0.10	-0.18*	-0.20*	-0.26**	-0.30***	-0.12	-0.41***	-0.06	-0.24***	-0.17**	-0.13*	-0.27***
θ_{v30}	-0.08	-0.08	-0.24**	-0.26**	-0.27**	-0.10	-0.36***	-0.05	-0.22***	-0.14*	-0.12*	-0.24***
BD_{10}	0.20*	-0.01	0.20*	0.14	0.15	0.09	-0.04	0.30***	0.21***	0.05	0.08	0.19***
BD_{20}	0.14	0.05	0.17	0.09	0.13	0.17*	-0.01	0.18**	0.08	0.17**	0.11*	0.16**
BD_{30}	0.08	0.05	0.22*	0.29**	0.27**	0.16*	0.11	0.19**	0.27***	0.08	0.23***	0.13*
PO_{10}	-0.20*	0.01	-0.20*	-0.14	-0.16	-0.09	0.04	-0.30***	-0.21***	-0.05	-0.08	-0.19***
PO_{20}	-0.14	-0.05	-0.17	-0.09	-0.13	-0.17*	0.01	-0.18**	-0.08	-0.17**	-0.11	-0.15**
PO_{30}	-0.09	-0.05	-0.22*	-0.29**	-0.27**	-0.17*	-0.11	-0.19**	-0.27***	-0.08	-0.23***	-0.13*
$WFPS_{10}$	-0.15	-0.13	-0.12	-0.32***	-0.27**	-0.28***	-0.29***	-0.02	-0.15*	-0.23***	-0.24***	-0.12*
$WFPS_{20}$	0.19*	0.15	0.18*	0.12	0.21*	0.18*	0.14*	0.30***	0.16**	0.20***	0.12*	0.24***
$WFPS_{30}$	-0.08	-0.07	-0.18*	-0.03	-0.07	-0.12	-0.17*	0.08	-0.06	-0.12*	-0.01	-0.15*
RF_{10}	0.07	-0.11	-0.14	0.02	-0.01	0.18*	-0.10	-0.15*	-0.07	-0.01	-0.12*	-0.01

RF_{20}	-0.17	-0.17	-0.11	-0.02	-0.10	-0.06	-0.10	-0.17*	-0.11*	-0.13*	-0.09	-0.17**
RF_{30}	-0.03	-0.14	-0.14	-0.07	-0.07	-0.01	-0.10	-0.15*	-0.10	-0.10	-0.15**	-0.06

Appendix 2.6: Correlation analyses between soil temperature (T_s) and soil volumetric water content (θ_v), bulk density (BD), total porosity (PORE), water filled pore space (WFPS), and rock fragments (RF) across the clone (1 – 5), stocking (stems ha^{-1}), fertilization (F = fertilized, NF = non-fertilized), and follow-up herbicide (H = herbicide, NH = no herbicide). The subscript values 10, 20 and 30 associated with given variables are soil depth. Correlation values are Pearson's coefficient. Notation of asterisk indicates significant correlations at *$p < 0.05$, **$p < 0.01$, and **$p < 0.001$.

Variables	CLONE					STOCK			FERT		HERB	
	1	**2**	**3**	**4**	**5**	**625**	**1250**	**2500**	**F**	**NF**	**H**	**NH**
θ_{v10}	0.10	0.08	-0.11	0.05	0.11	0.06	0.11	-0.04	0.00	0.09	0.12*	-0.05
θ_{v20}	-0.29**	-0.27**	-0.15	-0.25**	-0.29**	-0.22**	-0.41***	-0.14*	-0.22***	-0.28***	-0.26***	-0.25***
θ_{v30}	-0.22*	-0.19*	-0.22*	-0.24**	-0.31***	-0.16*	-0.34***	-0.24***	-0.22***	-0.26***	-0.26***	-0.22***
BD_{10}	0.05	0.04	0.06	0.06	0.04	0.03	0.12	0.02	0.06	0.04	0.02	0.08
BD_{20}	0.04	0.01	0.02	0.04	0.05	0.04	-0.03	0.07	0.02	0.04	0.01	0.05
BD_{30}	0.00	-0.02	0.02	0.00	-0.03	0.02	-0.06	-0.02	0.03	-0.05	0.06	-0.06
PO_{10}	-0.05	-0.04	-0.06	-0.06	-0.04	-0.03	-0.12	-0.02	-0.06	-0.04	-0.02	-0.08
PO_{20}	-0.04	-0.01	-0.02	-0.04	-0.05	-0.03	0.03	-0.07	-0.02	-0.04	-0.01	-0.04
PO_{30}	0.00	0.02	-0.02	0.00	0.03	-0.03	0.06	0.02	-0.03	0.05	-0.06	0.06
$WFPS_{10}$	-0.36***	-0.35***	-0.34***	-0.34***	-0.36***	-0.51***	-0.29***	-0.28***	-0.34***	-0.36***	-0.42***	-0.28***
$WFPS_{20}$	0.22*	0.21*	0.22*	0.23*	0.23*	0.20*	0.27***	0.22**	0.23***	0.22***	0.20***	0.24***
$WFPS_{30}$	-0.20	-0.19*	-0.16	-0.20*	-0.19*	-0.26	-0.17*	-0.16*	-0.13	-0.27***	-0.21***	-0.17**
RF_{10}	-0.03	-0.02	-0.04	-0.04	-0.02	0.06*	-0.06	-0.07	-0.04	-0.03	-0.02	-0.03
RF_{20}	-0.05	-0.02	-0.05	-0.06	-0.02	0.07	-0.09	-0.06	-0.04	-0.04	-0.02	-0.06
RF_{30}	-0.03	-0.02	-0.07	-0.04	0.00	0.02	0.00	-0.09	-0.03	-0.03	-0.04	-0.02

Appendix 3

Appendix 3.1: ANOVA statistics for the plot level analysis of data using linear mixed effects model. Fixed effects included stocking, fertilization, follow-up herbicide, and their interactions. The below-ground soil respiration (BSR), above-ground biomass production (AGB), the ratio (BSR/AGB), tree diameter (DBH), tree height (H), basal area (G), and leaf area index (LAI) were the response variables.

BSR						**AGB**				
Factors	numDF	denDF	F-value	p-value		Factors	numDF	denDF	F-value	p-value
(Intercept)	1	27	1484.217	<.0001		(Intercept)	1	27	9854.152	<.0001
Stock (S)	2	6	7.9627	**0.0205**		Stock (S)	2	6	29.907	**0.0008**
Fert (F)	1	27	0.8598	0.362		Fert (F)	1	27	2.953	0.0972
Herb (H)	1	27	3.3118	0.0799		Herb (H)	1	27	31.998	**<.0001**
S×F	2	27	0.2293	0.7966		S×F	2	27	1.58	0.2245
S×H	2	27	0.591	0.5608		S×H	2	27	4.165	**0.0265**
F×H	1	27	1.8803	0.1816		F×H	1	27	1.806	0.1902
S×F×H	2	27	1.5673	0.227		S×F×H	2	27	0.492	0.6165
BSR/AGB ratio						**DBH**				
Factors	numDF	denDF	F-value	p-value		Factors	numDF	denDF	F-value	p-value
(Intercept)	1	27	1,234.258	<.0001		(Intercept)	1	27	5,9626.82	**<.0001**
Stock (S)	2	6	5.3737	**0.046**		Stock (S)	2	6	1,184.46	**<.0001**
Fert (F)	1	27	1.5758	0.2201		Fert (F)	1	27	0.93	0.3423
Herb (H)	1	27	10.9036	**0.0027**		Herb (H)	1	27	75.74	**<.0001**
S×F	2	27	0.7123	0.4995		S×F	2	27	2.15	0.1362
S×H	2	27	0.0031	0.997		S×H	2	27	11.57	**0.0002**
F×H	1	27	0.6981	0.4108		F×H	1	27	1.15	0.2935
S×F×H	2	27	1.2879	0.2923		S×F×H	2	27	0.39	0.6778
H						**G**				

Factors	numDF	denDF	F-value	p-value		Factors	numDF	denDF	F-value	p-value
(Intercept)	1	27	8,890.945	<.0001		(Intercept)	1	27	23,408.82	<.0001
Stock (S)	2	6	17.581	**0.0031**		Stock (S)	2	6	293.374	**<.0001**
Fert (F)	1	27	1.281	0.2678		Fert (F)	1	27	1.405	0.2463
Herb (H)	1	27	22.737	**0.0001**		Herb (H)	1	27	46.133	**<.0001**
S×F	2	27	0.313	0.7339		S×F	2	27	1.801	0.1844
S×H	2	27	0.169	0.8454		S×H	2	27	4.163	**0.0266**
F×H	1	27	0.08	0.7794		F×H	1	27	1.138	0.2956
S×F×H	2	27	0.397	0.6763		S×F×H	2	27	1.171	0.3252
LAI										
Factors	numDF	denDF	F-value	p-value						
(Intercept)	1	27	1626.365	<.0001						
Stock (S)	2	6	0.5542	0.6014						
Fert (F)	1	27	0.2758	0.6038						
Herb (H)	1	27	0.3559	0.5558						
S×F	2	27	0.886	0.4239						
S×H	2	27	1.4156	0.2602						
F×H	1	27	0.218	0.6443						
S×F×H	2	27	0.5882	0.5623						

Appendix 3.2: ANOVA statistics for the clone level analysis of data using linear mixed effects model. Fixed effects included stocking, fertilization, follow-up herbicide, clone, and their two-way interactions. The below-ground soil respiration (BSR), above-ground biomass production (AGB), BSR/AGB ratio, tree diameter (DBH), tree height (H), and basal area (G) were the response variables.

BSR						**ABG**				
Factors	numDF	denDF	F-value	p-value		Factors	numDF	denDF	F-value	p-value
(Intercept)	1	172	1,484.209	<.0001		(Intercept)	1	172	9,854.017	<.0001
Stock (S)	2	6	7.9627	**0.0205**		Stock (S)	2	6	29.906	**0.0008**
Fert (F)	1	29	0.8274	0.3705		Fert (F)	1	29	2.859	0.1016
H (Herb)	1	29	3.1871	0.0847		H (Herb)	1	29	30.981	**<.0001**
Clone (C)	4	172	3.7011	**0.0064**		Clone (C)	4	172	56.516	**<.0001**
S×F	2	29	0.2207	0.8033		S×F	2	29	1.53	0.2336
S×H	2	29	0.5688	0.5724		S×H	2	29	4.033	**0.0285**
F×C	4	172	1.3693	0.2466		F×C	4	172	1.491	0.2069
H×C	4	172	2.1806	0.0732		H×C	4	172	2.431	**0.0494**
F×H	1	29	1.8096	0.189		F×H	1	29	1.748	0.1964
S×C	8	172	0.4683	0.8772		S×C	8	172	1.828	0.0747
BSR/AGB ratio						**DBH**				
Factors	numDF	denDF	F-value	p-value		Factors	numDF	denDF	F-value	p-value
(Intercept)	1	172	1,403.477	<.0001		(Intercept)	1	172	6,2432.81	**<.0001**
Stock (S)	2	6	6.4342	**0.0322**		Stock (S)	2	6	1243.94	**<.0001**
Fert (F)	1	29	1.8534	0.1839		Fert (F)	1	29	1.04	0.3162
H (Herb)	1	29	10.6716	**0.0028**		H (Herb)	1	29	78.14	**<.0001**
Clone (C)	4	172	14.8688	**<.0001**		Clone (C)	4	172	69.47	**<.0001**
S×F	2	29	0.712	0.4991		S×F	2	29	2.22	0.1265
S×H	2	29	0.0153	0.9848		S×H	2	29	12.02	**0.0002**

F×C	4	172	1.3983	0.2366		F×C	4	172	1.76	0.1389
H×C	4	172	0.2418	0.9143		H×C	4	172	2.8	**0.0277**
F×H	1	29	0.6039	0.4434		F×H	1	29	1.24	0.2748
S×C	8	172	1.2312	0.2835		S×C	8	172	1.19	0.3054
H						**G**				
Factors	numDF	denDF	F-value	p-value		Factors	numDF	denDF	F-value	p-value
(Intercept)	1	172	8,803.781	<.0001		(Intercept)	1	172	23,431.34	<.0001
Stock (S)	2	6	17.494	**0.0031**		Stock (S)	2	6	293.656	**<.0001**
Fert (F)	1	29	1.319	0.2601		Fert (F)	1	29	1.138	0.295
H (Herb)	1	29	23.531	**<.0001**		H (Herb)	1	29	37.363	**<.0001**
Clone (C)	4	172	61.463	**<.0001**		Clone (C)	4	172	60.934	**<.0001**
S×F	2	29	0.318	0.7299		S×F	2	29	1.459	0.2491
S×H	2	29	0.191	0.8274		S×H	2	29	3.372	**0.0482**
F×C	4	172	0.459	0.7654		F×C	4	172	1.66	0.1615
H×C	4	172	0.75	0.5594		H×C	4	172	2.052	0.0892
F×H	1	29	0.097	0.7572		F×H	1	29	0.922	0.345
S×C	8	172	0.301	0.9647		S×C	8	172	2.394	**0.018**

Appendix 3.3: Estimated plot level mean values BSR (tonne C ha^{-1} yr^{-1}), AGB (tonne C ha^{-1}), BSR/AGB ratio, DBH (cm), H (m), G (m^2 ha^{-1}), and LAI (m^2 m^{-2}) across three stockings (stems ha^{-1}), five clones (1 – 5), fertilization (F = fertilized, NF = non-fertilized), and follow-up herbicide (H = herbicide, NH = no herbicide) treatments. The treatment means within a category followed by the same letter do not differ significantly at α = 0.05 level using Tukey's HSD test.

Factor	Level	BSR	AGB	BSR/AGB	DBH	H	G	LAI
STOCK	625	5.93±0.30 a	49.39±0.96 a	0.25±0.009 b	24.28±0.14 c	13.56±0.17 b	29.32±0.41 b	3.31±0.14 a
	1250	7.52±0.30 b	56.76±0.96 b	0.21±0.009 a	19.28±0.14 b	13.21±0.17 b	37.03±0.41 b	3.35±0.14 a
	2500	6.29±0.30 ab	59.61±0.96 b	0.19±0.009 a	14.79±0.14 a	12.53±0.17 a	43.50±0.41 a	3.15±0.14 a
FERT	F	6.72±0.23 a	54.59±0.68 a	0.12±0.005 a	19.39±0.10 a	13.17±0.15 a	36.36±0.32 a	3.24±0.10 a
	NF	6.43±0.23 a	55.91±0.68 a	0.12±0.005 a	19.51±0.10 a	13.03±0.15 a	36.87±0.32 a	3.30±0.10 a
HERB	H	6.29±0.23 a	57.43±0.68 b	0.11±0.005 a	19.98±0.10 b	13.4±0.15 b	38.08±0.32 b	3.30±0.10 a
	NH	6.86±0.23 a	53.07±0.68 a	0.13±0.005 b	18.92±0.10 a	12.8±0.15 a	35.15±0.32 a	3.24±0.10 a
Mean		6.58±0.26	55.25±0.8	0.16±0.01	19.45±0.12	13.1±0.16	36.62±0.36	3.27±0.12

Appendix 3.4: Estimated clone level mean values of the BSR (tonne C ha^{-1} yr^{-1}), AGB (tonne C ha^{-1}), BSR/AGB ratio, DBH (cm), H (m), G (m^2 ha^{-1}), and LAI (m^2 m^{-2}) across five clones (1 – 5). The treatment means within a category followed by the same letter do not differ significantly at α = 0.05 level using Tukey's HSD test.

Factor	Level	BSR	AGB	BSR/AGB	DBH	H	G
CLONE	1	6.42±0.23 ab	62.81±0.96 c	0.10±0.001 a	20.56±0.14 c	13.42±0.15 c	41.11±0.53 c
	2	6.36±0.23 a	55.5±0.96 b	0.12±0.001 ab	19.43±0.14 b	12.78±0.15 b	36.58±0.53 b
	3	7.07±0.23 b	60.64±0.96 c	0.12±0.001 bc	20.41±0.14 c	13.87±0.15 d	40.47±0.53 c
	4	6.30±0.23 a	48.63±0.96 a	0.13±0.001 cd	18.26±0.14 a	12.38±0.15 a	32.29±0.53 a
	5	6.73±0.23 ab	48.67±0.96 a	0.14±0.001 d	18.55±0.14 a	13.02±0.15 b	32.62±0.53 a
Mean		6.58±0.23	55.25±0.96	0.12±0.001	19.44±0.14	13.09±0.15	36.62±0.53

Appendix 3.5: Stand density index (SDI) analysis of the *P. radiata* growing in the trial site. The first year of measurement was 2008 (3 years after planting) and last measurement was in 2017 (12 years after planting).

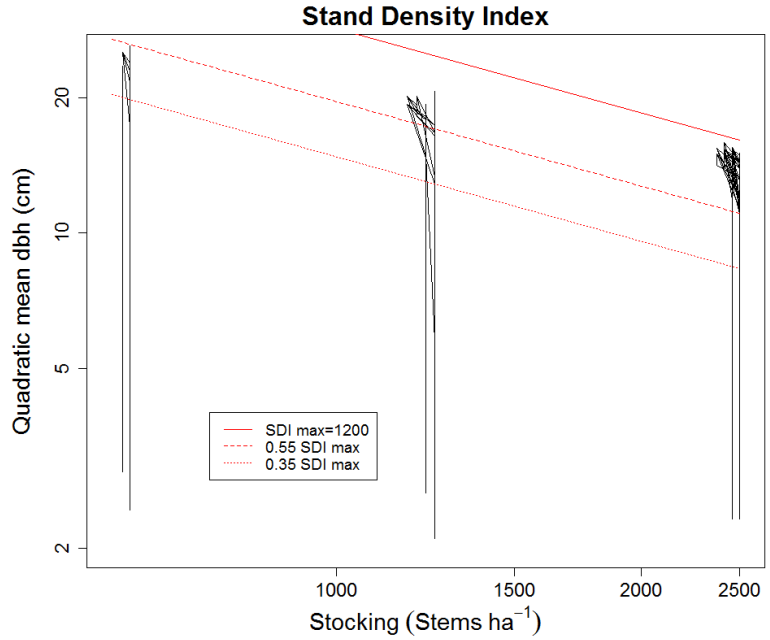

(A) SDI as indicated by quadratic mean DBH for the three different level of stocking (625, 1,250, and 2,500 stems ha^{-1})

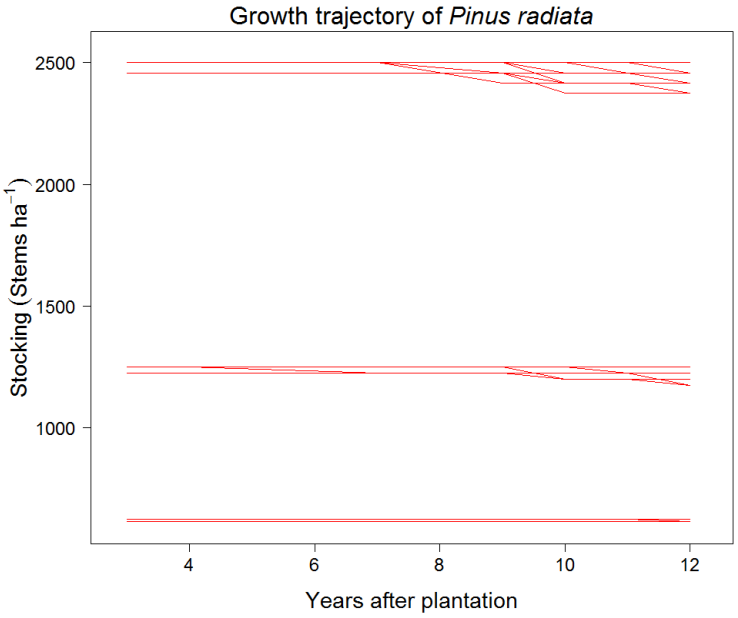

(B) Growth trajectories of *P. radiata* plantations with three different level of stocking in the trial site.